Magnetic And Interpolation Techniques In The Identification And Analysis Of Metal Contaminants In Urban Soils

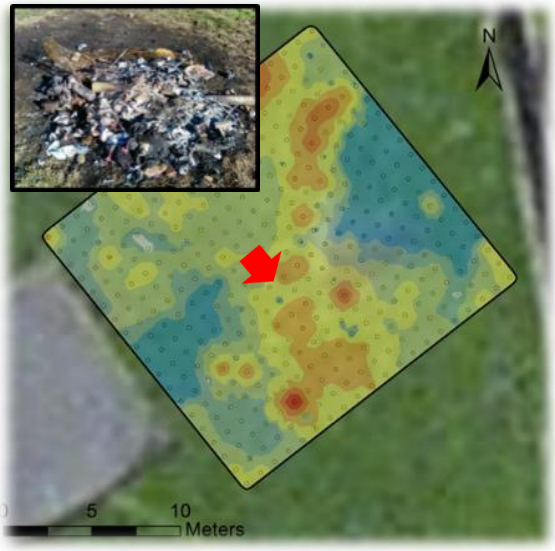

A thesis submitted to the National University of Ireland Galway for a degree of Doctor of Philosophy

June 2019

Nessa Golden

School of Geography and Archaeology & School of Natural Sciences,
National University of Ireland, Galway

Supervisors and affiliations:

Dr. Chaosheng Zhang

Discipline of Geography, School of Geography and Archaeology,
National University of Ireland Galway

Dr. Liam Morrison

Discipline of Earth and Ocean Sciences, School of Natural Sciences
and Ryan Institute, National University of Ireland Galway

NUI Galway
OÉ Gaillimh

Ryan Institute

TABLE OF CONTENTS

DECLARATION

This dissertation is my own original research work. It has not been previously submitted, in part or whole, to any university or institution for any degree, diploma, or other qualification.

The work described in chapter 2, detailing the spatial patterns of metal contaminants in soils of an urban bonfire site has previous been published as: Golden, N., Morrison, L., Gibson, P.J., Potito, A.P. and Zhang, C. (2015). 'Spatial patterns of metal contamination and magnetic susceptibility of soils at an urban bonfire site'. *Applied Geochemistry, 52*, 86-96. This work was performed and written by myself with co-authors in a teaching and supervisory capacity.

Chapter 3 describes the research published on the effects of grass coverage on magnetic susceptibility measurements of urban soils. This is published as: Golden, N., Zhang, C., Potito, A.P., Gibson, P.J., Bargary, N. and Morrison, L. (2017). 'Impact of grass cover on the magnetic susceptibility measurements for assessing metal contamination in urban soils'. *Environmental Research, 155*, 294-306. This work was carried out and written by myself with teaching and guidance from the co-authors.

The study outlined in chapter 4 is on the application of the ordinary cokriging method to produce good estimates of lead concentrations present in urban contaminated soils using magnetic susceptibility measurements as auxiliary data. This manuscript has been submitted for publication as: Golden, N., Zhang, C., Potito, A.P., Gibson, P.J., Bargary, N. and Morrison, L. 'Use of ordinary cokriging with magnetic susceptibility for mapping lead concentrations in soils of an urban contaminated site' is currently under review for publication in the *Journal of Soils and Sediments*. The work was carried out and the manuscript written by myself with guidance and advise on the topic provided by the co-authors.

Some passages have been quoted verbatim from these sources.

Signed: _____ Date: _____

nessa golden B.A
National University of Ireland, Galway

ABSTRACT

Soil pollution has been identified as the third most important threat to soil quality in Europe. There are an estimated ~2,000 potentially contaminated sites in Ireland alone. Metal contamination has been identified as one of the most common types of soil contamination. Urban soils are particularly susceptible to metal contamination as they are subjected to constant inputs of anthropogenic origin. This thesis describes cost and time saving methodological approaches involving the use of magnetic susceptibility (MS) measurements and spatial analysis techniques which can be applied in the preliminary and exploratory phases of site assessment of suspected metal contamination in urban topsoils.

The first study describes a methodological approach to the investigation of metal contamination of bonfire affected soils in a residential green space. Measurements of low frequency mass specific magnetic susceptibility (χlf) were recorded from the soil samples collected from a high density 1 x 1 m^2 grid. Local Moran's I hotspot analysis maps were produced for χlf and elemental concentrations of the soil samples. At this density, localized variations in susceptibility signals were distinguishable using the hotspot analysis technique to reveal statistically significant high value clusters where the most recent bonfire presided. Potential locations of historic bonfires were also identified. This application was shown to be effective, even when physical evidence on site was not obvious.

At a second site, two methodological-based studies were conducted on the use of volume magnetic susceptibility measurements in the identification of metal contamination in topsoil. The study area was a former unregulated landfill site and is currently used as a local amenity park.

The geostatistical analysis technique of ordinary cokriging (CK) was applied to the lead and volume magnetic susceptibility (κ) data collected to explore the use of this method in efficiently estimating the spatial distribution of lead present at the site. The objective was to improve spatial interpolation for lead using the auxiliary information of κ which could be more easily collected. The results were compared to ordinary kriging (OK) estimates of Pb concentrations. Root mean square errors (RMSE) and coefficients of

determination (R^2) signified a marked improvement in estimation capability of the CK procedure, demonstrating the efficiency of this method in an exploratory site investigation of this nature.

In addition to site assessments, practical experiments were conducted to aid others in investigations of this kind. The effects of grass cover on in-situ volume MS (κ) measurements of urban soils was also investigated at the former unregulated landfill site. The results suggested that the removal of grass coverage prior to obtaining in-situ κ measurements of urban soil is unnecessary. This layer does not impede the MS sensor from accurately measuring elevated κ in soils (in typical urban green spaces with low vegetation cover <10 cm), and therefore κ measurements recorded with grass coverage present can be reliably used to identify areas of urban soil metal contamination. During the examination of bonfire soils a small experiment was carried out to isolate what temperature the soils directly below the base of the bonfire ash likely reached and it was determined they likely reached a maximum of 300°C and at this temperature had minimal impact on the MS signal of the soils.

The methods of investigation detailed in this thesis can easily be adapted and applied in the inspection of suspected illegal burning or municipal waste disposal sites by local governing bodies charged with containing this issue.

ACKNOWLEDGEMENTS

I wish to thank my family, my mother, Mary, my two sisters, Aoife and Ciara and my late father, Michael for all their support during my studies. Thank you for always being there at the end of the phone, the trips away and for all the lifts! I owe you all a great deal of gratitude. My mother especially for her patience and financial support in the last year. My boyfriend, Barry has also been there for many years of my PhD. Thank you for all your support, advice, the proof-reading, the list goes on. I sincerely wish to thank them all. I know I could not have reached the final stage without them.

I would like to express my deep gratitude to Dr. Liam Morrison, my supervisor, for his patience, guidance and encouragement – including many, many pep talks as I reached my submission date. There was a time I thought I would not make it to this point, and I am eternally grateful to Dr. Morrison for stepping in as my supervisor, which empowered me to continue with my studies. I would like to express my very great appreciation to my GRC committee, in particular Dr. Aaron Potito, for constructive suggestions during planning and development of my research work and for regularly checking in to see how things were going. I would also like to thank Dr. Paul Gibson for providing me with an introduction to magnetic susceptibility techniques and demonstrating how to use the equipment.

I wish to extend a huge thank you to Dr. Siúbhan Comer. Whether I needed assistance with fieldwork or paperwork, Siúbhan was always so helpful and generous with her time. I also greatly appreciate assistance provided by Joe Fenwick, for demonstrating how to use the fluxgate gradiometer and for assisting me with fieldwork and the loan of equipment from the Discipline of Archaeology (MS2 meter and MS2D field probe, GPS and a fluxgate gradiometer).

And my peers and now good friends from Geography and the Ryan Institute. I wish to thank them for all the laughs and commiserations and everything that goes along with PhD life.

DEDICATION

In loving memory of my father,

Michael Golden R.I.P.

1. GENERAL INTRODUCTION

1.1. Background

Soil is an essential non-renewable resource, which performs many vital functions and ecosystem services including food production, buffering, carbon storage and filtration, all of which are of paramount environmental as well as socio-economic importance (Bullock & Gregory, 1990). Soil is, however, increasingly degrading. The remnants of past industrial activities in the form of derelict and contaminated land is a prevalent global soil issue (Rodriguez-Eugenio et al., 2018). Soil pollution has been identified as the third most important threat to soil functioning in Europe (FAO & ITSP, 2015). Metals have been reported as one of the most common types of soil contaminants (EEA, 2010) with an estimated > 5 million sites affected worldwide (Antoniadis et al., 2019). Soils of urbanized regions are particularly susceptible to metal contamination as they are subjected to constant inputs from anthropogenic sources, e.g. waste disposal, infill, mixing, construction, and atmospheric deposition (Alloway, 2013). Since urban expansion, soil has been used as a sink for the dumping of waste materials. In the past, waste buried *out of sight* in soils was not considered a potential threat to human health or environmental systems (Rodriguez-Eugenio et al. 2018). Until recent decades little attention was paid to the condition of urban soils or regulations issued for its protection (Bullock & Gregory, 2009). As a result, there are a conservatively estimated 22 million hectares of the world's soil affected by pollution (Oldeman, 1991 cited in Rodriguez-Eugenio et al. 2018). This thesis highlights time and cost saving methodological approaches (discussed in chapters 2, 3 & 4) involving the use of MS and spatial analysis techniques which can be applied in the preliminary and exploratory phases of investigation when soils are suspected of being contaminated with excess levels of potentially toxic elements.

Potentially contaminated sites are defined as areas of land suspected of containing elevated levels of metals and other possible contaminants in levels exceeding background values or not naturally present. In the context of this thesis, it mainly refers to sections of urban green spaces where metal contamination of anthropogenic origin is suspected in (at least) the superficial layers of soils.

1.2. Urban soils

Urban environments consist of a variety of green spaces including gardens, allotments, parks and playing fields, utilized as various recreational amenities. These spaces are an integral part of urban life and often individuals' only link to the natural environment. In Ireland, almost two-thirds of the population lived in urbanized areas in 2016 (CSO, 2017) and in 2018, 55% of the world's population lived in urban areas, which is projected to increase to 68% by 2050 (UN, 2018). For many years, little attention was paid to past activities on these parcels of land and the potential implications for future use. Few restraints were placed on industry and householders up until the latter half of the twentieth century in order to prevent contamination of soil. The emergence of related health problems drew attention to the importance of soil quality, the need for greater understanding, and for its protection. In recent decades, there has been increasing interest in examining the composition of these soils (Bullock & Gregory, 2009), often in the pursuit of identifying the potential threats they may pose. The genesis of urban soils can differ greatly from natural and agricultural systems; soils of urban areas represent a wide spectrum in terms of composition and development and can comprise of a wider range of materials than rural areas. Frequently, they may not present the classic vertical stratification or even the mineralogical and chemical composition found in natural or some agricultural soils (Argyraki & Kelepertzis, 2014). In addition to the typical silt, sand, clay and organic matter content, urban and suburban soils are subject to mixing, filling and contamination with metals, herbicides and pesticides (Thornton, 2009), and can contain materials such as building debris, buried wastes on disposal sites, bottom ashes and residues from industrial processes (Bullock and Gregory, 2009; Alloway, 2013).

1.3. Metal contamination in urban soils

Soil contamination refers to the presence in the soil of a chemical or substance out of place/present in higher concentrations than background values but not necessarily causing harm (Rodriguez-Eugenio et al., 2018). Since the industrial revolution, urban soils have been subject to contamination. The history of land use can be difficult to ascertain, as records of prior industrial

use or waste disposal are frequently poor or unknown (Thornton, 2009). Due to this legacy, the damage caused cannot always be attributed to guilty parties and the origin and type of contamination known. There may not even be any obvious visible evidence of contamination (Rodriguez-Eugenio et al., 2018). These conditions often relate to metal contaminated sites. Urban soils are generally contaminated with Pb, Zn, Cd, and Cu from traffic, paint and many other non-specific sources (Alloway, 2013, p.11). In particular, Pb, Cd and Zn are characteristic urban trace element contaminants (Alloway, 2013, p.35). Anthropogenic metal signatures in soils can persist for many decades after termination of source emissions due to the long residence times of metals in soils (Alloway, 2013, p.11; Argyraki & Kelepertzis, 2014). Concentrations of metals or elements of concern are often found in higher concentrations in urban soils in comparison to agricultural and rural soils (Alloway, 2013, p.35).

A common form of contamination in urban areas is point-source contamination (Rodriguez-Eugenio et al., 2018), which can occur as a once-off or series of events where contaminants are released into soils of a particular area and source(s) are identifiable. The bonfire site and former unregulated landfill sites investigated in this thesis are examples of point-source contamination. When a single point-source is not present, there may be many possible causes of soil contamination in urban soils including: deposition of dust and aerosols form industrial and vehicular emissions; corrosion of metal structures; technogenic materials incorporated into soils; contaminants from former land use (agricultural); fertilizers and composts used in urban gardens; deposition of waste onto soils; paints and other decorative materials and accidental fires (Alloway, 2013, p. 36).

It is important that potentially metal contaminated sites in urban areas are assessed in order to maintain a healthy environment; from a socio-environmental perspective, it benefits local residents and promotes tourism (Norra & Stüben, 2003). Elevated metals/metalloids in urban soils are an indication of inputs from anthropogenic sources such as atmospheric aerosols, which may affect human health through inhalation. Once absorbed into soils, elevated trace elements of concern can affect human health via direct

ingestion from unwashed hands, vegetables or pica behaviors; by inhalation and through intake of edible vegetation (Alloway, 2013, p.36).

Some geochemical surveys of urban soils have been conducted on the island of Ireland including a survey of Galway City (Zhang, 2006); Dublin City (Glennon et al., 2014) and Belfast City (McIlwaine et al., 2017). A consensus was found on the main anthropogenic *potentially toxic elements* (PTEs) present in these cities (Pb, Zn, Cu and As). Of particular concern are levels of Pb and As. Arsenic is a metalloid which in very small concentrations appears to be essential to animals and beneficial to plants (Alloway, 2013, p.242). However, arsenic is a class I carcinogen (IARC, 2012) and of particular concern when present in the form of As(III) (Niazi et al., 2018 cited in Antoniadis et al., 2019). The chronic toxicological effects of As are well recognized and have been exploited since ancient times (Alloway, 2013, p.242). In the late 20^{th} century, arsenic received global attention due to As-poisoning from contaminated drinking and irrigation groundwater supplies in many parts of the world (McGrory et al., 2017). When of anthropogenic origin in soils, lead is speciated into easily absorbed manganese and iron hydroxide and carbonate soil fractions (Teutsch et al., 2001) and to soil organic matter (Emmanuel and Erel, 2002; Sierra et al., 2010). Naturally occurring Pb is mostly found in the residual fractions which are considered non-bioavailable (Lee et al., 1997). Serious health hazards, particularly to young children, result from the inhalation of air-borne lead through the lungs, e.g. indoor leaded dust (Hunt et al., 2006), and absorption of lead through the gut, e.g. ingesting foods with high lead content (Chłopecka et al., 1996). Lead can also be absorbed via dermal contact, e.g. playing in urban soils (Holmes et al., 1999) and dusts (Yiin et al., 2000). Both the bonfire (chapter 2) and former landfill site (chapter 3 & 4) investigated in this study contained elevated levels of Pb, Cu and Zn. Iron, Cu and Zn play an essential role in plant development hence their maximum allowable intakes are orders of magnitude higher than elements with no known biological function like Pb, As and Hg (Antoniadis et al., 2019). However, at critical levels these elements can cause negative health impacts and as a result are considered PTEs.

1.4. EU legislation pertaining to potentially contaminated soil site assessment

At the European or national level in Ireland, there is currently no Soil Framework Directive in place for the protection of soil; the EU proposal was withdrawn in 2014. The strategy behind the former proposed framework was to implement a common policy for the protection of soil and remediation of contaminated land within the EU member states which would include the integration of soil related concerns into other policies, prevention of major threats to soils and lessening their impacts as well as the restoration of degraded soils (COM(2006)231). There are other policies such as 'Urban Wastewater Treatment Directive (UWWTD) 91/271/EEC' (1991), 'Dangerous Substances Directive (DSD) 67/548/EEC' (1967), 'Directive on Pesticides 2009/128/EC' (2009), 'Water Framework Directive (WFD) 2000/60/EC'(2000), 'Groundwater Directive (GWD) 2006/118/EC' (2006) and Directive on Industrial Emissions (IED) 2010/75/EU' (2010) which provided partial and incomplete protection to soils, but in indirect ways (COM(2006)232). The 7th Environmental Action Programme has stated that one of its main objectives was to "*protect, conserve and enhance the union's natural capital".* It provided that "*by 2020, land is managed sustainably in the Union, soil is adequately protected, and the remediation of contaminated sites is well underway*" (7th Environmental Action Programme, 2013). Although the development of newly contaminated areas is being inhibited by current policies, the legacy of historic contamination is a prevalent issue. The number of *potentially contaminated sites* in the EU is currently unknown, though it is estimate that there are around 2.5 m across the whole of Europe, with an estimated 340,000 expected to be *contaminated sites* of which 33% have been identified and 15% have been remediated (Van Liedekerke et al. 2014). The European Commission estimate the number of potentially contaminated sites in Ireland at 2,400 with possibly 200 contaminated (IPA, 2006). The proposed Directive on Soil Protection and Remediation of Contaminated Land (withdrawn in May 2014) highlighted the potential cost of preliminary site investigation at €1,300 - €4,900 (IPA, 2006). Based on these estimates, the cost of investigation at the preliminary stage alone in Ireland could potentially cost millions of euros. Aside from the financial

implications to site investigations, there is a compelling need for these sites to be assessed, even at the preliminary/exploratory stages of investigation, in order for potentially hazardous sites to be pinpointed for main site investigations and managed as necessary. In terms of progress in the management of contaminated sites in Ireland, there are defined targets for main site investigations and a national inventory of contaminated sites has been compiled. The main sources of soil contamination reported by Ireland are oil spills from transport operations, industrial and commercial activities (30%), waste disposal and treatment (13%) and storage (oil/chemical) (1%) (Van Liedekerke et al. 2014).

The EU-funded Environmental Assessment of Soil for Monitoring (ENVASSO Project (2006-08)) was commissioned with the objective of defining and documenting a soil monitoring system at the continental level for the protection of soil and was implemented to support the Soil Framework Directive (Huber et al. 2008). The projects involved the development of a soil database management system, compiling data on soil quality indicators, e.g. metal concentrations, and existing inventories and monitoring programs in place in member states. The project provides recommendations on procedures and protocols for selecting and monitoring sites and carrying out sampling and analytical procedures, with the aim of establishing a harmonized methodology for the comparison of monitored sites (Huber et al., 2008) which can easily be integrated into any site investigation.

1.5. Magnetic susceptibility measurements

Magnetic susceptibility (MS) is a measure of how magnetizable a material is. Soil is made up of many minerals of varying magnetic attraction. If a sample is ground to a fine fraction, a magnet passing over the sample will attract magnetic particles present like magnetite while particles of other minerals like quartz will not demonstrate any attraction. Thus, MS measurements can be used to tell us about the minerals (in particular, iron-bearing minerals) present in substances like rocks, sediments and soils. The magnetic susceptibility of a sample is approximately proportional to the mass of minerals present that have an attraction to a magnet. Minerals are affected by magnetism as a result of inherent forces created by electrons in the atoms of the minerals. The way

the electrons align determines the magnetic moment of the atoms. Therefore, the magnetic behaviour of a material is dependent on the arrangements and interactions of all the electrons and atoms present in the various minerals and other substances making up the material (Dearing, 1999).

Different minerals exhibit different magnetic behaviours dependent on their composition, e.g. water displays a diamagnetic behaviour and measures weak or negative susceptibility values. Ferromagnetism results in stronger magnetic signal than diamagnetism or paramagnetism and are not normally found freely in nature with the exception of ores. Minerals like magnetite in soils would produce a ferrimagnetic response with elevated MS values (Gibson and George, 2004, p.93). In theory, the magnetic susceptibility of a sample can be predicted based on the sum of all the magnetic susceptibility of minerals and materials making up the sample. Magnetite is a ferrimagnetic iron oxide found in virtually all environments. In the absence of ferromagnetic materials, the susceptibility of a material is controlled by its ferrimagnetic iron oxide content (Dearing, 1999). Four factors control magnetic susceptibility – mineral concentration, composition, crystal size and shape. In terms of crystal size, ferrimagnetic grains are made up of different regions of magnetization known as domains. The number of domains in a grain is related to the size of the crystal. Grains >110 μm tend to be multidomain (MD) grains which contain domains of equal magnetization (Dearing, 1999). In small grain sizes, single domain (SD) grains of <0.2 μm contain no domain walls and magnetic moments are strongly constrained to lie in particular directions, resulting in limited susceptibility (Liu et al., 2012). Pseudo-single domain grains (PSD) range between 0.2 – 110 μm and have the capability to contain more domains but act like SD grains. Ultra-fine superparamagnetic (SP) grains <0.03 μm are SD but are not constrained and result in a strong susceptibility (Liu et al., 2012).

A Bartington dual-frequency susceptibility meter was used to acquire magnetic susceptibility measurements. When an AC current produced by the MS2 meter passes through the wire coil of an attached sensor (MS2B, MS2D), this generates a weak magnetic field. The MS of a material is ascertained by comparing the magnetic permeability of air with the magnetic permeability of a material placed in the magnetic field. The magnetic

permeability of air is considered a constant with a very low ability to create internal fields. The MS2 meter reads the frequency values for air permeability and a sample permeability and uses these values to calculate the change in inductance of the wire coil or the magnetic permeability (Bartington® Instruments, 2016). Magnetic susceptibility is then calculated by the meter using the following equation from Bartington® Instruments (2016):

$$\mu_0 \chi_{vol} = \mu - \mu_0 \quad [1]$$

Where '$\mu_0\chi_{vol}$' refers to the volume magnetic susceptibility of a sample; 'μ' and 'μ_0' refer to the permeability of the sample and free space, respectively.

Field-based measurements of volume magnetic susceptibility (κ) are related to the top ~10 cm of the surface, in the shape of a toroid, obtained using the MS2D sensor and are measured in 10^{-5} SI units. Laboratory-based mass specific magnetic susceptibility (χ) are obtained using 10 cm^3 containers to house the samples (which must be packed to capacity) and a MS2B sensor. Values are calculated by the equipment by dividing κ of a sample by the density; measurements are taken in units of $m^3 kg^{-1}$ (Evans and Heller, 2003). Changing the operating frequency of the instrument when measuring mass specific magnetic susceptibility can assist in the identification of SD grains of <0.03 μm diameter that exhibit superparamagnetic behaviour. Bartington MS2 meters have two oscillations frequencies – low frequency (χlf) operates at ~460kHz and high frequency (χhf) operates at ~4,600 kHz (Oldfield, 1991). By switching to χhf, this causes the magnetization of materials containing very fine grain sizes near the SD/SP domain boundary to be blocked, when the frequency becomes similar to the relaxation frequency of the grains (Evans and Heller, 2003). High χfd% of 10-14% are estimated to be mainly SP grains (>75% of total measured) whereas χfd% of <2.0% are estimated to contain virtually no SP grains (Dearing, 1999). Frequency dependence % was computed by the equipment using the following equation:

Bartington® Instruments (2016):

$$fd\% = 100 \times \left(\frac{\chi lf - \chi hf}{\chi lf}\right) \quad [2]$$

Magnetic susceptibility has far reaching applications in environmental science. It can be used in the identification of magnetic minerals and used to calculate their total volume in a sample, in a similar way to other mineralogical techniques like x-ray diffraction (Dearing, 1999). MS can be used to classify different materials (Dearing, 1999) e.g. an exposed patch of limestone rock would have a much lower volume susceptibility value than a bare patch of basalt rock. It can also be used in the identification of the processes of Fe-bearing mineral formation (Dearing, 1999). In chapter 2, this application of MS is explored in the investigation of heat effects on mass specific susceptibility measurements of bonfire affected soils. It can also be used as a proxy of related environmental parameters (Dearing, 1999), examples of this can be seen in chapters 2, 3 and 4.

The measurements are ideal in reconnaissance studies where a large number of samples are needed in finding the average or typical values rather than having to obtain expensive or time-consuming analysis (Dearing, 1999). In recent times, studies have been conducted demonstrating the relationship between magnetic susceptibility and anthropogenically sourced elemental concentrations in soils (Heller et al., 1998; Jordanova et al. 2003; Blaha et al., 2008). Significant correlations between mass specific magnetic susceptibility (χ) and metals have been found in soils affected by metallurgic fly-ash deposition: Heller et al. (1998) found correlations of $r = 0.83$ and $r = 0.63$ between χ and Pb and Zn, respectively, in surface soils in the vicinity of coal-burning power plants in the Upper Silesian region, Poland. Significant relationships between χ and metals Pb and Cu ($r = 0.69$ and $r = 0.71$) were observed in suburban soils (Sofia, Bulgaria) near a metallurgic plant identified as the main source of pollution in the area (Jordanova et al. 2003). Additionally, Blaha et al. (2008) found highly correlated values of χ and metals Pb and Zn in contaminated surface forest soils near a steel mill (Loeben, Austria) with correlations of $r = 0.98$ and $r = 0.97$, respectively. Urban topsoils have also been analysed for their geochemical and magnetic susceptibility measurements, in an attempt to discern the level of environmental pollution in a region. Measurements of road-side topsoils of Beni Mellal City, Morocco, shared a highly positive correlation coefficient between χ and Pb ($r^2 = 0.93$); Cu ($r^2 = 0.70$) and Zn ($r^2 = 0.68$) (El Baghdadi

et al., 2012). The relationship between χ and metals was investigated using topsoil measurements collected from public parks and green strips along road-sides within Isfahan City, Iran, in determining the efficiency of magnetometry as a proxy for assessing heavy metal pollution of soils. Again, a strong correlation was found between χlf and elements Pb (r = 0.72) and Zn (r = 0.61) (Karimi et al., 2011). Further examples of studies demonstrating this strong correlation in anthropogenically influenced soils can be seen in chapters 2, 3 and 4.

As the magnetic susceptibility measurements obtained pertained to the magnetization of materials at the top ~10 cm layer of soil, a gradiometry survey was also conducted on a small section of the former landfill site featured in chapter 3 and 4 to investigate the presence of buried waste at the subsurface level. A fluxgate gradiometer was employed in this study which provides the gradient (or quantity measured by magnetic locators in land surveys) of a magnetic field (Schlinger, 1990). The presence of lateral variation in magnetic properties in the subsurface results in lateral variation in the magnetic field at the surface of the earth and this variation can be a result of voids or magnetic materials in the subsurface which can reduce or increase signals, respectively in relation to the background magnetic field value and these variations are known as anomalous values (Schlinger, 1990).

1.6. Spatial analysis

Spatial analysis is an umbrella term which covers a range of techniques and methods for analyzing events in geographical space. One example of exploratory spatial analysis is the identification of local patterns of spatial association (LISA). This technique was developed by Anselin (1995) and can be applied in the identification of clusters of non-stationarity in a study area, and can also be used to identify individual outliers. From each observation, a local indicator of spatial association is calculated as well as an associated z-score and p-value which indicates the level of significance of the local Moran's I value. A positive I value indicates neighbouring observations have a similarly high/low value and a negative I indicates neighbouring values are not similar and that the observation could be an outlier (Mitchell, 2005). Local

Moran's I is used to investigate the correlation between a sample and it's neighbouring samples and as such it is a form of autocorrelation analysis. This technique applied in chapter 2 and 3 was beneficial in the investigation of bonfire affected topsoils by metal contamination and magnetic susceptibility. Other examples of its use in previous studies are included in this chapter.

Interpolation techniques use measured sample point values at different locations within a landscape to predict a continuous surface of that measurement (or in some instances a related measurement). This can include any form of spatial data including landscape, subsurface and atmosphere like rainfall levels, population, soil organic carbon (%), elevation, soil properties such as metal concentration or gravel content (%). Interpolation techniques rely on the similarity of nearby samples to create a surface (Johnston et al., 2001). Two types of interpolation techniques have been applied in this thesis - deterministic and geostatistical.

The deterministic method of Inverse Distance Weighting (IDW) is based on surrounding points and uses a mathematical function to determine the smoothness of a continuous surface (Johnston et al., 2001). An arbitrary number of samples or distance radius is chosen which vary with the distribution and amount of points available and characteristics of the site of interest. Examples of the effective application of this technique can be seen in chapters 2 & 3.

Geostatistics is based on the Theory of Regionalized Variables, where a phenomena can be characterized by the distribution in space of a set of measured quantities known as regionalized variables (Journel, 2004). The interpolation is based on a stochastic process which accounts for various trends in the data including anisotropies and correlation with distance, in the prediction of unknown values (Geostatistics, p.69). Geostatistics is a class of statistics used to analyze and predict values of phenomena with spatial or spatio-temporal associations. Many geostatistical techniques have been developed to describe spatial patterns and interpolate values at unsampled locations (ESRI, 2018) including kriging. Geostatistical models can provide a measure of the level of uncertainty in predictions made; unlike deterministic models which are based on mathematical functions and do not share this function. Kriging is a weighted moving average technique which uses a

system of linear regressions and prior knowledge of the spatial dependence of the data to make predictions at unknown locations in creating a continuous surface (Fortin and Dale, 2008). It is known as a best linear unbiased predictor on point and block data because it minimizes errors and its predictions are unbiased (Oliver and Webster, 2015). Like IDW, the closest known values have the greatest influence, however the weights calculated in kriging procedures are dependent on the arrangement of sample points nearby and the semivariogram developed, which is based on the spatial structure of the data (Johnston et al., 2001). Kriging is a well-established application of geostatistics; it was developed by D.G. Krige in the 1950's for the estimation of gold ore reserves. Georges Matheron further developed the method by deriving formulas and establishing the field of linear geostatistics (Hengl, 2009). Ordinary kriging is the most commonly applied method of kriging however there are many advanced types developed for specific tasks (Oliver and Webster, 2015). Ordinary cokriging can be applied in the prediction of a continuous surface of a target variable when a co-variable is available which is significantly correlated with the target variable and is cheaper to measure or has been more densely sampled (Rossiter, 2007). In chapter 4, the techniques of Ordinary Kriging and Ordinary Cokriging have been applied in the estimation of Pb contamination in topsoils and both techniques are discussed in further detail.

1.7. Scope and objectives of this study

In terms of this thesis, the focus has predominantly been to provide a guidance for the investigation of potentially metal contaminated soils in urban environments using magnetic susceptibility and spatial analysis techniques.

The standard methodology to evaluate the degree of pollution present at a site involves the collection and chemical analysis of samples. This is a necessary practice; however, this study outlines procedures which can be followed by others to efficiently identify and map the spatial structure of metal contaminants in urban soils. These procedures involve the innovative combination of spatial analysis techniques including geostatistical applications and magnetic susceptibility data, which can greatly reduce costs and labour involved in a site assessment by reducing the number of soil samples needed traditionally, to carry out a comprehensive assessment.

The main objectives of this thesis were:

- to confirm the presence of anthropogenically influenced metals in these urban soils and provide high quality spatial distribution maps
- demonstrate how useful MS measurements can be in metal contaminated urban soil studies
- demonstrate the applicability of spatial analysis techniques (e.g. LISA and interpolation techniques) with MS measurements when investigating metal contaminated urban soils.
- to apply procedures which can be implemented by others to reduce costs and labour involved in the assessment of metal contaminated soils

At the bonfire site examined in chapter 2, the aims of this study were to determine the extent of influence of a bonfire on soils by investigating the spatial distribution of elevated metals present and the low frequency mass specific magnetic susceptibility (χlf) measurements of the soil samples collected on a high density grid (1 x 1 m^2). To further quantify the spatial patterns of contamination present at the site, local Moran's I hotspot analysis or LISA was used to identify outliers and spatial clusters of each of the metals and χlf. The relationships between χlf and metals were also examined to

explore the possibility of using χlf readings as a surrogate for the assessment of metal contamination in a bonfire site. The objectives of this study were to demonstrate χlf measurements can be used in discerning the presence and extent of burnt materials in surface soils and spatial distribution techniques like hotspot analysis, can be used to display the statistically significant outliers or high value clusters of environmental parameters.

In chapter 3, the aims of the study were to evaluate the use of field-based volume magnetic susceptibility (κ) measurements by: (1) investigating whether grass coverage impacts the reliability of κ as an indicator of metal contamination in urban soils; (2) evaluating κ as a proxy for metal contamination in soil by comparing spatial distribution maps of κ and metals. In addition, field-based κ spatial distributions were also compared to laboratory-based χlf. The novel objective of this study was to ascertain whether it was necessary to remove vegetation prior to κ measurement.

The aim of chapter 4 was to apply the interpolation technique CK with κ measurement for the mapping of anthropogenic lead loadings in urban soils. The objective was to evaluate the robustness of the procedure in comparison to OK using efficiency and error estimates. The findings could be applied to assist in reducing the costs and labour involved in the investigation of Pb contaminated or polluted urban topsoils.

Although I am referring to urban soils in this thesis, these techniques are also applicable to industrial, agricultural or soils containing naturally elevated metal concentrations, where appropriate. The scope of this project was limited to the investigation of surficial layers (0-10 cm) of *potentially contaminated sites* (PCS) with metals of concern. This is the most environmentally relevant soil layer in terms of risks posed to humans as there are many potential exposure pathways from contaminated surface soils. Further examination and additional analysis would be required for main site investigations, risk assessments or decisions relating to remediation.

1.8. General methodological approach

Fig. 1.1. *Location of study sites in Galway city, Ireland: inset a) investigated bonfire site located in a residential green space; (b) a former landfill site, presently used as a recreational park.*

The purpose of this thesis was to demonstrate techniques involving magnetic susceptibility which could be applied in the identification of metal contamination in urban topsoil (Main Aims and Objectives are outlined in Section 1.7: Scope of Thesis). For this purpose, two sites were selected as suitable case study sites within the vicinity of Galway City, Ireland (see Fig. 1.1.). The study featured in Chapter 2 is based on a bonfire site located in a residential green space and chapters 3 & 4 are both based on conditions found at a recreational park. This thesis follows a papers-based format and consists of three papers which are detailed in chapters 2, 3 and 4. Due to this thesis format there is some repetition among sections of these papers.

1.8.1. Preliminary investigations:

A regional geochemical survey was conducted by Zhang (2006). In this sampling campaign, sampling points were collected from the Inishannagh Park residential area and from South Park recreational park. At Inishannagh park, a hotspot of arsenic was detected. On visual inspection of the green

space, it was evident a section was being used for the illegal burning of municipal wastes.

Fig. 1.2. *Remains of a bonfire in the residential green space. [Image source: Personal files].*

At South Park, elevated levels of As, Pb, Cu and Zn were found by Zhang (2006). The site was formally known colloquially as 'The Swamp' and was used for many years as an illegal landfill. Subsequent studies have been conducted on the site, confirming the level of contamination present (Carr et al. 2008; Dao et al. 2013). A visual site investigation also confirmed the presence of reddish soils in the western section of the park.

1.8.2. Exploratory investigations:

A site-specific conceptual model of assessment was devised based on the main aims & objectives of this thesis.

At the bonfire site, Inishannagh Park, hypotheses were formulated on:

- the presence of other potential metal contaminants (other than As mg kg^{-1}) and associated enhanced magnetic susceptibility signals
- whether hotspot analysis could be used to identify the lateral extent of bonfire affected topsoils using χlf measurements
- what temperature the soil beneath a bonfire is subjected to
- whether the burnt materials were causing an enhancement of magnetic susceptibility in affected topsoils

At the former unregulated landfill site, South Park, hypotheses were formulated on whether:

a)

- anthropogenically enhanced magnetic susceptibility measurements of the topsoil were detectable
- MS measurements were correlated with metal contaminants present in the topsoil
- grass height has a significant effect on in-situ κ measurements of underlying urban topsoils

b)

- ordinary cokriging with MS measurements can be successfully applied in the prediction of the spatial distribution of Pb in topsoils
- CK of contaminated Pb using MS could 'outperform' OK of Pb contamination in urban topsoils

1.8.3. Methodological Workflow:

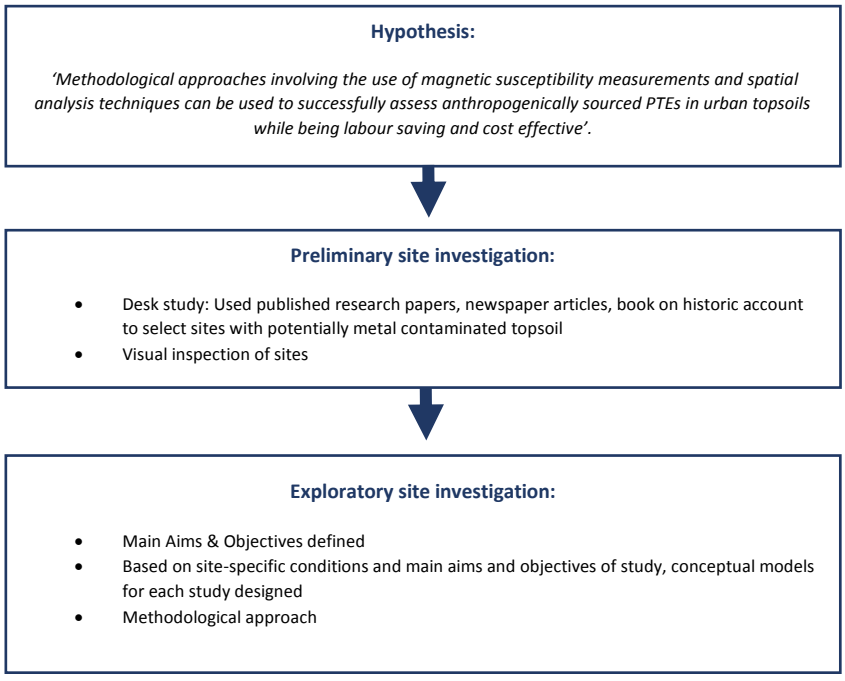

Chapter 1.

1.9. References

Alloway, Brian J. (2013). *Heavy Metals in Soils*. Dordrecht: Springer Netherlands.

Antoniadis, V., Shaheen, S.M., Levizou, E., Shahid, M., Khan Niazi, N., Vithanage, M., Sik Ok, Y., Bolan, N. and Rinklebe, J. (2019). 'A critical prospective analysis of the potential toxicity of trace element regulation limits in soils worldwide: Are they protective concerning health risk assessment? – A review'. *Environment International,* 127, pp. 819 – 847.

Anselin, L. (1995). 'Local Indicators of Spatial Association – LISA'. *Geographical Analysis*, 27(2), pp. 93-115.

Argyraki, A. & Kelepertzis, E. (2014). 'Urban soil geochemistry in Athens, Greece: The importance of local geology in controlling the distribution of potentially harmful trace elements'. *Science of the Total Environment*, 482-483(1), pp. 366–377.

Bartington Instruments (2016). *Operating Manuals for MS2 Magnetic Susceptibility System*. OM0408.

Blaha, U., Appel, E. & Stanjek, H. (2008). 'Determination of anthropogenic boundary depth in industrially polluted soil and semi-quantification of heavy metal loads using magnetic susceptibility'. *Environmental Pollution*, 156, pp. 278-289.

Bullock, P. & Gregory, P.J. (1991). *Soils in the Urban Environment*.1st edn. Oxford: Blackwell Scientific Publications.

Bullock, P. & Gregory, P.J. (2009). Soils: A Neglected Resource in Urban Areas, in *Soils in the Urban Environment*. 2nd edn. Oxford: Wiley Blackwell, pp. 1–4.

Carr, R., Zhang, C. and Moles, N. and Harder, M. (2008). 'Identification and mapping of heavy metal pollution in soils of a sports ground in Galway City, Ireland, using a portable XRF analyser and GIS'. *Environ Geochem Health* ,30, pp. 45–52.

Chłopecka, A. (1996). 'Assessment of form of Cd, Zn and Pb in contaminated calcareous and gleyed soils in southwest Poland'. *Science of The Total Environment*, 188 (2-3), pp. 253-262.

Commission Decision No. 1386/2013/EU (7th Environmental Action Programme), 2013 O.J. L 354/171.

Communication from the Commission to the Council, the European Parliament, the European Economic and Social Committee and the Committee of the Regions - Thematic Strategy for Soil Protection [SEC(2006)620] [SEC(2006)1165]

Creamer, R.E., Brennan, F., Fenton, O., Healy, M.G., Lalor, S.T.J., Lanigan, G.J., Regan, J.T. and Griffiths, B.S. (2010). 'Implications of the proposed Soil Framework Directive on Agricultural Systems in Atlantic Europe – a Review', *Soil Use and Management*, 26, pp. 198-211.

(CSO) Central Statistics Office (2017). *Profile 2 – Population and Distribution Movements*.https://www.cso.ie/px/pxeirestat/Statire/SelectVarVal/Define.asp?MainTable=E2004&TabStrip=Select&PLanguage=0&FF=1 (Accessed on 28.04.2019)

Dao, L., Morrison, L., Kiely, G. and Zhang, C. (2013). 'Spatial distribution of potentially bioavailable metals in surface soils of a contaminated sports ground in Galway, Ireland'. *Environ Geochem Hlth*, 35, pp. 227-238.

Dearing, J. (1999). *Environmental Magnetic Susceptibility. Using the Bartington MS2 System*. 2nd edn. Kenilworth, UK: Chi Publishing.

(EEA) European Environmental Agency (2010). *The European Environment – state and outlook 2010: synthesis*. European Environmental Agency, Copenhagen. Luxembourg: Publications Office of the European Union.

El Baghdadi, M., Barakat, A., Sajieddine, M. and Nadem, S. (2012). 'Heavy metal pollution and soil magnetic susceptibility in urban soil of Beni Mellal City (Morocco)'. *Environ. Earth Sci*., 66, pp. 141-155.

Emmanuel, S. and Erel, Y. (2002). 'Implications from concentrations and isotopic data for Pb partitioning processes in soils'. *Geochimica et Cosmochimica Acta*, 66(14), pp. 2517–2527.

Chapter 1.

ESRI (2018). *What is geostatistics?* http://desktop.arcgis.com/en/arcmap/latest/extensions/geostatistical-analyst/what-is-geostatistics-.htm (Accessed on 12.06.2019).

Evans, M. and Heller, F. (2003). *Environmental Magnetism: Principals and Applications of Enviromagnetics*. San Diego, California, USA: Academic Press.

FAO and ITPS (2015). *Status of the World's Soil Resources (SWSR) – Main Report*. Rome, Italy, Food and Agricultural Organization of the United Nations and the Intergovernmental Technical Panel on Soils. http://www.fao.org/3/a-i5I99e.pdf (Accessed on 28.04.2019)

Fortin, M.J. and Dale, M. (2008). Spatial Analysis of Sample Data, in *Spatial Analysis – A guide for Ecologists.* Cambridge, UK: University Press, pp.111-174.

Geostatistics – A Handful of the Theory of Regionalized Variables. https://shodhganga.inflibnet.ac.in/bitstream/10603/52562/13/13_chapter%204.pdf (Accessed on 12.06.2019).

Gibson, P.J. & George, D.M. (2004). Magnetic Geophysical Techniques, in *Environmental Applications of Geophysical Surveying Techniques*. Hauppauge, New York: Nova Science Publishers, pp. 85-124.

Glennon, M.M., Harris, P., Ottesan, R.T., Scanlon, R.P. and O'Connor, P.J. (2014). 'The Dublin SURGE Project: geochemical baseline for heavy metals in topsoil and spatial correlation with historical industry in Dublin, Ireland'. *Environ Geochem Health*, 36, pp.235-254.

Heller, F., Strzyszcz, Z. and Magiera, T. (1998). 'Magnetic record of industrial pollution in forest soils of Upper Silesia, Poland'. *Journal of Geophysical Research*, 103(B8), pp. 17,767-17,774.

Hengl, T. (2009). A Practical Guide to Geostatistical Mapping. JRC Scientific and Technical Reports, 2nd edn. Luxembourg: Office for Official Publication of the European Communities, Luxembourg.

Holmes, Jr., K.K., Shirai, J.H., Richter, K.Y. and Kissel, J.C. (1999). 'Field measurement of Dermal Soil Loadings in Occupational and Recreational Activities'. *Environmental Research Section A*, 80, pp. 148-157.

Huber, S., Prokop, G., Arrouays, D., Banko, G., Bispo, A., Jones, R.J.A., Kibblewhite, M.G., Lexer, W., Möller, A., Rickson, R.J., Shishkov, T., Stephens, M., Toth, G., Van den Akker, J.J.H., Varallyay, G., Verheijen, F.G.A and Jones A.R. (eds) (2008). *Environmental Assessment of Soil for Monitoring Volume I: Indicators & Criteria*. Luxembourg: Office for Official Publications of the European Communities.

Hunt, A., Johnson, D.L. and Griffith, D.A. (2006). 'Mass transfer of soil indoors by track-in on footwear'. *Science of The Total Environment*, 370, pp. 360-371.

(IARC) International Agency for Research on Cancer (2012). *Arsenic and Arsenic Compounds. Arsenic, Metals, Fibres and Dusts*. Lyon, International Agency for Research on Cancer (IARC Monographs on the Evaluation of Carcinogenic Risks to Humans, vol. 100) https://monographs.iarc.fr/wp-content/uploads/2018/06/mono100C-6.pdf (Accessed on 11.06.2019).

(IPA) Institute of Public Administration (2006). EU Policy Review. Analysis of recent legislation and policy for local and regional government. Number 5/06 – Aug-Sept 2006.

Johnston, K., ver Hoef, J.M., Krivoruchko, K. and Lucas, N. (2001) *Using ArcGIS™ Geostatistical Analyst - GIS by ESRI™*. Redlands, California: ESRI.

Johnson, C. and Ander, E.L. (2008). 'Urban geochemical mapping studies: how and why we do them'. *Environ Geochem Health*, 30, pp. 511–530.

Johnston, K., ver Hoef, J.M., Krivoruchko, K. and Lucas, N. (2001). *Using ArcGIS™ Geostatistical Analyst - GIS by ESRI™*. Redlands, California: ESRI.

Chapter 1.

Jordanova, N.V., Jordanova, D.V., Veneva, L., Yorova, K. and Petrovsky, E. (2003) Magnetic Response of Soils and Vegetation to Heavy Metal Pollution – A Case Study'. *Envir. Sci. Technol*., 37, pp. 4417-4424.

Journel, A.G. (2004). 'Geostatistics'. *Encyclopaedia of Statistical Sciences*. https://onlinelibrary.wiley.com/doi/full/10.1002/0471667196.ess0882 (Accessed on 12.06.2019).

Kapička, A., Petrovský, E., Ustjak, S. & Macháčková, K. (1999). 'Proxy mapping of fly-ash pollution of soils around a coal-burning power plant: a case study in the Czech Republic'. *Journal of Geochemical Exploration*, 66, pp.291-297.

Karimi, R., Ayoubi, S., Jalalian, A., Sheikh-Hosseini, A.R. and Afyuni, M. (2011). 'Relationship between magnetic susceptibility and heavy metals in urban topsoils in the arid region of Isfahan, central Iran'. *Journal of Applied Geophysics*, 74, pp. 1-7.

Lee, P.K., Touray, J.C., Baillif, P. and Ildefonse, J.P. (1997). 'Heavy metal contamination of settling particles in a retention pond along the A-71 motorway in Sologne, France'. *Science of the Total Environment*, 201, pp. 1-15.

Liu, Q., Roberts, A.P., Larrasoaña, J.C., Banerjee, S.K., Guyodo, Y., Tauxe, L. and Oldfield, F. (2012). 'Environmental Magnetism: Principals and Applications'. *Reviews of Geophysics*, 50, RG4002, pp. 1-50.

Lloyd, C.D. (2011). *Local Models for Spatial Analysis*. 2nd edn. Boca Raton, Fl: CRC Press.

McGrory, E.R., Brown, C., Bargary, N., Hunter Williams, N., Mannix, A., Zhang, C., Henry, T., Daly, E., Nicholas, S., Petrunic, B.M., Lee, M. and Morrison, L. (2017). 'Arsenic contamination of drinking water in Ireland: A spatial analysis of occurrence and potential risk'. *The Science of The Total Environment.*, 579, pp.1863–1875.

McIlwaine, R., Doherty, R., Cox, S.F. and Cave, M. (2017). 'The relationship between historical development and potentially toxic element concentrations in urban soils'. *Environmental Pollution*, 220, pp. 1036-1049.

Mitchell, A. (2005). *The ESRI Guide to GIS Analysis*, Vol. 2. Redlands, California: ESRI Press.

Niazi, N.K., Bibi, I., Shahid, M., Ok, Y.S., Burton, E.D., Wang, H., et al. (2018). 'Arsenic removal by perilla leaf biochar in aqueous solutions and groundwater: An integrated spectroscopic and microscopic examination. *Environmental Pollution*, 232, pp.31 – 41.

Norra, S. & Stüben, D. (2003). 'Urban soils'. *Journal of Soils and Sediments*, 3(4), pp.230–233.

Oldeman, L.R. **(**1991). *World map on status of human-induced soil degradation*. Nairobi, Kenya: Wageningen, Netherlands, UNEP; ISRIC.

Olea, R.A. (2009). *A Practical Primer on Geostatistics*. United States Geological Survey. Reston, Virginia. 2009.

Oliver, B.A. and Webster, R. (2015). Chapter 4: Geostatistical Prediction: Kriging, in *Basic Steps in Geostatistics: The Variogram and Kriging*. Cham, Switzerland: Springer, pp. 43-70.

Proposal for a Directive of the European Parliament and of the Council establishing a framework for the protection of soil and amending Directive 2004/35/EC, COM(06) 232, final.

Rodriguez-Eugenio, N., McLaughlin, M. and Pennock, D. (2018). *Soil Pollution: a hidden reality*. Rome, Food and Agricultural Organisation of the United Nations. 142 pp.

Rossiter, D.G. (2007). *Technical note: co-kriging with the gstat package of the R environment for statistical computing*, 2nd edn. International Institute for Geo-information Science & Earth Observation (ITC), Enschede, Netherlands.

Schlinger, C.M. (1990). 'Magnetometer and Gradiometer Surveys for Detection of Underground Storage Tanks'. *Bulletin of the Association of Engineering Geologists*, 17(1), pp. 37-50.

Sierra, C., Gallego, J.R., Afif, E., Menéndez-Aguado, J.M., Gonzálaz-Coto, F. (2010). 'Analysis of soil washing effectiveness to remediate a brownfield polluted with pyrite ashes'. *Journal of Hazardous Materials*, 180, pp. 602-608.

Chapter 1.

Teutsch, N., Erel, Y., Halicz, L. and Banin, A. (2001). 'Distribution of natural and anthropogenic lead in Mediterranean soils'. *Geochimica et Cosmochimica Acta*, 65(17), pp. 2853–2864.

Thornton, I., (2009). 'Metal contamination of soils in urban areas', in Bullock P. and Gregory P.J. (eds.) *Soils in the urban environment*. Oxford: Wiley Blackwell, pp. 47-75.

(UN) United Nations Department of Economic and Social Affairs Population Division, (2018). *World Urbanization Prospects: the 2018 Revision*. https://www.un.org/development/desa/en/news/population/2018-revision-of-world-urbanization-prospects.html (Accessed on 29.04.2019).

Van Liedekerke, M., Prokop, G., Rabl-Berger, S., Kibblewhite, M. and Louwagie, G. European Commission (2014). *Progress in the management of Contaminated Sites in Europe*. Luxembourg: Publications Office of the European Union.

Yiin, L.M., Rhoads, G.G. and Lioy, P.J. (2000). 'Seasonal influences on childhood lead exposure'. *Environmental Health Perspectives*, 108(2), pp. 177-182.

Zhang, C. (2006). 'Using multivariate analyses and GIS to identify pollutants and their spatial patterns in urban soils in Galway, Ireland'. *Environmental Pollution*, 142, pp.501-511.

Chapter 2.

2. SPATIAL PATTERNS OF METAL CONTAMINATION AND MAGNETIC SUSCEPTIBILITY OF SOILS AT AN URBAN BONFIRE SITE

This paper has been published in the journal of *Applied Geochemistry*, 52, pp. 86-96 (November, 2015).

Chapter 2:

SPATIAL PATTERNS OF METAL CONTAMINATION AND MAGNETIC SUSCEPTIBILITY OF SOILS AT AN URBAN BONFIRE SITE

1.2. Abstract

Bonfires are a major pollution source in urban soils. In this study, a total of 379 soil samples were collected from a traditional bonfire site on a 1×1 m^2 grid system and analysed for total metal concentration and low frequency magnetic susceptibility (χlf). High resolution maps of the spatial distribution of Cu, Fe, Mn, Pb, Sr, Ti, Zn and χlf were created and a significant relationship between each of the metals and χlf was revealed. Elevated levels of each metal were observed, indicating the site may pose a significant health hazard. The spatial patterns were generally consistent, encompassing the position of bonfires. The spatial extent of influence of bonfires was estimated at approximately 10 meters, in line with the extent of bonfire materials. The results of this study indicate the importance of metal contamination associated with bonfires in urban soils.

2.2. Introduction

The need for precise measurements of environmental pollution is increasing due to the adverse exposure effects of elevated concentrations of pollutants on human health and the environment. Bonfires are outdoor fires used in rituals and celebrations. Traditionally, non-hazardous wastes such as wood, straw and bones were used as kindling (Gailey and Adams, 1977). However, modern bonfire sites include less traditional items, such as materials of technogenic origin, municipal wastes such as electrical appliances, tyres and plastics (Dao et al., 2012). Bonfires are sources of CO, particulates, NO2, SO2, PAHs, dioxins, organic compounds and toxic metals (DEFRA, 2006). Previous studies revealed high levels of PAH and dioxin emissions in residential areas during bonfire season (Butterfield and Brown, 2012; DEFRA, 2006). Domestic solid fuel burning is a particular problem as it releases PAHs close to the ground level in areas of high population density, where their impact on the maximum recorded ground level concentration can be up to 100 times greater than the same mass of PAH emitted by an industrial process through a tall chimney stack (DEFRA, 2006). Dioxin concentrations were found to increase 30 fold (21-25 - 720 TEQ/m 3) at one bonfire site (DEFRA, 2006). Very few studies have investigated the potential contribution of metals from bonfires to the environment. High levels of Cu, Pb and Zn were reported at a bonfire site in a residential area in Galway, Ireland, demonstrating the uncontrolled burning of metal-bearing materials leading to metal accumulation in soils (Dao et al., 2012).

The use of magnetic parameters in the identification of pollution sources has become a widespread practice as a reliable, efficient and sensitive method for evaluating polluted sites (Blaha et al., 2008; Jordanova et al., 2003; Magiera et al., 2008; Wang and Qin, 2005). Anthropogenic pollution has a strong magnetic signature, in particular a strong correlation was observed between magnetic susceptibility (MS) and metal concentrations in the upper layers of soils and sediments (Chan et al., 2001; El Baghdadi et al., 2012). Although the determination of total metal concentrations is a routine analysis, soil magnetic measurements can provide valuable reference information in pollution studies (Blaha et al., 2008; Jordanova et al., 2003; Lu et al., 2012;

Magiera et al., 2008; Morton-Bermea et al., 2009; Wang and Qin, 2005; Strzyszcz and Magiera, 1998). It is now well established that by-products of incineration can possess a significant mineral magnetic component (Lu et al., 2012; Sapkota and Cioppa, 2012; Strzyszcz and Magiera, 1998).

Many studies have documented the correlation between magnetic properties and metal concentration in urban soils (El Baghdadi et al., 2012; Gudadhe et al., 2012; Lu and Bai, 2006; Lu et al., 2008; Wang and Qin, 2005), sediments (Botsou et al., 2011; Canbay et al., 2010;; Frančišković-Bilinski et al. 2014), dust (Zhang et al., 2012; Zhu et al., 2012, 2013) and paleoclimatology studies (Alekseeva et al., 2007; Blundell et al., 2009; Maher et al., 2002a, 2003b; Maher and Hallam, 2005). These investigations have highlighted the use of magnetic parameters as a proxy in the detection and mapping of metal contaminated areas. MS mapping of soils and sediments has become one of the most important tools for estimating anthropogenic pollution (Yang et al., 2012) and has been widely used in mapping metal contamination in many countries (Hanesch and Scholger, 2002; Zawadzki and Fabijańczyk, 2008).

MS may be used as an initial step for further investigations at regional, national, international scales and as a result of its compatibility with routine chemical analysis, it can be considered a simple, rapid, non-destructive proxy tool for mapping metal pollution (D'Emilio et al., 2012). However, due to large variations of the reference signal as a result of soil processes and other natural conditions such as bedrock lithology, the reliability of magnetic mapping still remains a challenge in unpolluted or relatively unpolluted soils (Kapička et al. 2003).

In geospatial terms, the index of local Moran's I is a useful tool in the identification of statistically significant pollution hotspots in urban soils and for classifying them into spatial clusters and outliers. Although other methods can help in the identification of spatial patterns, in pollution studies it is important that areas of high/low values in comparison to the surrounding area are identified, and local Moran's I examines the individual locations, enabling hotspots to be identified based on a comparison with the neighbouring samples. It has been applied successfully in various fields, including ecology (Sokal et al., 1998a, 1998b), geochemistry (Li et al., 2014; Zhang et al., 2008), crime (Levine, 2006), disease (McCullagh, 2006) and mortality rates (Zhang

and Lin, 2007). Early methods of local indicators of spatial autocorrelation (LISA) statistics were developed for geographical areas, such as municipal divisions (Anselin, 1995; Getis and Ord, 1992; Ord and Getis, 1995). However, more contemporary work has focused on point patterns, possibly driven by the need to identify crime patterns and disease outbreaks (McCullagh, 2006). Point patterns allow for more precision in analysis of hotspot identification (Jacquez, 1996).

In the present study, Local Moran's I has been applied to an annual bonfire site, and utilized to trace the locations and effects of past bonfires. Bonfire sites offer an ideal case study as spatial influences tend to be localised, e.g. extreme and immediate shifts in values are present within small areas, requiring high resolution mapping.

The aims of the present study included the investigation of the spatial distribution of metals (Cu, Fe, Mn, Pb, Sr, Ti, Zn) and low frequency mass specific magnetic susceptibility (χlf) in order to determine the spatial range of influences of a bonfire. To further quantify the spatial patterns of contamination present at the site, local Moran's I hotspot analysis was used to identify pollution hotspots, outliers and spatial clusters of each of the metals and χlf. The relationships between χlf and metals were also examined to explore the possibility of using χlf readings as a surrogate for the assessment of metal contamination in a bonfire site. In addition, laboratory based experiments examined the effects of temperature on the magnetic properties of soil.

2.3. Materials and Methods

2.3.1. Study area and Sampling grid

The study focused on a bonfire site located on a 380 m^2 residential and green area in Galway City (53° 16' 44 N, - 9° 04' 48 E), Ireland (Fig. 2.2.). A systematic sampling grid comprised of 379 points was employed using a 1 x 1 m^2 grid system (Fig. 2.1.). The location was selected in accordance with the position of known past bonfires, still visible on the surface of the topsoil (Fig. 2.2.).

The extent of the sampling boundary was based on the central position of the current bonfire site and the limitation of the range of the green area in order to investigate the influence of the burning of metallic materials on the metal concentration and MS of soil in close proximity to a bonfire. The sampling grid was laid using measuring tapes and plastic sticks as markers (Fig 2.3(a)) and the locations were recorded using a portable global positioning system (GPS) Trimble GeoExplorer ®.

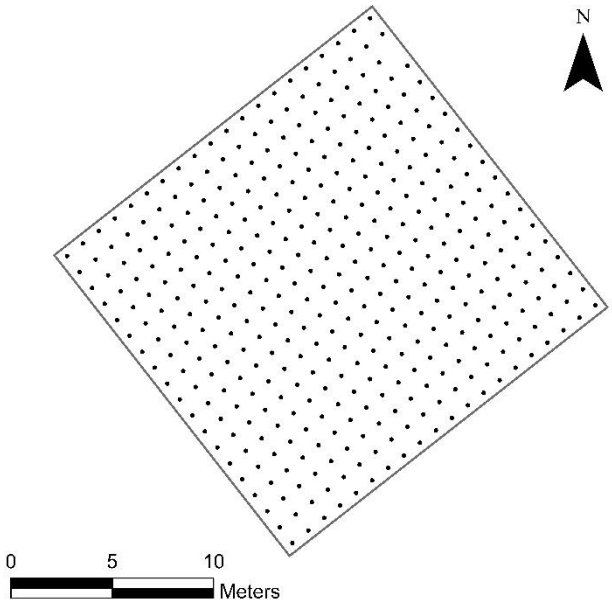

Fig. 2.1. *Sampling grid (1 x 1 m^2) featuring 379 sampling points*

Fig. 2.2. *Map of study area, Inishannagh Park, Galway, Ireland with previously known bonfire locations highlighted. (Image: Bing Aerial Map (© 2013 Microsoft Corporation) captured March 2012). Inset: Google™ Earth historical images, featuring past bonfires: 2005, 2007, 2008 and © OSi MapGenie ITM 2010 series, featuring 2010 bonfire.*

2.3.2. Sample collection and preparation

Soil samples were obtained using a stainless steel auger, which was cleaned in between samples and the first sub-sample at each point was discarded to avoid cross contamination (Fig. 2.3(b)). Five representative sub-samples (0 – 10 cm in depth (Dao et al. 2012)), one from the center point and four from the four quadrants of the 1 m ^{2} area of each point (Fig. 2.3(c)), were taken and combined to make one composite sample representing each point on the grid. Soil samples were stored in clean polythene bags, dried at room temperature (~ 20 °C) and gently disaggregated using a mortar and pestle and sieved (< 2 mm fraction).

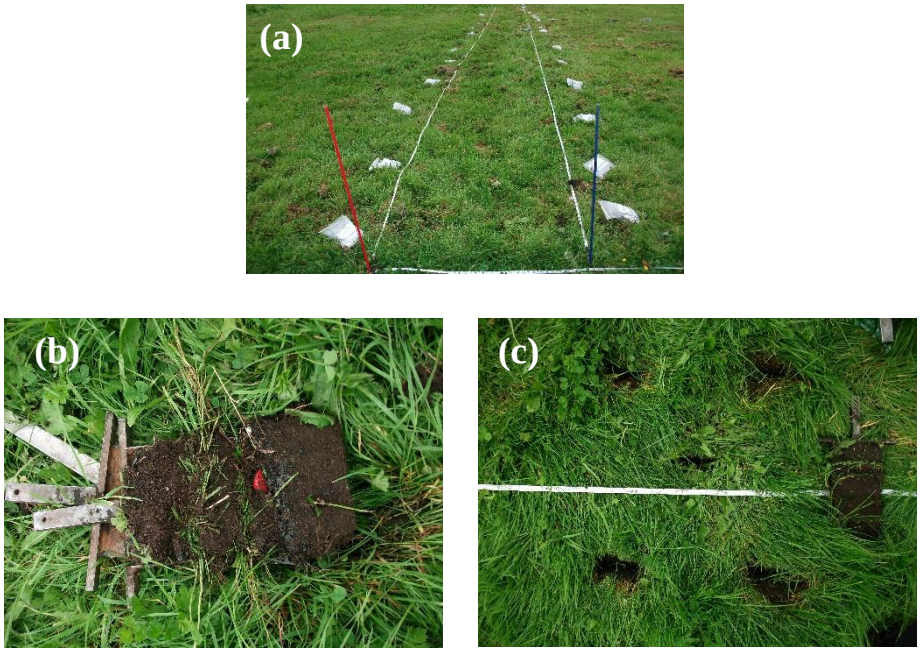

Fig. 2.3. *Sampling: a) Sampling grid (1 x 1 m^2); b) Sample taken using soil auger; c) Example of 5 subsample locations per sampling point*

2.3.3. Determination of total element concentration

A portable X-ray fluorescence analyser (PXRF, ©Innov-X Systems, Inc.) was employed to determine total metal concentrations of prepared composite soil samples. PXRF is a non-destructive method of investigating potentially contaminated sites which can rapidly provide in-situ laboratory quality soil/sediment chemistry of a range of metals including As, Ba, Cd, Co, Cr, Cu, Fe, Hg, K, Mn, Pb, Sr, Ti, Zn (Innov-X Systems, Inc., 2005).

A subset of the total number of samples collected (n=50) were analyzed via Inductively Coupled Plasma-Optical Emissions Spectroscopy (ICP-OES). "*ICP-OES is a trace level elemental analysis technique that uses the emission spectra of a sample to identify and quantify elements present*" (Lucideon.com, 2019). Samples were digested in preparation for analysis using a four-acid digestion procedure. The milled samples of 0.2 g were digested using 10 ml HF, 5 ml $HClO_4$, 2.5 ml HCl, and 2.5 ml HNO_3, dissolved in 20% *aqua regia* and made up to 10 ml for ICP-OES analysis of chemical elements.

2.3.4. Magnetic susceptibility measurements

Magnetic susceptibility measurements were carried out in the laboratory using a magnetic susceptibility 2 meter (©Bartington Instruments Ltd.) with a MS2B sensor attached (Fig. 2.4.), which generates a weak magnetic field from alternating currents (AC) and detects the magnetisation of the sample in response to the magnetic field. Magnetic susceptibility measured using the MS2B sensor is the ratio of the strength of the magnetisation (A m^{-1}) to a magnetic field of ~80 A m^{-1} and is expressed in SI units (Dearing, 1999). Mass specific magnetic susceptibility (χ) was calculated for the soil samples with units of 10^{-8} m^3 kg^{-1}. MS at low (0.46 kHz) frequency was measured and computed using Multisus v2.44 software for Windows (©Bartington Instruments Ltd.). The measurements are used to detect the presence of ultrafine (<0.03 μm) superparamagnetic ferromagnetic minerals occurring as crystals, produced largely by biochemical processes in soil.

The integrity of instrumental performance and calibration of the magnetic susceptibility sensor was ascertained through the use of a SRM calibration sample (supplied by ©Bartington Instruments Ltd.). The sample was reassessed throughout the measurement process. To verify the integrity of the values obtained, all samples were measured on the higher sensitivity range of 0.1 to assure weaker samples were measured as true to their real values as possible. At this range, small increments of instrumental drift between readings are more prominent and have to be corrected. To compensate for drift in measurements, air readings are taken before and after each measurement and the average subtracted. If there are significant differences between air readings, then the meter should be zeroed and the measurement retaken.

2.3.5. Impact of temperature on magnetic susceptibility

As bonfires will inevitably affect soil temperatures, an experiment was performed to investigate the impacts of bonfires on soil temperatures and associated influences on soil magnetic susceptibility at the study site. Soil (3 kg) was collected from the outer regions of the study area (away from the potential influence of bonfires), homogenised, sieved to < 2 mm fraction and

ground to a finer fraction using a laboratory disc mill (N.V. TEMA, Model T- 100 A).

Fig. 2.4. *Magnetic susceptibility 2 meter (©Bartington Instruments Ltd.) with a MS2B sensor attached.*

Smaller aliquots were measured and heated using a VWR DRY-Line, Model DL 115 (≤ 267 ˚C) and Nabertherm Laboratory furnace, Model LA 11/ 11 230 v (≤ 3000 ˚C). Individual aliquots were weighed using a Sartorius TE64 analytic balance (accurate to 0.0001 g), and heated to various temperatures: 50 °C; 100 ˚C; 150 ˚C; 200 ˚C; 300 ˚C; 400 ˚C; 500 ˚C; 600 ˚C; 700 ˚C; 800 ˚C; 900 ˚C; 1000 ˚C for 1, 2 and 4 hour intervals (n = 3 samples per test). After heating, the aliquots were reweighed and the loss of mass on ignition (LOI) was recorded. Three aliquots were retained in their unheated condition as control samples. A sample was also removed from beneath the ashes of a bonfire at the site (the following morning after a bonfire in 2012) for comparative purposes. The colours of soil samples were recorded using the Munsell Soil Colour Charts (Oyama and Takehara, 1967) after each burn, or in the case of the controls, prior to burning. The Munsell System records colour by hue, value and chroma, providing a standardized system of describing or quantifying colours (Shipman et al. 1984). A follow up experiment to determine remaining organic content (% mass) within the bonfire sample and among samples of similar colouration (100 ˚C, 150 ˚C; 200 ˚C; 300 ˚C; 400 ˚C) was carried out to clarify colouration similarities.

These samples were heated to 550 ˚C for two hours to burn off remaining organic content, and percentage mass loss for each sample was recorded.

Fig. 2.5*. Example of individual aliquots heated to different temperatures, resulting in visible changes in soil colour*

2.3.6. Quality control

For total metal concentration, soil certified reference materials (CRMs) (Montana I (2710a), Montana II (2711a) and San Joaquin (2709a)) from the National Institute of Standards and Technology, USA (NIST) were incorporated to ensure the validity of the PXRF technique. These CRMs have been developed for use in method development, method validation and routine quality assurance in the analysis of major, minor and trace element concentration of soils (Mackey et al., 2010).

2.3.7. Data analysis and statistics

Statistical analysis was carried out using SPSS 20 (IBM®SPSS® Statistics). The bonfire experiment graph was created using Sigmaplot® v 12.2 (©Systat Software Inc.). Spatial analysis was performed within a Geographical Information System (ESRI® ArcGIS® ArcMap™ 10) with the incorporation of satellite imagery from Ordnance Survey Ireland, MapGenie and Bing Aerial Maps. Local Moran's I cluster/outlier maps were produced using GeoDa™1.4.6. (Anselin et al. 2006) and magnetic measurements were computed using ©Bartington Instruments Ltd. Multisus v2.44 software.

2.4. Results

2.4.1. Quality Assurance

Table 2.1. *Recovery of metals (Cu, Fe, Mn, Pb, Sr, Ti, Zn) in three soil certified reference materials (Montana I, Montana II and San Joaquin, National Institute of Standards and Technology, USA) (n = 3)*

	SRM 2710a (Montana I)			SRM 2711a (Montana II)			SRM 2709a (San Joaquin)		
	[a] Cert.	[b] Meas.	[c] Rev. (%)	[a] Cert.	[b] Meas.	[c] Rev. (%)	[a] Cert.	[b] Meas.	[c] Rev. (%)
Cu	3420 ± 50	3231 ± 43	**94.4**	140 ± 2	124.3 ± 8	**88.7**	33.9 ± 0.5	36 ± 5	**106.1**
Fe	4.32 ± 0.08	4.59 ± 0.04	**106.2**	2.82 ± 0.04	2.4 ± 0.02	**85.1**	3.36 ± 0.07	3.05 ± 0.02	**90.8**
Mn	2140 ± 60	2821 ± 87	**131.8**	675 ± 18	703 ± 43	**96**	529 ± 18	554.8 ± 41	**104.9**
Pb	5520 ± 30	6521.6 ± 68	**118.1**	1400 ± 10	1610 ± 17	**115**	17.3 ± 0.1	16.3 ± 3	**94.3**
Sr	246.6 ± 7	253.6 ± 4	**102.8**	242 ± 10	233 ± 4	**96.2**	239 ± 6	234.6 ± 3	**98.1**
Ti	3310 ± 70	3766.6 ± 4	**113.7**	3170 ± 80	3033. 3 ± 3	**95.6**	3360 ± 70	3200 ± 3	**95.2**
Zn	4180 ± 20	4142.2 ± 48.4	**99.1**	414 ± 11	363 ± 9.2	**87.7**	103 ± 4	84.8 ± 5	**82.3**

[a] Cert. abbreviation for *certified reference value* of CRM; [b] Meas. abbreviation for *measured value* obtained; [c] Rev. (%) abbreviation for *recovery (%)* obtained of certified value

Three soil CRMs were analysed using the PXRF and the results were compared to certified values for Cu, Fe, Mn, Pb, Sr, Ti and Zn (Table 2.1.). PXRF systems are designed to provide reliable analysis of priority pollutant metals and other elements in soils (Innov-X Systems, Inc., 2005) and the results obtained highlight the efficiency of PXRF performance with good recoveries (Table 2.1.). One exception was the % recovery of Mn in 2710a. This CRM contains Mn at higher concentration than observed in 2709a, 2711a or the bonfire affected soils. In this CRM, variations in concentrations of other elements may be affecting the x-ray intensity of Mn and causing

enhancement, these occurrences are known as matrix effects (Kalnicky and Singhvi, 2001). In particular, QA provided high precision values for SRM2709a, depicting the suitability of the PXRF technique for the determination of total metal concentrations in the soil samples (Dao et al., 2012). Another confirmation of the validity of the PXRF technique is evident in Fig. 2.6., which shows the values obtained for total element concentration using the PXRF technique correlated well with values obtained via ICP-OES analysis. The error of the laboratory measurements of mass-specific magnetic susceptibility was found to be an acceptable level of < 15 % (recovery 85.92 %).

2.4.2. Basic statistics

Descriptive statistics for the raw data of the 7 elements determined by PXRF and χlf are summarized in Table 2.2. (n = 379). All elemental concentrations are above detection limits. A high degree of variation is visible, depicting the complexity of soil geochemistry across such a small area e.g. the minimum value of Zn (124 mg kg^{-1}) differs by several magnitudes to the maximum value (21,681 mg kg^{-1}). This may be due to the burning of Zinc oxide, which is used in tyres, paints, rubbers, cosmetics, plastics, inks, soap, batteries, pharmaceuticals and many other products (Barceloux, 1999b). Although elements such as Zn and Cu are bio-essential, these metals are potentially toxic at high levels (Barceloux, 1999a; 1999b). To obtain a better understanding of the degree of pollution present, a comparison between the median values obtained in this study and those previously published for the local Galway region (Zhang, 2006), national soil surveys (Zhang et al. 2008) and bonfire affected soils, located in Galway City (Dao et al. 2012) are presented in Table 2.3., demonstrating the elevated values present at this bonfire site. χlf also depicts high deviation from minimum to maximum values. The median χlf value of this study (125.2 x 10^{-8} m^3 kg^{-1}) were comparable to other contaminated urban soils, e.g. 107 x 10^{-8} m^3 kg^{-1} in Xuzhou, China (Wang and Qin, 2005) and 68 x 10^{-8} m^3 kg^{-1} in the coastal region of Izmit Gulf and Izaytas, Turkey (Canbay et al., 2010).

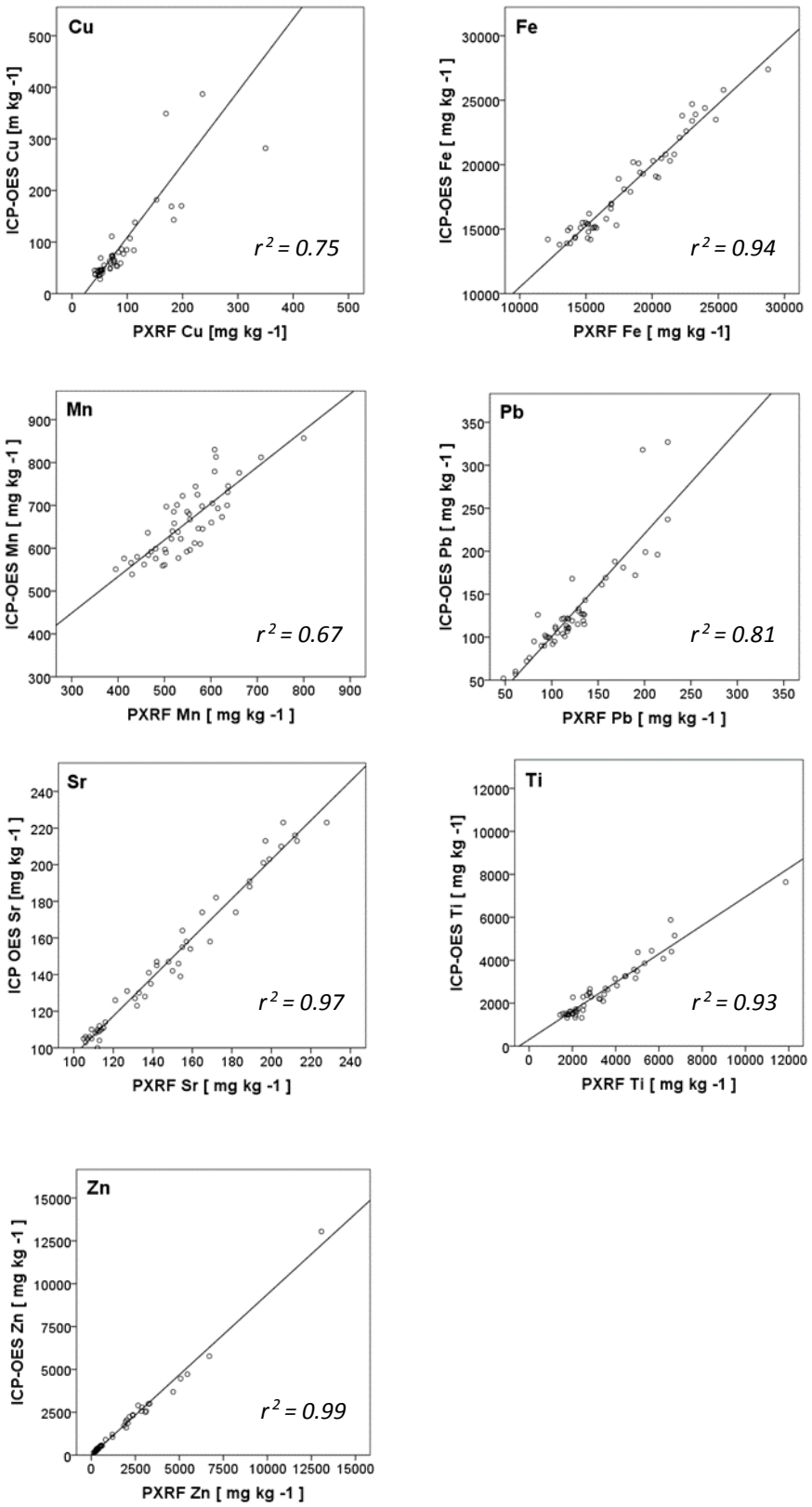

Fig. 2.6. *Comparison between total metal concentrations analysed using ICP-OES and PXRF (mg kg $^{-1}$)*

Table 2.2. *Descriptive statistics for total content of metals (mg kg $^{-1}$) analysed by PXRF and χlf (10 $^{-8}$ m ^{3} kg $^{-1}$)*

Element	Cu	Fe	Mn	Pb	Sr	Ti	Zn	χlf
Min	30	12122	377	34	95	1434	124	75.2
25%	51	14622	482	96	117	1994	315	109.9
Median	68	16256	532	114	140	2606	561	125.2
75%	95	19817	585	137	166	3955	1693	151
Max	1117	37724	964	985	2922	25510	21681	371.2
Mean	95.79	17471.2	538.7	134.54	162.39	3517.69	1354.74	139.5
SD	102.75	3687.93	84.17	98.78	162.67	2559.36	2015.95	46.4
Skewness[1]	5.33	1.26	0.96	5.2	13.65	3.29	4.55	1.9
Kurtosis[2]	37.78	2.09	2.47	33.47	222.29	17.3	32.66	4.27
K-S *p*	0	0	0.15	0	0	0	0	0

[1] Std. error of Skewness 0.13. [2] Std. error Kurtosis 0.25.

Table 2.3. *Comparison between median values of element concentrations in Galway soils (mg kg $^{-1}$) (Fe in %)*

Element	This study	Bonfire affected soils [a]	Galway region soils [a]	National soil survey (Ireland) [a]
Cu	68	19.1	27	16.2
Fe	1.62	1.12	1.7	1.87
Mn	532	384	539	462
Pb	114	42.1	58	24.8
Sr	140	-	114	49.7
Ti	2606	1495	1623	2133
Zn	561	93.4	85	62.6

[a] Data sources: Median values (mg kg $^{-1}$) (Fe in %) of bonfire affected soils (Dao et al. 2012); local Galway region soils (Zhang 2006); National soil survey, Ireland (Zhang et al. 2008).

2.4.3. Relationship between metals and χlf in soils

Laboratory experiments showed that high temperatures can potentially have a large impact on soil χlf, especially at temperatures above 400 - 500 °C (Fig. 2.7.). A plateauing effect emerges at first from 'Control' to 400 °C, after which we see a dramatic increase at 500 °C as χlf values continue to rise up to 800 °C, followed by a sharp decline from 900 - 1000 °C (carbon dioxide is evolved from carbonate at 900 - 1000 °C, possibly accounting for this loss).

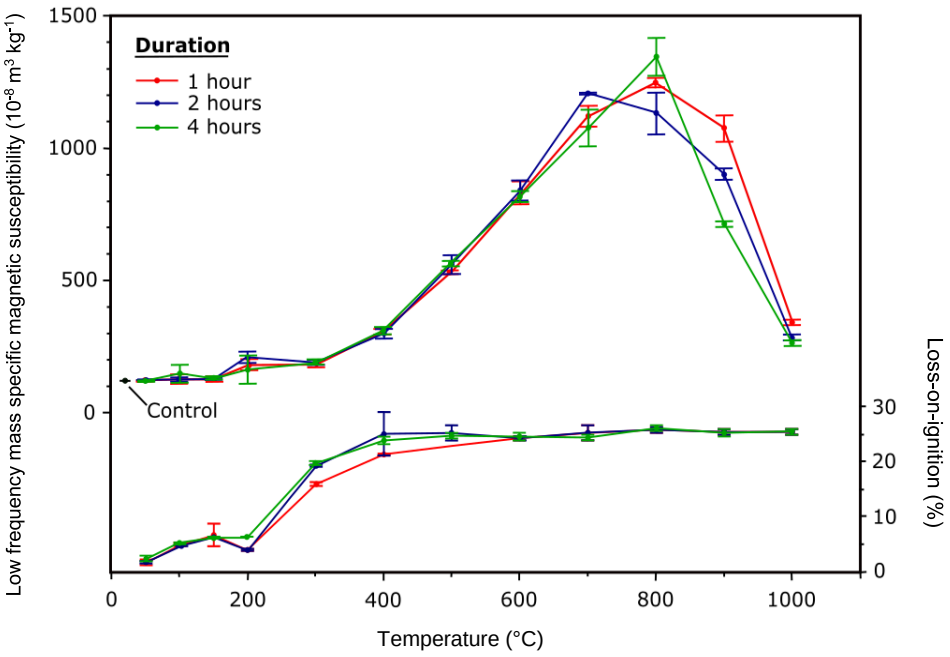

Fig. 2.7. *Relationship between χlf at different temperature intervals [n = 3 per temp] and Loss-On-Ignition (%) (Error bars = 1 st. dev.)*

These changes in χlf are not closely followed by LOI, showing that loss in moisture and organic content are likely not driving χlf values. χlf and LOI responses appear to be almost instantaneous, with longer intervals of heat exposure showing little to no added effect over the one-hour intervals in the experiment. However, a soil sample from beneath a 2012 bonfire site showed only slightly elevated χlf values, similar to aliquots burned at 200 - 300 °C. The soil beneath the 2012 bonfire site also exhibited discolouration similar to aliquots burned at 300 °C (Fig. 2.8.). Follow-up analysis to determine remaining organic content in similarly coloured samples was used to confirm the colour and LOI-inferred temperatures. The bonfire sample showed 11.0 % mass loss in the second burn, which was comparable to samples heated to 200 °C and 300 °C (10.5 % and 10.2 % mass loss, respectively), greater than samples heated to 100 °C and 150 °C (23.8 % and 22.9 % mass loss, respectively) and less than samples heated to 400 °C (3.0 % mass loss).The results of these experiments thus indicate that bonfires are likely to only raise soil temperatures to a maximum of 300 °C, and the associated effects of heat from bonfires on soil χlf are minimal. However, metals are significantly correlated with χlf, with Pearson's correlation coefficients (all significant at

$p < 0.01$) of (ln)χlf and elements (ln)Cu (0.558), (ln)Fe (0.527), (ln)Mn (0.368), (ln)Pb (0.332), (ln)Sr (0.471), (ln)Ti (0.567), (ln)Zn (0.615), following a test for normality and necessary data transformation (with details shown in the following sections). These relationships are illustrated using scatterplots in Fig. 2.9. The burning of metal laden objects in the bonfire, rather than the heating of the soil itself, would thus account for the majority of the effects on χlf in bonfire soils.

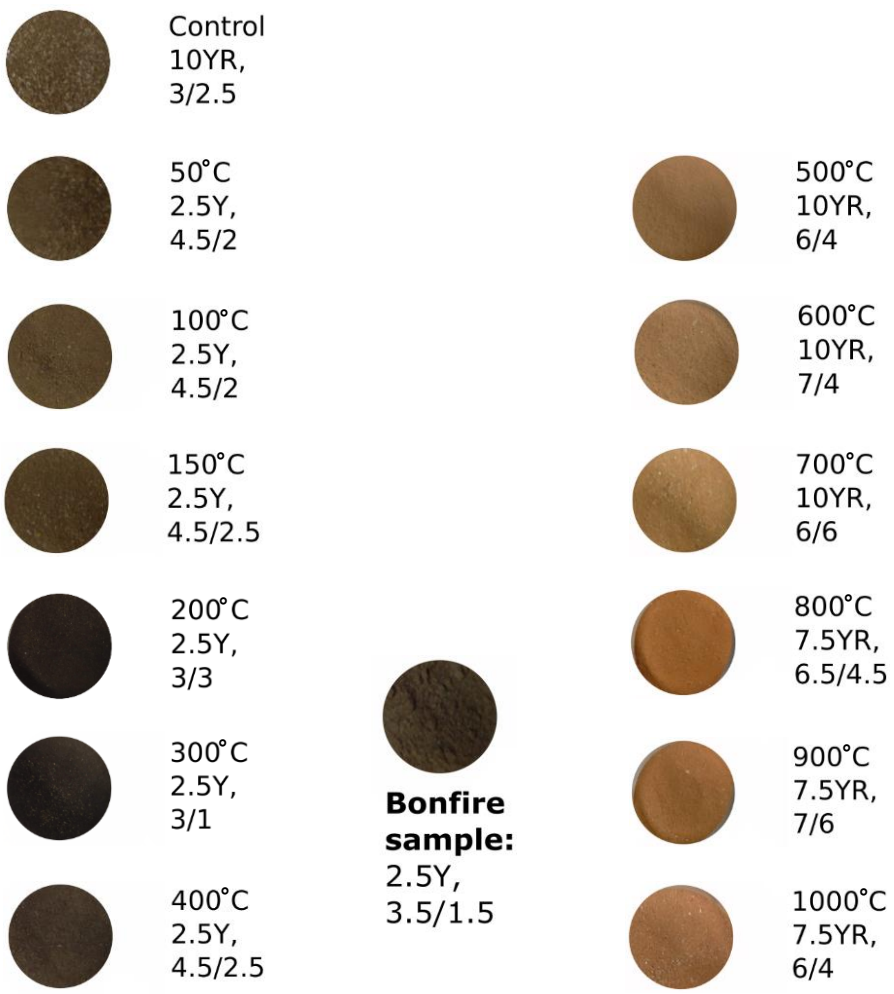

Fig. 2.8. *Relationship between sample colour and temperature (50 – 1000 °C) based on the Munsell Colour Chart (Oyama and Takehara, 1967), based on sample photographs*

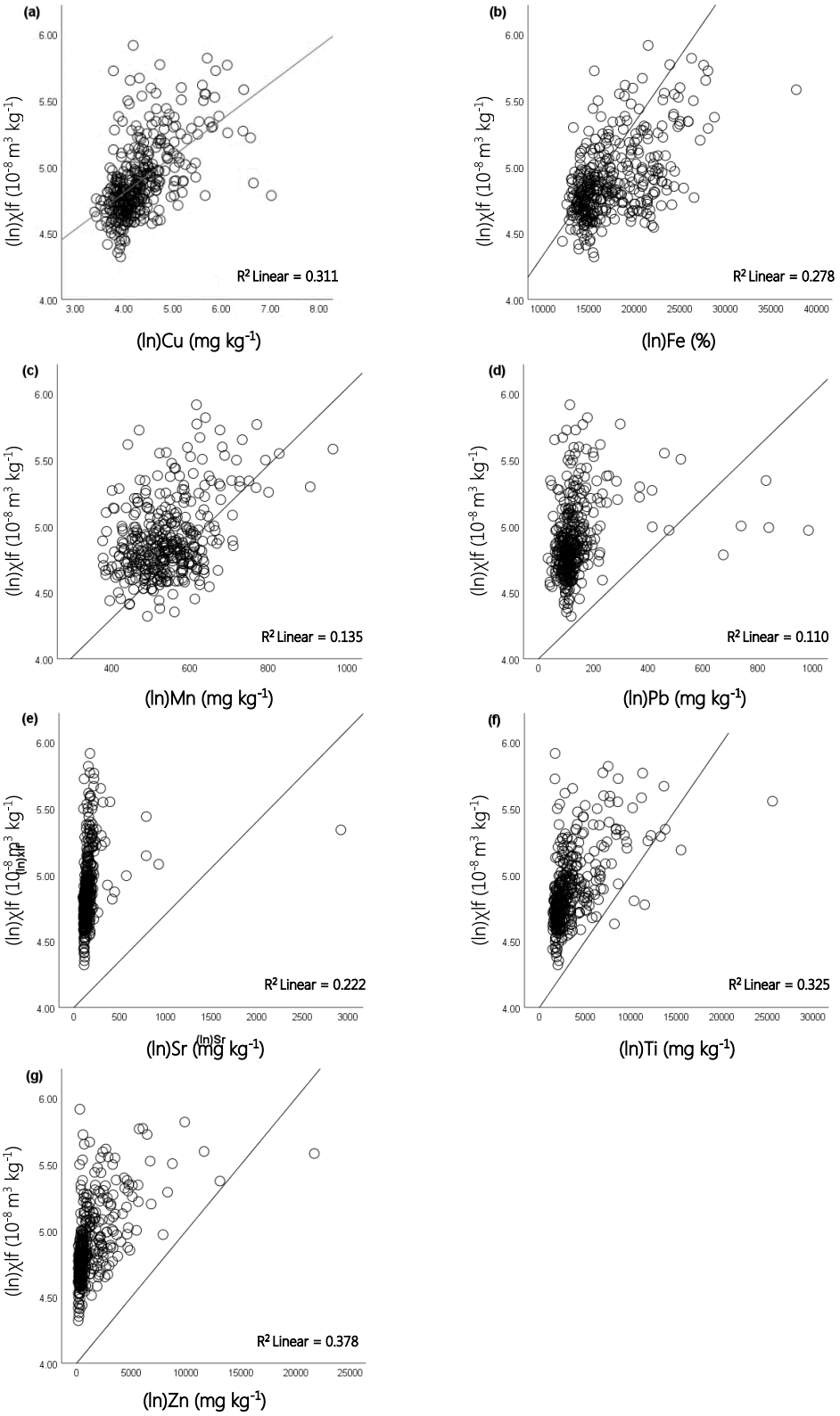

Fig. 2.9. *Comparison between total metal concentrations analysed using PXRF (mg kg $^{-1}$) and low frequency mass specific magnetic susceptibility measurements (χlf) (10 $^{-8}$ m ^{3} kg $^{-1}$) of the soil samples (n=379) collected from the bonfire affected soils.*

2.4.4. Spatial distribution with metals and χlf

The total concentrations analysed by PXRF and χlf data were first tested for skewness and kurtosis (see Table 2.2). As expected, the data was heavily skewed and kurtotic. A Kolmogorov-Smirnov test ($p < 0.05$) confirmed that the datasets did not pass the normality test, with the exception of Mn ($p = 0.15$). Therefore, the spatial interpolation method of inverse distance weighting (IDW) was employed as there are no assumptions for the probability distribution of data required for this analysis. Spatial distribution maps of total concentrations of Cu, Fe, Mn, Pb, Sr, Ti, Zn and χlf were produced (Fig. 2.10.) for comparative purposes.

2.4.5. Hotspot analysis

Local indicators of spatial association (LISA) (Anselin, 1995) maps of the elements Cu, Fe, Mn, Pb, Sr, Ti and Zn and χlf (see Fig. 2.10.) were produced to identify spatial clusters and spatial outliers within the bonfire site. As the raw datasets did not follow a normal distribution (with the exception of Mn), a natural logarithm transformation (ln) was performed on each of the variables (excluding Mn) to bring the datasets to approximate normal distributions, necessary for the calculation of a Local Morals I index. As the datasets involved are located on a 1 x 1 m^2 grid, the creation of the weight function was based on K-nearest neighbours (8 neighbours) rather than distance threshold.

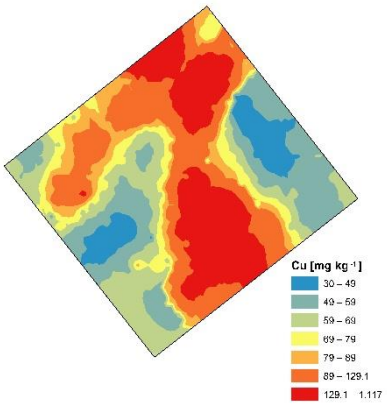
Cu [mg kg⁻¹]
30 – 49
49 – 59
59 – 69
69 – 79
79 – 89
89 – 129.1
129.1 1.117

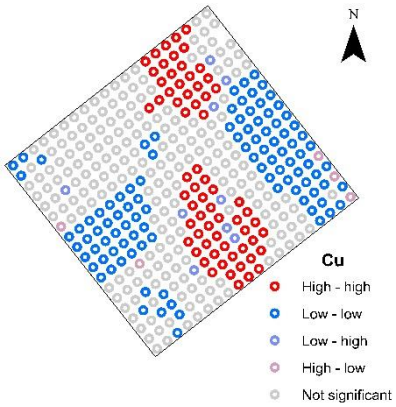
N
Cu
High - high
Low - low
Low - high
High - low
Not significant

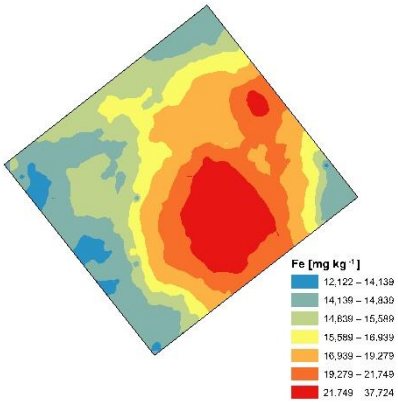
Fe [mg kg⁻¹]
12,122 – 14,139
14,139 – 14,839
14,839 – 15,589
15,589 – 16,939
16,939 – 19,279
19,279 – 21,749
21.749 37,724

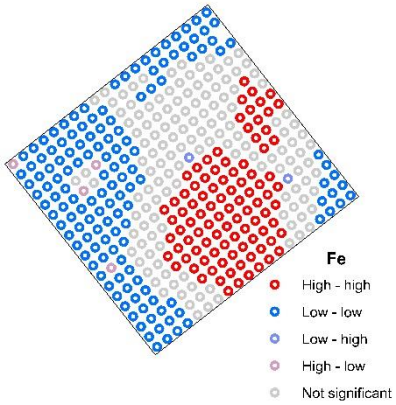
Fe
High - high
Low - low
Low - high
High - low
Not significant

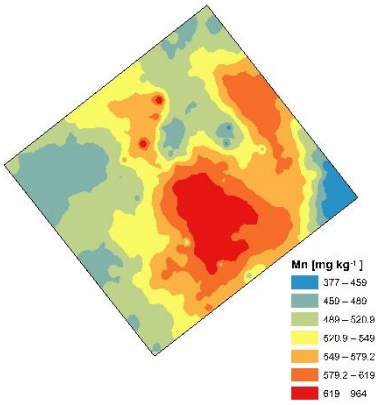
Mn [mg kg⁻¹]
377 – 459
459 – 489
489 – 520.9
520.9 – 549
549 – 579.2
579.2 – 619
619 964

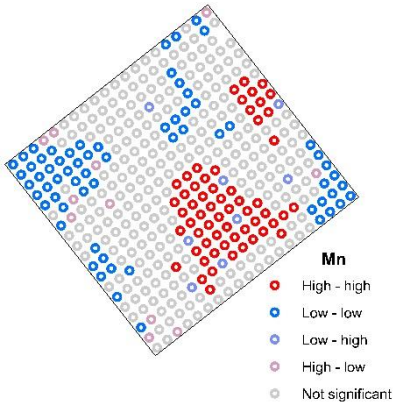
Mn
High - high
Low - low
Low - high
High - low
Not significant

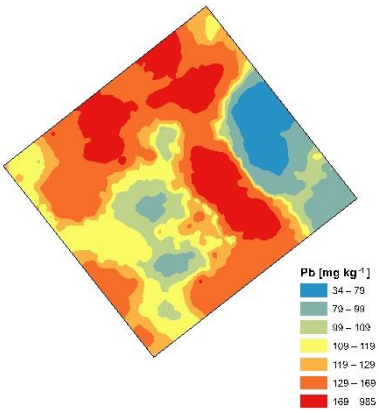
Pb [mg kg⁻¹]
34 – 79
79 – 99
99 – 109
109 – 119
119 – 129
129 – 169
169 985

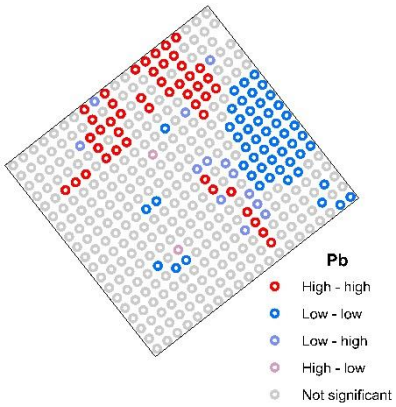
Pb
High - high
Low - low
Low - high
High - low
Not significant

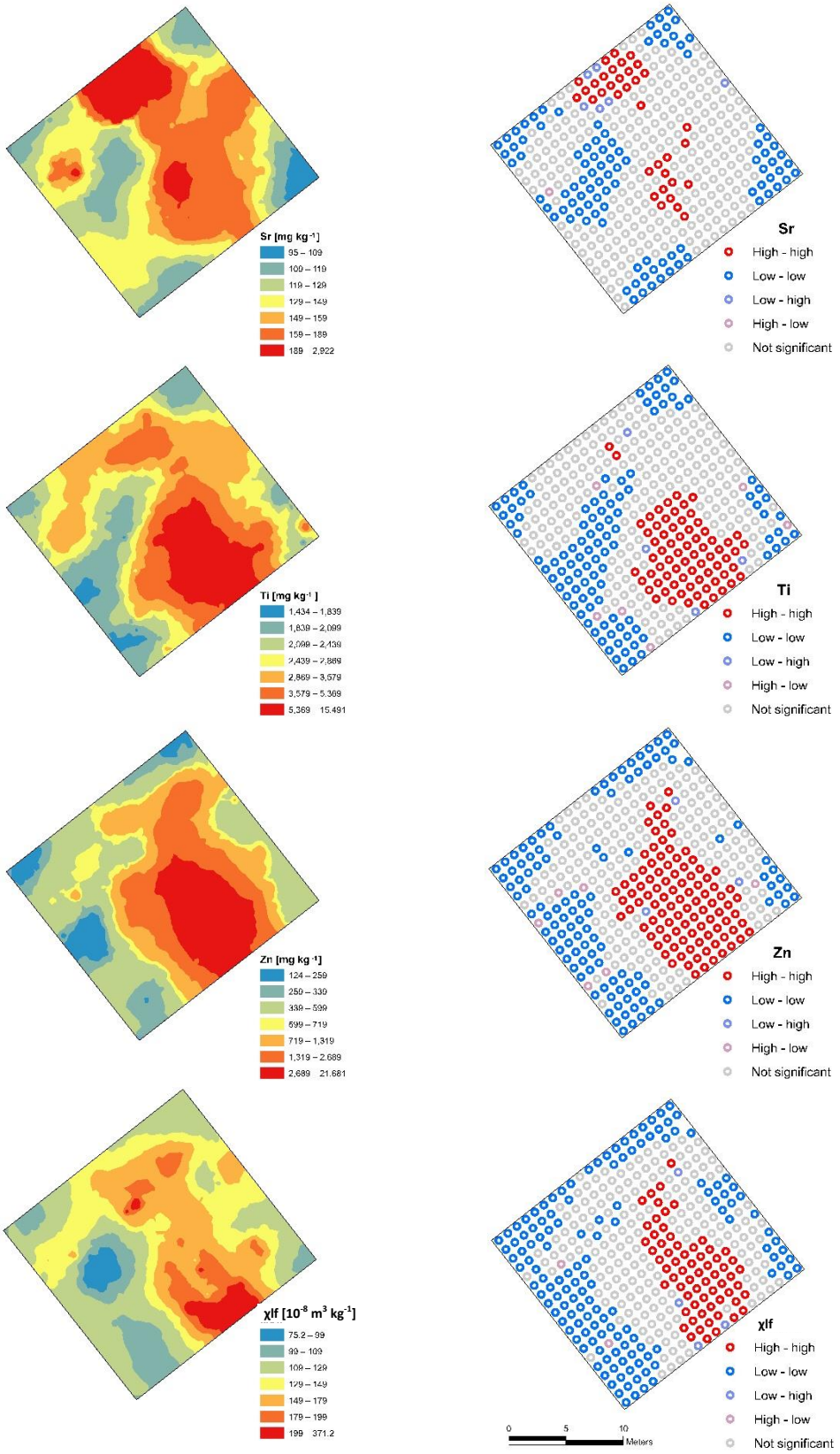

Fig. 2.10. *Spatial distribution and local Moran's I maps of Cu, Fe, Mn, Pb, Sr, Ti and Zn (mg kg $^{-1}$) and χlf (10 $^{-8}$ m ^{3} kg $^{-1}$)*

2.5. Discussion

Many studies have documented the maximum temperatures reached by fires (Stinson and Wright, 1969; Wright and Bailey, 1982), ranging from 600 °C – 900 °C. Livingstone Smith (2001) investigated the relationship between firing procedures (structures, fuel, schedule and scale) and some of the firing conditions (time and temperature) and found temperatures ranged between 65 - 1011 ˚C. Tylecote (1962) reports that 400 ˚C is a normal temperature for a campfire and proposed that such fires rarely reach 700 ˚C. Rowlett et al. (1974) stated that objects heated in campfires may reach temperatures of 380 - 550 ˚C. The impact of heating on soils varies depending on: a) the composition of materials burned: Sheehy (1988) found that temperatures ranged between 437 - 844 ˚C where materials included household refuse and vegetation (dried grass, cacti plants, cornstalks and small branches); b) soil moisture: Busse et al. (2005) found that maximum temperatures of 600 ˚C were reached in dry clay loam soil of pre-masticated woody shrubs covered areas (simulating wildfire conditions) and were 100 - 200 ˚C lower for moist soils (simulating Spring prescribed burning) and c) depth of soil: After a summer fire, soil temperatures above 40 ˚C were found up to 4.5 cm in depth, while temperatures above 60 ˚C were found only in the top 0.5 cms of soil (Auld and Bradstock, 1996). Very little is known about the processes by which fires enhances soil MS, however it has been theorised that high temperatures and changes in reduction conditions in the presence of organic matter to oxidation conditions during fires act to convert less magnetic iron oxy-hydroxides into more highly magnetic phases (Clement et al., 2010). Alternatively, Schwertmann and Fechter (1984) showed that heating aluminum substituted goethite produces aluminum substituted maghemite, a much more magnetic phase, which they suggest is a common mechanism by which wildfires cause enhancement of surface magnetization. Our evidence suggests soil temperatures reached approximately 200 - 300 °C, below the modern bonfire site, and the requisite effects on χlf at this temperature are minimal. Although heating could play an intrinsic role in magnetic enhancement, it cannot be considered fully accountable for the elevated χlf values beneath the bonfire site, indicating the influence of metal

contamination through direct metal inputs. This is further validated by the shared spatial patterns featured in Fig. 2.10.

General patterns exist throughout the elemental spatial distribution maps, with a hotspot visible in the central southeastern section of the site. When compared to the locations of previous bonfires (Fig. 2.2.), it is possible to propose that the presence of a high-high value cluster in the area is due to the activity of burning metal laden materials, as the χlf map and Moran's I maps also feature this pattern. Copper, iron and zinc encompass this area; known by-products of the burning of tyres (DEFRA, 2006). Both tyre threads (Fauser et al., 1999) and tyre dust (Adachia and Tainoshob, 2004) contain significant amounts of Zn. Brake housing dust and crushed brake pads analyses indicate high concentrations of Cu and Fe (Adachia and Tainoshob, 2004; Apeagyei et al., 2011). The mobility of Zn is poor and therefore severe Zn contamination occurs near the point source (Barceloux, 1999b). Although there are large variations across the metals, all appear to have elevated values in the northeasterly section, indicating the likely location of another historic bonfire. This northern point is the main Sr hotspot location. Sr is found in fireworks and sparklers, which is a possible traditional festive and entertainment source during the bonfire celebrations. The degree of elevation of this section differs greatly among the metals, with Cu, Pb, Sr and to a less extent Ti, featuring statistically significantly high-high values. However, the absence of Zn suggests tyres have never been burned at this section. Titanium is not known to have any adverse health effects, is ubiquitous and naturally occurring in soil (Salminen et al., 2005). However, due to its strong correlation with χlf and its spatial association with the main burning zone, it may have entered the site through burning. Ti is also associated with tyres and brake wear. Due to its similar dispersion pattern to Zn and Fe, it may also be present as a result of the burning of tyres (Apeagyei, et al., 2011). Historically, leaded-petrol was a major source of Pb (Von Storch et al., 2003) and its presence may infer its use as an ignition fluid for previous bonfires or another burning zone, as it also features exclusively in the northwestern section of the study zone. Pb is also found in common municipal waste e.g. paint, batteries, electrical appliances, ceramics and crystal glass (Stone, 1981), all of which are possible Pb sources. Like Pb, Cu is used in many

household items, glass making, jewellery, wiring and as a wood preservative (Barceloux, 1999a) and Cu treated household furniture items may have been used as fuel. The distribution of Cu and Pb is very similar, the main difference occurring in the location of the main bonfire in the central southeastern section. This may be due to the localised burning of leaded-paint, a major Pb pollution source (Stone, 1981) in the eastern section of the burning zone. The distribution maps infer the presence of an additional bonfire in the north western section of the site. In particular, this spatial pattern is visible for Cu, Pb, Sr, Ti and χlf. However, these are not statistically significant, with the exception of Pb. Outliers are identifiable as the cause of the assumed elevated values in the distribution maps. A disadvantage of IDW maps is that outliers may be exaggerated, to indicate regions of high values, which may not a true reflection of the sample data (Zhang et al., 2008). However, there appears to be symmetry across corresponding elementary maps, e.g. Fe distribution map compared to Fe Moran's I map. Since 2000, leaded petrol was removed from the market in the EU (Von Storch et al., 2003) and lead replacement petrols (LRP) with additives such as manganese were introduced (Barlow, 1999). Given the unique location of a high-high Mn and Fe values in the central eastern section of the site, Mn-bearing petrol may have been used as a possible ignition fuel. Significant low-low clusters are not as uniform across all maps, but in general occur in the western section and the south easterly edge of the site. These points and non-significant points are indicative that the soil here contains background values which have not been affected by bonfires.

The significant high-high values featured across the site indicate the presence of possibly 3 - 4 burning zones. These features are not visible on the available satellite imagery, with the exception of the main central southeastern burning zone. The spatial dispersion of metals is suggestive of a variety of materials being burnt in the bonfires. Zn presence is indicative of the burning of tyres, in a central eastern/central south eastern direction. Other metals indicate a bonfire in other locations where tyres were likely not burned, with significant high-high values in a north eastern direction of Cu, Pb and Sr high-high values of Pb in a western direction and Mn and Fe significantly high in the central

east of the site. The metals present are dependent in the materials burned in the bonfires.

2.6. Conclusion

By examining the metal and χlf maps and available satellite imagery, bonfires are recognized as a major pollution source in soils of the study area. The spatial range of influence of a bonfire is confined to the boundary of materials being burnt and is estimated at around 10 meters. The local Moran's I and spatial distribution maps presented here demonstrate the enhancement of metals and magnetic susceptibility of bonfire soils. The fast and inexpensive delineation of environmental pollution by PXRF and MS is also shown. This allows for high density sampling of sites, leading to the generation of high-resolution maps, possible in small-scale/regional studies. A study into the effects of heating on magnetization also revealed that soils under bonfires reached a maximum temperature of 300 °C, indicating heating is likely not a significant factor in the enhancement of magnetization. More research in to the materials burnt in bonfires is necessary to further investigate the impacts of bonfires on the environment. Furthermore, the environmental impacts of bonfires should be taken into consideration in future policy on soil protection.

Acknowledgements

We are grateful to Ligang Dao, Ta Na, Sorcha Dolan and Ellen Mc Grory for their assistance in sample collection and Ellen Mc Grory for assistance with the PXRF analysis. Also to the Discipline of Archaeology, NUI Galway for the loan of a MS2 meter.

2.7. References

Adachia, K. and Tainoshob, Y. (2004). 'Characterization of heavy metal particles embedded in tire dust'. *Environmental International,* 30, pp. 1009-1017.

Alekseeva, T., Alekseev, A., Maher, B.A. and Demkin, V. (2007). 'Late Holocene climate reconstructions for the Russian steppe, based on mineralogical and magnetic properties of buried palaeosols'. *Paleogeography, Paleoclimatology, Paleoecology,* 249, pp. 103-127.

Chapter 2.

Anselin, L. (1995). 'Local Indicators of Spatial Association – LISA'. *Geographical Analysis,* 27(2), pp. 93-115.

Anselin, L., Syabri, I. and Kho, Y. (2006). 'GeoDa: An Introduction to Spatial Data Analysis'. *Geographical Analysis,* 38(1), pp. 5-22.

Apeagyei, E., Bank, M.S. and Spengler, J.D. (2011). 'Distribution of heavy metals in road dust along an urban-rural gradient in Massachusetts'. *Atmospheric Environment,* 45(13), pp. 2310-2323.

Auld, T.D. and Bradstock, R.A. (1996). 'Soil temperatures after the passage of a fire: Do they influence the germination of buried seeds?' *Australian Journal of Ecology,* 21(1), pp. 106-109.

Barceloux, D.G. (1999). 'Copper'. *Clinical Toxicology,* 37(2), pp. 217-230.

Barceloux, D.G. (1999). 'Zinc'. *Clinical Toxicology,* 37(2), pp. 279-292.

Barlow, P.L. (1999). 'The lead ban, lead replacement petrol, and the potential for engine damage'. *Industrial Lubrication and Tribology,* 51(3), pp. 128-138.

Blaha, U., Appel, E. and Stanjek, H. (2008). 'Determination of anthropogenic boundary depth in industrially polluted soil and semi-quantification of heavy metal loads using magnetic susceptibility'. *Environmental Pollution,* 156, pp. 278-289.

Botsou, F., Karageorgis, A.P., Dassenakis, E. and Scoullos, M. (2011). 'Assessment of heavy metal contamination and mineral magnetic characterization of the Asopos River sediments (Central Greece)'. *Marine Pollution Bulletin,* 62, pp. 547-563.

Blundell, A., Dearing, J.A., Boyle, J.F. and Hannam, J.A. (2009). 'Controlling factors for the spatial variability of soil magnetic susceptibility across England and Wales'. *Earth-Science Reviews,* 95, pp. 158-188.

Busse, M.D., Hubbert, K.R., Fiddler, G.O., Shestak, C.J. and Powers, R.F. (2005). 'Lethal soil temperatures during burning of masticated forest residues'. *International Journal of Wildland Fire,* 14, pp. 267-276.

Butterfield, D.M. and Brown, R.J.C. (2012). *Report on Polycyclic Aromatic Hydrocarbons in Northern Ireland*. NPL Report AS66, Northern Ireland Department of Environment. February 2012. http://www.doeni.gov.uk/de/pah_in_ni_report_final_published_version_v2.pdf (Last visited 04.03.2014).

Canbay, M., Aydin, A. and Kurtulus, C. (2010). 'Magnetic susceptibility and heavy metal contamination in topsoils along the Izmit Gulf coastal area and IZAYTAS (Turkey)'. *Journal of Applied Geophysics,* 70, pp. 46-57.

Chan, L.S., Ng, S.L., Davis, A.M., Yim, W.W.S. and Yeung, C.H. (2001). 'Magnetic properties and heavy-metal contents of contaminated seabed sediments of Penny's Bay, Hong Kong'. *Marine Pollution Bulletin*, 42, pp. 569-583.

Clement, B.M., Javier, J., Sah, J.P. and Ross, M.S. (2010). 'The effects of wildfires on the magnetic properties of soils in the Everglades'. *Earth Surfaces Processes and Landforms*, pp. 1-7.

Dao, L., Morrison, L. and Zhang, C. (2012). 'Bonfires as potential source of metal pollutants in urban soils, Galway, Ireland'. *Applied Geochemistry*, 27, pp. 930-935.

Dearing, J.A. (1999). *Environmental Magnetic Susceptibility. Using the Bartington MS2 System*, 2nd edn. Kenilworth, England, UK: Chi Publishing.

D'Emilio, M., Macchiato, M., Ragosta, M. and Simoniello, T. (2012). 'A method for the integration of satellite vegetation activities observations and magnetic susceptibility measurements for monitoring heavy metals in soil'. *Journal of Hazardous Materials*, 241-242, pp. 118-126.

(DEFRA) Department for Environment, Food and Rural Affairs (2006). *A Review of Bonfire Smoke Nuisance Controls*. Report by Netcen to the Department for Environment, Food and Rural Affairs (UK). Department for the Environment, Northern Ireland. http://archive.defra.gov.uk/environment/quality/local/nuisance/smoke/documents/bonfiresmoke-report.pdf (Accessed 05.03.2014).

De Vos, W. and Tarvainen, T. (2005).'Geochemical Atlas of Europe. Part 2 – Interpretation of Geochemical Maps, Additional Tables, Figures, Maps and Related Publications'. *Geological Survey of Finland, Otamedia Oy, Espoo*, pp. 373-377.

El Baghdadi, M., Barakat, A., Sajieddine, M. and Nadem, S. (2012). 'Heavy metal pollution and soil magnetic susceptibility in urban soil of Beni Mellal City (Morocco)'. *Environmental Earth Sciences*, 66, pp. 141-155.

(EEA) European Environment Agency (2010). *Air and Health – Sources of Air pollution.* http://www.eea.europa.eu/publications/2599XXX/page010.html (Accessed 08.04.2014).

Fauser, P., Tjell, J.C., Mosbaek, H. and Pilegaard, K. (1999). 'Quantification of tire-thread particles using extractable organic zinc as tracer'. *Rubber Chemical Technology*, 72, pp. 969-977.

Frančišković-Bilinski, S., Bilinski, H., Scholger, R., Tomašić, N. and Maldini, K. (2014). 'Magnetic spherules in sediments of the karstic Dobra River (Croatia)'. *Journal of Soils and Sediments*, 14, pp. 600-614.

Gailey, A. and Adams, G.B. (1977). *The Bonfire in the North Irish Tradition*. Oxfordshire: Taylor & Francis, Ltd.

Getis, A. and Ord, J.K. (1992). 'The analysis of Spatial Association by Use of Distance Statistics'. *Geographical Analysis*, 24, pp. 189-206.

Gudadhe, S.S., Sangode, S.J., Patil, S.K., Chate, D.M., Meshram, D.C. and Badekar, A.G. (2012). 'Pre- and post-monsoon variations in the magnetic susceptibilities of soils of Mumbai metropolitan region: implications to surface redistribution of urban soils loaded with anthropogenic particulates'. *Environmental Earth Sciences*, 67, pp. 813-831.

Hanesch, M. and Scholger, R. (2002). 'Mapping of heavy metal loadings in soils by means of magnetic susceptibility measurements'. *Environmental Geology*, 42, pp. 857-870.

Chapter 2.

Heiri, O., Lotter, A.F. and Lemcke, G. (2001). 'Loss on ignition as a method for estimating organic and carbonate content in sediments: reproducibility and comparability of results'. *Journal of Paleolimnology*, 25, pp. 101-110.

Innov-X Systems, Inc. (2005). *Technical Data. Alpha Series™- analyzers provide on-site environmental metals testing*. http://www.fieldenvironmental.com/assets/files/Literature/InnovX%20XRF%20Specs.pdf (Accessed 20.02.2014).

Jacquez, G., Grimson, R., Waller, L. and Wartenberg, D. (1996). 'The analysis of disease clusters, part ii: Introduction to techniques'. *Infection Control and Epidemiology*, 17(6), pp. 385-397.

Jordanova, N.V., Jordanova, D.V., Veneva, L., Yorova, K. and Petrovsky, E. (2003). 'Magnetic Response of Soils and Heavy Metal Pollution – A Case Study'. *Environmental Science and Technology*, 37, pp. 4417-4424.

Kalnicky, D.J. and Singhvi, R. (2001). Field portable XRF analysis of environmental samples. *Journal of Hazardous Materials*, 83, pp. 93-122.

Kapička A., Jordanova N., Petrovský E. and Podrázský V. (2003). 'Magnetic study of weakly contaminated forest soils'. *Water, Air & Soil Pollution*, 148, pp. 31−44.

Levine, N. (2006). 'Crime mapping and the CrimeStat program'. *Geographical analysis*, 38(1), pp. 41-56.

Li, W., Xu, B., Song, Q., Liu, X., Xu, J. and Brookes, P.C. (2014). 'The identification of 'hotspots' of heavy metal pollution in soil-rice systems at a regional scale in eastern China'. *Science of Total Environment*, 472, pp. 407-420.

Lucideon.com (2019). *Inductively Coupled Plasma Optical Emission Spectroscopy (ICP-OES Analysis)*. https://www.lucideon.com/testing-characterization/techniques/inductively-coupled-plasma-optical-emission-spectroscopy-icp-oes (Accessed on 28.08.2019).

Livingstone Smith A. (2001). 'Bonfire II: The Return of Pottery Firing Temperatures'. *Journal of Archaeological Science* 28, pp. 991-1003.

Lu, S.G. and Bai, S.Q. (2006). 'Study on the correlation of magnetic properties and heavy metals content in urban soils of Hangzhou City, China'. *Journal of Applied Geophysics*, 60, pp. 1-12.

Lu, S.G., Bai, S.Q. and Fu, L.X. (2008). 'Magnetic Properties as Indicators of Cu and Zn Contamination in soils'. *Pedosphere*, 18(4), pp. 479-485.

Lu, S.G., Wang, H.G. and Chen, Y.Y. (2012). 'Enrichment and solubility of trace metals associated with magnetic extracts in industrially derived contaminated soils'. *Environmental Geochemistry and Health*, 34, pp. 433-444.

Mackey, E.A., Christopher, S.J., Lindstrom, R.M., Long, S.E., Marlow, A.F., Murphy, K.E., Paul, R.L., Popelka-Filcoff, R.S., Rabb, S.A., Sieber, J.R., Spatz, R.O., Tomlin, B.E., Wood, L.J., Yen, J.H., Yu, L.L., Zeisler, R., Wilson, S.A., Adams, M.G., Brown, Z.A., Lamothe, P.L., Taggart, J.E., Jones, C., Nebelsick, J. (2010). 'Certification of Three NIST Renewal Soil Standard Reference Materials for Element Content: SRM 2709a San Joaquin Soil, SRM 2710a Montana Soil I, and SRM 2711a Montana Soil II'. *NIST Special Publication,* 260-172. US Department of Commerce and the National Institute of Standards and Technology.

Magiera, T., Kapička, A., Petrovský, E., Strzyszcz, Z., Fialová, H. and Rachwał, M. (2008). 'Magnetic anomalies of forest soils in the Upper Silesia-Northern Moravia region'. *Environmental Pollution*, 156, pp. 618-627.

Maher, B.A., Alekseev, A. and Alekseeva, T. (2002). 'Variation of soil magnetism across the Russian steppe: its significance for use of soil magnetism as a paleorainfall proxy'. *Quaternary Science Reviews*, 21, pp. 1571-1576.

Maher, B.A., Alekseev, A. and Alekseeva, T. (2003). 'Magnetic mineralogy of soils across the Russian Steppe: climatic dependence of

pedogenic magnetite formation'. *Paleogeography, Paleoclimatology, Paleoecology*, 201, pp. 321-341.

Maher, B.A. and Hallam, D.F. (2005). 'Paleomagnetic correlation and dating of Pilo/Pleistocene sediments at the southern margins of the North Sea Basin'. *Journal of Quaternary Science*, 20(1), pp. 67-77.

McCullagh, M.J. (2006). *Detecting Hotspots in Time and Space*. ISG06. https://www.academia.edu/699868/Detecting_hotspots_in_time_and_space (Accessed 08.04.2014).

Morton-Bermea, O., Hernandez, E., Martinez-Pichardo, E., Soler-Arechalde, A.M., Lozano Santa-Cruz, R., Gonzalez-Hernandez, G., Beramendi-Orosco, L. and Urrutia-Fucugauchi, J. (2009). 'Mexico City topsoils: Heavy metals vs. magnetic susceptibility'. *Geoderma*, 151, pp. 121-125.

Ord, J.K. and Getis, A. (1995). 'Local Spatial Autocorrelation Statistics: Distribution Issues and an Application'. *Geographical Analysis*, 27(4): pp. 286-306.

Oyama, M., Takehara, H. (1967). *Revised standard soil color charts.* National Institute of Agricultural Sciences, Forest Experiment Station, Japan Color Research Institute, Japan.

Rowlett, R.M., Mandeville, M.D. and Zeller, E.J. (1974). 'The interpretation and dating of humanly worked siliceous materials by thermoluminescent analysis'. *Proceedings of the Prehistoric Society*, 40, pp. 37-44.

Sapkota, B. and Cioppa, M.T. (2012). 'Using magnetic and chemical measurements to detect atmospherically-derived metal pollution in artificial soils and metal uptake in plants'. *Environmental Pollution*, 170, pp. 131-144.

Schwertmann, U. and Fechter, H. (1984). 'The influence of aluminum on iron oxides: XI. Aluminum-substituted maghemite in soils and its formation'. *Soil Science Society of America Journal*, 48, pp. 1462-1463.

Sheehy, J.J. (1988). ‘Ceramic ecology and the clay/fuel ratio: modelling fuel consumption in Tlajina 33, Teotihuacan, Mexico’. In Kolb, C.C. (Ed.), *Ceramic Ecology Revisited* (1987): *The Technology and Socio Economics of Pottery, Part 1. BAR International Series,* 436, p. 199

226.

Shipman, P., Foster, G. and Schoeninger, M. (1984). ‘Burnt Bones and Teeth: an Experimental Study of Color, Morphology, Crystal Structure and Shrinkage’. *Journal of Archaeological Science,* 11, pp. 307-325.

Sokal, R.R., Oden, N.L. and Thomson, B.A. (1998). ‘Local spatial autocorrelation in biological variables’. *Biological Journal of the Linnean Society,* 65, pp. 41-62.

Sokal, R.R., Oden, N.L. and Thomson, B.A. (1998). ‘Local spatial autocorrelation in a Biological Model’. *Geographical Analysis,* 30(4), pp. 331-354.

Stinson, K.J. and Wright, H.A. (1969). ‘Temperature headfires in the southern mixed prairie of Texas’. *Journal Range Management,* 22, pp. 169-174.

Stone, H.M. (1981). ‘Lead’. *Journal of Chemical Education,* 51(9), pp. 722-724.

Strzyszcz, Z. and Magiera, T. (1998). ‘Magnetic Susceptibility and Heavy Metals Contamination in Soils of Southern Poland’. *Physics and Chemistry of the Earth,* 23(9-10), pp. 1127-1131.

Tylecote, R.F. (1962). Metallurgy in Archaeology. London: Arnold Press.

Von Storch, H., Costa-Cabral, M., Hagner, C., Feser, F., Pacyna, J., Pacyna, E. and Kolb, S. (2003). ‘Four decades of gasoline lead emissions and control policies in Europe: a retrospective assessment’. *Science of the Total Environment,* 311(1-3), pp. 151-176.

Wang, X.S. and Qin, Y. (2005). ‘Correlation between magnetic susceptibility and heavy metals in urban topsoil: a case study from the city of Xuzhou, China’. *Environmental Geology,* 49, pp. 10-18.

Wright, H. and Bailey, P.W. (1982). *Fire Ecology: United States and Southern Canada*. New York: John Wiley & Sons.

Yang, T., Liu, Q., Zeng, Q. and Chan, L. (2012). 'Relationship between magnetic properties and heavy metals of urban soils with different soil types and environmental settings: implications for magnetic mapping'. *Environmental Earth Sciences*, 66, pp. 409-420.

Zawadzki, J. and Fabijańczyk, P. (2008). 'Reduction of soil contamination uncertainty assessment using magnetic susceptibility measurements and co-est method'. *Proceedings of ECOpole,* 2(1), pp. 171-174.

Zhang, C. (2006). 'Using multivariate analyses and GIS to identify pollutants and their spatial patterns in urban soils in Galway, Ireland'. *Environmental Pollution*, 142, pp. 501-511.

Zhang, C., Luo, L., Xu, W. and Ledwith, V. (2008). 'Use of local Moran's I and GIS to identify pollution hotspots of Pb in urban soils of Galway, Ireland'. *Science of Total Environment,* 398, pp. 212-221.

Zhang, C., Qiao, Q., Appel, E. and Huang, B., (2012). 'Discriminating sources of anthropogenic heavy metals in urban street dusts using magnetic and chemical methods'. *Journal of Geochemical Exploration*, 119-120, pp. 60-75.

Zhang, T. and Lin, G., (2007). 'A decomposition of Moran's I for cluster detection'. *Computational Statistics & Data Analysis*, 51, pp. 6123-6137.

Zhu, Z., Han, Z., Bi, X. and Yang, W., (2012). 'The relationship between magnetic parameters and heavy metal contents of indoor dust in e-waste recycling impacted area, Southeast China'. *Science of Total Environment*, 433, pp. 302-308.

Zhu, Z., Sun, G., Bi, X., Li, Z. and Yu, G., (2013). 'Identification of trace metal pollution in urban dust from kindergartens using magnetic, geochemical and lead isotopic analyses'. *Atmospheric Environment*, 77, pp. 9-15

3. *IMPACT OF GRASS COVER ON THE MAGNETIC SUSCEPTIBILITY MEASUREMENTS FOR ASSESSING METAL CONTAMINATION IN URBAN TOPSOIL*

This paper has been published in the journal of *Applied Geochemistry*,52, pp. 86-96 (November,2015).

Chapter 3:

IMPACT OF GRASS COVER ON THE MAGNETIC SUSCEPTIBILITY MEASUREMENTS FOR ASSESSING METAL CONTAMINATION IN URBAN TOPSOIL

3.1. Abstract

In recent decades, magnetic susceptibility monitoring has developed as a useful technique in environmental pollution studies, particularly metal contamination of soil. This study provides the first ever examination of the effects of grass cover on magnetic susceptibility (MS) measurements of underlying urban soils. Magnetic measurements were taken in situ to determine the effects on κ (volume magnetic susceptibility) when the grass layer was present (κ^{grass}) and after the grass layer was trimmed down to the root ($\kappa^{no\ grass}$). Height of grass was recorded in situ at each grid point. Soil samples (n=185) were collected and measurements of mass specific magnetic susceptibility (χ) were performed in the laboratory and frequency dependence (χfd%) calculated. Metal concentrations (Pb, Cu, Zn and Fe) in the soil samples were determined and a gradiometry survey carried out in situ on a section of the study area. Significant correlations were found between each of the MS measurements and the metal content of the soil at the p<0.01 level. Spatial distribution maps were created using Inverse Distance Weighting (IDW) and Local Indicators of Spatial Association (LISA) to identify common patterns. κ^{grass} (ranged from 1.67-301.00 x 10^{-5} SI) and $\kappa^{no\ grass}$ (ranged from 2.08-530.67 x 10^{-5} SI) measured in situ are highly correlated [r=0.966, n=185, p<0.01]. The volume susceptibility datasets in the presence and absence of grass coverage share a similar spatial distribution pattern. This study re-evaluates in situ κ monitoring techniques and the results suggest that the removal of grass coverage prior to obtaining in situ κ measurements of urban soil is unnecessary. This layer does not impede the MS sensor from accurately measuring elevated κ in soils, and therefore κ measurements

recorded with grass coverage present can be reliably used to identify areas of urban soil metal contamination.

3.2. Introduction

Metal contaminants are a useful indicator of environmental pollution in urban soils. The assessment of magnetic susceptibility of soils has become an established reliable and efficient proxy for metal contamination. The magnetic susceptibility of soils mainly depends on ferromagnetic mineral content which are a result of natural and anthropogenic processes. Natural processes can include weathering of rocks (Kapička et al., 2008) or occur during pedogenic processes which can be mediated by microorganisms (D'Emilio et al., 2007). Magnetic particles occurring in industrial and urban dusts have an anthropogenic source and are referred to as technogenic magnetic particles (TMPs). These iron minerals are formed as a result of technological processes at very high temperatures which are released into the atmosphere (Hanesch and Scholger, 2002; Magiera et al., 2011). Fossil-fuel burning power plants are a significant source of airborne TMPs (Hanesch and Scholger, 2002; Evans and Heller, 2003). Combustion of coal causes the release of sulfur gas and formation of spherical iron particles which can oxidize to form magnetite (Fe_3O_4) (Flanders, 1999; Hanesch and Scholger, 2002), pyrrhotite (Fe_7S_8) and other minerals can also form which are rarely found in the natural environment (technogenic ferrites) (Lukasik et al., 2015). In the event where natural processes are not a significant contributing factor in the magnetization of soil, magnetic susceptibility has emerged as an alternative technique for monitoring environmental metal pollution (Chianese et al., 2006). Particulates resulting from anthropogenic emissions may integrate potentially toxic elements (PTEs) into their structure. Magnetic particles TMPs can act as a host of metals and contaminants by either incorporating metals into the crystalline structure during combustion, or PTEs may adhere onto their exterior after formation (Chaparro et al., 2006; Kapička et al., 2008).

Magnetic parameters are widely applied in many fields including archaeology and environmental science. The application of magnetic studies to

environmental features of archaeology was first established in the 1950's which concerned the magnetic susceptibility of soils. Le Borgne observed enhanced magnetism in topsoils in comparison to the underlying bedrock (Evans and Heller, 2003). Initially, magnetic susceptibility was used to investigate magnetic enhancement of soils relating to fire which could be a result of natural or human activity or pedogenic processes (Dalan, 2008). More modern applications include the locating, mapping and interpretation of earthworks and also as part of the excavation process, carrying out magnetic susceptibility surveys on walls and floors at the microscale to add an additional layer of data to an excavation (Dalan, 2008). Environmental magnetism involves relating magnetic properties of mineral assemblages to the environmental conditions that govern them (Liu et al., 2012). The technique has been developed over the past thirty years and the range of applications of magnetic susceptibility conveyed by many (i.e. Thompson and Oldfield, 1986; Verosub and Roberts, 1995; Maher and Thompson, 1999; Evans and Heller, 2003; Gibson and George, 2003).

The use of magnetic parameters as a proxy for environmental metal contamination in urban environments is established (Canbay et al., 2010; El Baghdadi et al., 2012; Girault et al., 2016; Golden et al., 2015; Liu and Bai, 2006; Morton-Bermea et al.; Yang et al., 2012; Zhang et al., 2012 and Zhu et al., 2012). Environmental magnetic methods have been extensively used to examine the extent and causes of anthropogenic contamination, providing a simple, rapid, non-intrusive and feasible tool in the identification of metal pollutants (Chianese et al., 2006; Zhang et al., 2012).

Magnetic susceptibility can be measured in the laboratory as mass specific magnetic susceptibility (χ) and in situ as volume magnetic susceptibility (κ) and is a quick and economical technique compared to traditional chemical methods of analysis for soil geochemistry (Jordanova et al., 2003; Soodan et al., 2014).

Volume magnetic susceptibility has been applied as a proxy for metal contamination in many environmental samples such as sediments (Canbay et al., 2010), leaves (Gautam et al., 2005), tree bark (Kletetschka et al., 2003), mosses (Fabian et al., 2011), lichens (Salo et al., 2012), fly ash (Kapička et

al., 1999; Zawadzki et al., 2010) and soils (Bityukova et al., 1999; Hoffmann et al., 1999; Boyko et al., 2004; Schmidt et al., 2005; Canbay et al., 2010). The capability of κ to provide instant measurements make it possible to determine relative pollution impacts directly in the field (Jordanova et al., 2003). The main limitation of this technique in relation to environmental studies is the depth of analysis. In situ magnetic susceptibility studies are limited to the upper topsoil horizon as significant MS properties may lie below this horizon.

MS mapping has developed as an important technique in soil analyses and monitoring of temporal changes in environmental studies (Petrovský and Ellwood, 1999; Hanesch et al., 2007). Many studies have incorporated the use of κ to assist in soil metal pollution mapping studies particularly in urban soils (Wang and Qin, 2005; Fialová et al., 2006; Lu et al., 2007). Urban soils occur within populated areas and provide many ecosystem services, natural resources and recreational amenities for communities globally and are considered vulnerable to metal contamination from industrial and domestic sources. Some studies have explored the impact of a vegetative layer on magnetic susceptibility in varying soil environments including a former mining site (Schmidt et al., 2005), a laboratory setting (D'Emilio et al., 2007) and a forest floor (Zawadzki et al., 2010). However, the effects of a vegetative layer on magnetic susceptibility measurements in urban soils remains unknown.

The main aim of this paper was to identify for the first time whether grass coverage significantly affects volume magnetic susceptibility (κ) of underlying urban soils. The study area is a well-established metal contamination hotspot and hence ideal to test this hypothesis. In addition, field-based magnetic susceptibility measurements were evaluated as a proxy for metal contamination in soil by comparing spatial distribution maps of κ and metals. Laboratory-based magnetic susceptibility (χ) and a magnetic gradient survey on a section of the study area was carried out to assess the field-based κ measurements obtained. Percentage frequency dependence (χfd%) was also calculated to identify the possible locations of anthropogenic

magnetic minerals. The findings will potentially impact methodological approaches in environmental soil science.

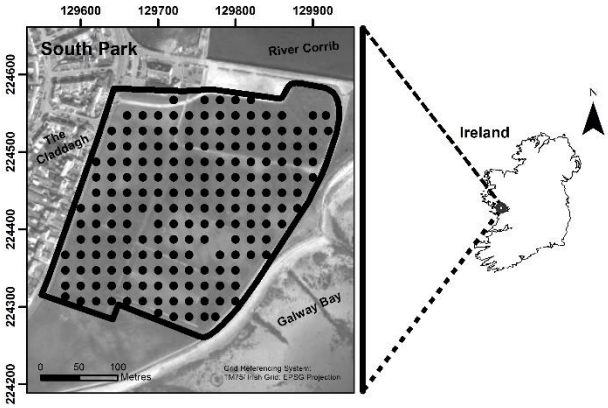

Fig. 3.1. *Map of study area, South Park, Galway, Ireland, featuring 185 soil sampling points and two datasets of κ measurement locations taken 1)* κ^{grass} *- before grass was removed and 2)* $\kappa^{no\ grass}$ *- after grass layer was removed*

3.3. Materials and Methods

3.3.1. Study area and vegetation cover

The study site is located in an urban park of approximately 20 acres of former swampy seaside wetland known as South Park in the Claddagh region (O'Dowd, 1993 as cited in Carr et al., 2008) of Galway City (53° 15' 56 N, -9° 03' 10 E), Ireland (Fig. 3.1.). In the past, the site has been considered a metal contamination hotspot (due to its use as an unregulated waste deposit site) prior to its current use as a green space amenity. A first attempt at reclaiming the flood prone region into a recreational site occurred at the beginning of the twentieth century with the development of a half-mile track around the perimeters of the area (Galway Advertiser, 2008). Much of the track layout is used as a pedestrian walkway/ bicycle path surrounding the green area. This was not a successful undertaking and it was soon after this that the site was used as a municipal landfill. The landfill was potentially in use for twenty to thirty years until in 1931, a grant was provided to develop

part of the site into a number of playing pitches. Development occurred gradually until the early 1950's when the area was fully converted into a municipal park (Galway Advertiser, 2008). It is not known whether its use as a municipal dump continued during this development phase. Colloquially, it is claimed that the removal of deposited materials such as glass and tin from the topsoil was required post-development of the playing pitches (Galway Advertiser, 2008). A previous study conducted at the site revealed very high levels of As, Pb and Cu present in the soils. In the past, a fertilizer plant was situated adjacent to the park and the type of pollution identified was similar to the industrial waste originating from a fertilizer plant processing pyrite ores (U.S. EPA 1997 as cited in Carr et al., 2008).

While the main soil type in the region is brown earths, the surface soils in South Park were imported, which were used to cover the rubbish when the sportsground was built. There were no natural horizons in the soils and the thickness of the imported soil varied across the study area, e.g. the west and north parts were relatively poorly covered.

Fig. 3.2. The site comprises of a number of playing pitches used for various

sporting activities including soccer, gaelic football and rugby. *Photographs taken at the study site featuring: a) Galway Bay to the east of the park, b) the central eastern pitch and c) north-western pitch and d) the south-eastern pitch.*

The study site (Fig. 3.2.) is comprised of the widespread cultivation of the grass species *Lolium*-mix, predominately *Lolium perenne* L., also known as Ryegrass, Ray Grass or Eavers. This versatile species is commonly found in agricultural settings; in improved or reseeded neutral grassland, livestock grazing pasture and fodder (Beddows, 1967); as a turfgrass species used in domestic gardens, parks, recreational amenities, commercial landscapes and other green belts (Bandaranayake et al., 2003) and on disturbed or waste ground (Averis, 2013). *Lolium perenne* is tolerable to grazing and environmental contamination (Cockerham et al., 1990) and as a result is commercially important globally, with widespread uses in urban and amenity spaces (e.g. football pitches, roadsides and waste places).

3.3.2. Sampling grid

A systematic 20 x 20 m ^{2} sampling grid was employed in the collection of 185 soil samples and two datasets of 185 corresponding κ measurements: 1) κ^{grass} - measured with the grass layer present and 2) $\kappa^{no\ grass}$ - measured after the grass layer was trimmed down to the root. The locations of a selection of sampling points were altered due to obstructions present in the field e.g. gravelled areas, tarmacked pavements or water-logged areas. A portable global positioning system (GPS) Trimble GeoExplorer® was used to locate and record sampling point coordinates.

3.3.3. Soil collection, preparation and analysis

At each point on the sampling grid, three soil samples were collected using a plastic scoop at a depth of ~0-10cm within 1m^2 area of the sampling point. The soils samples were combined to form one composite sample and stored in polythene bags. Special attention was paid to ensure the soil samples were removed from the same points as the κ sub-measurements. Soil samples were

air-dried at ~20 °C (Fig. 3.2.a)), before being gently disaggregated using a mortar and pestle and sieved using a 2 mm stainless steel sieve (Fig. 3.2.b)).

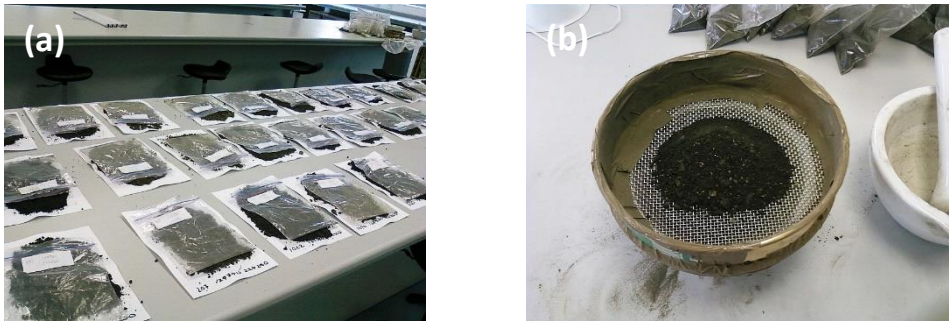

Fig. 3.2. *a) Soil samples left to air dry at ambient temperature; b) samples were sieved using a 2 mm sieve with stainless steel mesh*

A portable X-ray fluorescence analyser, Innov-X Alpha Series 6500 (PXRF, ©Innov-X Systems, Inc.) was used to analyse the metal content of the soil samples. PXRF is a non-destructive method of examining possible contaminated sites which can perform accurate quantitative analysis over a whole host of elements including Ba, Hg, Cd, As, Cr, Pb, Mn, Sr, Cu, K, Co, Ti, Fe and Zn (Soodan et al., 2014). XRF measurement uncertainties are within a specified relative standard deviation of the measurement, which are as follows: Cu(± 4), Fe(± 286), Pb(± 13) and Zn(± 9). The XRF was operated for 120 seconds per sample to generate data for elements lead (Pb), copper (Cu), zinc (Zn) and iron (Fe). The limits of detection are relatively low ranging from ~10 ppm (Innov-X Systems Inc., 2013). Tangible limits are dependent upon the sample type and matrix (Innov-X Systems Inc., 2013).

Fig. 3.3. *a) A portable X-ray fluorescence analyser, Innov-X Alpha Series 6500 (PXRF, ©Innov-X Systems, Inc.); b) prepared composite soil sample of at least 50g analysed for elemental content via PXRF*

3.3.4. Volume magnetic susceptibility (κ)

Volume magnetic susceptibility measurements were obtained using a Bartington MS2 meter (©Bartington Instruments Ltd.) in situ with a MS2D search loop. The field penetration depth of the MS2D sensor used is approximately 10 cm. The majority of the susceptibility signal, approximately 95%, comes from the upper 8cm in the shape of a toroid with an integrated volume of approximately 0.0043m^3 (Lecoanet et al., 1999). Values of volume magnetic susceptibility (κ) are dimensionless and expressed as 10^{-5} SI units (Zawadzki et al., 2015).

Volume magnetic susceptibility was measured in two phases within a 1 m^2 sampling location: Firstly, three sub-measurements were recorded with the grass layer present. The approximate length of grass coverage was noted to determine whether the presence of this layer had a significant impact on the magnetic measurements obtained. The length of grass was recorded by removing blades of grass from the sampling locations and measuring them. Measurements were rounded to the nearest cm. Lastly, the grass layers were trimmed to the root from each of the three previously measured locations and a secondary κ of the bare soils beneath were recorded. Three sub-measurements were taken at each location because high variability can occur between field measurements even at close distances (Lees et al., 1999). The mean of two air measurements (taken before and after) was subtracted from each surface measurement. The mean of the three surface measurements is then used as the representative measurement for each location.

Fig. 3.4. *In situ κ measurements: a) Bartington MS2 meter with a MS2D sensor attached; b) Grass height being recorded at a sub-measurement point; c) plastic marker placed at center of measurement point and vegetation cover removed; d)* $\kappa^{no\ grass}$ *measurement recorded after vegetation removed.*

3.3.5. Mass specific magnetic susceptibility (χ)

The mass specific magnetic susceptibility of the homogenized soil samples was measured using a Bartington MS2 meter with a dual-frequency MS2B sensor in the laboratory. Samples were measured at the low frequency range (0.46 kHz) expressed as χlf and at the high frequency range (4.6 kHz) expressed as χhf. Frequency dependence is the difference between the two frequencies and is expressed in %. Percentage frequency dependence (χfd%) was calculated to detect the presence of ultrafine (<0.03 μm) superparamagnetic ferrimagnetic minerals (Dearing, 1999). Samples were

measured in compact 10 cm^3 plastic cylinders. In order for true comparisons to be made between magnetic susceptibility measurements, mass specific magnetic susceptibility values were converted to volume magnetic susceptibility in accordance with the methodology applied by Dearing (1999) which states that $\chi(10^{-6}\ m^3\ kg^{-1})$ can be calculated by dividing κ by sample mass and then dividing by 10. Therefore the following formula was used to calculate κ^{lab}:

$$(\chi lf * 10) * sample\ mass = \kappa^{lab} \quad \textbf{[1]}$$

3.3.6. Fluxgate gradiometry survey

Measurements of magnetic gradient were taken using a Bartington 601 fluxgate gradiometer. These instruments feature two sets of two fluxgate sensors placed vertically above one another, separated by 1m and measure the vertical component of the Earth's magnetic field (Gaffney and Gater, 2003). Measurements were taken at regular 0.5 m intervals along a series of parallel transects positioned 1 m apart within 8 grid panels measuring 20m x 20m. Measurements were taken facing north along each transect. The survey grid design was based on the technique employed by Fenwick (2004).

3.3.7. Quality control

To evaluate the precision of the chemical analysis by PXRF, the determination of the studied elements was performed using the soil certified reference materials (CRMs) San Joaquin (SRM 2709a), Montana I (SRM 2710a) and Montana II (SRM 2711a) from the National Institute of Standards and Technology, USA (NIST). These CRMs have been established for use in technique development, technique validation and routine quality assurance in the analysis of major, minor and trace element concentrations of soils (Mackey et al., 2010). PXRF exhibited particularly good analytical accuracy for Cu and Zn (Table 3.1.).

Table 3.1. *Recovery of metals (Cu, Fe, Pb and Zn) in three soil certified reference materials (Montana I, Montana II and San Joaquin, National Institute of Standards and Technology, USA) (n = 3)*

CRM		Cu	Fe	Pb	Zn
2709a	Certified	33.9 ± 0.5	33600 ± 700	17.3 ± 0.1	103 ± 4
San Joaquin	Measured	31 ± 6	32875 ± 296	13 ± 3	97 ± 5
	Recovery (%)	91.44%	97.84%	75.14%	94.17%
2710a	Certified	3420 ± 50	43200 ± 800	5520 ± 30	4180 ± 20
Montana I	Measured	3518 ± 46	50503 ± 497	5564 ± 58	4412 ± 51
	Recovery (%)	102.87%	116.90%	100.80%	105.55%
2711a	Certified	140 ± 2	28200 ± 400	1400 ± 10	414 ± 11
Montana II	Measured	118 ± 8	25753 ± 244	1402 ± 18	374 ± 9
	Recovery (%)	84.29%	91.32%	100.14%	90.34%

The field sensor calibration was performed prior to carrying out the survey. Every time the meter was switched on, after an appropriate amount of time (approx. 10 minutes) a test point was measured ~10 times to check the measurement consistency. Variance was < (±) 3%. To maintain the accuracy of field-based κ measurements, air measurements were taken in between surface measurements to allow for any drift in the measurement sequence to be identified. The meter was 'zeroed' if air measurements fell outside the ± 0.5 x 10^{-5} tolerance level applied.

The MS2B sensor is calibrated electronically, to ensure the validity of the κ^{lab} values obtained, a calibration standard was used to check the stability of the measurement (Dearing, 1999). The calibration sample has a value of 3062 x 10^{-5} SI units. Every 10 samples, the calibration sample measurement was repeated. If a drift in air measurements was detected, samples were removed from the sensor, the meter was zeroed and the measurement repeated. The soil samples were compressed into each container to capacity and weights ranged from 8.48g to 14.55g.

3.3.8. Spatial analysis of metals and MS

Inverse Distance Weighting (IDW) was applied for the interpolation of elemental and magnetic data. Spatial interpolation maps (Fig. 3.6.) were prepared using the extension Geostatistical Analyst within ArcGIS® ArcMap™ v.10.2 (©2013 ESRI). This method is based on the assumption that the value of a particular variable at a location which has not been sampled is the weighted average of known values of that variable within its vicinity. Weights are inversely associated with the distances between the unknown value point location and determined value point locations. The inverse distance weight is dependent on a constant, known as a power parameter. Points closer to the unknown value point can have much more influence over the determined value based on the power parameter (Lu and Wong, 2008). In the current study, a power parameter of 2 was applied to the elemental and magnetic data during geostatistical analysis. Maps produced using a power parameter of 2 attribute more weight to samples closer to the unknown value. This results in a much more abrupt surface which highlights the complexity of the metal concentrations and the magnetic susceptibility signature present.

Local indicators of spatial association (LISA) (Anselin, 1995) maps of metals Pb, Cu, Zn and Fe and magnetic measurements κ and χ_{fd}% (see Fig. 3.6.) were created to identify statistically significant spatial clusters including high value areas (‘*high-high’*) and low value areas (‘*low-low’*) within the urban park. Spatial outliers are also featured, these are denoted as ‘*high-low*’ and ‘*low-high*’ on the LISA maps representing statistically significant outliers of high and low values in comparison to surrounding data values. Prior to LISA analysis, each of the datasets were transformed to an approximate normal distribution using a natural logarithm transformation (ln). The weight function used was based on K-nearest neighbours (8 neighbours) (Golden et al., 2015).

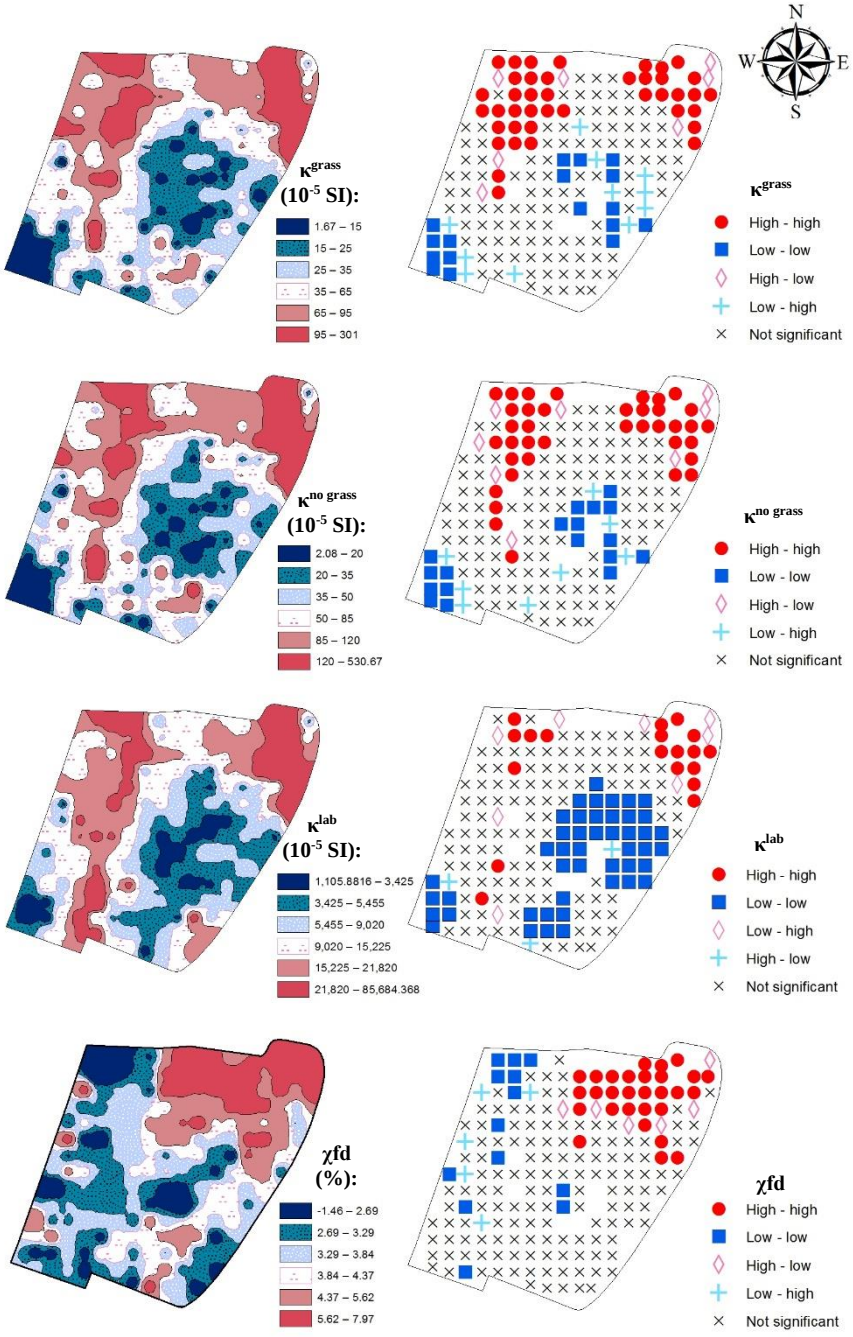
N
W
E
S
κgrass (10-5 SI):
1.67 – 15
15 – 25
25 – 35
35 – 65
65 – 95
95 – 301
κgrass
High - high
Low - low
High - low
Low - high
Not significant
κno grass (10-5 SI):
2.08 – 20
20 – 35
35 – 50
50 – 85
85 – 120
120 – 530.67
κno grass
High - high
Low - low
High - low
Low - high
Not significant
κlab (10-5 SI):
1,105.8816 – 3,425
3,425 – 5,455
5,455 – 9,020
9,020 – 15,225
15,225 – 21,820
21,820 – 85,684.368
κlab
High - high
Low - low
Low - high
High - low
Not significant
χfd (%):
-1.46 – 2.69
2.69 – 3.29
3.29 – 3.84
3.84 – 4.37
4.37 – 5.62
5.62 – 7.97
χfd
High - high
Low - low
High - low
Low - high
Not significant

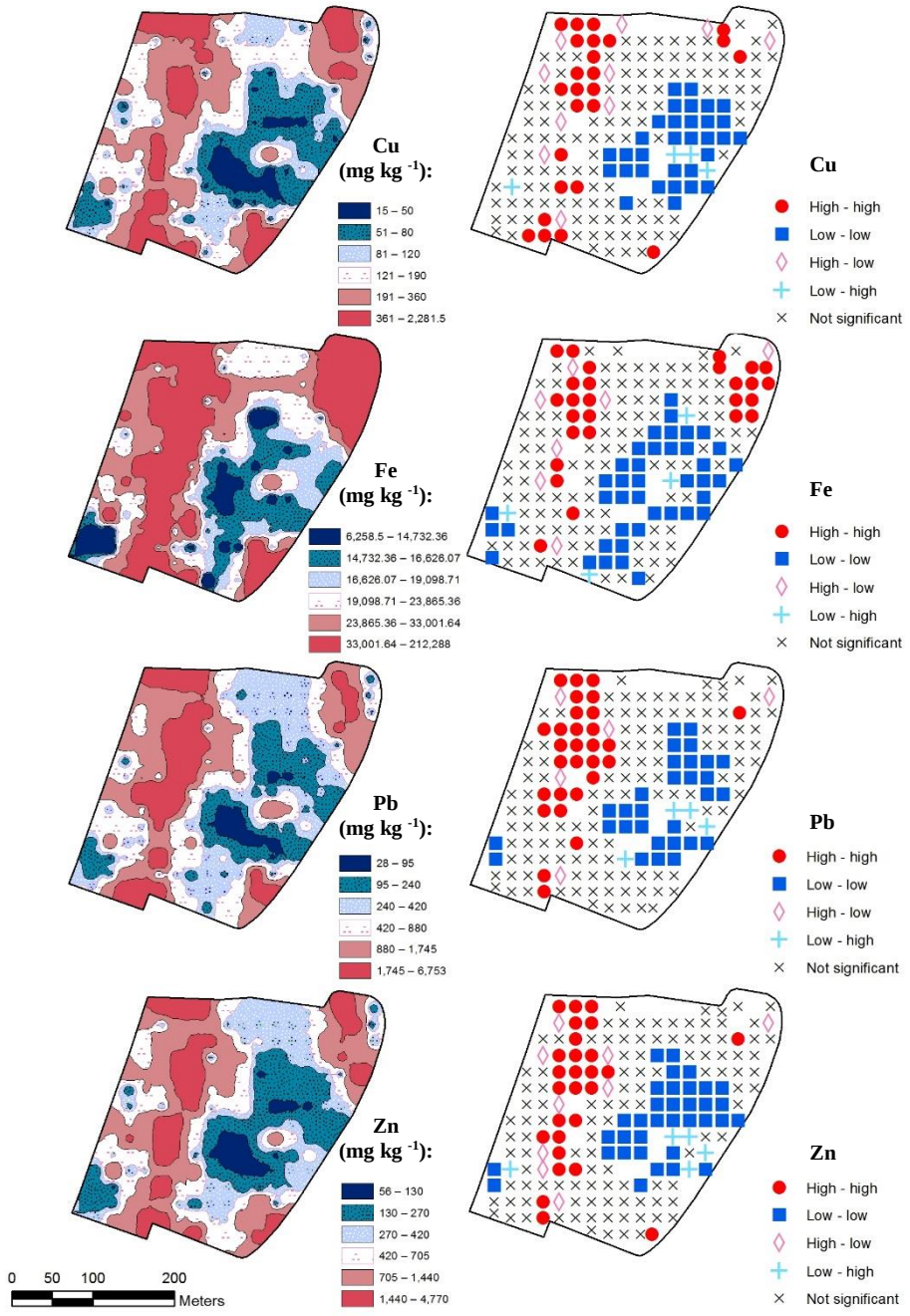

Fig. 3.6. *Total concentration distributions and local Moran's I maps of volume magnetic susceptibility – κ^{grass} and $\kappa^{no\ grass}$ (10^{-5} SI), mass specific magnetic susceptibility – κ^{lab} (10^{-5} SI), percentage frequency dependence – χ_{fd}% and metal concentrations – Cu, Fe, Pb and Zn (mg kg $^{-1}$).*

3.3.9. Principal Component Analysis (PCA)

Principal Component Analysis is a technique used for data reduction (Boruvka et al., 2005; Manta et al., 2002). The data must be correlated in order for PCA to be employed. Standardization is applied when variables are measured at different scales or in circumstances where some variables may have much larger variance than others and dominate the first principal component (Miller and Miller, 2005). This is avoided by making all variables carry equal weight. PCA is employed in the current study to aid in the interpretation of interrelations between metals and magnetic susceptibility in the contaminated urban topsoils.

3.3.10. Data transformation

Due to the heterogenic nature of geochemistry, a Kolmogorov-Smirnov test of normality was applied to the metal and MS datasets. A Kolmogorov-Smirnov test is based on the maximum deviation of the observed value series from the theoretical model (Webster and Oliver, 2007). Each of the MS sampled populations were non-normally distributed at the significance level of $p < 0.01$. A natural logarithmic transformation (ln) was performed in an attempt to transform the measured values to a new scale on which the distributions are closer to normality. Distributions of Cu(ln)=0.200, Pb(ln)=0.200, Zn(ln)=0.200 and $\kappa^{no\ grass}$(ln)0.083, $p<0.05$ were found to follow a normal distribution while Fe(ln)=0.000 and κ^{grass}=0.035, $p<0.05$ were brought close to a normal distribution as illustrated in fig. 3.7.

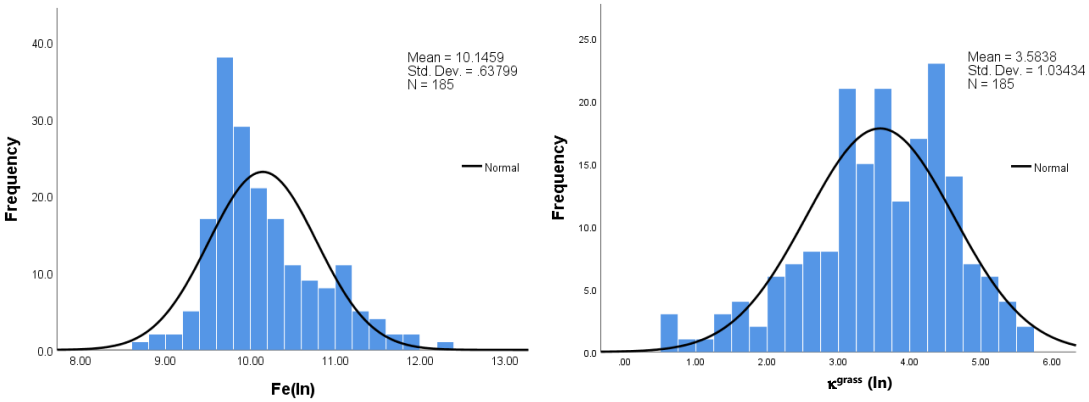

Fig. 3.7. *Histograms with normal distribution curves of Fe(ln) and* κ^{grass}*(ln)*

3.3.11. Integrated Pollution Index (IPI)

The degree of metal contamination at the site was also demonstrated by the calculation of an accumulation factor (Integrated Pollution Index (IPI)) (Jung, 2001 as cited in Morton-Bermea et al., 2009) in relation to background regional values (Zhang, 2006) for quantitative purposes. Integrated pollution index (IPI) refers to the mean value of all Pollution Indices (PI) of all the metals being investigated (Morton-Bermea et al., 2009). PI are commonly used to discriminate metal contamination and evaluate the degree of environmental pollution present at a site (Dong et al., 2014). An IPI was calculated for the soil samples defined as:

$$IPI = ((PI_{Cu}) + (PI_{Fe}) + (PI_{Pb}) + (PI_{Zn})) / 4 \quad \textbf{[2]}$$

Where $PI = (Concentration^{median}{}_i / Background^{median}{}_i)$, $_i$ = metal

3.3.12. Data analysis and statistics

Data management was carried out in Microsoft® Excel 2010. Statistical analysis was performed using SPSS 21 (IBM®SPSS® Statistics). Hotspot analysis was applied to the data using GeoDa™1.4.6. (Anselin et al., 2006) and spatial analysis was carried out within a Geographical Information System (ESRI® ArcGIS® ArcMap™ 10.2) using ArcGIS World Imagery

basemap service. Mass specific magnetic susceptibility measurements were determined using Multisus v2.44 software.

3.4. Results and Discussion

3.4.1.Effects of grass coverage on Magnetic susceptibility (MS)

A strong linear relationship is shown (fig. 3.8.) between κ^{grass}, $\kappa^{no\ grass}$ and κ^{lab}. The two κ(ln) datasets exhibited a strong positive Pearson's correlation coefficient of $r^2 = 0.966$, $n = 185$, $p < 0.01$. In general, κ^{grass} obtained initially, prior to the grass layer being disturbed, are lower than $\kappa^{no\ grass}$. This is because the sensitivity of the sensor for magnetic susceptibility measurements diminishes exponentially with distance from material (Lecoanet et al., 1999). The MS2D search loop is affected by material up to ~10 cm from the sensor. For example, a layer of vegetation 0.5 cm in depth can possibly reduce the MS2D measurement to 75% of the expected value compared to if the sensor was directly placed on the soil surface (Dearing, 1999). The gap between the sensor and the soil surface is a contributing factor in relation to grass height effects. This gap was at least 1.5cm from the sensor to the soil surface for grasses < 10 cm and 1.5-2 cm for grasses > 10-15 cm.

In this study, a substantial amount of magnetic susceptibility data was obtained in the field. The length of grass blades were also recorded at each sampling point. The grass heights ranged from 2-15 cm. A possible negative relationship between grass height and the difference in κ values was explored and a Spearman's rho correlation revealed a weak significant r_s value between these parameters ($r_s = 0.253$, $n = 185$, $p < 0.05$).

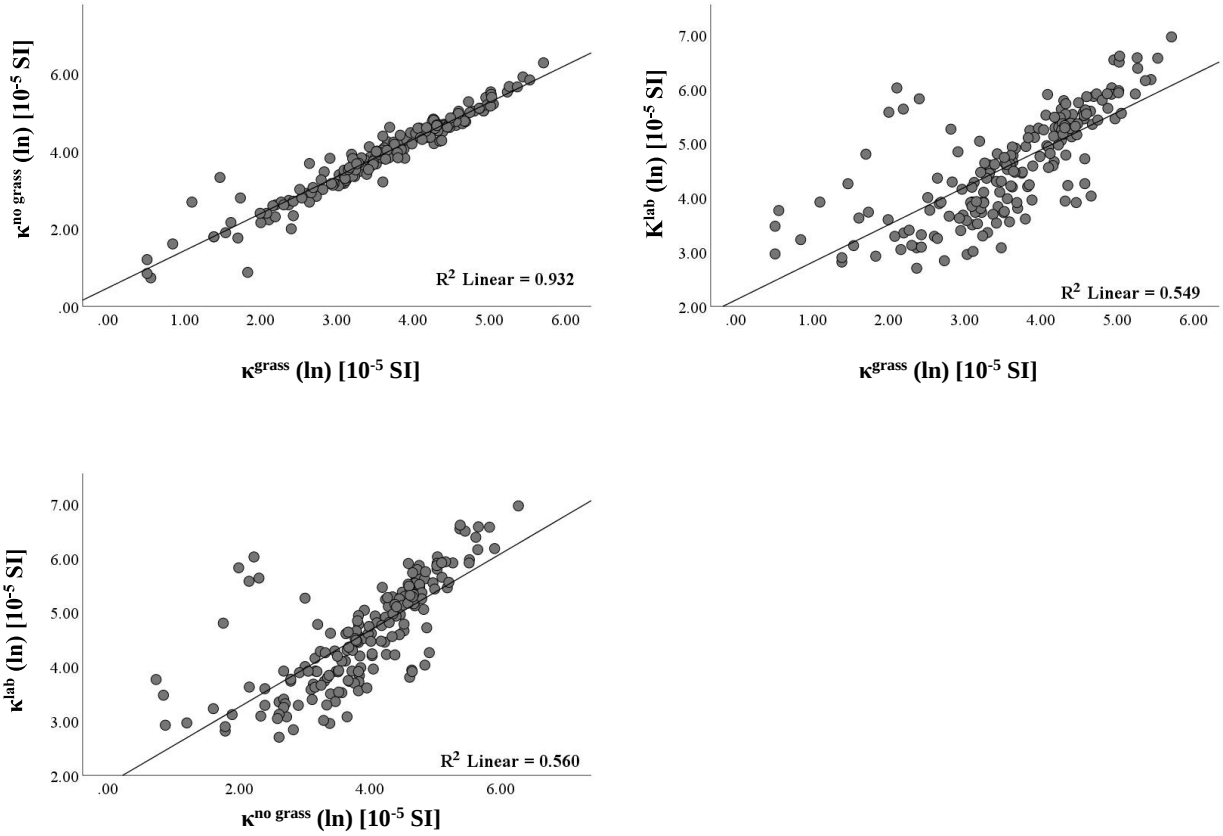

Fig. 3.8. *Relationships between three log-transformed magnetic susceptibility measurements: field-based volume magnetic susceptibility (10^{-5} SI) taken with and without grass coverage ($\kappa^{grass}(ln)$ and $\kappa^{no\ grass}(ln)$, respectively) and volume magnetic susceptibility of soil samples ($\kappa^{lab}(ln)$).*

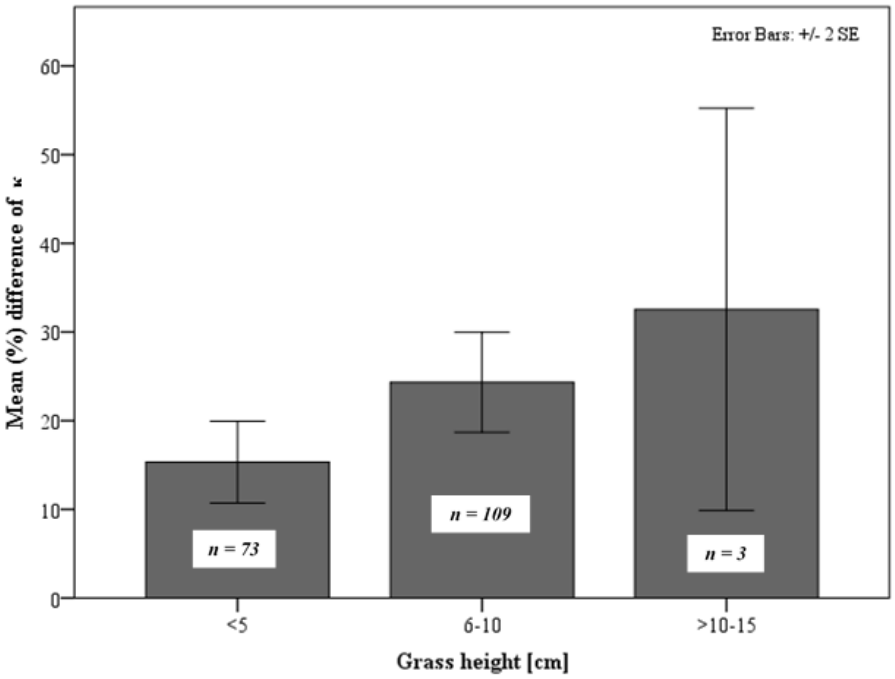

Fig. 3.9. *Effects of grass blade length on approximate mean (%) κ measurement error at grass height ranges: ≤5, 6-10 and >10-15 cm*

Where $\kappa^{no\ grass}$ was considered as the true κ magnetic susceptibility measurement for each sampling point, κ^{grass} measurements were treated as a recovery percentage and the (%) κ measurement error determined using the following calculation: $100 - (\kappa^{grass}/\kappa^{no\ grass} * 100) = \%\ \kappa$ error. This graph demonstrates a trend in the data and infers an inverse relationship between grass coverage height and κ. Error bars are included to depict the level of variance within each of the three grass height groups. The level of variance is smaller in group 1 (<5 cm) and group 2 (6-10 cm) in comparison to group 3(>10-15 cm). This is related to site specific conditions at the study area. The study site is a well-maintained urban park. Grass is mowed on a regularly basis resulting in a low average blade height of 6 cm at the sampled points. This demonstrates that grass height has the potential to effect measurements but not in the present study where maintained grass dominates the study area.

Based on these results, it is not possible to create a model to identify approximate (%) κ measurement error at varying grass heights. The level of variance across the grass height groups mean the results are not robust enough

to back calculate to create a model. The (%) difference calculated in this study can be used as an indicator for other urban soil studies carrying out κ surveys where grass coverage maybe a factor.

It is possible that where very high grasses are present in e.g. wastelands or roadsides that grass height may affect κ measurement obtained. But due to the small number of sample points with grass blade height >10 cm (n = 3), it does not affect the predictive power in the current study.

Four magnetic susceptibility datasets, two volume magnetic susceptibility (κ^{grass} and $\kappa^{no\ grass}$) one mass specific magnetic susceptibility of soil samples converted to volume MS measurement (κ^{lab}) and percentage frequency dependence (χfd%), were obtained in this study and the descriptive statistics are summarized in Table 3.2. The measurements suggested there are elevated and varied levels of magnetic particulates present in these urban soils. Shape parameters of each of the volume datasets were positively skewed to the right (1.724-2.274) with high levels of peakness (3.533-7.625). Strong correlation between the MS measurements were identified with positive correlations between κ^{lab}(ln) and the in-situ measurements of κ^{grass}(ln) and $\kappa^{no\ grass}$(ln) of r^2 =0.752 and r^2 =0.756, n =185, p <0.01, respectively.

Table 3.2. *Summary of κ magnetic susceptibility (10^{-5} SI) taken in the field, mass specific magnetic susceptibility represented as κ magnetic susceptibility of soil samples κ^{lab} (10^{-5} SI) and frequency dependence (%) of soil samples. Measurement uncertainties are within a standard deviation of the measurements, which are as follows: κ^{lab} (± 0.37), χ_{fd}% (± 1.8) and κ (± 0.3).*

	κ^{lab}	χ_{fd}%	κ_{grass}	$\kappa_{no\ grass}$
	κ [10^{-5} SI]	**[%]**	**κ [10^{-5} SI]**	**κ [10^{-5} SI]**
Min	2091	-1.46	1.7	2.1
25 %	4328	2.87	21.8	27.5
Median	9022	3.84	37.7	53.3
75 %	18764	4.70	74.8	105.3
Max	85684	7.97	301.0	530.7
S.D.	12290	1.51	50.8	73.8

A small number of studies have recognised and addressed the issue of conformity in experimental protocols for field-based magnetic susceptibility monitoring (Schibler et al., 2002; Schmidt et al., 2005; D'Emilio et al., 2007 and Zawadzki et al., 2010). As part of the MAGPROX team, Schibler et al. (2002) evaluated the data reproducibility of a magnetic susceptibility sensor. The team established a few standard procedures including: "*The preferred surface is covered well in litter and no surface preparation is allowed, except for removing high grass or branches*" (Schibler et al., 2002, p.47). Different perspectives exist in the literature on whether the removal of a vegetation layer is necessary (Table 3.3). Some studies do not explicitly state their methodological approach. In contrast, others have recommended the removal of vegetation prior to measuring magnetic susceptibility, in their unique soil environments. A magnetic susceptibility field survey was carried out at a brownfield site in close proximity to a former industrial iron production and processing site. The strong metal contamination signal and shallow and deep χ measurements of the brownfield site were interpreted to be related to historic localised deposition associated with nearby mining activity whereas the κ of the grass layer was inferred to represent more recent airborne particulate pollution (Schmidt et al., 2005). A forested region was the chosen site for an investigation of the relationship between the κ of different soil horizons of the forest floor. The removal of a thick organic layer was found to increase the magnetic susceptibility measurements of forest topsoils (Zawadzki et al., 2010). In the laboratory, the κ measurement reproducibility of soil, covered by vegetation and after the vegetation was removed was also examined. Based on the distribution shapes of each dataset, the removal of the vegetation layer during field surveys was considered necessary due to its inhomogeneity (D'Emilio et al., 2007).

Table 3.3. *Summary of literature that used a MS2D sensor with the objective of obtaining magnetic susceptibility measurements in soil studies.*

Author(s)	Vegetation Cover
Kapička et al., 1997, p.392	Not stated. *"Attention was paid to keep constant conditions at the measurement sites (regarding e.g. vegetation cover)"*
Ďurža, 1999	Not stated.
Lecoanet et al., 1999	Not stated. Measurements taken at graduated distances from ground.
Petrovský et al., 2000	Not stated.
Strzyszcz and Magiera, 2001	Not stated.
Schibler et al., 2002, p.47	Vegetation. *"The preferred measurement surface is covered well in litter. No surface preparation is allowed, except for removing high grass or branches".*
Boyko et al., 2004	Vegetation. Followed procedure prescribed by Schibler *et al.,* 2002.
Gautam et al., 2004	Not stated.
Schmidt et al., 2005	Grass/Grass removed.
D'Emilio et al., 2007	Grass/Grass removed
Magiera and Zawadzki, 2007, p.21	Vegetation. "Measurements were taken without any surface preparation, except for cutting of high grass or removal of twigs".
Zawadzki et al., 2007, p.115	Vegetation. "Measurements were taken without any surface preparation, except for cutting of high grass or removal of twigs".
Kapička et al., 2008	Grass
Magiera et al., 2008	Vegetation. Followed procedure prescribed by Schibler *et al.,* 2002.
D'Emilio et al., 2010	Grass removed
Zawadzki et al., 2010	Vegetation/ Without vegetation layer (referred to as organic layer (OL)
D'Emilio et al., 2012	Grass removed
Łukasik et al., 2015	Surface measured using an MS2D Bartington loop.
Grison et al., 2016	The soil surface volume magnetic susceptibility was measured.

In regards to urban soils, the results of this study suggest it is not necessary to remove the grass prior to obtaining magnetic susceptibility measurements in the field. Although vegetation can cause reduced contact with the soil surface, the shape and penetration range of the instrument sensor (to a depth of 10cm) allow for the detections of anthropogenic particles present in deeper horizons. Lower value, diamagnetic minerals in the upper organic layers may dilute the measurement slightly but not detrimentally particularly when greater levels of particles are present. The main argument in favour of removing the vegetation layer is that most anthropogenic contaminants accumulate at a depth of 3-7 cm (Zawadzki et al., 2010) but this may be pathway specific, e.g. atmospheric deposition versus landfill leachate. Furthermore, a vegetative cover, including *Lolium perenne* prevents the spreading of metal-associated particles via wind erosion or water and reduces the mobility of metals through root secretion and precipitation processes (Vangronsveld et al., 1995).

Thick upper organic layers may significantly influence the measured κ due to limitations of the penetration range, e.g. 50% of the magnetic susceptibility measurement comes from the top 1.5cm (Lecoanet et al., 1999). Unlike urban soils, undisturbed soils are likely to be allowed to develop over time naturally and accumulate anthropogenic particles via atmospheric deposition. Urban soils are transient as urban environments are constantly modified, leading to a more complicated contamination sources and pathways.

3.4.2. Metals

The anthropogenic influence at the park is evident in the Pb, Cu and Zn concentrations, the result of previous municipal and industrial waste disposal activities. However, there is a much smaller PI for Fe between the park soil samples and median regional background values (Zhang, 2006). The maximum pollution indices are 84.5 for Cu, 116.43 for Pb and 56.12 for Zn. Concentrations of Fe did not differ much from background levels and this is reflected in a PI of 1.25. This may be because Fe content in topsoil is largely related to the parent rock (Morton-Bermea et al., 2009). Based on the metal concentration PIs we can speculate that the soils of this urban park remain

heavily contaminated with Pb as the largest contributor. The park has a complex history of contamination and remediation activities and this leads to a diverse genetic origin. Pearson correlation values between Pb(ln) and Cu(ln) r^2 =0.931, Pb(ln) and Zn(ln) r^2 =0.941 and Cu(ln) and Zn(ln) r^2 =0.962, n=185, p <0.01 show a strong positive linear correlation suggesting the same contamination source, resulting from industrial waste. There is also a positive correlation between Fe(ln) and Pb(ln) r^2 =0.841, Fe(ln) and Cu(ln) r^2 = 0.883 and Fe(ln) and Zn(ln) r^2 =0.863, n =185, p <0.01 but it is slightly lower. These soils subjected to high levels of contamination with elevated concentrations of Pb, Cu and Zn show slightly lower Fe content and this may be due to Fe being associated with low levels of anthropogenic influence (Morton-Bermea et al., 2009).

Table 3.4. *Summary of total concentrations of metals (mg kg^{-1}) analysed by PXRF.*

	***n* = 185**	**Cu**	**Fe**	**Pb**	**Zn**
		mg kg $^{-1}$	%	mg kg $^{-1}$	mg kg $^{-1}$
Min		15.00	0.06	28.00	56
R_Q[a]		60.50	0.16	171.50	197
Median		121.00	0.22	420.00	421
Max		2281.50	2.12	6753	4770
PI (median)[b]		4.48	0.13	7.24	4.95
Regional soils (median)[c]		27.00	1.70	58.00	85.00

[a] R_Q: Interquartile range
[b] PI: Enrichment factor
[c] Local Galway regional soils (Zhang, 2006)

3.4.3. Spatial distribution of metals and magnetic susceptibility

Elevated levels of magnetic susceptibility can be found throughout this urban amenity signifying the strong presence of magnetic particles in these soils. The contents of metals Cu, Pb and Zn in the surveyed samples exhibit a considerable enhancement compared to regional background values. Total Pb concentrations ranged from 28 to 6753 mg kg $^{-1}$. Copper concentrations were found to vary from 15 to 2281.50 mg kg $^{-1}$ and Zn ranged from 56 to 4770 mg kg $^{-1}$. In the north east corner, soils are reddish in colour indicating the presence of industrial waste. Historically, a fertilizer plant was situated adjacent to the park. It processed pyrite ores. There are some high value

outliers of Cu, Zn and particularly Pb in this area. In particular, a '*high-high*' value cluster of Fe, κ^{grass}, $\kappa^{no\ grass}$ and κ^{lab} are a feature of this area which coincides with a '*high-high'* value cluster of χ_{fd}%. High χ_{fd}% and Fe are associated with natural processes. Reddish soils can also be found in the central west region of the sports ground, covering the main football pitch where patches of bare soil are visible particularly around goal posts (Carr et al., 2008). The magnetic susceptibility sensor was also capable of detecting these sections of the park as the most highly contaminated. The northern and western sections are the most heavily laden with ferro/ferri magnetic particulates; this is demonstrated by the '*high-high'* value clusters featured in fig. 3.6. Volume magnetic susceptibility measured with a grass vegetative layer present shared a very similar spatial dispersal pattern of high magnetic susceptibility with measurements taken without the grass layer present and with the laboratory-based mass specific susceptibility of the soil samples.

A small inversely proportional relationship exists between χ_{fd}% and metal concentrations Cu(ln) r^2=-0.176, Fe(ln) r^2=-0.148, Pb(ln) r^2=-0.162 and Zn(ln) r^2=-0.206, n =185, p <0.05. '*Low-low'* value clusters of χ_{fd}% featured in the north western region of the study area contrast with '*high-high'* value clusters in each of the volume magnetic susceptibility and metal concentration spatial distribution maps. A useful magnetic criteria proposed for the identification of soils containing significant concentrations of pollution particles includes elevated χ(>380 x 10^{-8} m^3 kg^{-1}) and frequency dependence of <3% (Evans and Heller, 2003).

Some remediation work has occurred in the central eastern region of the park and there is a clear distinction in soil depth where soils have been imported and placed there. The less contaminated soils are found in this central eastern area. Volume magnetic susceptibility values are < 85 x 10^{-5} SI units in these imported soils. However, there are still some elevated levels of Pb (201-500 mg kg^{-1}) and Zn (201-500 mg kg^{-1}) present which are much greater than the median Galway regional background values (Zhang, 2006) see Table 3.4. There is also a statistically significant low level of ferro/ferri magnetic particulates featured in each of the magnetic susceptibility maps in the

southern western tip of the park. The metal maps feature *relatively* low value concentrations in this area also.

3.4.4. Comparison between κ and gradiometry surveys

A single magnetic reading cannot determine the exact depth or source of magnetic anomalies in soils. However, with a magnetometer in gradiometer mode acquiring two simultaneous readings from two sensors located at different heights it is possible to estimate the depth of magnetic anomalies based on their associated measurements (Gibson and George, 2004). A spatial distribution map of the surveyed sub-section of the study area can be seen in figure 3.10. It is possible to identify magnetic anomalies in the lower half of the surveyed region visible as white spots. The gradient value observed is very much dependent on what the anomaly (materials) present is in the subsurface. A material such as a tin can exhibiting paramagnetic behavior would contribute to the anomaly value whereas a glass would have a diamagnetic behavior and result in a reduced gradient. The appearance of the anomaly values observed in fig. 3.10. suggest the presence of metallic objects below the surface. A comparison to the results obtained in this survey can be made with field- and laboratory-based κ measurements and Fe content of soils samples taken in this section of the park. Each of these parameter maps featured elevated measurements in same locale as the gradiometry survey. This infers that the enhanced magnetic measurements recorded in this area are related to anthropogenic waste as proposed and not naturally occurring.

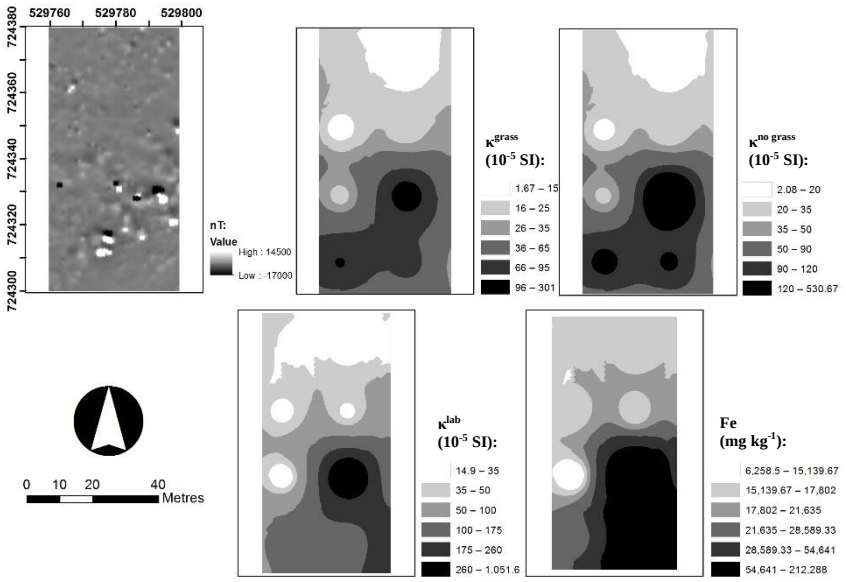

Figure 3.10. *Gradiometry survey (up to ~ 2 m depth of subsurface) of a south eastern section of the park compared to* κ^{grass}*(10* $^{-5}$ *SI),* $\kappa^{no\ grass}$*(10* $^{-5}$ *SI),* κ^{lab}*(10* $^{-5}$ *SI) and Fe(mg kg* $^{-}$*1), of the same section.*

3.4.5.Relationship between metals and κ

A Pearson's correlation was performed, after necessary data transformations between magnetic susceptibility datasets κ^{grass}(ln), $\kappa^{no\ grass}$(ln) and κ^{lab}(ln) and metals Cu(ln), Fe(ln), Pb(ln) and Zn(ln). The *r* coefficients revealed a statistically significant relationship (see fig. 3.11.) between each of the metals and magnetic susceptibility at the p <0.01 level. As expected, the strongest correlation was present between κ^{lab}(ln) and each of the metals: Cu(ln) 0.855, Fe(ln) 0.859, Pb(ln) 0.826 and Zn(ln) 0.834, p <0.01. However, importantly both κ^{grass} (ln) and $\kappa^{no\ grass}$(ln) are also strongly correlated to each of the metals and share a similarity in r^2 value (κ^{grass}(ln): Cu(ln) 0.589, Fe(ln) 0.599, Pb(ln) 0.601, Zn(ln) 0.591;$\kappa^{no\ grass}$(ln):Cu(ln) 0.591, Fe(ln) 0.600, Pb(ln) 0.605, Zn(ln) 0.587, n =185, p <0.01.

Strong linear relationships are visible between each of the (ln)magnetic susceptibility datasets and the (ln)metals. It is evident that the magnetic signal is increased for soils affected by anthropogenic waste.

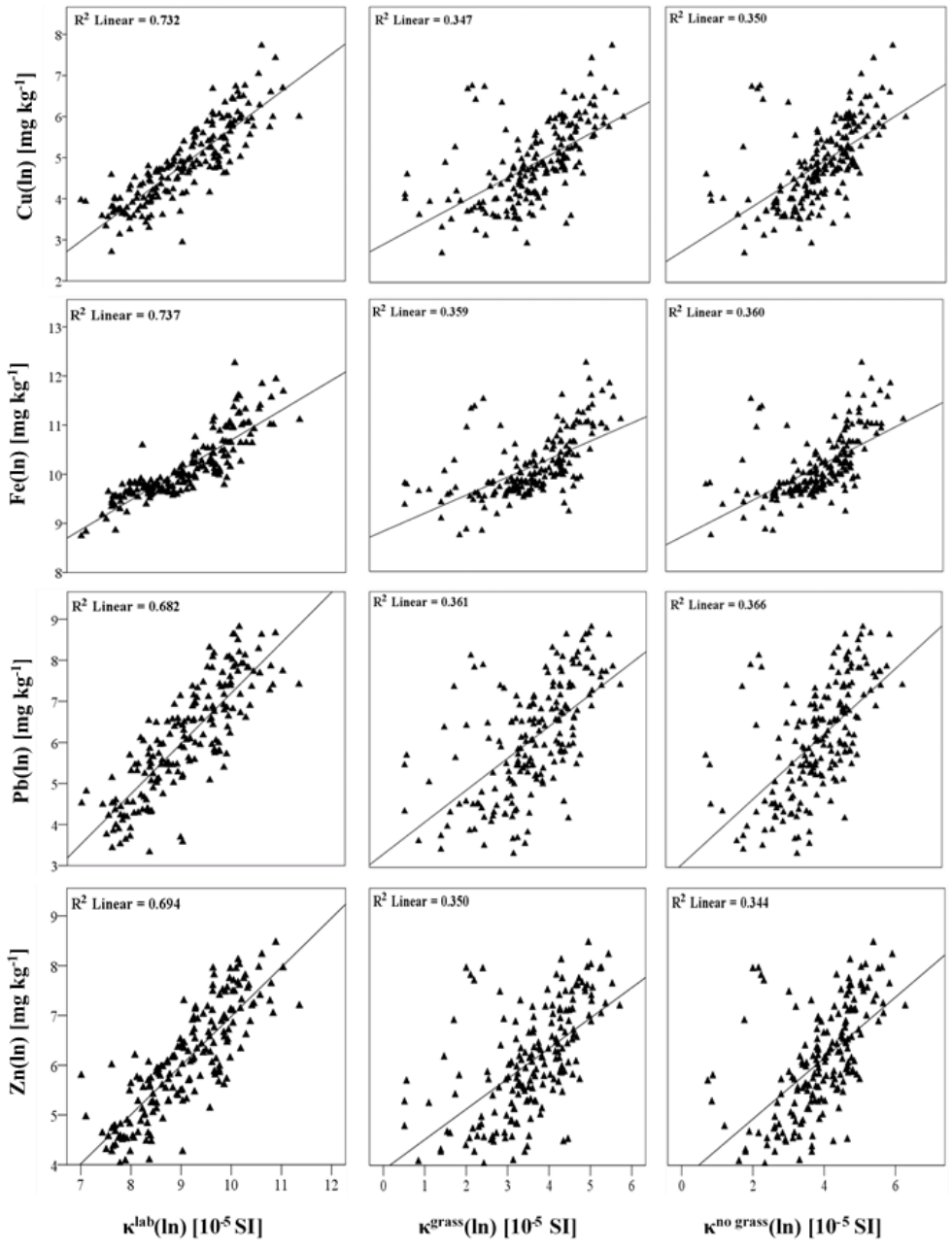

Figure 3.11. *Scatterplots demonstrating the relationship between log-transformed metal concentrations Cu, Fe, Pb and Zn (mg kg^{-1}) and volume magnetic susceptibility measurements of soil samples (κ^{lab}) and field-based measurements (κ^{grass} and $\kappa^{no\ grass}$) (10^{-5} SI).*

3.4.6. Principal Component Analysis (PCA)

A Principal Component Analysis (PCA) was applied to the metal and magnetic susceptibility datasets. Prior to carrying out PCA, the variables were standardised as they were on different measurement scales.

Table 3.5. *Values of extracted rotated Factor loadings for volume magnetic susceptibility measurements and metal concentrations and estimated communalities of the variables.*

	Variable	Factor I	Factor II	Communalities
Volume magnetic susceptibility	κ^{grass}	0.317	0.800*	0.960
	$\kappa^{no\ grass}$	0.286	0.928*	0.980
Volume magnetic susceptibility	κ^{lab}	0.493*	0.948*	0.883
Metals	Cu	0.871*	0.321	0.861
	Fe	0.853*	0.395*	0.884
	Pb	0.873*	0.292	0.848
Metals	Zn	0.907*	0.322	0.926
Cumulative % variance		75.978	90.621	
Rotated sum of cumulative % variance		49.955	40.666	

* Dominant variable in each Factor.

Based on the eigenvalues and scree plot results, two principal components (Factor I and Factor II) were selected. The obtained Factors were rotated using varimax which allows an easier interpretation of factor loadings (Boruvka et al., 2005; Manta et al., 2002). The resulting rotated Factor loadings and Communalities can be found in Table 3.5. The cumulative variance % explained by Factor I and Factor II is >90%.

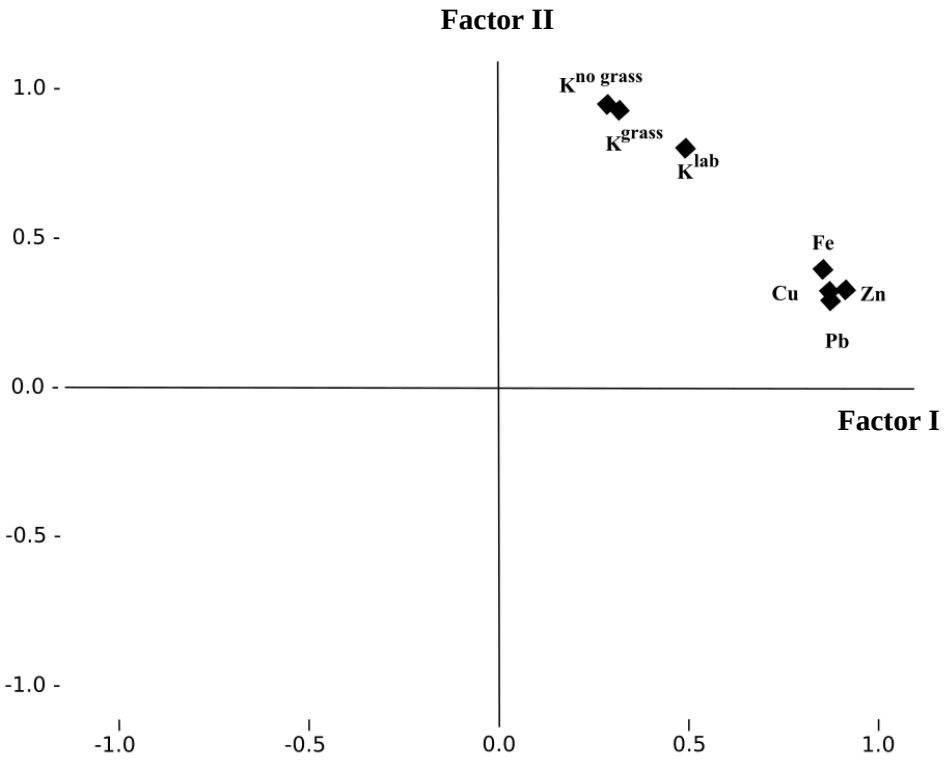

Figure 3.12. *Projection featuring the correlation between the soil parameters magnetic susceptibility measurements and metal concentrations and principal components Factor I and Factor II.*

A projection of the components is illustrated in figure 3.12. All three magnetic susceptibility measurements are positively loaded close to the second axis. κ^{grass} and $\kappa^{no\ grass}$ are particularly close reiterating the similarity between the before and after in-situ magnetic susceptibility measurement of the topsoil. Factor I is dominated by Cu, Fe, Pb and Zn. Based on the history of the site, the spatial distributions and Pearson correlations of these metals, they are interpreted as having an anthropogenic origin. The concentrations of Cu, Pb and Zn are tightly clustered close to the first axis and indicate they are of the same anthropogenic origin in the topsoil sampled. The position of Fe close to this clustering is understandable as Fe is heavily associated with the anthropogenic metals. It is also being pulled up towards the Factor II group as magnetic susceptibility measurements are associated with Fe-minerals. Laboratory-based κ^{lab} features in between both clusters but is more closely associated with Factor II. Based on previous interpretations of the

relationships of κ^{lab} and the other soil parameters the reason for this positioning may be related to this technique being a more sensitive measure of the field-based MS measurements and because the measurements were made on the same homogenised soil samples as were used to obtain the metal concentrations. The results of the PCA were also plotted on two maps which correspond well with the spatial distribution maps of magnetic susceptibility and metal concentrations. Factor I which was dominated by the metal variables (Cu, Fe, Pb and Zn mg kg^{-1}) closely resembles the distributions of metals which feature elevated concentrations expanding the length of the western section and dominating the northeast corner. Factor II primary elevated values are spread across the northern section and down the western pitch, a pattern mirrored by the volume magnetic susceptibility distribution maps.

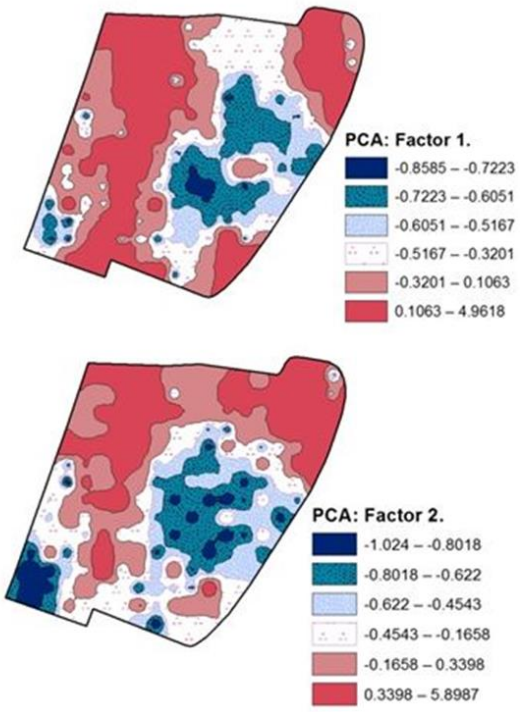

Figure 3.13. *Map of spatial distribution of Factor I (metal concentrations) and Factor II (magnetic susceptibility).*

3.5. Conclusions and Recommendations

This study reaffirms the suitability of in-situ magnetic susceptibility technique as a proxy for metal contamination in soils, particularly where high levels of metal contamination are present. However magnetic susceptibility monitoring may not be as efficient at identifying less contaminated levels of metals in soils. Importantly, it demonstrates that a grass layer has little effect on the ability to identify metal contaminated soils using magnetic susceptibility techniques (in particular, when grass height <10cm). Therefore, we suggest that the removal of a grass layer prior to determination of magnetic susceptibility is unnecessary for urban soils. This is reflected in the similarity between the magnetic susceptibility maps and correlation coefficients. Highly spatially associated maps of volume magnetic susceptibility were created from datasets obtained with/without grass layer present during measurement. κ^{grass} also shared a good linear correlation and similarity in spatial distribution with κ^{lab} and concentrations of Cu, Fe, Pb and Zn. Although a robust model to assist in identifying when grass coverage height significantly affects κ measurement could not be calculated. It is worth bearing in mind the % κ measurement errors obtained in this study particularly when surveying in long grasses.

Overall, magnetic surveying is a viable alternative to geochemical surveying and can be used for large scale campaigns investigating potentially contaminated soils with anthropogenic particulates.

Acknowledgements

The authors would like to thank He Yaxin, Ellen McGrory, Sorcha Dolan, Joe Fenwick and Siubhán Comer for their assistance during fieldwork. The authors wish to acknowledge funding from the Department of Communications, Energy and Natural Resources under the National Geoscience Programme 2007-2013 (Griffiths Award). The views expressed in the study are the authors' own and do not necessarily reflect the views and

opinions of the Minister for Communications, Energy and Natural Resources or any government body.

3.6. References

Anselin, L. (1995). 'Local indicators of spatial association – LISA'. *Geographical Analysis*, 27(2), pp. 93-115.

Anselin, L., Syabri, I., Kho, Y. (2006). 'GeoDa: An Introduction to Spatial Data Analysis'. *Geographical Analysis*, 38(1), pp. 5-22.

Arienzo, M., Adamo, P., Cozzolino, V. (2004). 'The potential of *Lolium perenne* for revegetation of contaminated soil from a metallurgical site'. *The Science of Total Environment*, 319, pp. 13-25.

Averis, B. (2013). *Plants and Habitats: An introduction to common plants and their habitats in Britain and Ireland*. East Linton, UK: Ben Averis,.

Bandaranayake, W., Qian, Y.L., Parton, W.J., Ojima, D.S., Follett, R.F., (2003). 'Estimation of Soil Organic Carbon Changes in Turfgrass Systems Using the CENTURY Model'. *Agronomy Journal*, 95, pp. 558-563.

Beddows, A.R. (1967). 'Lolium Perenne L'. *Journal of Ecology*, 55(2), pp. 567-587.

Bityukova, L., Scholger, R., Birke, M. (1999). 'Magnetic susceptibility as indicator of environmental pollution of soils in Tallinn'. *Physics and Chemistry of the Earth (A)*, 24(9), pp. 829–835.

Boruvka, L., Vacek, O. and Jehlička, (2005). 'Principal component analysis as a tool to indicate the origin of potentially toxic elements in soils'. *Geoderma*, 128, pp. 289-300.

Boyko, T., Scholger, R., Stanjek, H., MAGPROX Team (2004). 'Topsoil magnetic susceptibility mapping as a tool for pollution monitoring: repeatability of in-situ measurements'. *Journal of Applied Geophysics*, 55(3–4), pp. 249–259.

Canbay, M., Aydin, A., Kurtulus, C. (2010). 'Magnetic susceptibility and heavy metal contamination in topsoils along the Izmit Gulf Coastal area and IZAYTAS (Turkey)'. *Journal of Applied Geophysics*, 70(1), pp. 46-57.

Carr, R., Zhang, C., Moles, N., Harder, M. (2008). 'Identification and mapping of heavy metal pollution of a sports ground in Galway City, Ireland, using a portable XRF analyser and GIS'. *Environmental Geochemistry and Health*, 30(1), pp. 45-52.

Chaparro, M.A.E., Gogorza, C.S.G., Chaparro, M.A.E., Irurzun, M.A., Sinito, A.M. (2006). 'Review of magnetism and pollution studies of various environments in Argentina'. *Earth Planets Space*, 58(10), pp. 1411–1422.

Cockerham, S.T., Gibeault, V.A., Van Dam, J., Leonard, M.K. (1990). 'Tolerance of several cool- season turfgrasses to simulated sports traffic'. In: Schmidt et al. (Eds.), *Natural and artificial playing fields: Characteristics and safety features*. American Society for Testing and Materials. STP 1073, pp. 85–95.

Dalan, R.A. (2008). 'A Review of the Role of Magnetic Susceptibility in Archaeogeophysical Studies in the USA: Recent Developments and Prospects'. *Archaeological Prospection*, 15, pp. 1-30.

Dao, L., Morrison, L. and Zhang, C. (2012). 'Bonfires as a potential source of metal pollutants in urban soils, Galway, Ireland'. *Applied Geochemistry*, 27 (4), pp. 930-935.

Dao, L., Morrison, L., Zhang, H. and Zhang, C. (2014). 'Influences of traffic on Pb, Cu and Zn concentrations in roadside soils of an urban park in Dublin, Ireland'. *Environmental Geochemistry and Health*, 36 (3), pp. 333-343.

Dao, L., Morrison, L., Kiely, G. and Zhang, C. (2013). 'Spatial distribution of potentially bioavailable metals in surface soils of a contaminated sports ground in Galway, Ireland'. *Environmental Geochemistry and Health*, 35 (2), pp. 227-238.

Dao, L., Morrison, L. and Zhang, C. (2010). 'Spatial variation of urban soil geochemistry in a roadside sports ground in Galway, Ireland'. *Science of the Total Environment*, 408 (5), pp. 1076-1084.

Dearing, J.A. (1999). *Environmental Magnetic Susceptibility. Using the Bartington MS2 System*, 2nd edn. Kenilworth, England, UK: Chi Publishing.

D'Emilio, M., Chianese, D., Coppola, R., Macchiato, M., Ragosta, M. (2007). 'Magnetic susceptibility measurements as proxy method to monitor soil pollution: Development of experimental protocols for field surveys'. *Environmental Monitoring and Assessment*, 125, pp. 137-146.

D'Emilio, M., Caggiano, R., Coppola, R., Macchiato, M., Ragosta, M. (2010). 'Magnetic susceptibility measurements as proxy method to monitor soil pollution: the case study of S. Nicola di Melfi'. *Environmental Monitoring and Assessment*, 169, pp. 619-630.

D'Emilio, M., Macchiato, M., Ragosta, M. and Simoniello, T. (2012). 'A method for the integration of satellite vegetation activities observations and magnetic susceptibility measurements for monitoring heavy metals in soil'. *Journal of Hazardous Materials*, 241-242, pp. 118-126.

Dong, C., Zhang, W., Ma, H., Feng, H., Lu, H., Dong, Y., Yu, L. (2014). 'A magnetic record of heavy metal pollution in the Yangtze River subaqueous delta'. *Science of Total Environment*, 476-477, pp. 368-377.

Ďurža, O. (1999).' Heavy metals contamination and magnetic susceptibility in soils around a metallurgical plant'. *Physics and Chemistry of the Earth (A)*, 24, pp. 541-543.

El Baghdadi, M., Barakat, A., Sajieddine, M., Nadem, S. (2012). 'Heavy metal pollution and soil magnetic susceptibility in urban soil of BeniMellal City (Morocco)'. *Environmental Earth Sciences*, 66(1), pp. 141-155.

Evans, M.E. and Heller, F. (2003). *Environmental Magnetism: Principles and Applications of Enviromagnetics*. San Diego, California, USA: Academic Press.

Fabian, K., Reimann, C., McEnroe, S.A., Willemoes-Wissing, B. (2011). 'Magnetic properties of terrestrial moss (*Hylocomium splendens*) along a north–south profile crossing the city of Oslo, Norway'. *Science of the Total Environment*, 409(11), pp. 2252-2260.

Fenwick, J. (2004). *An Integrated Approach to Archaeological Survey Design, Methodology and Data Management. Computer Applications and Quantitative Methods in Archaeology. Computer Applications in Archaeology, Faculty of Archaeology*. Leiden University 2004.

Fialová, H., Maier, G., Petrovský, E., Kapička, A., Boyko, T., Scholger, R., MAGPROX Team (2006). 'Magnetic properties of soils from sites with different geological and environmental settings'. *Journal of Applied Geophysics*, 59(4), pp. 273-283.

Flanders, P.J. (1999). 'Identifying fly ash at a distance from fossil fuel power stations'. *Environmental Science and Technology*, 33(4), pp. 528-532.

Gaffney, C. and Gater, J. (2003). *Revealing The Buried Past. Geophysics for Archaeologists*. Stroud, Gloucestershire: Tempus Publishing Ltd,.

Galway Advertiser (2008). *A May procession in the Claddagh, c1935*. Galway Advertiser, 2 October 2008.

http://www.advertiser.ie/galway/article/2313/a-may-procession-in-the-claddagh-c1935 (Accessed on 22.07.2016).

Gautam, P., Blaha, U., Appel, E., Neupane, G. (2004). 'Environmental magnetic approach towards the quantification of pollution in Kathmandu urban area, Nepal'. *Physics and Chemistry of the Earth*, 29, pp. 973-984.

Gautam, P., Blaha, U., Appel, E. (2005). 'Magnetic susceptibility of dust-loaded leaves as a proxy of traffic-related heavy metal pollution in Kathmandu city, Nepal'. *Atmospheric Environment*, 39(12), pp. 2201-2211.

Gibson, P. J. and George, D. M. (2013). *Environmental applications of geophysical surveying techniques*, 2nd edn. New York: Nova Science Publishers Inc.

Girault, F., Perrier, F., Poitou, C., Isambert, A., Théveniaut, H., Laperche, V., Clozel-Leloup, B., Douay, F. (2016). 'Effective radium concentration in topsoils contaminated by lead and zinc smelters'. *Sci. Total Environ*, 566-567, pp. 865-876.

Golden, N., Morrison, L., Gibson, P.J., Potito, A.P., Zhang, C. (2015). 'Spatial patterns of metal contamination and magnetic susceptibility of soils at an urban bonfire site'. *Applied Geochemistry*, 52, pp. 86-96.

Grison, H., Petrovský, E., Kapička, A., Stejskalova, S. (2016). 'Magnetic and chemical parameters of andic soils and their relation to selected pedogenesis factors'. *Catena*, 139, pp. 179-190.

Hanesch, M., Rantitsch, G., Hemetsberger, S., Scholger, R. (2007). 'Lithological and pedological influences on the magnetic susceptibility of soil: Their consideration in magnetic pollution mapping'. *Science of the Total Environment*, 382(2-3), pp. 351-363.

Hoffmann, V., Knab, M., Appel, E. (1999). 'Magnetic susceptibility mapping of roadside pollution'. *Geochemistry International*, 66(1–2), pp. 313–326.

Innov-X Systems, Inc. (2013). *Handheld XRF Revolutionizes Environmental Testing. The Best Environmental Analyzer in the World*. <http://yosemite.epa.gov/r9/sfund/r9sfdocw.nsf/3dc283e6c5d6056f88257426007417a2/e599199dc919b049882576a300616943/$FILE/Attachment%202.pdf> (Accessed on 15.09.14).

Jordanova, D., Veneva, L., Hoffmann, V. (2003). 'Magnetic susceptibility screening of anthropogenic impact on the Danube River sediments in Northwestern Bulgaria-preliminary results'. *Studia Geophysica et Geodaetica*, 47, pp. 403–418.

Jung, M.A. (2001). 'Heavy metal contamination of soils and waters in and around the Imcheon Au-Ag mine, Korea'. *Applied Geochemistry*, 16, pp. 1369-1375.

Kapička, A., Petrovský, E., Jordanova, N. (1997). 'Comparison of in-situ Field Measurements of Soil Magnetic Susceptibility with Laboratory Data'. *Studia Geophysica et Geodaetica*, 41(4), pp. 391–395.

Kapička, A., Petrovský, E., Ustjak, S., Macháčková, K. (1999). 'Proxy mapping of fly-ash pollution of soils around a coal-burning power plant: a case study in Czech Republic'. *Journal of Geochemical Exploration*, 66(1), pp. 291–297.

Kapička, A., Petrovský, E., Fialová, H., Podrázský, V., Dvořák, I. (2008). 'High resolution mapping of anthropogenic pollution in the Giant Mountains Natural Park using soil magnetometry'. *Studia Geophysica et Geodaetica*, 52(2), pp. 271-284.

Kletetschka, G., Žila, V., Wasilewski, P.J. (2003). 'Magnetic anomalies on the tree trunks'. *Studia Geophysica et Geodaetica*, 47(2), pp. 371−379.

Lecoanet, H., Lévêque, F., Segura, S. (1999). 'Magnetic susceptibility in environmental applications: comparison of field probes'. *Physics of the Earth and Planetary Interiors*, 115, pp. 191-204.

Lees, J.A. (1999). 'Evaluating magnetic parameters for use in source identification, classification and modelling of natural and environmental materials'. In: Walden, J., Oldfield, F., Smith, J. (Eds.), *Environmental Magnetism: A Practical Guide, Technical Guide*, vol.6. Quaternary Research Association, London.

Liu, S.G., Bai, S.Q. (2006). 'Study on the correlation of magnetic properties and heavy metals content in urban soils of Hangzhou City, China'. *Journal of Applied Geophysics*, 60, pp. 1-12.

Liu, Q.S., Roberts, A.P., Larrasoana, J.C., Banerjee, S.K., Guyodo, Y., Tauxe, L. and Oldfield, F. (2012). 'Environmental Magnetism: Principles and Applications'. *Reviews of Geophysics*, 50(4), pp. 1-50.

Lu, S.G., Bai, S.Q., Xue, Q.F. (2007). 'Magnetic properties as indicators of heavy metals pollution in urban topsoils: a case study from the city of Luo Yang, China'. *Geophysical Journal International*, 171, pp. 568-580.

Lu, G.Y., Wong, D.W. (2008). 'An adaptive inverse-distance weighting spatial interpolation technique'. *Computers & Geosciences*, 34, pp. 1044-1055.

Lucideon.com (2019). *Inductively Coupled Plasma Optical Emisson Spectroscopy (ICP-OES).* https://www.lucideon.com/testing-characterization/techniques/inductively-coupled-plasma-optical-emission-spectroscopy-icp-oes (Accessed on 28.08.2019).

Łukasik, A., Szuszkiewicz, M., Magiera, T. (2015). 'Impact of artifacts on topsoil magnetic susceptibility enhancement in urban parks of the Upper Silesian Conurbation datasets'. *Journal of Soils and Sediments*, 15(8), pp. 1836-1846.

Mackey, E.A., Christopher, S.J., Lindstrom, R.M., Long, S.E., Marlow, A.F., Murphy, K.E., Paul, R.L., Popelka-Filcoff, R.S., Rabb, S.A., Sieber, J.R., Spatz, R.O., Tomlin, B.E., Wood, L.J., Yen, J.H., Yu, L.L., Zeisler, R., Wilson, S.A., Adams, M.G., Brown, Z.A., Lamothe, P.L., Taggart, J.E., Jones, C., Nebelsick, J. (2010). 'Certification of Three NIST Renewal Soil Standard Reference Materials for Element Content: SRM 2709a San Joaquin Soil, SRM 2710a Montana Soil I, and SRM 2711a Montana Soil II'. *NIST Special Publication,* 260-172. US Department of Commerce and the National Institute of Standards and Technology.

Magiera, T., Zawadzki, J. (2007). 'Using of high-resolution topsoil magnetic screening for assessment of dust deposition: comparison of forest and arable soil datasets'. *Environmental Monitoring and Assessment*, 125(1-3), pp. 19-28.

Magiera, T., Kapička, A., Petrovský, E., Strzyszcz, Z., Fialová, H., Rachwał, M., (2008). 'Magnetic anomalies of forest soils in the upper Silesia—Northern Moravia region'. *Environmental Pollution,* 156(3), pp. 618-627.

Magiera, T., Jabłońska, M., Strzyszcz, Z. and Rachwal, M. (2011). 'Morphological and mineralogical forms of technogenic magnetic particles in industrial dusts'. *Atmospheric Environment,* 45(25), pp. 4281-4290.

Maher, B.A. and Thompson, R. (Eds.) (1999). *Quaternary Climates, Environments and Magnetism*. Cambridge, UK.: Cambridge University Press,

Manta, D.S., Angelone, M., Bellanca, A., Neri, R. and Sprovieri, M. (2002). 'Heavy metals in urban soils: a case study from the city of Palermo (Sicily), Italy'. *The Science of the Total Environment*, 300, pp. 229-243.

Miller, J.N. and Miller, J.C. (2005). *Statistics and Chemometrics for Analytical Chemistry*. England, UK.: Pearson Education Ltd.

Morton-Bermea, O., Hernandez-Alvarez, E., Martinez-Pichardo, E., Soler-Arechalde, A.M., Lozano Santa-Cruz, R., Gonzalez, G., Beramendi-Orosco, L., Urrutia-Fucugauchi, J. (2009). 'Mexico City Topsoils: Heavy metals vs. magnetic susceptibility'. *Geoderma,* 151(3-4), PP. 121-125.

Norland, M.R., Veith, D.L. (1995). 'Revegetation of course taconite iron ore tailing using municipal solid waste compost'. *Journal of Hazardous Materials,* 41, PP. 123-134.

O'Dowd, P. (1993). *Down by the Claddagh*. Galway, Ireland: Kenny's Bookshop and Art Galleries Ltd.

Petrovský, E., Ellwood, B. (1999). 'Magnetic monitoring of air, land and water pollution'. In: Maher B.A. and Thompson, R. (Eds.), *Quaternary climates, environment and magnetism.* Cambridge, England, UK: Cambridge University Press.

Petrovský, E., Kapička, A., Jordanova, N., Knab, M., Hoffmann, V. (2000). 'Low-field magnetic susceptibility: a proxy method of estimating increased pollution of different environmental systems'. *Environmental Geology*, 39(3-4), pp. 312-318.

Salo, H., Bućko, M.S., Vaahtovuo, E., Limo, J., Mäkinen, J., Pesonen, L.J., (2012). 'Biomonitoring of air pollution in SW Finland by magnetic and chemical measurements of moss bags and lichens'. *Journal of Geochemical Exploration*, 115(1), pp. 69-81.

Schibler, L., Boyko, T., Ferdyn, M., Gajda, M., Höll, S., Jordanova, N., Rösler, N., MAGPROX Team (2002). 'Topsoil magnetic susceptibility mapping: data reproducibility and compatibility, measurement strategy'. *Studia Geophysica et Geodaetica*, 46(1), pp. 43–57.

Schmidt, A., Yarnold, R., Hill, M., Ashmore, M. (2005). 'Magnetic susceptibility as proxy for heavy metal pollution: a site study'. *Journal of Geochemical Exploration*, 85(3), pp. 109-117.

Soodan, R.K., Pakade, Y.B., Nagpal, A., Katnoria, J.K. (2014). 'Analytical techniques for estimation of heavy metals in soil ecosystem: A tabulated review'. *Talanta*, 125, pp. 405-410.

Strzyszcz, Z., Magiera, T. (2001). 'Record of industrial pollution in polish ombrotrophic peat bogs'. *Physics and Chemistry of the Earth, Part A: Solid Earth and Geodesy*, 26(11-12), pp. 859-866.

Thompson, R. and Oldfield, F. (1986). *Environmental Magnetism*. Winchester, Massachusetts: Allen and Unwin.

Vangronsveld, J., Van Assche, F., Clijsters, H. (1995). 'Reclamation of a bare industrial area contaminated by non-ferrous metals: In-situ metal immobilization and revegetation'. *Environmental Pollution*, 87(1), pp.51-59.

Verosub, K.L. and Roberts, A.P. (1995). 'Environmental Magnetism: Past, present and future'. *Journal of Geophysical Research*, 100, pp. 2175-2192.

Wang, X. S. and Qin, Y. (2005). 'Correlation between magnetic susceptibility and heavy metals in urban topsoil: a case study from the city of Xuzhou, China'. *Environmental Geology*, 49(1), pp. 10-18.

Webster, R. and Oliver, M.A. (2007). *Geostatistics for Environmental Scientists. Statistics in Practice*, 2nd edn. Chichester, West Sussex, England: Wiley & Sons Ltd.

Yang, T., Liu, Q., Zeng, Q., Chan, L. (2012). 'Relationship between magnetic properties and heavy metals of urban soils with different soil types and environmental settings: implications for magnetic mapping'. *Environmental Earth Sciences*, 66(2), pp. 409-420.

Zawadzki, J., Fabijańczyk, P., Magiera, T. (2007). 'The influence of forest stand and organic horizon development on soil surface measurement of magnetic susceptibility'. *Polish Journal of Soil Science*, XL(2), pp. 113−124.

Zawadzki, J., Fabijańczyk, P., Magiera, T., Strzyszcz, Z. (2010). 'Study of litter influence on magnetic susceptibility measurements of urban forest topsoils using the MS2D sensor'. *Environmental Earth Sciences*, 61(2), pp. 223-230.

Zawadzki, J., Fabijańczyk, Magiera, T., Rachwał, M. (2015). 'Geostatistical Microscale Study of Magnetic Susceptibility in Soil Profile and Magnetic Indicators of Potential Soil Pollution'. *Water, Air & Soil Pollution*, 226(5), pp. 142-149.

Zhang, C. (2006). ‘Using multivariate analysis and GIS to identify pollutants and their spatial patterns in urban soils in Galway, Ireland’. *Environmental Pollution*, 142(3), pp. 501-511.

Zhang, C., Qiao, Q., Appel, E., Haung, B. (2012). ‘Discriminating sources of anthropogenic heavy metals in urban street dusts using magnetic and chemical methods’. *Journal of Geochemical Exploration*, 119-120, pp. 60-75.

Zhu, Z., Han, Z., Bi, X., Yang, W. (2012). ‘The relationship between magnetic parameters and heavy metal contents of indoor dust in e-waste recycling impacted area, Southeast China’. *Science of the Total Environment*, 433, pp.302-308.

Chapter 4.

4. USE OF ORDINARY COKRIGING WITH MAGNETIC SUSCEPTIBILITY FOR MAPPING LEAD CONCENTRATIONS IN SOILS OF AN URBAN CONTAMINATED SITE

Chapter 4.

This manuscript has been submitted to the *Journal of Soils and Sediments* for peer review and consideration of publication (March, 2019).

Chapter 4:

USE OF ORDINARY COKRIGING WITH MAGNETIC SUSCEPTIBILITY FOR MAPPING LEAD CONCENTRATIONS IN SOILS OF AN URBAN CONTAMINATED SITE

4.1. Abstract

Lead contamination is a prevalent issue affecting cities worldwide. Traditional fieldwork and laboratory analysis techniques can be time-consuming and costly. The purpose of this study was to evaluate the performance of ordinary cokriging (CK) when volume magnetic susceptibility (κ) is used as a co-variable for spatial interpolation of Pb in contaminated urban soils. The study was conducted in contaminated urban soils of a former unregulated landfill site. A total of 76 surface samples (0-10 cm) were collected using a systematic sampling grid separated by 20m intervals. Magnetic susceptibility measurements were taken at a higher density of 10m intervals with 288 measurements. Thus, it was used as an auxiliary variable to predict Pb concentrations by the CK procedure with an aim to improve spatial interpolation of Pb. To determine the effectiveness of CK over ordinary kriging (OK) procedure, the spatial density of samples was reduced prior to interpolation. A total of ~15%, 25%, 35% and 50% of the Pb samples were randomly selected and reserved for validation. Omnidirectional semivariograms and covariograms were fitted using log-transformed data prior to interpolation. Measurements of κ shared a significant relationship with Pb concentrations by the Spearman's Rho correlation analysis (r_s = 0.676, p < 0.01). The effectiveness of the CK procedure over OK was determined using validation datasets. Statistically, the results showed that lnPb when its auxiliary relations with lnκ were used in CK had overall lower "Root Mean Square Error" (RMSE) and predicted lnPb values from the CK procedure had a higher r^2 value with measured lnPb than OK. A model produced by the CK procedure with a reduced spatial density of 49 Pb points

provided the more accurate map with a RMSE of 0.550 and an r^2 value of 0.730, $p < 0.01$ level. This technique can potentially reduce fieldwork and soil analysis costs considerably. Measurements of Pb and κ must share a substantial level of spatial continuity to implement CK effectively Where applicable, it can be used in the site-specific evaluation of hazard posed by Pb exposure to ecosystems, human health or water bodies in urban green spaces, roadside soils, allotments or brownfield sites.

4.1. Introduction

In recent years, geostatistical interpolation techniques have increasingly been employed in the prediction of spatial distributions of metal contaminants in urban soils (Zawadzki and Fabijańczyk 2008; Xie et al. 2011; Dankoub et al. 2012; Dao et al. 2013; Li 2016; Zawadzki et al. 2016; Hou et al. 2017; Wang et al. 2018). Spatial predictions of soil geochemistry are often important for planning, risk assessment and decision-making purposes in environmental management (Li 2016). However, anthropogenic influences on urban soils can be from a combination of sources including industrial, commercial or domestic activities and from local or diffused sources (Cheng et al. 2014). Lead in particular is ubiquitous in nature and can be emitted from the burning of low-grade coal, fuel combustion, flaking of leaded paint and industrial processing of ores. As a result, the needs for remedial practices may vary within the field; mapping the spatial distribution is a key component of site-specific pollution management (Posthuma et al. 2008). However, due to costs involved in fieldwork and chemical analysis, it may not always be possible to conduct dense sampling campaigns or obtain repeat measurements (Xie et al. 2011) and these factors can greatly influence the quality and accuracy of spatial distribution prediction models of contaminants like Pb in urban soils.

The contamination of urban soils and green spaces by lead and other known toxic metals is a prevalent issue affecting many cities worldwide (Mielke 1994; Chlopecka et al. 1996; Facchinelli et al. 2001; Möller et al. 2005; Chen et al. 2007; Lu et al. 2009; Mielke et al. 2011; Cheng et al. 2014; Motuzova et al. 2014; Wawer et al. 2015; Gu et al. 2016). In comparison to other non-essential elements, lead contamination is widespread (Flegal and Smith 1992) and persistent (Mielke et al. 2011). The accumulation of lead dust in soils has

been identified as a major health concern for children (Louis et al. 2006). Consequently, accurate interpolations of potentially toxic elements like Pb in urban soils is vitally important from an ecological and human health perspective.

Magnetic susceptibility (MS) measurements provide an indication of a material's ability to be magnetised in an external magnetic field. In natural materials like soil, MS measurements can provide an indication of the types of minerals present, particularly iron-bearing minerals (Dearing 1999) like technogenic magnetic particles associated with anthropogenic activities. Soil magnetic susceptibility (MS) is already frequently used to determine potential anthropogenic soil pollution (Strzyszcz et al. 1996; Strzyszcz and Magiera 1998; Ďurža 1999; Kapička et al. 1999; Petrovský et al. 2000; Hanesch and Scholger 2002; Jordanova et al. 2003; Canbay et al. 2010; Karimi et al. 2011; Dankoub et al. 2012; Lu et al. 2016; Magiera et al. 2016; Fabijańczyk et al. 2017; Rachwał et al. 2017). Different sensors are required to determine the magnetic susceptibility of different materials and each measure at different sensitivity levels. Mass specific magnetic susceptibility (χ) can be measured using a MS2B sensor attached to a MS2 meter (Bartington® Instruments 2019) and is recorded at a high sensitivity (10^{-8} m^3 kg^{-1}). It can be used to detect very fine ferrimagnetic minerals in 10 cm^3 mass specific samples. While volume magnetic susceptibility (κ) is a field-based surface technique, measured at 10^{-5} SI units and can be acquired using a MS2D probe attached to a MS2 meter (Bartington® Instruments 2019), measuring to a depth of ~10cm; it is used mainly for mapping and reconnaissance surveys (Dearing 1999). Anthropogenically influenced lead has been shown to have strong associations with MS in urban and industry-affected soils. A strong correlation coefficient was observed between κ and Pb (r = 0.927) in Morocco (El Baghdadi et al. 2012). Strong correlations were also found (r = 0.72) in Iran (Karimi et al. 2011) and in Turkey (r = 0.78) (Canbay et al. 2010) between χ measurements and Pb concentrations in urban soils. High correlation coefficients of Pb and χ are prevalent in industry affected soils (Heller 1998; Jordanova et al. 2003; Blaha et al. 2008; Dankoub et al. 2012). Magnetic minerals and pollutants are genetically related (Kapička et al. 1999; Hanesch and Scholger 2002). During high temperature combustion, Fe oxides

such as hematite, magnetite and oxyhydroxides like goethite are formed from iron sulphides (Flanders 1994; Hanesch and Scholger 2002). These magnetic minerals can act as carriers of metals through adsorption (El Baghdadi et al. 2012) and incorporation into their crystalline structures (Kapička et al. 1999; Waychunas et al. 2005). Magnetic particles and metals may also be produced at the same time but form separate particles (Kapička et al. 1999).

Geostatistical techniques, such as kriging, have been used successfully to describe and predict the spatial variability of environmental parameters and to integrate this information into mapping through spatial interpolation (Elbasiouny et al. 2014). Ordinary kriging is a basic application of the kriging technique. It is known as the best linear unbiased predictor (BLUP) because it assumes that the mean value of the estimation error is equal to zero therefore minimizing the variance of the estimation error (Zawadzki et al. 2009). There are many examples in the literature where it has been used for the spatial evaluation of soil parameters including: soil depths (Knotters et al. 1995), soil hydraulic conductivity (Basaran et al. 2011), soil organic carbon (Bhunia et al. 2018) and soil contamination (Hooker and Nathanail 2006; Rossiter 2007; Zawadzki et al. 2009; Xie et al. 2011; Dao et al. 2013; Hou et al. 2017). A novel use of magnetometry measurements with geostatistical analysis to predict soil contamination was applied by Zawadzki and Fabijańczyk (2008) and involved the application of the Co-Est method to reduce soil contamination prediction uncertainties by transforming the auxiliary variable (MS measurements of the soil surface) into measurements of the target variable (measurements of the soil profile) and then carrying out an ordinary kriging interpolation of the resulting primary variable. An advantage of the kriging technique over deterministic methods is the generation of estimates of the uncertainty surrounding each interpolated value (Johnston et al. 2001; Pereira et al. 2017). A condition of the OK procedure is the availability of an adequate number and distribution of observed values of the geochemical variable of interest. When this requirement is not met, CK can potentially be applied as an alternative method when related measurements are collected at a higher density. The CK procedure is a variant of kriging, which enables the use of multiple measurements as co-variables in the interpolation of a target geochemical measurement when the co-variables and target variable are

correlated (Zawadzki and Fabijańczyk 2008), have spatial autocorrelation and share spatial cross-correlation.

The use of indicator cokriging with MS measurements to assess soil contamination has also been explored (Zawadzki et al. 2009; Fabijańczyk et al. 2017). A critical or threshold value system for magnetic susceptibility measurements was developed whereby the values established are dependent upon the natural background values of the study area and pilot geochemical measurements used as an indicator of soil metal content (Fabijańczyk et al. 2017). Indicator kriging maps were also developed to create probability distribution maps of metal concentrations in order to evaluate the performance of MS probability maps, as indicators of metal contamination in forest soils (Zawadzki et al. 2009). Geostatistical techniques have been applied in the past to predict the distribution of lead contamination in urban soils (Hooker and Nathanail 2006; Dao et al. 2013). Lead was also used as an auxiliary variable in the cokriging of Cd and Zn concentrations in contaminated agricultural soils (Juang and Lee 1998). However, the combined use of ordinary cokriging, κ and Pb have not previously been used in the assessment and interpolation of lead contamination in urban soils.

The aim of the present study was to apply the interpolation technique CK with κ measurement for the mapping of anthropogenic lead loadings in urban soils. The objective was to evaluate the robustness of the procedure in comparison to OK using efficiency and error estimates. The spatial density of the Pb dataset was reduced multiple times (-15%, -25%, -35% and -50%) with the objective of identifying a limit to the spatial density required of the target variable when implementing the CK procedure. The findings could potentially reduce the chemical analysis costs involved in the investigation of Pb contaminated or polluted urban topsoils by reducing the number of samples required for analysis that would otherwise be required if not applying the CK technique of interpolation.

4.3. Materials & Methods

4.3.1. Study site

The study site comprises of an urban green space which covers an area of approximately 4 ha and is located in the Claddagh region, Galway City,

Ireland. Formerly, the region now known as South Park was an area of marshland on the seafront which was periodically flooded by spring tides. Gradually the site was infilled and used as an unregulated municipal landfill site until the 1970s. Some of the waste disposed of at the site consisted of ash waste from an artificial fertilizer plant and various other wastes including glass, plastics, cans, bottle caps, wires, etc. The site was remediated in the 1980s and has since been used as a recreational park containing playing pitches. Attention was drawn to the site in 2004 after a city-wide study of pollutants present in soils was carried out (Zhang 2006). Since this initial study, a number of studies have been conducted at the site relating to soil contamination (Carr et al. 2006; Dao et al. 2013; Golden et al. 2017).

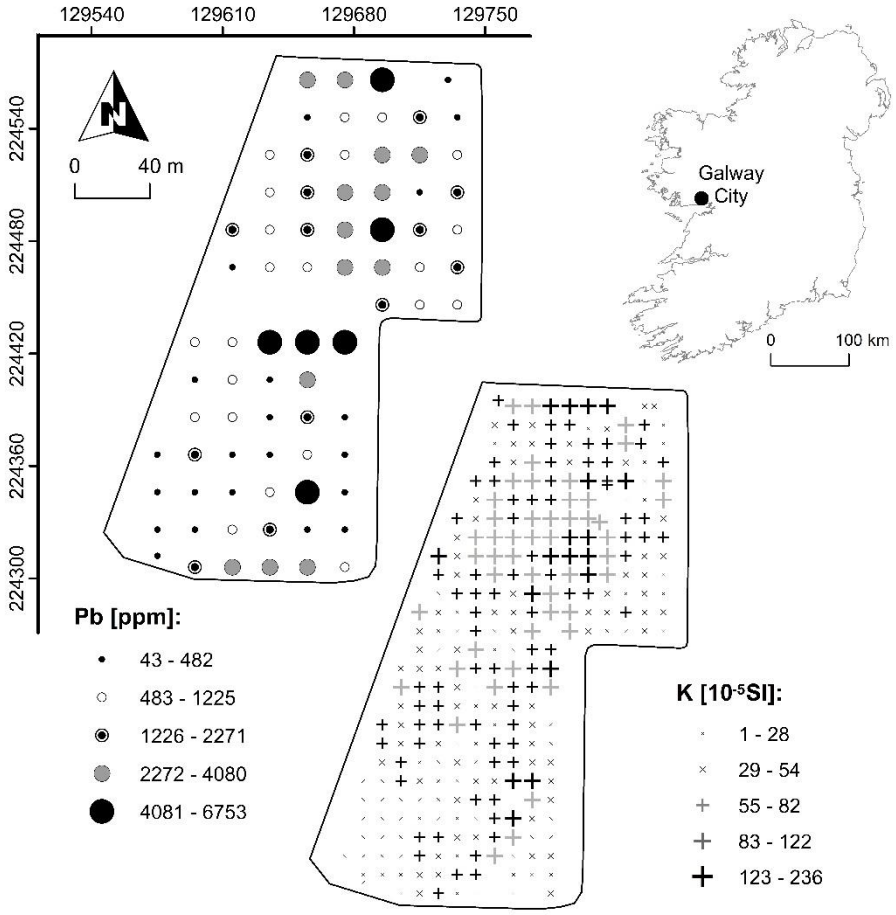

Fig. 4.1. *Geographical location of study area, soil samples (n=76) with lead concentrations (in ppm) and volume magnetic susceptibility (n=288) measurement points*

4.3.2. Soil sampling and analysis of Pb content

Soil samples (*n*=76) were collected using a systematic sampling grid from the superficial soil layer of 0-10 cm. To achieve systematic soil sampling a rectangular grid separated by 20-meter intervals was overlaid on a map using a GIS. Soil samples were collected at each sampling point on the grid (Fig. 4.1.) and consisted of three soil subsamples collected within a 1m radius of the sampling point on the grid. The sub-samples were composited and placed in labelled polythene bags for analysis.

In preparation for analysis, soil samples were dried at room temperature ~20°C and sieved to <2 mm fraction. Samples were analyzed for total metal content using a portable X-ray fluorescence analyser (PXRF, ©Innov-X Systems, Inc.). A PXRF is an analytical tool used for the rapid, non-destructive, simultaneous multi-elemental determination of a wide range of materials. It can be used to determine contamination patterns and define metals present at the site for comprehensive site investigation. The XRF technique can be used as a preliminary screening tool as it allows one to locate areas of interest to be investigated further (Moioli and Seccaroni 2000). The Innov-X employed is capable of the simultaneous analysis of 25 separate elements in seconds including As, Ba, Cd, Co, Cr, Cu, Fe, Hg, K, Mn, Pb, Sr, Ti, Zn (Weindorf et al. 2014).

XRF analysis allows you to identify the composition of a material. The technique works by discharging an x-ray beam into the material's atomic structure with primary radiation, which then makes the electrons in the material excited and it emits secondary radiation. The energy from this fluorescence is measured and its characteristics can then be analysed and identified (Bruker.com 2019).

To carry out the analysis, soil samples are kept in polythene bags and measured for 120 s. Two measurements of the lead concentration from each composite soil sample were determined by PXRF, and the average of the two measurements was calculated and used to represent each soil sample. The limit of detection (LOD) varies by element, with higher atomic numbered elements generally allowing for lower detection limits (Weindorf et al. 2011). Pb has LODs of 10-15 ppm (dependent on sample types and presence of interfering elements) (Innov-X Systems 2019).

4.3.3. Volume magnetic susceptibility (κ)

A Bartington MS2 meter (©Bartington Instruments Ltd.) with a MS2D probe attached was used to obtain the κ measurements. It contains a coil, which is attached to a source of alternating voltage and produces an alternating magnetic field. When a material is placed within a close proximity of the magnetic field produced, the frequency of this field changes with the magnetization of the material (Schibler et al. 2002). The magnetic susceptibility is calculated, and the value is displayed by the instrument in SI units ($x10^{-5}$ SI) (Schibler et al. 2002). In terms of surface soil measurements, the magnetic response is attributed to the top 6-10 cm of the land surface (Dearing 1999).

A systematic sampling grid at 10-meter intervals was employed to collect the *n*=288 volume magnetic susceptibility measurements (κ). This grid intercepted the soil sampling grid at 20-meter intervals where both soil samples and κ measurements were collected together. Care was taken to ensure the soil samples were removed from the same points as the κ measurements were recorded. At each point on the sampling grid, three surface measurements were taken. The mean of two air measurements taken before and after each measurement was subtracted from each surface κ measurement and represented a blank-value correction, and the mean of the three surface measurements taken at each grid point was used as the representative measurement for each location (Golden et al. 2017).

4.3.4. Quality control

Soil certified reference materials (CRMs) (Montana I (SRM 2710a) and Montana II (SRM 2711a)) from the National Institute of Standards and Technology, USA (NIST) were selected for validation of the PXRF analysis technique. These CRMs contain mean total concentrations of anthropogenic Pb loadings at intermediate (SRM 2711a) and high (SRM 2710a) levels and were included to provide a robust test of the analytical procedure. Every ten measurements, a CRM was analysed for quality control purposes. Table 4.1. displays the percentage recovery of total Pb in the soil CRMs as determined by PXRF. SRM 2710a and SRM 2711a demonstrated particularly good recovery rates of ~100%.

A standard value for 'background' κ measurements on-site was established. A location was designated, and measurements were recorded at this point at the beginning of each survey campaign. The mean background measurement of 49.2 10^{-5} SI was calculated with a standard deviation of ± 1.6 and on average, the measurements taken at this point differed ± 2.6% from the mean. These results indicate a high level of stability in the instrument's performance.

4.3.5. Geostatistical analysis

In the present study, volume magnetic susceptibility measurements (κ) were taken on a high-density sampling grid and soil samples were collected on a lower density grid and analyzed for total Pb concentration (Fig. 4.1.). A percentage of the original dataset of *n*=76 soil samples analyzed for lead content were excluded from the semivariogram and covariogram modelling procedures. The process of reducing the original dataset by 15%, 25%, 35% and 50% at random, was repeated multiple times to obtain 10 datasets each of: $\ln Pb_{-15\%}$, $\ln Pb_{-25\%}$, $\ln Pb_{-35\%}$ and $\ln Pb_{-50\%}$ for validation purposes. Semivariogram models were created for each reduced dataset (*n*=66; *n*=57; *n*=49 and *n*=38, respectively) of lnPb to conduct the kriging procedures. Covariogram models were also developed using the reduced lnPb datasets, and the co-variable lnκ (*n*=288).

Geostatistical methods are a type of interpolation method based on statistical models that include spatial autocorrelation. These methods can provide a measure of the uncertainty of the predictions. Kriging methods weigh the surrounding measured points to calculate a prediction for each unknown location. The weights are based on the distance between measured points and the overall spatial arrangements among the measured points. The spatial autocorrelation of the measured points must be determined when using the spatial arrangements in calculating the weights (Johnston et al. 2001).

Kriging (Adhikary et al. 2015):

$$Z(x_0) = \sum_{i=1}^{n} w_i Z(x_i) \qquad \textbf{[1]}$$

$Z(x_0)$ refers to the prediction value at location (x_0); $Z(x_i)$ refers to measured points nearby the location of the predicted value; w_i refers to the weights of the nearby measured points estimated using parameters of variograms and n refers to the total number of nearby measured points included.

Cokriging (Knotters et al. 1995):

$$\hat{Z}_u(x_0) = \sum_{i=1}^{n} w_i \mathrm{Z}_u(x_i) + \sum_{j=1}^{p} s_j Z_v(x_j) \qquad \textbf{[2]}$$

Z_u represents the measured value of the variable of interest at *ith* location from n surrounding locations and Z_v represents the measured value of a parameter variable at *jth* location from p surrounding locations that shares covariance with the measured value of the variable of interest; w_i and s_i are kriging weights estimated from parameters of the covariogram.

Variogram clouds are initially plotted to illustrate the experimental semivariogram values of all paired samples. Lags are automatically calculated using the variogram modelling method in the gstat package to produce the experimental semivariograms with bins. The 'binned' experimental semivariograms are used to examine the spatial dependence of each dataset and based on a visual best fit, model-functions are chosen and fitted to the experimental semivariograms using the weighted least square fit, to describe the spatial structure of the datasets. The term $\gamma(h)$ refers to the semivariogram, it is a graph used to depict the difference in paired sample values at a distance h apart. The measurement units used are the sample measurement units e.g. ppm squared ($(ppm)^2$). The y-axis represents the value of the variogram, and the x-axis represents the distance or 'h'. Both axes always start at '0' and as the distances between the paired samples increases along the x-axis, the semivariogram value increases along the y-axis. In a perfect example, when the distance becomes very large the sample values will become independent of each other. At this point the semivariogram will become constant and the semivariogram will be calculating the difference between sets of independent samples (Clark 1979). The covariogram model works in a similar manner to the semivariogram. The x-axis represents paired target variables and co-variables sampled at the same 'h' distances apart and the y-axis represents the variogram values. A model is then fitted to the empirical semivariograms.

The shape of the model influences the prediction of the unknown values e.g. a sharper curve close to '0' will result in a 'spikier' predicted surface. Commonly used functions for modelling the empirical semivariogram include the spherical model and the exponential model. There are other model functions which can be applicable depending on the spatial characteristics of the data, including circular, linear and gaussian. The chosen model is fitted through the points in the experimental semivariogram using the weighted least squares fit, which fits the line so that the weighted squared difference between each point and the line is as small as possible (Johnson et al. 2001). The experimental semivariogram and covariograms were calculated using the following equations:

Semivariogram (Clark 1979):

$$2\gamma*(h) = \frac{1}{N(h)} \sum_{i=1}^{N(h)} [z(x)_i - z(x_i + h)]^2 \quad \textbf{[3]}$$

Covariogram (Basaran et al. 2011):

$$2\gamma_{uv}(h) = \frac{1}{N(h)} \sum_{i=1}^{N(h)} [\, Z_u(x)_i - Z_u(x_i + h)][Z_v(x_i) - Z_v(x_i + h)] \quad \textbf{[4]}$$

Where $z(x_i)$ represents the measured value and location of the target variable and $N(h)$ refers to the number of paired samples at lag (h) distance apart. In equation 4, u and v represent the target variable and the co-variable, respectively.

Spherical or exponential models were fitted to each experimental semivariogram and covariogram model. All geostatistical analysis was carried out in R software version 3.0.1. using the 'gstat' package (© The R Foundation, R Core Team, 2017).

4.3.6. Validation

The performance of CK produced maps of Pb was assessed by comparing efficiency and error estimates with OK produced maps. The sample points (n=76) were divided at random, into two datasets with $\ln Pb_{-15\%}$ (n=66), $\ln Pb_{-25\%}$ (n=57), $\ln Pb_{-35\%}$ (n=49) and $\ln Pb_{-50\%}$ (n=38) used to train the model and

the remaining points making up corresponding datasets of $val_{15\%}$ (n=10), $val_{25\%}$ (n=19), $val_{35\%}$ (n=27) and $val_{50\%}$ (n=38), used to validate the models. This process was repeated 10 times for each reduced dataset. Datasets of observed values of lnPb ($val_{15\%}$, $val_{25\%}$, $val_{35\%}$ and $val_{50\%}$) were estimated using the interpolation models generated e.g. the OK and CK models generated from using training dataset $lnPb_{-15\%}$(no.3) were used to estimate the values of validation dataset $val_{15\%}$(no.3). The accuracy of these interpolations were calculated using performance metrics root mean square errors (RMSE), mean errors (ME), and coefficients of determination (r^2) (Pereira et al. 2018).

4.3.7. Statistical analysis

Descriptive statistics, data transformations, normality tests and geostatistical analysis were carried out using basic functions available in R. The main packages required to carry out the methodology were 'lattice' for data plotting; 'sp' for spatial analysis and 'gstat' for interpolation in R software version 3.0.1 (© The R Foundation, R Core Team, 2019). Some statistical analysis was calculated in Open Office Calc (The Apache software foundation ®).

4.4. Results

4.4.1. Lead

The basic statistical parameters for total content of Pb in soil sampled are listed in Table 4.2. The large variances in minimum and maximum values and the CV (>100%) indicate the heterogeneous nature of soil geochemistry at the park. Due to the level of skewness of the Pb dataset the data were transformed using a natural logarithmic (ln) transformation to allow for easy interpretation of the results. A substantial percentage (89.5%) of the soil samples collected had levels of Pb above the recommended 200 ppm limit advised for a sports field or park and all samples analyzed were above background levels (Rossiter 2007).

Table 4.1. *Recovery of Pb in certified reference materials (Montana I and Montana II, National Institute of Standards and Technology, USA) (n=2)*

CRMs		Pb (ppm)
2710a Montana I	Certified	5520 ± 30
	Measured	5564 ± 58
	Recovery (%)	100.80%
2711a Montana II	Certified	1400 ± 10
	Measured	1402 ± 18
	Recovery (%)	100.14%

4.4.2. Volume magnetic susceptibility (κ)

Basic statistics for κ are summarized in Table 2. The data exhibited a log-normal distribution function rather than normal, as did the lead concentrations. There is a high level of variation present in κ measurements (>75%). This is due to anthropogenic pressures on the soil in previous years. A natural logarithmic transformation was applied to the dataset to bring it towards a normal distribution necessary to carry out the geostatistical analysis.

Table 4.2. *Summary of basic statistics of Pb (ppm) and κ measurements (10^{-5} SI) in soil samples, and log-transformed versions.*

	Pb	lnPb	κ	lnκ
n	76	76	288	288
Min.	43	3.76	1.67	0.51
Median	970.50	6.88	50.77	3.93
Mean	1596.85	6.80	61.78	3.75
Std. Dev.	1614.69	1.20	46.64	1.02
Max.	6753	8.82	229.87	5.44
K-S test	.000	.200	.002	.066

4.4.3. Relationship between Pb and κ

A Pearson's correlation was performed, after necessary data transformations between lnκ and lnPb (n=76) datasets. The relationship was found to be

favourable with a r coefficient of 0.635, $p < 0.001$. The feature-space relationship shown in Fig. 4.1. also illustrated a good level of spatial continuity between Pb and κ levels in the surface soils. Pearson's correlations of $r = 0.571$; 0.799; 0.662; and 0.636, $p < 0.001$ were found between lnκ and reduced spatial density datasets of lnPb (lnPb$_{-15\%}$, lnPb$_{-25\%}$, lnPb$_{-35\%}$ and lnPb$_{-50\%}$, respectively). These datasets were used in the modelling and interpolation results featured in Table 4.3. The cokriging procedure results in better predictions than kriging when the correlation between the target and the auxiliary variables > 0.5 and when the auxiliary variable is sampled more densely (Basaran et al. 2011).

4.4.4. Spatial structure modelling

Variogram clouds of the lnPb datasets and lnκ were created initially and no discernible directional influences were detected in the dispersal patterns. Therefore, omnidirectional semivariograms were constructed. The same parameters relating to maximum distance and bin width were applied to each semivariogram. Lags of ~20 m apart were assigned to the lnPb empirical semivariograms and lags of ~10 m were assigned to the covariograms and exponential or spherical models were selected based on visual best fit. The initial variogram parameters of nugget (C_0), sill (C) and range (a) were chosen based on the shape of the 'binned' experimental semivariograms and covariograms. Details of selected models used in the interpolations of lnPb are featured in Table 4.3. and the resulting fitted models of regionalisation and co-regionalisation of lnPb are featured in Fig. 4.2. and Fig. 4.3, respectively. In accordance with the defined classes of spatial dependence of soil properties (Cambardella et al. 1994), lnPb and lnκ combined, shared a 4% spatial dependence. Individually, lnPb and lnκ demonstrated a moderate level of spatial correlation, 32.3 % and 30.6 %; indicating a similar level of randomness in both soil parameter's spatial variability (Shahandeh et al. 2005).

Table 4.3. *Summary of best performing variogram model-functions from each spatial density of Pb samples used in the interpolations of lnPb*

Variogram model	Variable	*n*	model	Nugget	Partial sill	Range (m)
Semivariograms	$lnPb_{-15\%}$	66	Spherical	0.4514	0.9469	58
	$lnPb_{-25\%}$	57	Spherical	0.7440	0.7023	75
	$lnPb_{-35\%}$	49	Spherical	1.0138	0.2602	151
	$lnPb_{-50\%}$	38	Spherical	0.000	1.4647	42
	lnκ	288	Exponential	0.2361	0.535	33
Covariograms	$lnPb_{-15\%}$/lnκ	66/288	Exponential	0.0407	0.9405	14
	$lnPb_{-25\%}$/lnκ	57/288	Exponential	0.0462	0.9213	14
	$lnPb_{-35\%}$/lnκ	49/288	Exponential	-0.0512	1.1258	14
	$lnPb_{-50\%}$/lnκ	38/288	Exponential	0.1310	0.8369	14

Fig. 4.2. *Fitted models of regionalisation of lnPb using datasets: (a) $lnPb_{-15\%}$ (b) $lnPb_{-25\%}$ (c) $lnPb_{-35\%}$ and (d) $lnPb_{-50\%}$*

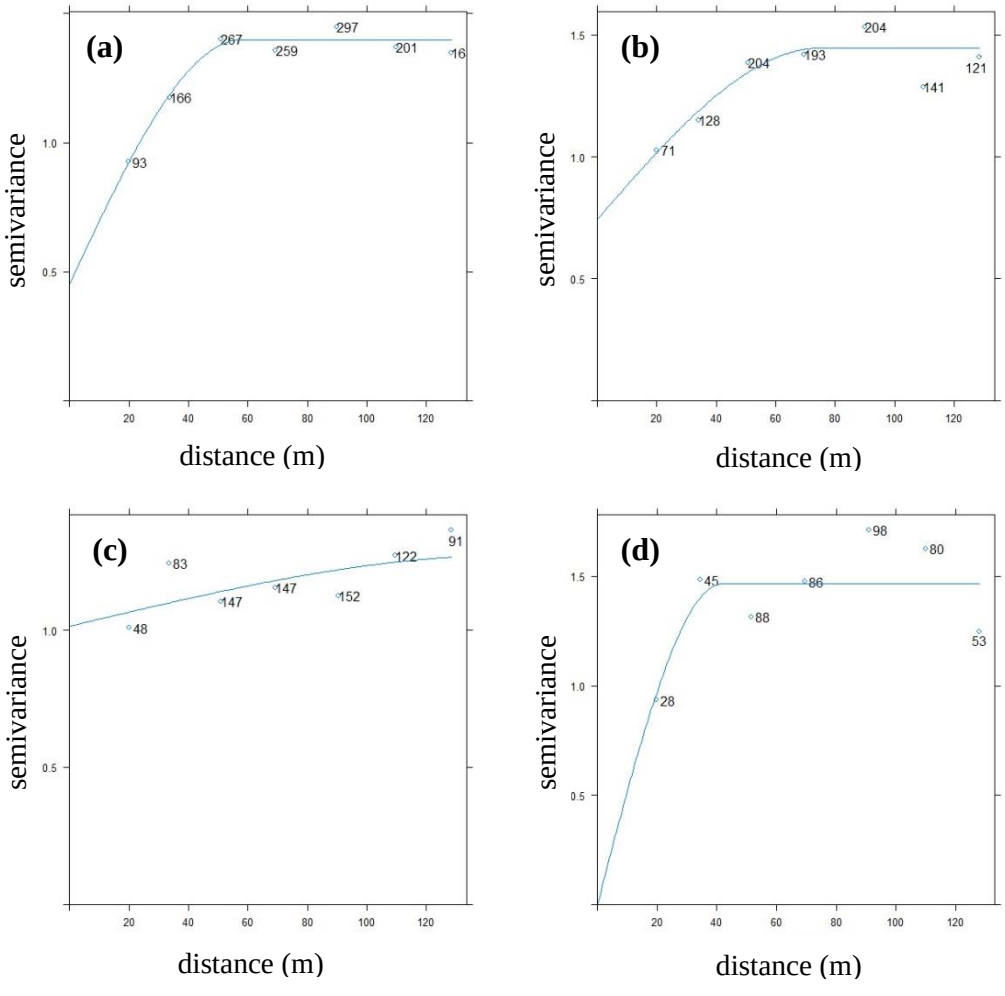

Table 4.4. *Prediction metrics: Mean and standard deviation values of estimated mean error, root mean square error and coefficient of determination (R^2) of the ordinary kriging and cokriging estimations of lnPb validation datasets ($val_{15\%}$ (n=10), $val_{25\%}$ (n=10), $val_{35\%}$ (n=10) and $val_{50\%}$ (n=10)*

Dataset Type	lnPb-15%		lnPb-25%		lnPb-35%		lnPb-50%	
Interpolation	**OK**	**CK**	**OK**	**CK**	**OK**	**CK**	**OK**	**CK**
ME								
Mean	0.021	-0.053	-0.125	-0.216	-0.007	0.007	-0.173	-0.083
St. Dev. ±	0.27	0.29	0.22	0.23	0.22	0.15	0.2	0.18
RMSE								
Mean	1.242	1.175	1.09	1.092	1.158	0.997	1.155	1.018
St. Dev. ±	0.17	0.26	0.13	0.2	0.1	0.21	0.14	0.14
R								
Mean	0.244	0.413	0.166	0.351	0.187	0.455	0.191	0.451
St. Dev. ±	0.15	0.17	0.12	0.18	0.09	0.17	0.1	0.1

Fig. 4.3. *Fitted models of co-regionalisation of lnPb using lnκ data (n=288) and datasets: (a) $lnPb_{-15\%}$ (b) $lnPb_{-25\%}$ (c) $lnPb_{-35\%}$ and (d) $lnPb_{-50\%}$*

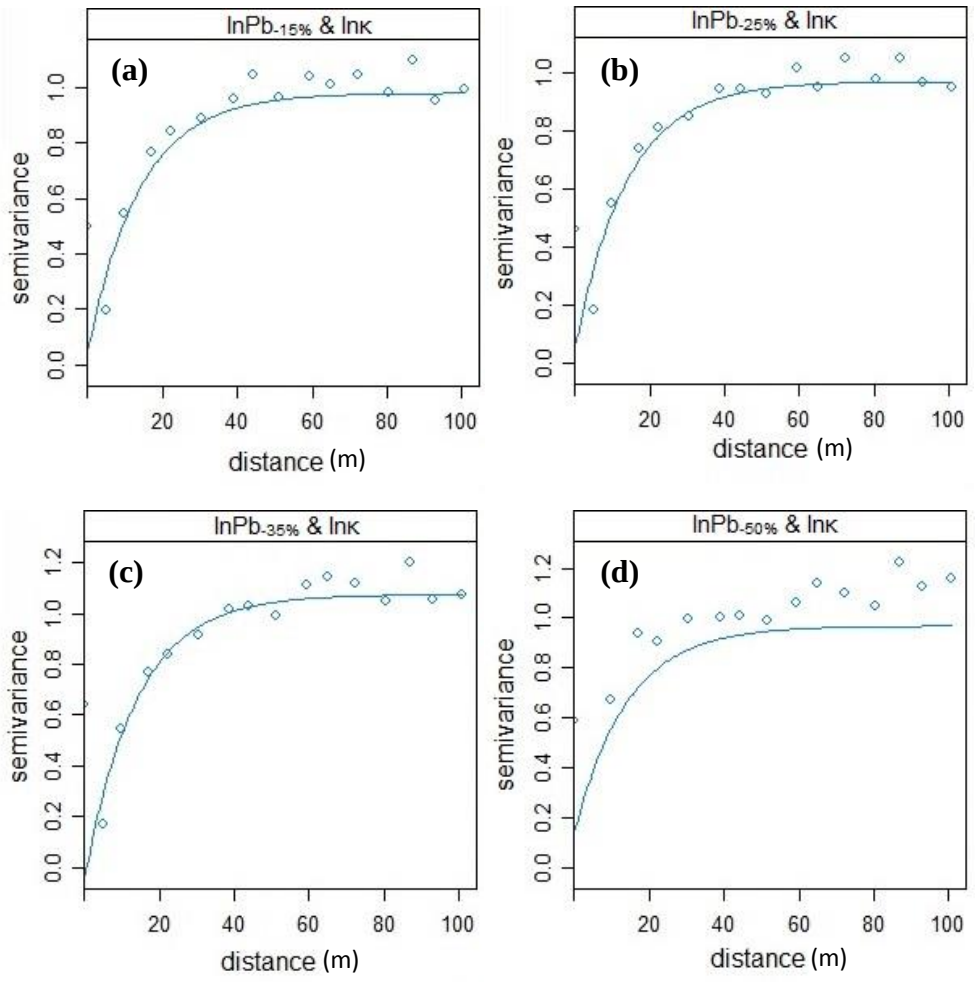

Chapter 4.

4.4.5. Validation

The models were judged by comparing the prediction errors (mean error and RMSE) produced in the prediction of the validation datasets and by comparing how close the estimated values were to the measured validation data (R^2). The precision errors and coefficients are summarized in Table 4.4. Mean Error values did not differ greatly between OK and CK validation results. Values ranged from: -422.2 to -956.7(for OK $lnPb_{-15\%}$ models) and 214.7 to 849.5(for CK $lnPb_{-15\%}$ models); -257.5 to -1546(for OK $lnPb_{-25\%}$ models) and -34.2 to -910.7 (for CK $lnPb_{-25\%}$ models); -265.3 to -876.4 (for OK $lnPb_{-35\%}$ models) and 466.6 to -646.5 (for CK $lnPb_{-35\%}$ models); and -126.8 to -1129.1 (for OK $lnPb_{-50\%}$ models) and 170.4 to -906.5 (for CK $lnPb_{-50\%}$ models). There is a negative bias in mean error values obtained with both types of interpolation models tending to underestimate the validation data. In general, the RMSE values indicate a weak level of precision obtained by the models. Ideally, the RMSE should be close to '0', '1' is considered a high level of error. However, overall RMSE values were lower for the CK models (with the exception of $lnPb_{-25\%}$), signifying an improvement in prediction capability in comparison to the OK models produced.

Table 4.5. *Summary of prediction metrics for best performing (a) ordinary kriging and (b) ordinary cokriging models from each spatial density of Pb samples*

(a) Ordinary Kriging

Dataset Type	R^2	RMSE	ME
$lnPb_{-15\%}$	0.596	0.902	0.037
$lnPb_{-25\%}$	0.431	0.926	-0.185
$lnPb_{-35\%}$	0.359	1.258	0.293
$lnPb_{-50\%}$	0.332	0.952	-0.056

(b) Ordinary Cokriging

Dataset Type	R^2	RMSE	ME
$lnPb_{-15\%}$	0.848	0.600	0.300
$lnPb_{-25\%}$	0.545	0.890	-0.093
$lnPb_{-35\%}$	0.730	0.550	0.090
$lnPb_{-50\%}$	0.622	0.765	-0.220

Coefficients of determination (R^2) were applied as a statistical measure of each model's ability to predict the validation points. Each set of interpolated predicted values shared on average, a statistically significant relationship with observed lnPb. The mean R^2 value of the CK models were consistently greater than the OK R^2 values obtained. A summary of the prediction metrics of the selected models used in the mapping of Pb at the study site are featured in Table 4.5. These models represent the best performing ordinary kriging and ordinary cokriging models from each lnPb spatial density applied ($lnPb_{-15\%}$, $lnPb_{-25\%}$, $lnPb_{-35\%}$ and $lnPb_{-50\%}$), based on efficiency and error estimates. The estimations made using the cokriging model with a spatial density of 49 points of lnPb and the complete lnκ (n = 288) dataset appeared to work the best with the lowest RMSE of 0.550 and a high coefficient of determination value of 0.730, at the 0.001 level. However, predictions made using the CK $lnPb_{-50\%}$ model were also acceptable, relative to the errors and r^2 values of the OK validation results (Table 4.5.).

Fig. 4.4. *Prediction and error maps of Pb(ppm) generated using ordinary cokriging models. Data was back-transformed prior to creation of prediction maps. Error maps were interpolated using the log-transformed data.*

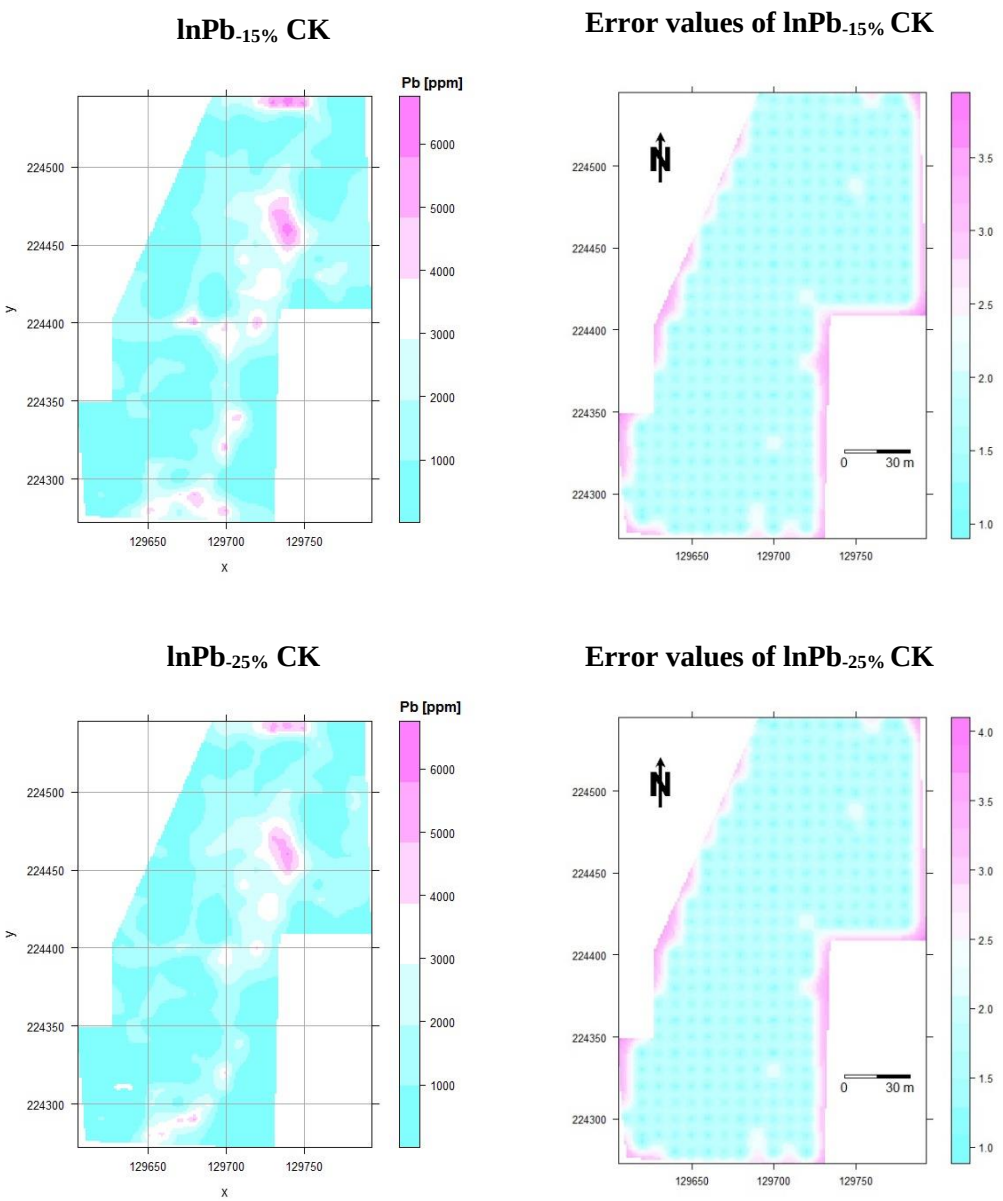

lnPb$_{-35\%}$ CK

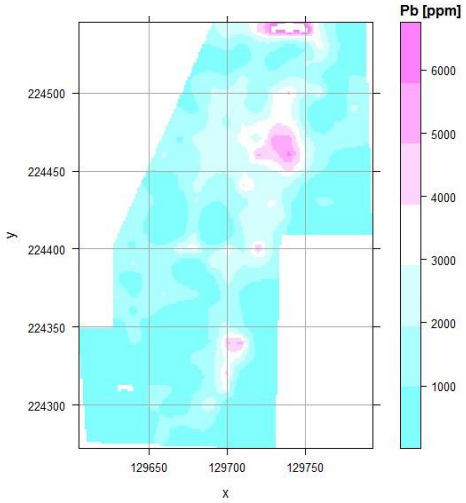

Error values of lnPb$_{-15\%}$ CK

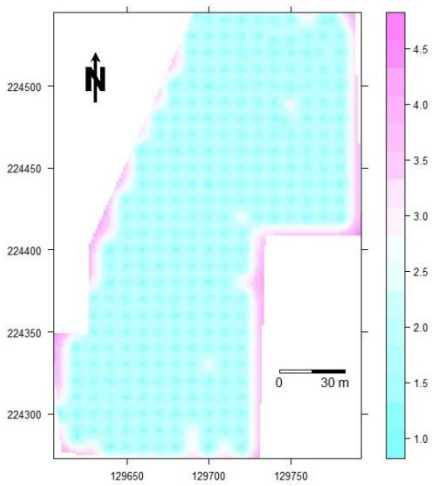

lnPb$_{-50\%}$ CK

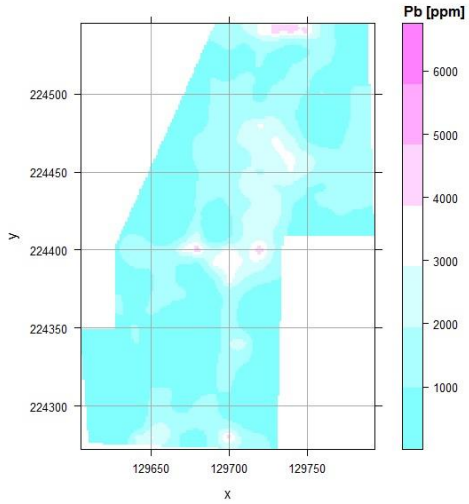

Error values of lnPb$_{-25\%}$ CK

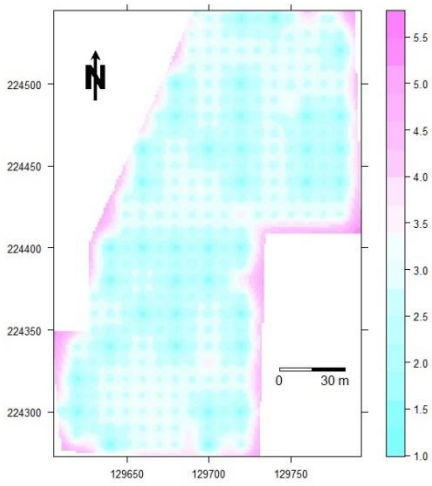

Fig. 4.5. *Prediction and error maps of Pb(ppm) generated using ordinary kriging models. Data was back-transformed prior to creation of prediction maps. Error maps were interpolated using the log-transformed data.*

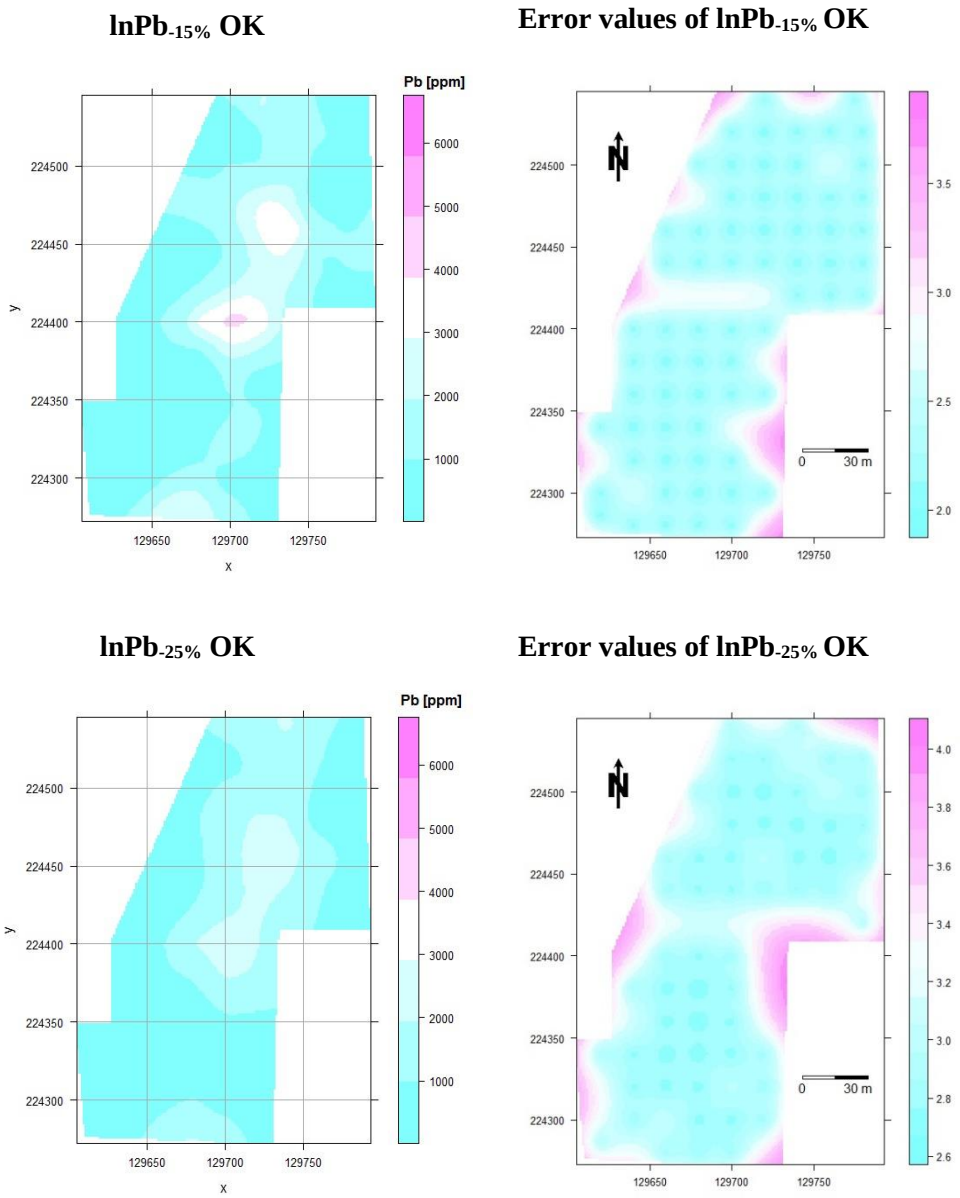

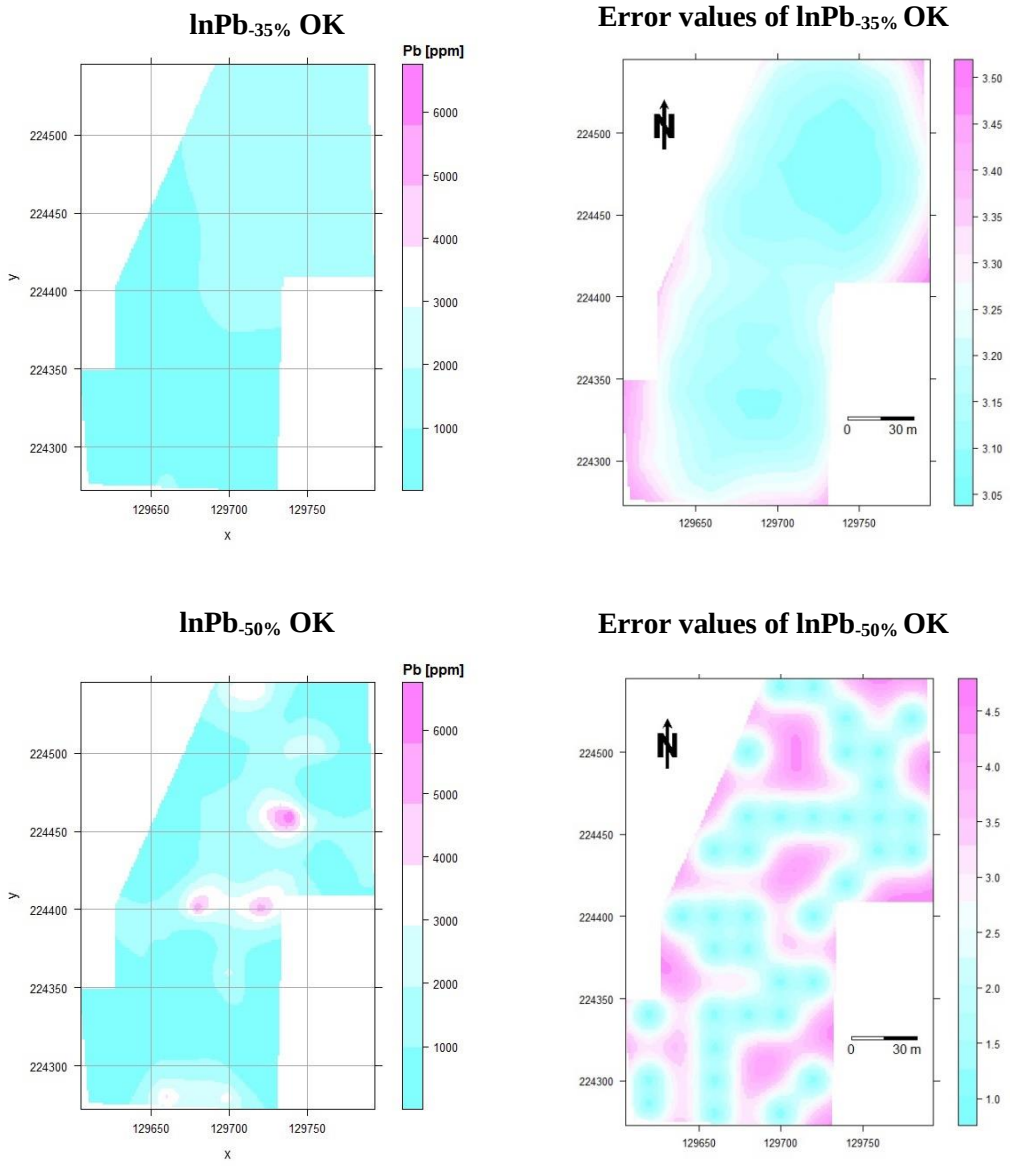

4.5. Discussion

The selected best performing semivariogram and covariogram models of lnPb and lnκ are presented in Fig. 4.2. and 4.3. The sill and nugget represent the general and random variance of the regional variable, respectively and the range represents the extent of spatial autocorrelation (Cao et al. 2017). The optimum parameters selected for the covariogram model resulted in a short range of 14 m. If the range is too short, there is a risk it will result in a 'spiky' map (Fortin et al. 2002). However, the resulting CK maps (Fig. 4.4.) illustrate a high level of localised variation throughout the region which corresponded

to the spatial distribution of the 'Pb (ppm) graduated symbols map' featured in Fig.4.1. A range of approximately 50–67% the spatial extent of the sample area's shortest perimeter is recommended (Clark 1979). The site is approximately 100 m in E–W direction and 325 m in the N–S direction. Ranges of 42 - 151 m were automatically applied to the OK procedures using the modelling function in gstat (R) (Fig. 4.5.). The longer ranges of fitted model-functions $lnPb_{-15\%}$ and $lnPb_{-25\%}$ account for much of the smoothing effect visible in these interpolations. The empirical binned data of $lnPb_{-35\%}$ does not follow a prominent curve shape like the other models of regionalisation. It is evident from the fitted model that the empirical data has poor spatial correlation at this range. This is also demonstrated in the OK $lnPb_{-35\%}$ map of Pb(ppm) which fails to adequately depict the spatial variation of Pb present at the site. The OK map of Pb(ppm) generated using $lnPb_{-50\%}$ displays hotspots of lead located in the centre, north-west and south of the site. A range of 42 m was applied to this model of regionalisation. Overall, this model worked adequately with areas of concern identified and the range of ~40 m appears a suitable extend for this study area. Gradual migration of Pb from 'hotspot' points of origin with levels exceeding 4,000 ppm are a feature of each CK interpolation and OK maps $lnPb_{-15\%}$ and $lnPb_{-50\%}$. A linear transect of elevated lead >2,000 ppm runs the entire extend of the site in a N-S direction with four main Pb-enhanced hotspots. Each cokriging map provides a more detailed and accurate illustration of the locations of elevated Pb; individual sample points of elevated Pb >1,000 ppm are more easily identifiable due to the shorter range applied in modelling. However, this level of detail is not available on the OK maps due to strong smoothing effects and in the case of OK $lnPb_{-50\%}$, due to the reduced spatial density of Pb points. In the CK $lnPb_{-50\%}$ map, the spatial distribution of elevated Pb concentrations is very similar to the CK $lnPb_{-15\%}$ map. This is due to the influence of the densely measured κ measurements included in the interpolation. The error maps provide an illustration of the spatial distribution of the reduced datasets (and κ dataset used in CK interpolations) used in the interpolation of each corresponding Pb prediction map displayed, as the level of variance is lowest at the location of sample points. The areas in the OK $lnPb_{-50\%}$ with the greatest discrepancies from the 'Pb ppm graduated symbol map' in Fig.4.1 are the

north (x 129750, y 224600) and at the south (x 129700, y 224325). However, in the CK $lnPb_{-50\%}$ map, the elevated concentrations of Pb >3,000 ppm present in these areas are illustrated. The error map of OK $lnPb_{-50\%}$ demonstrated a high level of variance was estimated at these points and it evident from this map that the Pb points sampled at these locations were not included in the interpolation of this map. These results infer that when an auxiliary variable shares spatial continuity with the target variable (r >0.5) and is located on a regular grid of suitable density, this greatly impacts the quality of the map produced. The use of the grid provided an evenly spaced number of measurements of the magnetic susceptibility (auxiliary variable) with a reduced sampling bias, which is very useful in reconnaissance type assessments. This application of the cokriging method with magnetic susceptibility could be applied in the assessment of a number of contaminants in soils. Based on the findings of this study, I would recommend the use of the cokriging procedure with a spatial density limit of 38 Pb points and an optimum spatial density of 288 κ measurements. Referring to the $lnPb_{-50\%}$ maps alone, the influence of κ measurements as the auxiliary variable at this spatial density was a crucial factor in the quality of map produced.

Although the error estimates obtained in this study are relatively high, similar validation results were reported in other related studies involving the use of geostatistical analysis of magnetic susceptibility measurements. Prediction errors of OK and Co-Est models ranging from 0.993 to 1.265 were estimated for RMSE and mean error ranged from 0.024 to 1.034 (Zawadzki and Fabijańczyk, 2008).

This geostatistical application using magnetic susceptibility as an auxiliary variable can potential be applied to other environmental pollution studies. Magnetic susceptibility has been found to have strong associations with daily sampled particulate matter (PM) in urban and industrial areas (Muxworthy et al. 2003). This technique could be applied to an urban area to assess air pollution levels of pollutants such as PAHs and NO2 using air filters as sample collectors. Lichens and mosses are natural biomonitors of air quality, strong correlations have been found between magnetic susceptibility and metals such as Cd, Cu, Ni, Pb and Zn in these biomonitors (Salo et al. 2012). Another potential application of this method could involve the assessment of

magnetic susceptibility of lichens or mosses within a region affected by air pollution, a subset of the biomonitors could be measured for Pb content, then the cokriging method could be applied to predict the concentration of lead in PM across the affected region.

4.6. Conclusions

Overall, the cokriging map appears to be the optimum choice of model. Based on validation prediction metrics of RMSE and r^2, a moderate level of precision was observed for the fitted model function generated using $lnPb_{-35\%}$ and lnκ. Predictions made using the model of co-regionalisation $lnPb_{-50\%}$ and lnκ yielded lower RMSE and a higher r^2 value than all the OK prediction models. Predictions made using the fitted semivariogram model function for $lnPb_{-50\%}$ were poor in comparison the covariogram fitted model function prediction metrics. Precision is highly dependent on the spatial autocorrelation of the target and auxiliary variable and the spatial continuity between the target variable and covariable. The feature-space correlation was not very strong between measured Pb and κ at longer ranges at the site. However, by applying a shorter range the level of spatial dependence was very strong and the success of the model was demonstrated by the high-resolution map produced detailing Pb content >1,000 ppm at close range and the strong r^2 value obtained between predicted and observed lnPb values using the selected CK models (see Table 5(b)) for interpolation. This method of kriging can potentially reduce fieldwork and analysis costs substantially in the investigation of potential soil contamination. This technique can be used in site-specific evaluation of brownfield sites, allotments, gardens or roadside soils with high levels of anthropogenically produced lead contamination in the assessment of risk posed to human health, ecosystems or ground and surface waters. It can also be applied to air pollution studies to assist in the assessment of pollutants such as $NO_{2,}$, PAHs and metal particulate matter.

4.7. References

Adhikary SK, Yilmaz AG, Muttil N (2015) Optimal design of rain gauge network in the Middle Yarra River catchment, Australia. Hydrol Process 29:2582-2599

Basaran M, Erpul G, Ozcan AU, Saygin DS, Kilbar M, Bayramin I, Yilman FE (2011) Spatial information of soil hydraulic conductivity and performance of cokriging over kriging in a semi-arid basin scale. Environ Earth Sci 63:827-838

Bhunia GS, Shit PK, Maiti R (2018) Comparison of GIS-based interpolation methods for spatial distribution of soil organic carbon (SOC). Journal of the Saudi Society of Agricultural Sciences 17:114-126

Blaha U, Appel E, Stanjek H (2008) Determination of anthropogenic boundary depth in industrially polluted soil and semi-quantification of heavy metal loads using magnetic susceptibility. Environ Pollut 156:278-289

Bruker.com, 2019. *Handheld XRF: How it works.* https://www.bruker.com/products/x-ray-diffraction-and-elemental-analysis/handheld-xrf/how-xrf-works.html (Accessed on 28.08.2019).

Cambardella CA, Moorman TB, Novak JM, Parkin TB, Karlen DL, Turco RF, Konopka AE (1994) Field scale variability of soil properties in central Iowa soils. SSSAJ 58:1501-1511

Canbay M, Aydin A, Kurtulus C (2010) Magnetic susceptibility and heavy-metal contamination in topsoils along the Izmit Gulf coastal area and IZAYTAS (Turkey). J Appl Geophy 70(1):46-57

Cao S, Lu A, Wang J, Huo L (2017) Modeling and mapping of cadmium in soils based on qualitative and quantitative auxiliary variables in a cadmium contaminated area. Sci Total Environ 580:430-439

Chen A, Cai B, Dietrich KN, Radcliffe J, Rogan WJ (2007) Lead Exposure, IQ, and Behavior in Urban 5- to 7-Year-Olds: Does Lead Affect Behavior Only by Lowering IQ? Pediatrics 119(3):650-658

Cheng H, Li M, Zhao C, Li K, Peng M, Qin A, Cheng X (2014) Overview of trace metals in the urban soil of 31 metropolises in China. J Geochem Explor 139:31-52

Chlopecka A, Bacon JR, Wilson MJ, Kay J (1996) Heavy Metals in the Environment – Forms of Cadmium, Lead and Zinc in Contaminated Soils from Southwest Poland. J Environ Qual 25:69-79

Clark I (1979) Practical Geostatistics. Applied Science Publishers Ltd., Essex, England

Dankoub Z, Ayoubi S, Khademi H, Lu SG (2012) Spatial Distribution of Magnetic Properties and Selected Heavy Metals in Calcareous Soils as Affected by Land Use in the Isfahan Region, Central Iran. Pedosphere 22(1):33-47

Dao L, Morrison L, Zhang C (2010) Spatial variation of urban soil geochemistry in a roadside sports ground in Galway, Ireland. Sci Total Environ 408:1076-1084

Dao L, Morrison L, Zhang C (2012) Bonfires a potential source of metal pollution in urban soils, Galway, Ireland. Appl Geochem 27(4):930-935

Dao L, Morrison L, Kiely G, Zhang C (2013) Spatial distribution of potentially bioavailable metals in surface soils of a contaminated sports ground in Galway, Ireland. Environ Geochem Hlth 35:227-238

Dao L, Morrison L, Zhang H, Zhang C (2014) Influences of traffic on Pb, Cu and Zn concentrations in roadside soils of an urban park in Dublin, Ireland. Environ Geochem Hlth 36(3):333-343

Dearing JA (1999) Environmental Magnetic Susceptibility. Using the Bartington MS2 System, 2nd edn. Chi Publishing, Kenilworth, England

Ďurža O (1999) Heavy Metals Contamination and Magnetic Susceptibility in Soils Around Metallurgical Plant. Phys Chem Earth (A) 24(6):541-543

El Baghdadi, M., Barakat, A., Sajieddine, M. and Nadem, S. (2012) Heavy metal pollution and soil magnetic susceptibility in urban soil of Beni Mellal City (Morrocco). Environ Earth Sci 66:141-155

Elbasiouny H, Abowaly M, Abu_Alkheir A, Gad AA (2014) Spatial variation of soil carbon and nitrogen pools by using ordinary Kriging method in an area of north Nile Delta, Egypt. Catena 113:70-78

Fabijańczyk P, Zawadzki J, Magiera T (2017) Magnetometric assessment of soil contamination in problematic area using empirical Bayesian and

indicator kriging: A case study in Upper Silesia, Poland. Geoderma 308:69-77

Facchinelli A, Sacchi E, Mallen L (2001) Multivariate statistical and GIS-based approach to identify heavy metal sources in soils. Environ Pollut 114:313-324

Flanders PJ (1994) Collection, measurement, and analysis of airborne magnetic particulates from pollution in the environment. J Appl Phys 75:5931-5936

Flegal AR, Smith DR (1992) Current needs for increased accuracy and precision in measurements of low levels of lead in blood. Environ Res 58(1-2):25-133

Fortin MJ, Dale MRT, ver Hoef J (2002) Spatial analysis in ecology. Encyclopedia of Environmetrics 4:2051-2058

Golden N, Morrison L, Gibson PJ, Potito AP and Zhang C (2015) Spatial patterns of metal contamination and magnetic susceptibility of soils at an urban bonfire site. Appl Geochem 52:86-96

Golden N, Zhang C, Potito AP, Gibson PJ, Bargary N, Morrison L (2017) Impact of grass cover on the magnetic susceptibility measurements for assessing metal contamination in urban topsoil. Environ Res 155:294-306

Gu YG, Gao YP, Lin Q (2016) Contamination, bioaccessibility and human health risk of heavy metals in exposed-lawn soils from 28 urban parks in southern China's largest city, Guangzhou. Appl Geochem 67:52-58

Hanesch M, Scholger R (2002) Mapping of heavy metal loadings in soils by means of magnetic susceptibility measurements. Environ Geol 42:857-870

Heller F (1998) Magnetic record of industrial pollution in forest soils of Upper Silesia, Poland. J Geophys Res 103(B8):17,767-17,774

Hengl T (2009) A Practical Guide to Geostatistical Mapping. JRC Scientific and Technical Reports, 2nd edn. Office for Official Publication of the European Communities, Luxembourg

Hooker PJ and Nathanail CP (2006) Risk-based characterisation of lead in urban soils. Chem Geol 226: 340-351

Hou X, He Y, Jones BT (2004) Recent Advances in Portable X-Ray Fluorescence Spectrometry. Appl Spec 39(1):1-25

Hou D, O'Connor D, Nathanail P, Tian L, Ma Y (2017) Integrated GIS and multivariate statistical analysis for regional scale assessment of heavy metal soil contamination: A critical review. Environ Pollut 231:1188-1200

Innov-X Systems, Inc. (2011) Portable XRF for Environmental Assessment https://www.spektrometry.cz/analyzatory/delta_soil.pdf Last viewed on 04.03.2019

Innov-X Systems, Inc. (2019) Handheld XRF Tests Lead (Pb) in Soil, Dusts, and on Surfaces https://www.olympus-ims.com/en/applications/xrf-tests-lead-soil-surfaces/ Last viewed on 04.03.2019

Johnston K, ver Hoef JM, Krivoruchko K, Lucas N (2001) Using ArcGIS™ Geostatistical Analyst - GIS by ESRI™. ESRI, Redlands, California

Jordanova NV, Jordanova DV, Veneva L, Yorova K, Petrovský E (2003) Magnetic Response of Soils and Vegetation to Heavy Metal Pollution – A Case Study. Environ Sci Techn 37:4417-4424

Juang KW, Lee DY (1998) A comparison of three kriging methods using auxiliary variables in heavy-metal contaminated soils. J Environ Qual 27(2):355-363

Kapička A, Petrovský E, Ustjak S, Macháčková K (1999) Proxy mapping of fly-ash pollution of soils around a coal-burning power plant: a case study in the Czech Republic. J Geochem Explor 66:291-297

Karimi R, Aoyoubi S, Jalalian A, Sheikh-Hosseini AR, Afyuni M (2011) Relationships between magnetic susceptibility and heavy metals in urban topsoils in the arid region of Isfahan, central Iran. J Appl Geophys 74:1-7

Knotters M, Brus DJ and Oude Voshaar JH (1995) A comparison of kriging, co-kriging and kriging combined with regression for spatial interpolation of horizon depth with censored observations. Geoderma 67:227-246

Li J (2016) Assessing spatial predictive models in the environmental sciences: Accuracy measures, data variation and variance explained. Environ Model Software 80:1-8

Louis GB, Damstra T, Diaz-Barriga F et al (2006) Principles for evaluating health risks associated with exposure to chemicals. World Health Organization Environmental Health Criteria 237

Lu X, Wang L, Lei K, Huang J, Zhai Y (2009) Contamination assessment of copper, lead, zinc, manganese and nickel in street dust of Baoji, NW China. J Hazard Mater 161:1058-1062

Lu S, Yu X, Chen Y (2016) Magnetic properties, microstructure and mineralogical phases of technogenic magnetic particles (TMPs) in urban soils: Their source identification and environmental implications. Sci Total Environ 543:239-247

Magiera T, Mendakiewicz M, Szuszkiewicz M, Jabłońska M, Chróst L (2016) Technogenic magnetic particles in soils as evidence of historical mining and smelting activity: A case of the Brynica River Valley, Poland. Sci Total Environ 566-567:536-551

Mielke HW (1994) Lead in New Orleans soils: new images of an urban environment. Environ Geochem Hlth 16(3-4):123-128

Mielke HW, Laidlaw MAS, Gonzales CR (2011) Estimation of leaded (Pb) gasoline's continuing material and health impacts on 90 US urbanized areas. Environ Int 37:248–257

Moioli P, Seccaroni C (2000) Analysis of art objects using a portable x-ray fluorescence spectrometer. X-Ray Spectrom 29:48-52

Möller A, Müller HW, Abdullah A, Abdelgawad G, Uttermann J (2005) Urban soil pollution in Damascus, Syria: concentrations and patterns

of heavy metals in the soils of the Damascus Ghouta. Geoderma 124:63-71

Motuzova GV, Minkina TM, Karpova EA, Barsova NU, Mandzhieva SS (2014) Soil contamination with heavy metals as a potential and real risk to the environment. J Geochem Explor 144(B):241-246

Muxworthy, AR, Matzka, J, Fernandez Davila, A and Petersen, N (2003) Magnetic signature of daily sampled urban atmospheric particles. Atmospheric Environment 37(29): 4163-4169

Pereira P, Brevik E, Muñoz-Rojas M, Miller B, Brevik E (2017) Soil Mapping and Process Modeling for Sustainable Land Use Management. Elsevier, Saint Louis

Petrovský E, Kapička A, Jordanova N, Knab M, Hoffmann V (2000) Low-field magnetic susceptibility: a proxy method of estimating increased pollution of different environmental systems. Environ Geol 39(3-4):312-318

Posthuma L, Eijsackers HJP, Koelmans AA, Vijver MG (2008) Ecological effects of diffuse mixed pollution are site-specific and require higher-tier risk assessment to improve site management decisions: A discussion paper. Sci Total Environ 406:503-517

Rachwał M, Kardel K, Magiera T, Bens O (2017) Application of magnetic susceptibility in assessment of heavy metal contamination of Saxonian soil (Germany) caused by industrial dust deposition. Geoderma 295:10-21

Rossiter DG (2007) Technical note: co-kriging with the gstat package of the R environment for statistical computing, 2nd edn. International Institute for Geo-information Science & Earth Observation (ITC), Enschede, Netherlands.

Salo, H, Bucko, MS, Vaahhtovuo, E., Limo, J, Makinen, J and Pesonen, LJ (2012) Biomonitoring of air pollution in SW Finland by magnetic and chemical measurements of moss bags and lichens. Journal of Geochemical Exploration 115:69-81

Shahandeh H, Wright AL, Hons FM, Lascano RJ (2005) Spatial and Temporal Variation of Soil Nitrogen Parameters Related to Soil Texture and Corn Yield. Agron J 97:772-782

Schibler L, Boyko T, Ferdyn M, Gajda M, Höll S, Jordanova N, Rösler N, MAGPROX Team (2002) Topsoil magnetic susceptibility mapping: data reproducibility and compatibility, measurement strategy. Stud Geophys Geod 46(1):43–57

Sierra C, Gallego JR, Afif E, Menéndez-Aguado JM, González-Coto F (2010) Analysis of soil washing effectiveness to remediate a brownfield polluted with pyrite ashes. J Hazard Mater 180:602-608

Soodan RK, Pakade YB, Nagpal A, Katnoria JK (2014) Analytical techniques for estimation of heavy metals in soil ecosystem: A tabulated review. Talanta 125:405-410

Strzyszcz Z, Magiera T, Heller F (1996) The influence of industrial immissions on the magnetic susceptibility of soils in the Upper Silesia. Stud Geophys Geod 40:276-286

Strzyszcz Z, Magiera T (1998) Magnetic Susceptibility and Heavy Metals Contamination in Soils of Southern Poland. Phys Chem Earth 23(9-10):1127-1131

Wang B, Xia D, Yu Y, Chen H Jia J (2018) Source apportionment of soil-contamination in Baotou City (North China) based on a combined magnetic and geochemical approach. Sci Total Environ 642:95-104

Wawer M, Magiera T, Ojha G, Appel E, Kusza G, Hu S, Basavaiah N (2015) Traffic-Related Pollutants in Roadside Soils of Different Countries in Europe and Asia. Water Air Soil Pollut 226(216):1-14

Waychunas GA, Kim CS, Banfield JF (2005) Nanoparticulate iron oxide minerals in soils and sediments: unique properties and contaminant scavenging mechanisms. J Nanoparticle Res 7:409-433

Weindorf DC, Bakr N, Zhu Y (2014) Chapter One - Advances in Portable X-ray Fluorescence (PXRF) for Environmental, Pedological, and Agronomic Applications. Adv Agron 128:1-45

Xie Y, Chen TB, Lei M, Yang J, Guo QJ, Song B, Zhou XY (2011) Spatial distribution of soil heavy metal pollution estimated by different interpolation methods: Accuracy and uncertainty analysis. Chemosphere 82:468-476

Zawadzki J, Fabijańczyk P (2008) Reduction of soil contamination uncertainty assessment using magnetic susceptibility measurements and CO_EST method. Proceedings of ECOpole 2(1):169-174

Chapter 4.

Zawadzki J, Magiera T, Fabijańczyk P (2009) Geostatistical evaluation of magnetic indicators of forest soil contamination with heavy metals. Stud Geophys Geod 53:132-149

Zawadzki J, Szuszkiewicz M, Fabijańczyk P, Magiera T (2016) Geostatistical discrimination between different sources of soil pollutants using a magneto-geochemical data set. Chemosphere 164:668-676

5. GENERAL DISCUSSION

5.1. General Discussion

There are estimated to be in excess of 2,000 potentially contaminated sites in Ireland (IPA, 2006). Typically, the procedures involved in the investigation of potentially metal contaminated soils involves sending a small number of soil samples to a commercial lab for chemical analysis. Even at the preliminary phase of an investigation, time-scales and costs can mount. The cost of a preliminary site investigation is estimated at between €1,300 - €4,900 (IPA, 2006). This study provides a new approach for the assessment of metal contamination in urban topsoils, employing magnetic susceptibility measurements and spatial analysis techniques. The establishment of site investigation protocols for addressing different forms of contamination at a local scale will be beneficial for local governing bodies tasked with managing potentially affected sites.

5.2. Key Findings

The main findings from the previous three chapters of this thesis are discussed below in relation to the overall aims, which were to:

- Identify locations of anthropogenic loadings in surface soils where levels of a PTEs of interest may be present using magnetic susceptibility measurements, and create high-quality spatial distribution maps.
- Demonstrate how MS measurements can be incorporated with PTE data and spatial analysis techniques in the mapping of anthropogenically affected topsoils.
- Outline procedures which can be implemented by others in the assessment of metal contaminated soils.

Recommendations are made from the findings of this study to inform on procedures which can be adopted for urban topsoil metal contamination assessment. Also provided are sections on the limitations of the study and suggestions for future research.

i) The application of magnetic susceptibility measurements (mass specific MS) using Local Moran's I hotspot analysis in locating and identifying

the extent of historic bonfires was shown to be effective, even when physical evidence on site is not obvious.

The use of magnetic measurements in the identification of human control fires from ancient times is an established archaeological technique (Barbetti, 1986; Morinaga et al., 1999). Burning produces an enhanced magnetic signature and consequently fire ash is well suited to magnetic-related studies (Peters et al. 2001). Heating temperature appears to play a significant role in the intensity of susceptibility enhancement. It has been theorised that high temperatures and changes in reduction conditions associated with the presence of organic matter to oxidation conditions during fires act to convert less magnetic iron oxy-hydroxides into more highly magnetic phases (Clement et al., 2010). The evidence detailed in chapter 2 suggests soil temperatures reached approximately 200 - 300 °C, below the modern 2012 bonfire site, and the requisite effects on χlf at this temperature are minimal. Although heating could play an intrinsic role in magnetic enhancement, it cannot be considered fully accountable for the elevated χlf values beneath the bonfire site, indicating the influence of metal contamination through direct metal inputs. This is further validated by the communal high-high value cluster featured in the southeastern section of the site in all the Local Moran's I hotspot and outlier analysis maps generated (Fig. 2.10., p. 46-47). When compared to the locations of previous bonfires (Fig. 2.2.), it is possible to propose that the presence of a high-high value cluster in the area is due to the activity of burning metal laden materials. High χlf value points featured in the northeastern section of the contour map indicate the presence of an additional historic bonfire location in this area. This theory is further strengthened by the occurrence of elevated Cu, Pb and Sr (mg kg^{-1}) in this section.

The spatial dispersion of metals is suggestive of a variety of materials being burnt in the bonfires. Zn presence is indicative of the burning of tyres. Other metals indicate a bonfire in other locations where tyres were likely not burned, with significant high-high values in a north eastern direction of Cu, Pb, and Sr, high-high values of Pb in a western direction and Mn and Fe were significantly high in the central east of the site. The metals present were dependent on the materials burned in the bonfires. Potential sources of these contaminants are discussed in chapter 2.

Based on the Local Moran's I maps quantified, the spatial range of influence of a bonfire is confined to the boundary of materials being burnt and was estimated at around 10 meters.

ii) Grass coverage height has a limited impact on *in-situ* volume magnetic susceptibility measurements

A strong linear relationship is shown (fig. 3.8., p. 81) between κ^{grass}, $\kappa^{no\ grass}$ and κ^{lab}. The two κ(ln) datasets exhibited a strong positive Pearson's correlation coefficient of $r^2 = 0.966$, $n = 185$, $p < 0.01$. In general, κ^{grass} obtained initially, prior to the grass layer being disturbed, are lower than $\kappa^{no\ grass}$. This is because the sensitivity of the sensor for magnetic susceptibility measurements diminishes exponentially with distance from material (Lecoanet et al., 1999). The MS2D search loop is affected by material up to ~10 cm from the sensor. The gap between the sensor and the soil surface is a contributing factor in relation to grass height effects. A possible negative relationship between grass height and the difference in κ values was explored and a Spearman's rho correlation revealed a weak significant r_s value between these parameters ($r_s = 0.253$, $n = 185$, $p < 0.05$). It is possible that where very high grasses are present in e.g. wastelands or roadsides that grass height may affect κ measurement obtained. But due to the small number of sample points with grass blade height >10 cm ($n = 3$), it does not affect the predictive power in the current study.

iii) Ordinary cokriging can be employed to generate high resolution spatial distribution maps of PTEs when volume magnetic susceptibility is incorporated as the auxiliary variable

The feature-space relationship shown in fig.4.1. (p.113) illustrated a good level of spatial continuity between the analyzed PTE Pb and κ levels in the surface soils. The reduced dataset of lnPb (n =66) employed in the best performing interpolations of both models shared a statistically significant relationship of $r = 0.571$, $p < 0.001$. According to the findings of Yates and Warrick (1987) the cokriging procedure results in better predictions than kriging when the correlation between the target and the auxiliary variables are above 0.5 and when the auxiliary variable is more densely sampled.

Based on evaluation metrics, the ordinary cokriging procedure was an improvement on the ordinary kriging. Root Mean Square Error was calculated as a measure of precision. Although all interpolation models resulted in relatively high RMSE, the RMSE of the ordinary cokriging procedures was lower on average than ordinary kriging. This is despite ordinary cokriging integrating additional variability into the interpolation by incorporating the auxiliary variable lnκ. Coefficients of determination (R^2) were applied as a statistical measure of each model's ability to predict the validation points. The mean R^2 value of the CK models were consistently greater than the OK predictions. On an individual basis, a CK model was the more superior in prediction error to the best of the OK models produced of lnPb, with a RMSE of 0.600 and a r^2 value of 0.848 in comparison to a RMSE of 0.902 and a r^2 of 0.596 for the corresponding OK model.

In general, all the maps feature a linear transect of elevated lead >2,000 ppm running the entire extend of the site in a N-S direction with four main Pb-enhanced hotspots (with the exception of $lnPb_{-35\%}$ OK map). The OK procedure appears to have smoothed out elevated Pb >4,000 ppm (with the exception of $lnPb_{-50\%}$ OK map) whereas these hotpots are evident on the ordinary cokriging map. The ordinary cokriging maps provide a more detailed and accurate illustration of the locations of elevated Pb with individual sample points of elevated Pb >1,000 ppm more easily identifiable.

iv) Example protocol for assessment of metal contamination in topsoils

The following is a basic procedure for the preliminary and exploratory phases of an investigation of metal contamination in topsoil:

- Hypothesis formed on condition of site
- Conceptual model developed – what are the aims & objectives of the assessment.

Preliminary phase of the investigation:

- Desk study – gather information on prior use, geology, etc.
- Reconnaissance κ survey:

- A control point is measured where contamination is not expected, providing an indication of background values of the soil in the vicinity
- A MS2D sensor could be employed in a walkthrough of the suspected site measuring in continuous mode.
- A small number of soil samples should also be analysed for elemental concentrations throughout the site using the PXRF

Exploratory phase of investigation:

- The chosen sampling design will then be dependent on the level of variation evident from this reconnaissance survey,
- A systematic sampling grid with 3-5 sub-measurements per grid point is recommended for an unbiased analysis
- Sampling grid points should be geo-referenced for spatial analysis
- A small number of soil samples could be collected from the same sampling grid as the MS survey but at a lower volume e.g. every second grid point collect a composite sample from the same locations as the κ measurements
- Soils samples can be collected:
  - 3-5 sub-samples, from same location as κ
  - 0-10 cm depth using stainless steel auger or plastic scoop
  - Stored in polythene bags and labelled
- Preparation:
  - Dried at ambient temperature
  - Gentle desegregated and homogenized
  - Sieved to <2 mm fraction
  - Placed in new bags for analysis
- PXRF analysis:
  - Analyze samples in soil mode for 120 s

- Instrument should be calibrated using certified reference materials such as NIST Montana I 2710a or Montana II 2711a soil CRMs
- Report only on elements which have efficient recovery rates of >85%. Elements reporting enhancements in recovery rates should be investigated further as potentially matrix effects are causing interferences (chemical analysis may be required for these elements).
- Analyze each sample 3 times, every 10 measurements measure a calibration sample.
- Prepare data in spreadsheets for analysis

- Explore basic statistics of the κ and elemental data of interest using descriptive statistics and histograms, line charts with error bars etc.
- Carryout log-transformation if not normally distributed
- On the transformed data significant relationships between κ and the elements of interest obtained can be explored using Pearson's correlation analysis and scatterplots.
- Spatial distribution maps using deterministic interpolation techniques can be produced using free software like QGIS or geostatistical models can also be produced in R.
- Alternatively, a hotspot and outlier analysis can be conducted on the transformed data using GeoDa™1.4.6. (Anselin et al., 2006) software
- From the statistical and spatial analysis, it can be confirm/denied whether significant levels of anthropogenically influenced contaminants are present in the topsoils.
- A Main Site Investigation may be necessary involving the collection of additional environmental properties such as bore hole, groundwater, soil pH, chemical analysis of soil.

5.3. Recommendations

- There is no worldwide consensus on what specific trace elements should be covered by regulations, and although there is no European Directive for the protection of soil, some EEA countries have put in place legislation pertaining to trace element limits including Poland, Germany, Netherlands, Belgium and the UK. Some countries have distinctions in limits of trace elements based on land use and others based on soil properties (Antoniadis et al. 2019). In the England and Wales, different ranges of concentration limits have been established for some metals and inorganic compounds known as Category 4 Screening levels (C4SLs). These values have been calculated based on different land uses such as garden allotments, residential spaces and commercial soils (CL:AIRE, 2014). In Germany, critical values have been set for some trace elements by the Berlin Environmental Atlas (1992). A critical value for Pb has been included for sports fields or parks where soil may become bare at < 200 ppm and the natural background value established at < 30 ppm. In the Netherlands, Dutch quality standards for soil are enforced for maximum value for residential and industrial soils and intervention values for a range of elements/ substances including Pb, Cu and Zn (ppm) (Lamé and Maring, 2014). It is advisable to refer to other European countries' legislated trace element limits such as the examples provided when undertaking a site assessment.

- Reference to regional background values is also recommended. 'The Soil Geochemical Map of Ireland' (Fay et al., 2007) and the 'Atlas of Topsoil Geochemistry of the Northern Counties of Ireland' (Gallagher, et al., 2016) provides baseline soil geochemical data for Irish soils up to a depth 10 cm and can provide a valuable reference material for the distribution and concentration of elements.

- A portable X-ray fluorescence analyser (PXRF, ©Innov-X Systems, Inc.) was employed to determine total metal concentrations of prepared composite soil samples. PXRF is a non-destructive method of investigating potentially contaminated sites which can rapidly provide in-situ laboratory quality soil/sediment chemistry of a range

of metals including As, Ba, Cd, Co, Cr, Cu, Fe, Hg, K, Mn, Pb, Sr, Ti, Zn (Innov-X Systems, Inc., 2005). However, due to low limits of detection or matrix effects, some elements present may not be detectable. It is advisable to employ a PXRF in the preliminary and exploratory phases of a site assessment. However, when levels of elements appear to reach intervention limits, a more precise analytical approach is required.

- Principal component analysis (PCA) is of practical use when differentiating between sources or groups of metals observed. Based on their eigenvalue they are separated into associated Factors for easy interpretation.
- A simple pollution index can be useful to provide perspective on the level of contamination present at a site, such as the example provided in chapter 3. A PI can be particularly helpful when critical values are not available.
- Deterministic interpolation techniques like Inverse Distance Weighting (IDW) are very useful for providing visual depictions of spatial dispersal patterns of elements. However, they can have a 'bulls eye effect' on outliers, as occurred in chapter 2. When an outlier of Cu, Pb, Sr and Ti (ppm) appeared as a potential hotspot or additional bonfire location in the west of the site. After cross-referencing with Local Moran's I hotspot maps of each element, this location was identified as an outlier.

5.4. Further Research

In the study detailed in chapter 3, a substantial amount of magnetic susceptibility data was obtained in the field. The length of grass blades were also recorded at each sampling point. The grass heights ranged from 2-15 cm with just n =3 locations with grass height > 10 cm. This is related to site specific conditions at the study area, it is a well-maintained urban park. Grass is mowed on a regularly basis resulting in a low average blade height of 6 cm at the sampled points. This demonstrates that grass height has the potential to effect measurements but not in the present study where maintained grass dominates the study area. It is possible that where very high grasses are present in e.g. wastelands or roadsides that grass height may affect κ

measurement obtained. In future, it would be interesting to investigate grass height effects > 10 cm at incremental levels at a control site which has been subjected to anthropogenic pressures.

The procedure reported in chapter 4 established that by applying the ordinary cokriging technique with volume magnetic susceptibility as an auxiliary variable, predicted surfaces of the target variable Pb ppm could be generated with lower root mean square error and a high correlation coefficient. It would be beneficial to further explore the dynamics of this procedure in terms of sample numbers of the target variable. The target variable sample number could be reduced by 20, 25 or 30 % and the analysis applied again to see if the CK procedure is even possible and a viable option with uncertainty errors similar to values obtained in this chapter 4.

Although magnetic susceptibility has been recognized as an excellent proxy measurement of metal contamination in international literature, it has not been included in metal contamination investigation protocols. This thesis provides details on how MS measurements can be incorporated into an assessment and used with spatial analysis tools like interpolation and hotspot analysis.

5.5. References

Anselin, L., Syabri, I. and Kho, Y. (2006). 'GeoDa: An Introduction to Spatial Data Analysis'. *Geographical Analysis*, 38(1), pp. 5-22.

Antoniadis, V., Shaheen, S.M., Levizou, E., Shahid, M., Khan Niazi, N., Vithanage, M., Sik Ok, Y., Bolan, N. and Rinklebe, J. (2019). 'A critical prospective analysis of the potential toxicity of trace element regulation limits in soils worldwide: Are they protective concerning health risk assessment? – A review'. *Environment International*, 127, pp. 819 – 847.

Barbetti, M. (1986). 'Traces of fire in the archaeological record, before one million years ago?'. *Journal of Human Evolution*, 15(8), pp. 771-781.

Berlin Environmental Atlas (1992). *Lead in Soils.* http://www.stadtentwicklung.berlin.de/umwelt/umweltatlas/ei1031.htm (Accessed on10.04.2019).

Clark, I. (1979). *Practical Geostatistics*. Essex, England: Applied Science Publishers Ltd.

Clement, B.M., Javier, J., Sah, J.P. and Ross, M.S. (2010). 'The effects of wildfires on the magnetic properties of soils in the Everglades'. *Earth Surfaces Processes and Landforms*, pp. 1-7.

Contaminated Land: Applications in Real Environments (CL:AIRE) (2014). *Appendix H Provisional C4SLs for lead*. SP1010 – Development of Category 4 Screening Levels for Assessment of Land Affected by Contamination Final Project Report (Revision 2). 24th September 2014.

Fay, D., Zhang, C., McGrath, D. and Grennan, E. (2007). *Soil Geochemical Atlas of Ireland*. Teagasc and Environmental Protection Agency.

Gallagher, V., Knights, K., Carey, S., Glennon, M. and Scanlon, R. (2016). *Atlas of Topsoil Geochemistry of the Northern Counties of Ireland Data from the Tellus and Tellus Border Projects*. Geological Survey of Ireland.

Innov-X Systems, Inc. (2005). *Technical Data. Alpha Series™- analyzers provide on-site environmental metals testing*. http://www.fieldenvironmental.com/assets/files/Literature/InnovX%20XRF%20Specs.pdf (Accessed 20.02.2014).

(IPA) Institute of Public Administration (2006). EU Policy Review. Analysis of recent legislation and policy for local and regional government. Number 5/06 – Aug-Sept 2006.

Jeffries, J. & Martin, I. (2009). *Updated technical background to CLEA model. Science Report SC050021/SR3*. Environmental Agency, UK. https://webarchive.nationalarchives.gov.uk/20140328153908/http://www.environment-agency.gov.uk/static/documents/Research/CLEA_Report_-_final.pdf (Accessed on 11.06.2019).

Lamé, F. and Maring, L. (2014). 'Into Dutch Soils', 2nd edn. Rijkswaterstaat (November, 2014). https://rwsenvironment.eu/publish/pages/126603/into_dutch_soils.pdf (Accessed on 04.06.2019).

Lecoanet, H., Lévêque, F., Segura, S. (1999). 'Magnetic susceptibility in environmental applications: comparison of field probes'. *Physics of the Earth and Planetary Interiors*, 115, pp. 191-204.

Morinaga, H., Inokuchi, H., Yamashita, H., Ono, A. and Hada, T. (1999). 'Magnetic detection of heated soils at Paliolithic sites in Japan'. *Geoarchaeology An International Journal*, 14(5), pp. 377-399.

Peters, C. and Church, M. (2001). 'Investigation of fire ash residues using mineral magnetism'. *Archaeological prospection*, 8(4), pp. 227-237.

Yates, S.R. and Warrick, A.W. (1987). 'Estimating soil water content using cokriging'. *Soil Sci. Soc. Am. J.*, 51, pp. 25-30.

6. APPENDICES

Applied Geochemistry 52 (2015) 86–96

Contents lists available at ScienceDirect

Applied Geochemistry

journal homepage: www.elsevier.com/locate/apgeochem

Spatial patterns of metal contamination and magnetic susceptibility of soils at an urban bonfire site

Nessa Golden [a], Liam Morrison [b], Paul J. Gibson [c], Aaron P. Potito [a], Chaosheng Zhang [a,*]

[a] School of Geography and Archaeology, National University of Ireland, Galway, Ireland
[b] Earth and Ocean Sciences, School of Natural Sciences and Ryan Institute, National University of Ireland, Galway, Ireland
[c] Environmental Geophysics Unit, Department of Geography, National University of Ireland, Maynooth, Ireland

ARTICLE INFO

Article history:
Available online 11 November 2014
Editorial handling by M. Kersten

ABSTRACT

Bonfires are a major pollution source in urban soils, but there is a lack of knowledge about the impacts and spatial extent of bonfires on soil metal concentration and magnetic properties. In this study, a total of 379 soil samples were collected from a traditional bonfire site on a 1×1 m^2 grid system and analysed for total metal concentration and low frequency magnetic susceptibility ($MS\chi_{lf}$). High resolution maps of the spatial distribution of Cu, Fe, Mn, Pb, Sr, Ti, Zn and $MS\chi_{lf}$ were created and a significant relationship between each of the metals and $MS\chi_{lf}$ was revealed. Elevated levels of each metal were observed, with median and maximum values of 68 and 1117 mg kg^{-1} for Cu, 114 and 985 mg kg^{-1} for Pb and 561 and 21 681 mg kg^{-1} for Zn in particular, indicating the site may pose a significant health risk. The spatial patterns were generally consistent, with Zn and Fe in particular, encompassing the position of bonfires. The spatial extent of influence of bonfires was estimated at approximately 10 m, in line with the extent of bonfire materials. In addition, laboratory based experiments involving soil colour and the effect of temperature on $MS\chi_{lf}$ indicated that bonfires only raise soil temperatures to a maximum of 300 °C, having little effect on $MS\chi_{lf}$. The results of this study indicate the importance of metal contamination associated with bonfires in urban soils.

1. Introduction

The need for precise measurements of environmental pollution is increasing due to the adverse exposure effects of elevated concentrations of pollutants on human health and the environment. Bonfires are outdoor fires used in rituals and celebrations. Traditionally, non-hazardous wastes such as wood, straw and bones were used as kindling (Gailey and Adams, 1977). However, modern bonfire sites include less traditional items, such as materials of technogenic origin, municipal wastes such as electrical appliances, tyres and plastics (Dao et al., 2012), making them a potentially major pollution source in urban soils. According to an EPA survey on Irish people's attitudes on environmental issues, 1 in 10 admitted to burning household wastes. This problem continues to grow despite 80% of adults being aware of the environmental and health risks associated with illegal burning. Two findings of particular concern are that 15% of adults consider illegal burning to be an adequate form of disposal and half of those admitting to burning did so with knowledge of the public health implications (EPA, 2006). Bonfires are sources of CO, particulates, NO_2, SO_2, PAHs, dioxins, organic compounds and toxic metals (DEFRA, 2006). Previous studies revealed high levels of PAH and dioxin emissions in residential areas during bonfire season (Butterfield and Brown, 2012; DEFRA, 2006). Domestic solid fuel burning is a particular problem as it releases PAHs close to the ground level in areas of high population density, where their impact on the maximum recorded ground level concentration can be up to 100 times greater than the same mass of PAH emitted by an industrial process through a tall chimney stack (DEFRA, 2006). Dioxin concentrations were found to increase 30 fold (from 21–25 to 720 TEQ/m^3) at one bonfire site (DEFRA, 2006). Very few studies have investigated the potential contribution of metals from bonfires to the environment. High levels of Cu, Pb and Zn were reported at a bonfire site in a residential area in Galway, Ireland, demonstrating the uncontrolled burning of metal-bearing materials leading to metal accumulation in soils (Dao et al., 2012).

The use of magnetic parameters in the identification of pollution sources has become a widespread practice as a reliable, efficient and sensitive method for evaluating polluted sites (Blaha et al., 2008; Jordanova et al., 2003; Magiera et al., 2008; Wang and Qin, 2005). Anthropogenic pollution has a strong magnetic signature, in particular a strong correlation was observed between magnetic susceptibility (MS) and metal concentrations in the

* Corresponding author. Tel.: +353 91 492375; fax: +353 91 495505.
E-mail address: Chaosheng.Zhang@nuigalway.ie (C. Zhang).

http://dx.doi.org/10.1016/j.apgeochem.2014.11.004
0883-2927/

upper layers of soils and sediments (Chan et al., 2001; El Baghdadi et al., 2012). Although the determination of total metal concentrations is a routine analysis, soil magnetic measurements can provide valuable reference information in pollution studies (Blaha et al., 2008; Jordanova et al., 2003; Lu et al., 2012; Magiera et al., 2008; Morton-Bermea et al., 2009; Wang and Qin, 2005; Strzyszcz and Magiera, 1998). It is now well established that by-products of incineration can possess a significant mineral magnetic component (Lu et al., 2012; Sapkota and Cioppa, 2012; Strzyszcz and Magiera, 1998).

Many studies have documented the correlation between magnetic properties and metal concentration in urban soils (El Baghdadi et al., 2012; Gudadhe et al., 2012; Lu and Bai, 2006; Lu et al., 2008; Wang and Qin, 2005), sediments (Botsou et al., 2011; Canbay et al., 2010; Frančišković-Bilinski et al., 2014), dust (Zhang et al., 2012; Zhu et al., 2012, 2013) and paleoclimatology studies (Alekseeva et al., 2007; Blundell et al., 2009; Maher et al., 2002, 2003; Maher and Hallam, 2005). These investigations have highlighted the use of magnetic parameters as a proxy in the detection and mapping of metal contaminated areas. MS mapping of soils and sediments has become one of the most important tools for estimating anthropogenic pollution (Yang et al., 2012) and has been widely used in mapping metal contamination (Hanesch and Scholger, 2002; Zawadzki and Fabijańczyk, 2008).

MS may be used as an initial step for further investigations at regional, national, international scales and as a result of its compatibility with routine chemical analysis, it can be considered a simple, rapid, non-destructive proxy tool for mapping metal pollution (D'Emilio et al., 2012). However, due to large variations of the reference signal as a result of soil processes and other natural conditions such as bedrock lithology, the reliability of magnetic mapping still remains a challenge in unpolluted or relatively unpolluted soils (Kapička et al., 2003).

In geospatial terms, the index of local Moran's I is a useful tool in the identification of statistically significant pollution hotspots in urban soils and for classifying them into spatial clusters and outliers. Although other methods can help in the identification of spatial patterns, in pollution studies it is important that areas of high/low values in comparison to the surrounding area are identified, and local Moran's I examines the individual locations, enabling hotspots to be identified based on a comparison with the neighbouring samples. It has been applied successfully in various fields, including ecology (Sokal et al., 1998a, 1998b), geochemistry (Li et al., 2014; Zhang et al., 2008), crime (Levine, 2006), disease (McCullagh, 2006) and mortality rates (Zhang and Lin, 2007). Early methods of local indicators of spatial autocorrelation (LISA) statistics were developed for geographical areas, such as municipal divisions (Anselin, 1995; Getis and Ord, 1992; Ord and Getis, 1995). However, more contemporary work has focused on point patterns, possibly driven by the need to identify crime patterns and disease outbreaks (McCullagh, 2006). Point patterns allow for more precision in analysis of hotspot identification (Jacquez et al., 1996).

In the present study, Local Moran's I has been applied to an annual bonfire site, and utilised to trace the locations and effects of past bonfires. Bonfire sites offer an ideal case study as spatial influences tend to be localised, e.g. extreme and immediate shifts in values are present within small areas, requiring high resolution mapping.

The aims of the present study included the investigation of the spatial distribution of metals (Cu, Fe, Mn, Pb, Sr, Ti, Zn) and low frequency magnetic susceptibility ($MS\chi_{lf}$) in order to determine the spatial range of influences of a bonfire. To further quantify the spatial patterns of contamination present at the site, local Moran's I hotspot analysis was used to identify pollution hotspots, outliers and spatial clusters of each of the metals and $MS\chi_{lf}$. The relationships between $MS\chi_{lf}$ and metals were also examined to explore the possibility of using $MS\chi_{lf}$ readings as a surrogate for the assessment of metal contamination in a bonfire site. In addition, laboratory based experiments examined the effects of temperature on the magnetic properties of soil.

2. Materials and methods

2.1. Study area and sampling grid

The study focused on a bonfire site located on a 380 m^2 residential and green area in Galway City (53°16′44N, −9°04′48E), Ireland (Fig. 1). A systematic sampling grid comprised of 379 points was employed using a 1×1 m^2 grid system (Fig. 2). The location was selected in accordance with the position of known past bonfires, still visible on the surface of the topsoil (Fig. 1). The extent of the sampling boundary was based on the central position of the current bonfire site and the limitation of the range of the green area in order to investigate the influence of the burning of metallic materials on the metal concentration and MS of soil in close proximity to a bonfire. The sampling grid was laid using measuring tapes and plastic sticks as markers and the locations were recorded using a portable global positioning system (GPS) Trimble GeoExplorer®.

2.2. Sample collection and preparation

Soil samples were obtained using a stainless steel auger, which was cleaned in between samples and the first sub-sample at each point was discarded to avoid cross contamination. Five representative sub-samples (0–10 cm in depth (Dao et al., 2012)), one from the centre point and four from the four quadrants of the 1 m^2 area of each point, were taken and combined to make one composite sample representing each point on the grid. Soil samples were stored in clean polythene bags, dried at room temperature (~20 °C) and gently disaggregated using a mortar and pestle and sieved (<2 mm fraction).

2.3. Determination of total element concentration

An Innov-X Alpha Series 6500 portable X-ray fluorescence analyser (PXRF, ©Innov-X Systems, Inc.) was employed to determine total metal concentrations. PXRF is a non-destructive method of investigating potentially contaminated sites which can rapidly provide in-situ laboratory quality soil/sediment chemistry of a range of metals including As, Ba, Cd, Co, Cr, Cu, Fe, Hg, K, Mn, Pb, Sr, Ti, Zn (Innov-X Systems, Inc., 2005). An element is defined by its characteristic X-ray emissions wavelength (λ) or energy (E). PXRF determines the amount of an element present by measuring the intensity of this characteristic line. The instrument contains a miniature (1.6 kg in weight) energy-dispersive spectrometer with a 35-kV Ag target excitation source. Fluorescence spectra are detected through a 3.5-mm^2 analysis window by a high resolution Si PIN diode detector. The XRF provides relatively low limits of detection of elements, ranging from 10 ppm. Actual limits of detection depend upon specific sample types and presence of interfering elements (Innov-X Systems, Inc., 2013). The equipment is fitted with a removable Personal Digital Assistant (PDA) containing the necessary software for running the different analysis modes. After data acquisition, results can be shown on the PDA display and downloaded to a PC for further processing.

2.4. Magnetic measurements

Magnetic measurements were carried out in the laboratory using a magnetic susceptibility 2 m (©Bartington Instruments

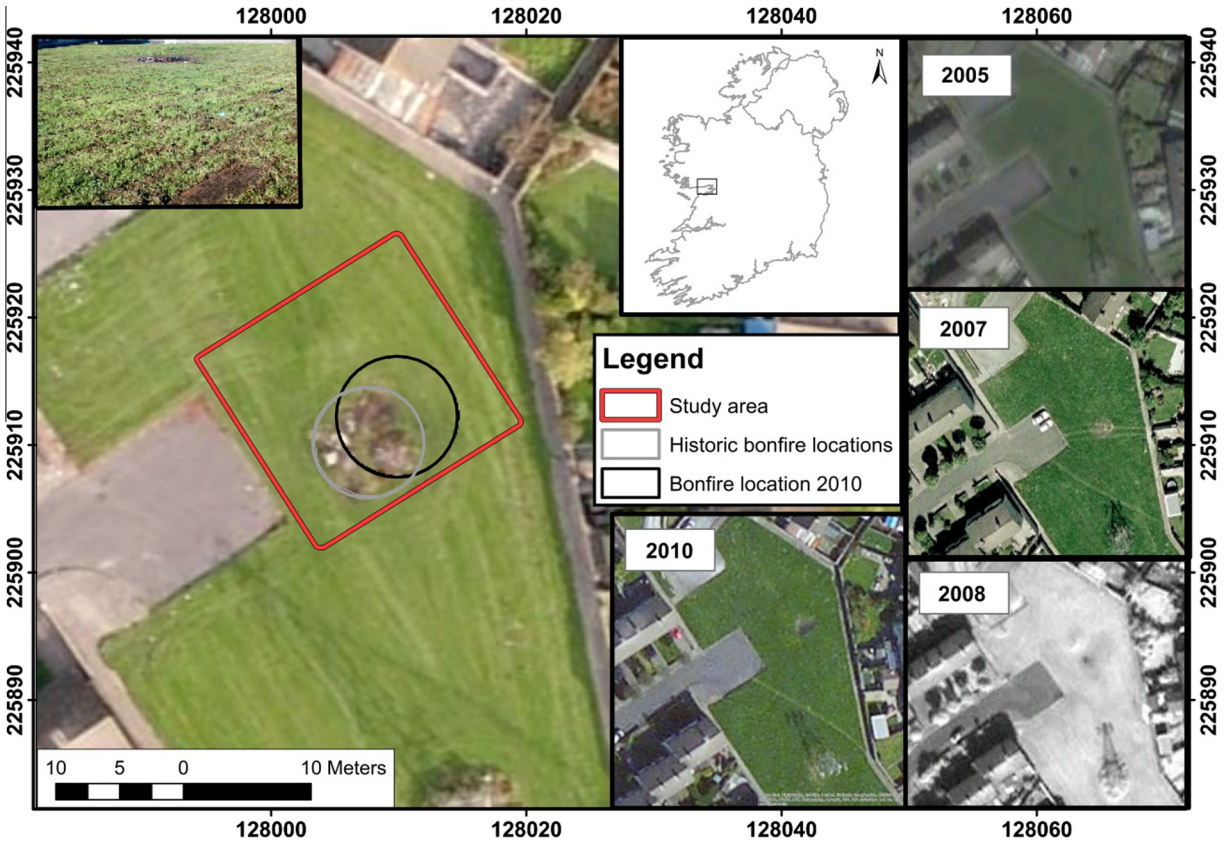

Fig. 1. Map of study area, Inishannagh Park, Galway, Ireland with previously known bonfire locations highlighted (Image: Bing Aerial Map (© 2013 Microsoft Corporation) captured March 2012). Inset: Google™ Earth historical images, featuring past bonfires: 2005, 2007, 2008 and © OSi MapGenie ITM 2010 series, featuring 2010 bonfire.

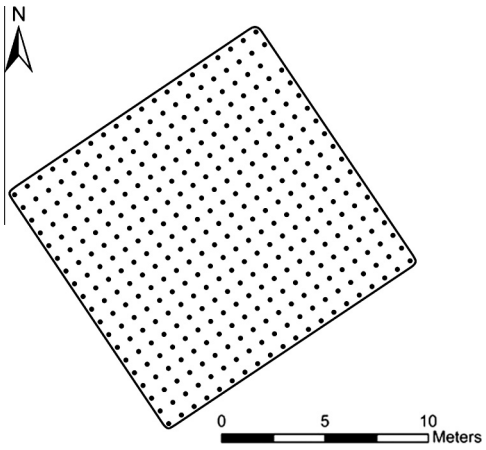

Fig. 2. Sampling grid ($1 \times 1\ m^2$) featuring 379 sampling points.

Ltd.) with a MS2B sensor attached, which generates a weak magnetic field from alternating currents (AC) and detects the magnetisation of the sample in response to the magnetic field. Magnetic susceptibility measured using the MS2B sensor is the ratio of the strength of the magnetisation ($A\ m^{-1}$) to a magnetic field of $\sim$80 $A\ m^{-1}$ and is expressed in SI units (Dearing, 1999). Mass specific susceptibility (χ) was calculated for the soil samples with units of $10^{-8}\ m^3\ kg^{-1}$. MS at low (χ_{lf}, 0.46 kHz) frequency was measured and computed using Multisus v2.44 software for Windows (©Bartington Instruments Ltd.). The measurements are used to detect the presence of ultrafine (<0.03 μm) superparamagnetic ferromagnetic minerals occurring as crystals, produced largely by biochemical processes in soil.

The integrity of instrumental performance and calibration of the magnetic susceptibility sensor was ascertained through the use of a SRM calibration sample (supplied by ©Bartington Instruments Ltd.). The sample was reassessed throughout the measurement process. To verify the integrity of the values obtained, all samples were measured on the higher sensitivity range of 0.1 to assure weaker samples were measured as true to their real values as possible. At this range, small increments of instrumental drift between readings are more prominent and have to be corrected. To compensate for drift in measurements, air readings were taken before and after each measurement and the average subtracted. If there were significant differences between air readings, then the meter was zeroed and the measurement retaken.

2.5. Impact of temperature on magnetic susceptibility

As bonfires will inevitably affect soil temperatures, an experiment was performed to investigate the impacts of bonfires on soil temperatures and associated influences on soil magnetic susceptibility at the study site. Soil (3 kg) was collected from the outer regions of the study area (away from the potential influence of bonfires), homogenised, sieved to <2 mm fraction and ground to a finer fraction using a laboratory disc mill (N.V. TEMA, Model T-100 A). Smaller aliquots were measured and heated using a VWR DRY-Line, Model DL 115 (⩽267 °C) and Nabertherm Laboratory furnace, Model LA 11/11 230 v (⩽3000 °C). Individual aliquots were weighed using a Sartorius TE64 analytic balance (accurate to 0.0001 g), and heated to various temperatures: 50 °C; 100 °C; 150 °C; 200 °C; 300 °C; 400 °C; 500 °C; 600 °C; 700 °C; 800 °C;

900 °C; 1000 °C for 1, 2 and 4 h intervals (n = 3 samples per test). After heating, the aliquots were reweighed and the loss of mass on ignition (LOI) was recorded. Three aliquots were retained in their unheated condition as control samples. A sample was also removed from beneath the ashes of a bonfire at the site (the following morning after a bonfire in 2012) for comparative purposes. The colours of soil samples were recorded using the Munsell Soil Colour Charts (Oyama and Takehara, 1967) after each burn, or in the case of the controls, prior to burning. The Munsell System records colour by hue, value and chroma, providing a standardised system of describing or quantifying colours (Shipman et al., 1984). A follow up experiment to determine remaining organic content (% mass) within the bonfire sample and among samples of similar colouration (100 °C, 150 °C; 200 °C; 300 °C; 400 °C) was carried out to clarify colouration similarities. These samples were heated to 550 °C for 2 h to burn off remaining organic content (Heiri et al., 2001), and percentage mass loss for each sample was recorded.

2.6. Quality control

For total metal concentration, soil certified reference materials (CRMs) (Montana I (SRM 2710a), Montana II (SRM 2711a) and San Joaquin (SRM 2709a)) from the National Institute of Standards and Technology, USA (NIST) were incorporated to ensure the validity of the PXRF technique. These CRMs have been developed for use in method development, method validation and routine quality assurance in the analysis of major, minor and trace element concentration of soils (Mackey et al., 2010).

Three soil SRMs were analysed using the PXRF and the results were compared to certified values for Cu, Fe, Mn, Pb, Sr, Ti and Zn (Table 1). PXRF systems are designed to provide reliable analysis of priority pollutant metals and other elements in soils (Innov-X Systems Inc., 2005) and the results obtained highlight the efficiency of PXRF performance with good recoveries (Table 1). In particular, QA provided high precision values for SRM2709a, depicting the suitability of the PXRF technique for the determination of total metal concentrations in soil samples (Dao et al., 2012). Another confirmation of the validity of the PXRF technique is evident in Fig. 3, which shows that values obtained for total element concentration using the PXRF technique correlated well with values obtained via ICP-OES analysis for 50 samples taken systematically through the study area. The error of the laboratory measurements of mass-specific magnetic susceptibility was found to be an acceptable level of <15% (recovery 85.92%).

2.7. Data analysis and statistics

Statistical analysis was carried out using SPSS 20 (IBM®SPSS® Statistics). The bonfire experiment graph was created using Sigmaplot® v 12.2 (©Systat Software Inc.). Spatial analysis was performed within a Geographical Information System (ESRI® ArcGIS® ArcMap™ 10) with the incorporation of satellite imagery from Ordnance Survey Ireland, MapGenie and Bing Aerial Maps. Local Moran's I cluster/outlier maps were produced using GeoDa™1.4.6. (Anselin et al., 2006) and magnetic measurements were computed using ©Bartington Instruments Ltd. Multisus v2.44 software.

3. Results

3.1. Basic statistics

Descriptive statistics for the raw data of the 7 elements determined by PXRF and MSχ_{lf} are summarised in Table 2 (n = 379). All elemental concentrations are above detection limits. A high degree of variation is visible, depicting the complexity of soil geochemistry across such a small area e.g. the minimum value of Zn (124 mg kg^{-1}) differs by several magnitudes to the maximum value (21,681 mg kg^{-1}). This may be due to the burning of Zinc oxide, which is used in tyres, paints, rubbers, cosmetics, plastics, inks, soap, batteries, pharmaceuticals and many other products (Barceloux, 1999b). Although elements such as Zn and Cu are bio-essential, these metals are potentially toxic at high levels (Barceloux 1999a, 1999b). To obtain a better understanding of the degree of pollution present, a comparison between the median values obtained in this study and those previously published for the local Galway region (Zhang, 2006), national soil surveys (Zhang et al., 2008) and bonfire affected soils, located in Galway City (Dao et al., 2012) are presented in Table 3, demonstrating the elevated values present at this bonfire site. MSχ_{lf} also depicts high deviation from minimum to maximum values. The median MSχ_{lf} value of this study (125.2×10^{-8} m^3 kg^{-1}) was comparable to other contaminated urban soils, e.g., 107×10^{-8} m^3 kg^{-1} in Xuzhou, China (Wang and Qin, 2005) and 68×10^{-8} m^3 kg^{-1} in the coastal region of Izmit Gulf and Izaytas, Turkey (Canbay et al., 2010).

3.2. Relationship between metals and MSχ_{lf} in soils

Laboratory experiments showed that high temperatures can potentially have a large impact on soil MSχ_{lf}, especially at temperatures above 400–500 °C (Fig. 4a). A plateauing effect emerges at first from 'Control' to 400 °C, after which we see a dramatic increase at 500 °C as MSχ_{lf} values continue to rise up to 800 °C, followed by a sharp decline from 900 to 1000 °C (carbon dioxide is evolved from carbonate at 900–1000 °C (Heiri et al., 2001), possibly accounting for this loss). These changes in MSχ_{lf} are not closely followed by LOI, showing that loss in moisture and organic content are likely not driving MSχ_{lf} values. MSχ_{lf} and LOI responses appear to be almost instantaneous, with longer intervals of heat exposure showing little to no added effect over the 1-h intervals in the experiment. A soil sample from beneath a 2012 bonfire site showed only slightly elevated MSχ_{lf} values, similar to aliquots

Table 1
Recovery of metals (Cu, Fe, Mn, Pb, Sr, Ti, Zn) in three soil certified reference materials (Montana I, Montana II and San Joaquin, National Institute of Standards and Technology, USA) (n = 3).

CRM		Cu	Fe	Mn	Pb	Sr	Ti	Zn
SRM 2710a (Montana I)	Certified	3420 ± 50	4.32 ± 0.08	2140 ± 60	5520 ± 30	246.6 ± 7	3310 ± 70	4180 ± 20
	Measured	3231 ± 43	4.59 ± 0.04	2821 ± 87	6521.6 ± 68	253.6 ± 4	3766.6 ± 4	4142.2 ± 48.4
	Recovery (%)	94.4%	106.2%	131.82%	118.1%	102.8%	113.7%	99.09%
SRM 2711a (Montana II)	Certified	140 ± 2	2.82 ± 0.04	675 ± 18	1400 ± 10	242 ± 10	3170 ± 80	414 ± 11
	Measured	124.3 ± 8	2.4 ± 0.02	703 ± 43	1610 ± 17	233 ± 4	3033.3 ± 3	363 ± 9.2
	Recovery (%)	88.7%	85.1%	96%	115%	96.2%	95.6%	87.68%
SRM 2709a (San Joaquin)	Certified	33.9 ± 0.5	3.36 ± 0.07	529 ± 18	17.3 ± 0.1	239 ± 6	3360 ± 70	103 ± 4
	Measured	36 ± 5	3.05 ± 0.02	554.8 ± 41	16.3 ± 3	234.6 ± 3	3200 ± 3	84.8 ± 5
	Recovery (%)	106.1%	90.77%	104.87%	94.3%	98.1%	95.2%	82.33%

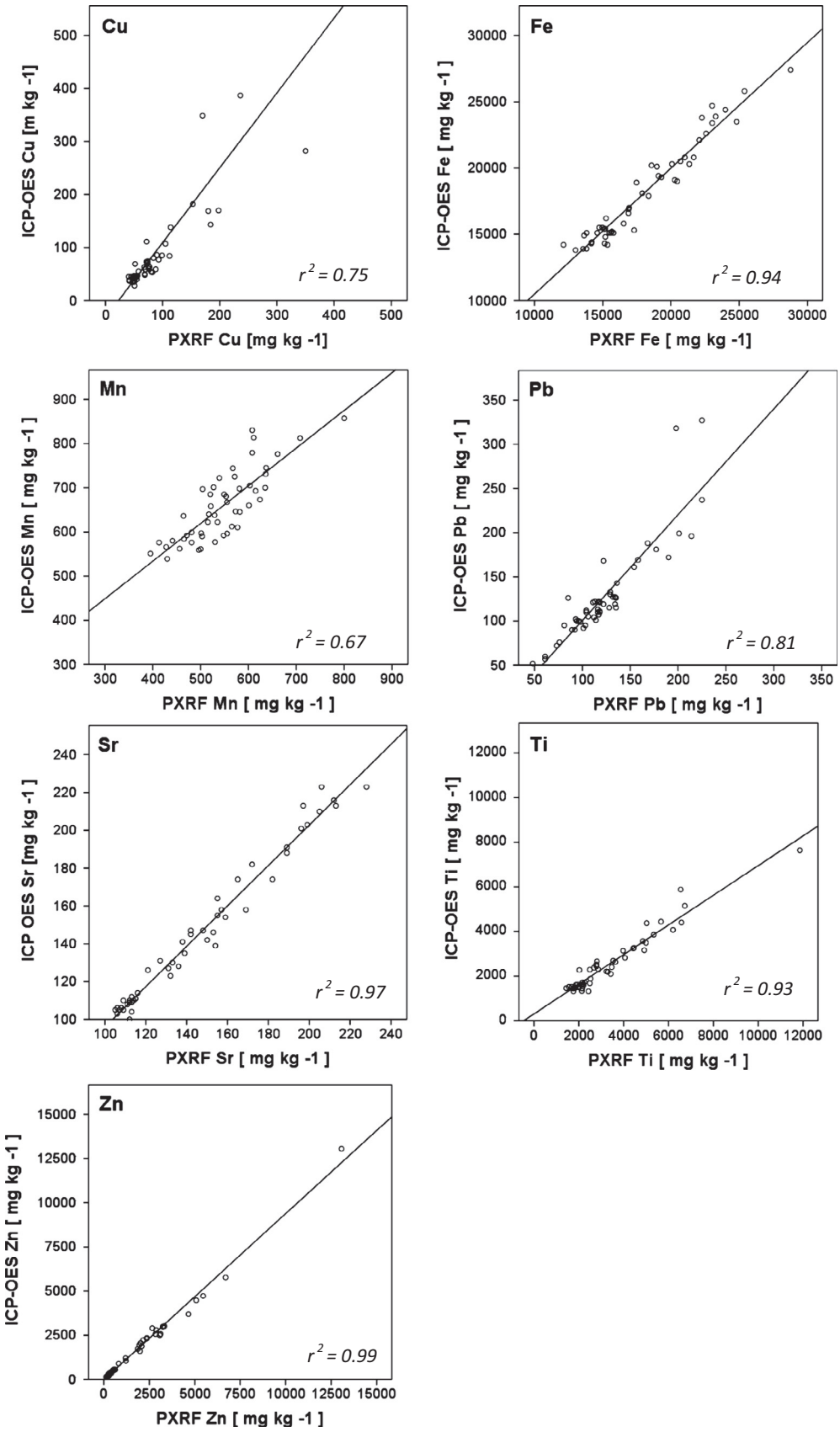

Fig. 3. Comparison between total metal concentrations analysed using ICP-OES and PXRF (mg kg^{-1}) ($n = 50$).

Table 2
Descriptive statistics for total content of metals (mg kg^{-1}) analysed by PXRF and $MS\chi_{lf}$ (10^{-8} m^3 kg^{-1}).

Element	Min	25%	Median	75%	Max	Mean	SD	Skewness	Kurtosis	K–S *p*
Cu	30	51	68	95	1117	95.79	102.75	5.33	37.78	0.00
Fe	12,122	14,622	16,256	19,817	37,724	17471.20	3687.93	1.26	2.09	0.00
Mn	377	482	532	585	964	538.69	84.17	0.96	2.47	0.15
Pb	34	96	114	137	985	134.54	98.78	5.20	33.47	0.00
Sr	95	117	140	166	2922	162.39	162.67	13.65	222.29	0.00
Ti	1434	1994	2606	3955	25,510	3517.69	2559.36	3.29	17.30	0.00
Zn	124	315	561	1693	21,681	1354.74	2015.95	4.55	32.66	0.00
$MS\chi_{lf}$	75.2	109.9	125.2	151	371.2	139.5	46.4	1.9	4.27	0.00

Table 3
Comparison between median values of element concentrations in Galway soils (mg kg^{-1}) (Fe in %).

Element	This study	Bonfire affected soils[a]	Galway region soils[a]	National soil survey (Ireland)[a]
Cu	68	19.1	27	16.2
Fe	1.62	1.12	1.7	1.87
Mn	532	384	539	462
Pb	114	42.1	58	24.8
Sr	140	–	114	49.7
Ti	2606	1495	1623	2133
Zn	561	93.4	85	62.6

[a] Data sources: median values (mg kg^{-1}) (Fe in %) of bonfire affected soils (Dao et al., 2012); local Galway region soils (Zhang, 2006); National soil survey, Ireland (Zhang et al., 2008).

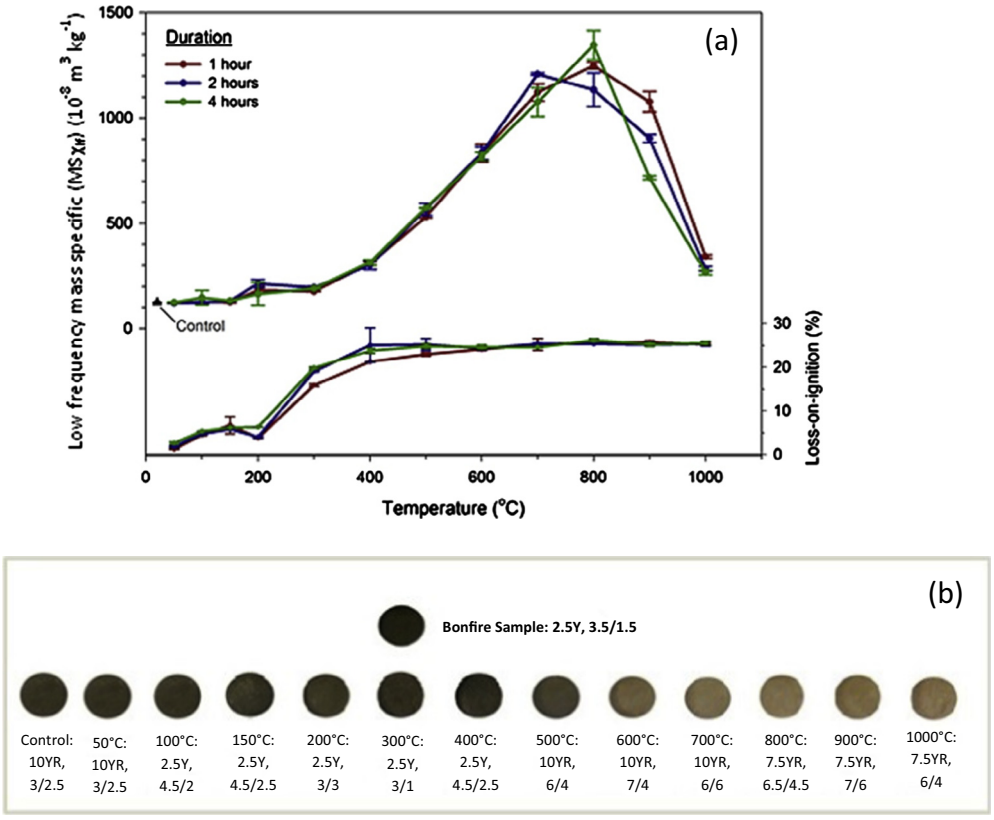

Fig. 4. (a) Relationship between $MS\chi_{lf}$ at different temperature intervals [n = 3 per temp] and Loss-On-Ignition (%) (error bars = 1 st. dev.); (b) relationship between sample colour and temperature (50–1000 °C) with Munsell Colour Chart descriptions (Oyama and Takehara, 1967), based on sample photographs.

burned at 200–300 °C. The soil beneath the 2012 bonfire site also exhibited discolouration similar to aliquots burned at 300 °C (Fig. 4b). Follow-up analysis to determine remaining organic content in similarly coloured samples was used to confirm the colour and LOI-inferred temperatures. The bonfire sample showed 11.0% mass loss in the second burn, which was comparable to samples heated to 200 °C and 300 °C (10.5% and 10.2% mass loss, respectively), greater than samples heated to 100 °C and 150 °C (23.8% and 22.9% mass loss, respectively) and less than samples heated to 400 °C (3.0% mass loss). The results of these experiment thus indicate that bonfires likely only raise soil temperatures to a maximum of 300 °C, and the associated effects of heat from bonfires on

soil MSχ_{lf} are minimal. The exact materials incinerated at the bonfire site are unknown and therefore the impact of burning specific materials on soil MSχ_{lf} cannot be fully quantified. However, metals are highly correlated with MSχ_{lf}. Pearson's correlation coefficients (all significant at $p < 0.01$) of MSχ_{lf} and elements are as shown: Cu (0.558), Fe (0.527), Mn (0.368), Pb (0.332), Sr (0.471), Ti (0.567), Zn (0.615), following a test for normality and necessary data transformation (with details shown in the following sections). The significant correlations between MSχ_{lf} and the elements and the similarity in the spatial distribution of MSχ_{lf} and associated elemental distributions are evident. Therefore, the enhancement of MS is directly related to metal contamination caused by the material deposition, rather than the heating of the soil itself.

3.3. Spatial distribution with metals and MSχ_{lf}

The total concentrations analysed by PXRF and MSχ_{lf} data were first tested for skewness and kurtosis (see Table 2). As expected, the data was heavily skewed and kurtotic. A *Kolmogorov–Smirnov* test ($p < 0.05$) confirmed that the datasets did not pass the normality test, with the exception of Mn ($p = 0.15$). Therefore, the spatial interpolation method of *inverse distance weighting* (IDW) (Bartier and Keller, 1996) was employed as there are no assumptions for the probability distribution of data required for this analysis. Spatial distribution maps of total concentrations of Cu, Fe, Mn, Pb, Sr, Ti, Zn and MSχ_{lf} were produced (Fig. 5) for comparative purposes.

3.4. Hotspot analysis

Local indicators of spatial association (LISA) (Anselin, 1995) maps of the elements Cu, Fe, Mn, Pb, Sr, Ti and Zn and MSχ_{lf} (see Fig. 5) were produced to identify spatial clusters and spatial outliers within the bonfire site. As the raw datasets did not follow a normal distribution (with the exception of Mn), a natural logarithm transformation (ln) was performed on each of the variables (excluding Mn) to bring the datasets to approximate normal distributions, necessary for the calculation of a Local Morals I index. As the datasets involved are located on a 1×1 m^2 grid, the creation of the weight function was based on K-nearest neighbours (8 neighbours) rather than distance threshold.

4. Discussion

Many studies have documented the maximum temperatures reached by fires (Stinson and Wright, 1969; Wright and Bailey, 1982), ranging from 600 °C to 900 °C. Livingstone (2001) investigated the relationship between firing procedures (structures, fuel, schedule and scale) and some of the firing conditions (time and temperature) and found temperatures ranged between 65 and 1011 °C. Tylecote (1962) reports that 400 °C is a normal temperature for a campfire and proposed that such fires rarely reach 700 °C. Rowlett et al. (1974) stated that objects heated in campfires may reach temperatures of 380–550 °C. The impact of heating on soils varies depending on: (a) the composition of materials burned: Sheehy (1988) found that temperatures ranged between 437 and 844 °C where materials included household refuse and vegetation (dried grass, cacti plants, cornstalks and small branches); (b) soil moisture: Busse et al. (2005) found that maximum temperatures of 600 °C were reached in dry clay loam soil of pre-masticated woody shrubs covered areas (simulating wildfire conditions) and were 100–200 °C lower for moist soils (simulating Spring prescribed burning) and c) depth of soil: After a summer fire, soil temperatures above 40 °C were found up to 4.5 cm in depth, while temperatures above 60 °C were found only in the top 0.5 cm of soil (Auld and Bradstock, 1996). Very little is known about the processes by which fires enhances soil MS, however it has been suggested that high temperatures and changes in reduction conditions in the presence of organic matter to oxidation conditions during fires act to convert less magnetic iron oxy-hydroxides into more highly magnetic phases (Clement et al., 2010). Alternatively, Schwertmann and Fechter (1984) showed that heating aluminium substituted goethite produces aluminium substituted maghemite, a much more magnetic phase, which they suggest is a common mechanism by which wildfires cause enhancement of surface magnetisation. Our evidence suggests soil temperatures reached approximately 200–300 °C below the modern bonfire site, and the requisite effects on MSχ_{lf} at this temperature are minimal.

The current study is an investigation into the impacts of soil pollution by metals and associated changes to MSχ_{lf} at an annual urban bonfire site in a residential area. Considering the MSχ_{lf} results on the modern bonfire sample, it could be surmised that heating can play an intrinsic role in magnetic enhancement. However, it cannot be considered fully accountable for the elevated MSχ_{lf} values beneath the bonfire site, indicating the influence of metal contamination through direct metal inputs. This is further validated by the shared spatial patterns featured in Fig. 5. MSχ_{lf} can be influenced by a multitude of mechanisms. There are numerous uncertainties in the composition, combustion profile, environmental conditions, etc. of a bonfire. However, enhancement of magnetic properties at a bonfire location is an indication the pollution activity of burning ferrous objects has occurred.

General patterns exist throughout the elemental spatial distribution maps (Fig. 5), with a hotspot visible in the central southeastern section of the site. When compared to the locations of previous bonfires (Fig. 1), it is possible to propose that the presence of a *high–high* value cluster in the area is due to the activity of burning metal laden materials, as the MSχ_{lf} map and Moran's I maps also feature this pattern. Cu, Fe and Zn, in particular, encompass this area, both of which are by-products of the burning of tyres (DEFRA, 2006). Both tyre threads (Fauser et al., 1999) and tyre dust (Adachia and Tainoshob, 2004) contain significant amounts of Zn. Brake housing dust and crushed brake pads analyses also indicate high concentrations of Cu and Fe (Adachia and Tainoshob, 2004; Apeagyei et al., 2011). Under certain conditions, the mobility of Zn is poor and therefore Zn contamination can occur near the point source (Barceloux, 1999b). Although there are large variations across the metals, all appear to have elevated values in the northeasterly section, indicating the likely location of another historic bonfire. This northern point is the main Sr hotspot location. Sr is found in fireworks and sparklers (Stewart, 2014), which is a possible traditional festive and entertainment source during the bonfire celebrations. The degree of elevation of this section differs greatly among the metals, with Cu, Pb, Sr and to a less extent Ti, featuring statistically significantly high–high values. However, the absence of Zn suggests tyres have never been burned at this section. Titanium is not known to have any adverse health effects, and is ubiquitous and naturally occurring in soil (De Vos and Tarvainen, 2005). However, due to its strong correlation with MSχ_{lf} and its spatial association with the main burning zone, it may have entered the site through burning. Ti is also associated with tyres and brake wear (Apeagyei et al., 2011). Due to its similar dispersion pattern to Zn and Fe, high concentrations may also be as a result of the burning of tyres (Apeagyei et al., 2011). Historically, leaded-petrol was a major source of Pb (Von Storch et al., 2003) and its presence may infer its use as an ignition fluid for previous bonfires or another burning zone, as it also features exclusively in the northwestern section of the study zone. Pb is also found in common municipal waste e.g. paint, batteries, electrical appliances, ceramics and crystal glass (Stone, 1981), all of which are

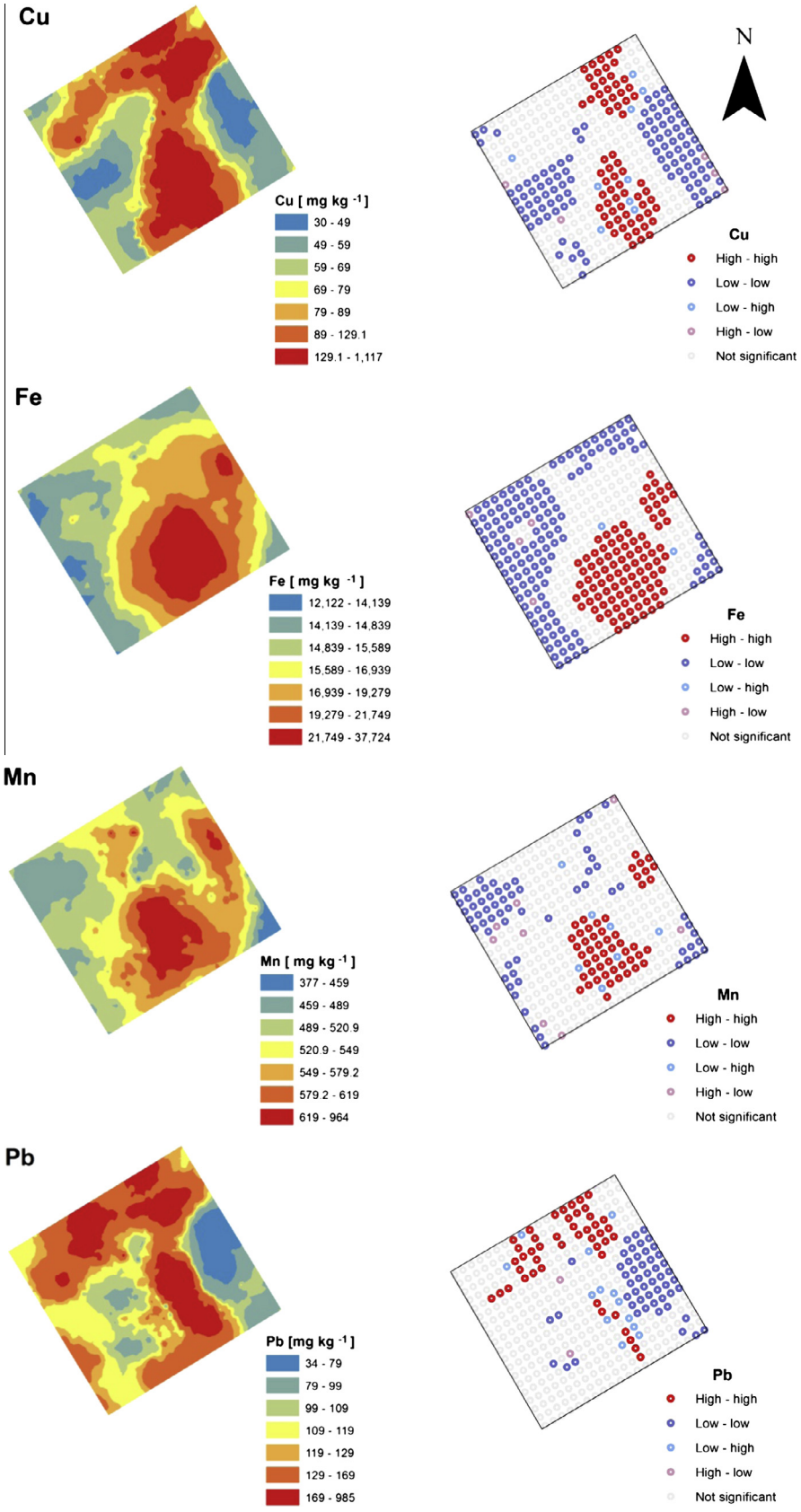

Fig. 5. Total concentrations distribution and local Moran's I maps of Cu, Fe, Mn, Pb, Sr, Ti and Zn (mg kg^{-1}) and low frequency magnetic susceptibility ($MS\chi_{lf}$) (10^{-8} m^3 kg^{-1}).

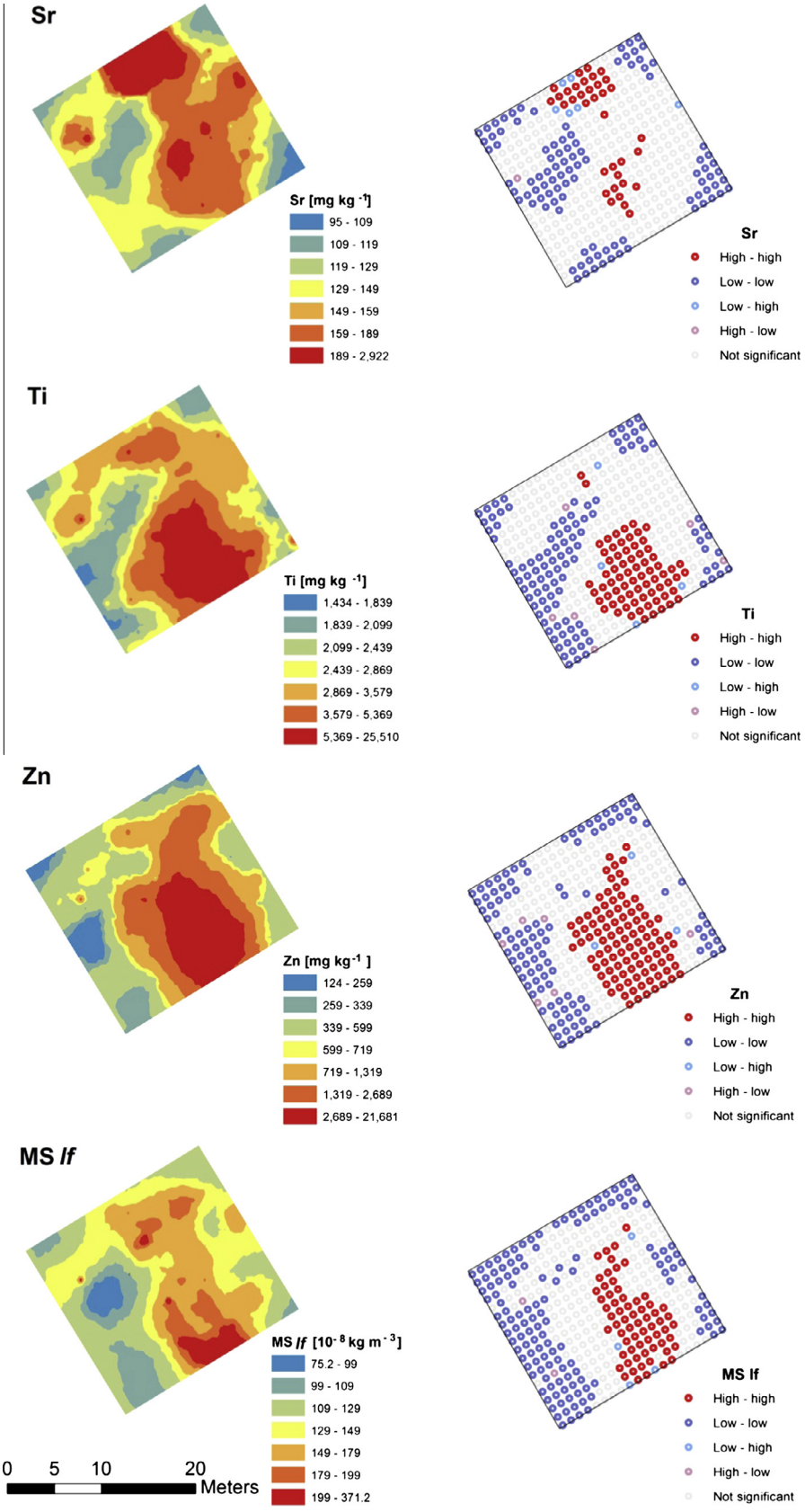

Fig. 5 (*continued*)

possible Pb sources. Like Pb, Cu is used in many household items, glass making, jewellery, wiring and as a wood preservative (Barceloux, 1999a) and Cu treated household furniture items may have been used as fuel. The distributions of Cu and Pb are very similar, the main difference occurring in the location of the main bonfire in the central southeastern section. This may be due to the localised burning of leaded-paint, a major Pb pollution source (Stone, 1981), in the eastern section of the burning zone. The distribution maps infer the presence of an additional bonfire in the northwestern section of the site. In particular, this spatial pattern is visible for Cu, Pb, Sr, Ti and MSχ_{lf}. However, these are not statistically significant, with the exception of Pb. Outliers are identifiable as the cause of the assumed elevated values in the distribution maps. A disadvantage of IDW maps is that outliers may be exaggerated, to indicate regions of high values, which may not a true reflection of the sample data (Zhang et al., 2008). However, there appears to be symmetry across corresponding elementary maps, e.g. Fe distribution map compared to Fe Moran's I map. Since 2000, leaded petrol was removed from the market in the EU (Von Storch et al., 2003) and lead replacement petrols (LRP) with additives such as manganese were introduced (Barlow, 1999). Given the unique location of a high–high Mn and Fe values in the central eastern section of the site, Mn-bearing petrol may have been used as a possible ignition fuel. Significant *low–low* clusters are not as uniform across all maps, but in general occur in the western section and the south easterly edge of the site. These points and non-significant points are indicative that the soil here contains background values which have not been affected by bonfires.

The significant high–high values featured across the site indicate the presence of possibly 3–4 burning zones. These features are not visible on the available satellite imagery, with the exception of the main central southeastern burning zone. The spatial dispersion of metals is suggestive of a variety of materials being burnt in the bonfires. Zn presence is indicative of the burning of tyres, in a central eastern/central southeastern direction. Other metals indicate a bonfire in other locations where tyres were likely not burned, with significant high–high values in a north eastern direction of Cu, Pb, Sr and Ti, high–high values of Pb in a western direction and Mn and Fe significantly high in the central east of the site. The metals present, as well as the metal–MS correlations, are thus mainly dependent on the materials burned in the bonfires. This study provides novel information of spatial changes of metals and MS of bonfire site soil, as well as their spatial relationship and patterns.

5. Conclusion

By examining the metal and MSχ_{lf} maps and available satellite imagery, bonfires are recognised as a major pollution source in soils of the study area. The spatial range of influence of a bonfire is confined to the boundary of materials being burnt and is estimated at around 10 m such an extent is in line with the size of the bonfire under study, demonstrating the spread of bonfire-caused metal pollution in soils is quite limited. The local Moran's I and spatial distribution maps presented here demonstrate the enhancement of metals and magnetisation in bonfire soils. The fast and inexpensive delineation of environmental pollution by PXRF and MS is also shown. This allows for high density sampling of sites, leading to the generation of high resolution maps, possible in small-scale/regional studies. A study into the effects of heating on magnetisation also revealed that soils under bonfires reached a maximum temperature of 300 °C, indicating heating is likely not a significant factor in the enhancement of magnetisation. More research into the materials burnt in bonfires is necessary to further investigate the impacts of bonfires on the environment. Finally, the environmental impacts of bonfires should be taken into consideration in future policy on soil protection.

Acknowledgements

This study was partly sponsored by the Department of Communications, Energy and Natural Resources under the National Geoscience Programme of Ireland 2007–2013 (Griffiths Research Award). We are grateful to Ligang Dao, Ta Na, Sorcha Dolan and Enda Mc Grory for their assistance in sample collection and Enda Mc Grory for assistance with the PXRF analysis. Also to the Department of Archaeology, NUI Galway for the loan of a MS2 meter.

References

Adachia, K., Tainoshob, Y., 2004. Characterization of heavy metal particles embedded in tire dust. Environ. Int. 30, 1009–1017.
Alekseeva, T., Alekseev, A., Maher, B.A., Demkin, V., 2007. Late Holocene climate reconstructions for the Russian steppe, based on mineralogical and magnetic properties of buried palaeosols. Paleogeogr., Paleoclimatol., Paleoecol. 249, 103–127.
Anselin, L., 1995. Local indicators of spatial association – LISA. Geogr. Anal. 27 (2), 93–115.
Anselin, L., Syabri, I., Kho, Y., 2006. GeoDa: an introduction to spatial data analysis. Geogr. Anal. 38 (1), 5–22.
Apeagyei, E., Bank, M.S., Spengler, J.D., 2011. Distribution of heavy metals in road dust along an urban–rural gradient in Massachusetts. Atmos. Environ. 45 (13), 2310–2323.
Auld, T.D., Bradstock, R.A., 1996. Soil temperatures after the passage of a fire: do they influence the germination of buried seeds? Aust. J. Ecol. 21 (1), 106–109.
Barceloux, D.G., 1999a. Zinc. Clin. Toxicol. 37 (2), 279–292.
Barceloux, D.G., 1999b. Copper. Clin. Toxicol. 37 (2), 217–230.
Barlow, P.L., 1999. The lead ban, lead replacement petrol, and the potential for engine damage. Ind. Lubr. Tribol. 51 (3), 128–138.
Bartier, P.M., Keller, C.P., 1996. Multivariate interpolation to incorporate thematic surface data using inverse distance weighting (IDW). Comput. Geosci. 22 (7), 795–799.
Blaha, U., Appel, E., Stanjek, H., 2008. Determination of anthropogenic boundary depth in industrially polluted soil and semi-quantification of heavy metal loads using magnetic susceptibility. Environ. Pollut. 156, 278–289.
Blundell, A., Dearing, J.A., Boyle, J.F., Hannam, J.A., 2009. Controlling factors for the spatial variability of soil magnetic susceptibility across England and Wales. Earth Sci. Rev. 95, 158–188.
Botsou, F., Karageorgis, A.P., Dassenakis, E., Scoullos, M., 2011. Assessment of heavy metal contamination and mineral magnetic characterization of the Asopos River sediments (Central Greece). Mar. Pollut. Bull. 62, 547–563.
Busse, M.D., Hubbert, K.R., Fiddler, G.O., Shestak, C.J., Powers, R.F., 2005. Lethal soil temperatures during burning of masticated forest residues. Int. J. Wildland Fire 14, 267–276.
Butterfield, D.M., Brown, R.J.C., 2012. Report on Polycyclic Aromatic Hydrocarbons in Northern Ireland. NPL Report AS66, Northern Ireland Department of Environment. February 2012. <http://www.doeni.gov.uk/de/pah_in_ni_report_final_published_version_v2.pdf> (last visited 03.05.14).
Canbay, M., Aydin, A., Kurtulus, C., 2010. Magnetic susceptibility and heavy metal contamination in topsoils along the Izmit Gulf coastal area and IZAYTAS (Turkey). J. Appl. Geophys. 70, 46–57.
Chan, L.S., Ng, S.L., Davis, A.M., Yim, W.W.S., Yeung, C.H., 2001. Magnetic properties and heavy-metal contents of contaminated seabed sediments of Penny's Bay, Hong Kong. Mar. Pollut. Bull. 42, 569–583.
Clement, B.M., Javier, J., Sah, J.P., Ross, M.S., 2010. The effects of wildfires on the magnetic properties of soils in the Everglades. Earth Surf. Process. Landforms, 1–7.
Dao, L., Morrison, L., Zhang, C., 2012. Bonfires as potential source of metal pollutants in urban soils, Galway, Ireland. Appl. Geochem. 27, 930–935.
De Vos, W., Tarvainen, T., 2005. Geochemical Atlas of Europe. Part 2 – Interpretation of Geochemical Maps, Additional Tables, Figures, Maps and Related Publications. Geological Survey of Finland, Otamedia Oy, Espoo, pp. 373–377.
Dearing, J., 1999. Environmental Magnetic Susceptibility. Using the Bartington MS2 System, second ed. Chi Publishing, Kenilworth, England, UK.
Department for Environment, Food and Rural Affairs (DEFRA), 2006. A Review of Bonfire Smoke Nuisance Controls. Report by Netcen to the Department for Environment, Food and Rural Affairs (UK). Department for the Environment, Northern Ireland. <http://archive.defra.gov.uk/environment/quality/local/nuisance/smoke/documents/bonfiresmoke-report.pdf> (last visited 03.05.14).
D'Emilio, M., Macchiato, M., Ragosta, M., Simoniello, T., 2012. A method for the integration of satellite vegetation activities observations and magnetic susceptibility measurements for monitoring heavy metals in soil. J. Hazard. Mater. 241–242, 118–126.
El Baghdadi, M., Barakat, A., Sajieddine, M., Nadem, S., 2012. Heavy metal pollution and soil magnetic susceptibility in urban soil of Beni Mellal City (Morocco). Environ. Earth Sci. 66, 141–155.
Environmental Protection Agency (EPA), 2006. Halloween Bonfires not an Excuse to Dispose of Waste. <http://www.epa.ie/newsandevents/news/previous/2006/name,48003,en.html> (last visited 03.09.14).

Fauser, P., Tjell, J.C., Mosbaek, H., Pilegaard, K., 1999. Quantification of tire-thread particles using extractable organic zinc as tracer. Rubber Chem. Technol. 72, 969–977.
Frančišković-Bilinski, S., Bilinski, H., Scholger, R., Tomašić, N., Maldini, K., 2014. Magnetic spherules in sediments of the karstic Dobra River (Croatia). J. Soils Sediments 14, 600–614.
Gailey, A., Adams, G.B., 1977. The Bonfire in the North Irish Tradition. Taylor & Francis Ltd., Oxfordshire.
Getis, A., Ord, J.K., 1992. The analysis of spatial association by use of distance statistics. Geogr. Anal. 24, 189–206.
Gudadhe, S.S., Sangode, S.J., Patil, S.K., Chate, D.M., Meshram, D.C., Badekar, A.G., 2012. Pre- and post-monsoon variations in the magnetic susceptibilities of soils of Mumbai metropolitan region: implications to surface redistribution of urban soils loaded with anthropogenic particulates. Environ. Earth Sci. 67, 813–831.
Hanesch, M., Scholger, R., 2002. Mapping of heavy metal loadings in soils by means of magnetic susceptibility measurements. Environ. Geol. 42, 857–870.
Heiri, O., Lotter, A.F., Lemcke, G., 2001. Loss on ignition as a method for estimating organic and carbonate content in sediments: reproducibility and comparability of results. J. Paleolimnol. 25, 101–110.
Innov-X Systems, Inc., 2005. Technical Data. Alpha Series™-analyzers Provide on-site Environmental Metals Testing. <http://www.fieldenvironmental.com/assets/files/Literature/InnovX%20XRF%20Specs.pdf> (last visited 03.05.14).
Innov-X Systems, Inc., 2013. Handheld XRF Revolutionizes Environmental Testing. The Best Environmental Analyzer in the World. <http://yosemite.epa.gov/r9/sfund/r9sfdocw.nsf/3dc283e6c5d6056f88257426007417a2/e599199dc919b049882576a300616943/$FILE/Attachment%202.pdf> (last visited 15.09.14).
Jacquez, G., Grimson, R., Waller, L., Wartenberg, D., 1996. The analysis of disease clusters, part ii: Introduction to techniques. Infect. Control Epidemiol. 17 (6), 385–397.
Jordanova, N.V., Jordanova, D.V., Veneva, L., Yorova, K., Petrovsky, E., 2003. Magnetic response of soils and heavy metal pollution – a case study. Environ. Sci. Technol. 37, 4417–4424.
Kapička, A., Jordanova, N., Petrovský, E., Podrázský, V., 2003. Magnetic study of weakly contaminated forest soils. Water Air Soil Pollut. 148, 31–44.
Levine, N., 2006. Crime mapping and the CrimeStat program. Geogr. Anal. 38 (1), 41–56.
Li, W., Xu, B., Song, Q., Liu, X., Xu, J., Brookes, P.C., 2014. The identification of 'hotspots' of heavy metal pollution in soil–rice systems at a regional scale in eastern China. Sci. Total Environ. 472, 407–420.
Livingstone, Smith A., 2001. Bonfire II: the return of pottery firing temperatures. J. Archaeol. Sci. 28, 991–1003.
Lu, S.G., Bai, S.Q., 2006. Study on the correlation of magnetic properties and heavy metals content in urban soils of Hangzhou City, China. J. Appl. Geophys. 60, 1–12.
Lu, S.G., Bai, S.Q., Fu, L.X., 2008. Magnetic properties as indicators of Cu and Zn contamination in soils. Pedosphere 18 (4), 479–485.
Lu, S.G., Wang, H.G., Chen, Y.Y., 2012. Enrichment and solubility of trace metals associated with magnetic extracts in industrially derived contaminated soils. Environ. Geochem. Health 34, 433–444.
Mackey, E.A., Christopher, S.J., Lindstrom, R.M., Long, S.E., Marlow, A.F., Murphy, K.E., Paul, R.L., Popelka-Filcoff, R.S., Rabb, S.A., Sieber, J.R., Spatz, R.O., Tomlin, B.E., Wood, L.J., Yen, J.H., Yu, L.L., Zeisler, R., Wilson, S.A., Adams, M.G., Brown, Z.A., Lamothe, P.L., Taggart, J.E., Jones, C., Nebelsick, J., 2010. Certification of Three NIST Renewal Soil Standard Reference Materials for Element Content: SRM 2709a San Joaquin Soil, SRM 2710a Montana Soil I, and SRM 2711a Montana Soil II. NIST Special Publication 260-172. US Department of Commerce and the National Institute of Standards and Technology.
Magiera, T., Kapička, A., Petrovský, E., Strzyszcz, Z., Fialová, H., Rachwał, M., 2008. Magnetic anomalies of forest soils in the Upper Silesia-Northern Moravia region. Environ. Pollut. 156, 618–627.
Maher, B.A., Hallam, D.F., 2005. Paleomagnetic correlation and dating of Pilo/Pleistocene sediments at the southern margins of the North Sea Basin. J. Quat. Sci. 20 (1), 67–77.
Maher, B.A., Alekseev, A., Alekseeva, T., 2002. Variation of soil magnetism across the Russian steppe: its significance for use of soil magnetism as a paleorainfall proxy. Quatern. Sci. Rev. 21, 1571–1576.
Maher, B.A., Alekseev, A., Alekseeva, T., 2003. Magnetic mineralogy of soils across the Russian Steppe: climatic dependence of pedogenic magnetite formation. Paleogeogr., Paleoclimatol., Paleoecol. 201, 321–341.
McCullagh, M.J., 2006. Detecting Hotspots in Time and Space. ISG06. <https://www.academia.edu/699868/Detecting_hotspots_in_time_and_space> (last visited 03.05.14).
Morton-Bermea, O., Hernandez, E., Martinez-Pichardo, E., Soler-Arechalde, A.M., Lozano Santa-Cruz, R., Gonzalez-Hernandez, G., Beramendi-Orosco, L., Urrutia-Fucugauchi, J., 2009. Mexico City topsoils: heavy metals vs. magnetic susceptibility. Geoderma 151, 121–125.
Ord, J.K., Getis, A., 1995. Local spatial autocorrelation statistics: distribution issues and an application. Geogr. Anal. 27 (4), 286–306.
Oyama, M., Takehara, H., 1967. Revised Standard Soil Color Charts. National Institute of Agricultural Sciences, Forest Experiment Station, Japan Color Research Institute, Japan.
Rowlett, R.M., Mandeville, M.D., Zeller, E.J., 1974. The interpretation and dating of humanly worked siliceous materials by thermoluminescent analysis. Proc. Prehist. Soc. 40, 37–44.
Sapkota, B., Cioppa, M.T., 2012. Using magnetic and chemical measurements to detect atmospherically-derived metal pollution in artificial soils and metal uptake in plants. Environ. Pollut. 170, 131–144.
Schwertmann, U., Fechter, H., 1984. The influence of aluminum on iron oxides: XI. Aluminum-substituted maghemite in soils and its formation. Soil Sci. Soc. Am. J. 48, 1462–1463.
Sheehy, J.J., 1988. Ceramic ecology and the clay/fuel ratio: modelling fuel consumption in Tlajina 33, Teotihuacan, Mexico. In: Kolb, C.C. (Ed.), Ceramic Ecology Revisited, 1987: The Technology and Socio Economics of Pottery, Part 1. BAR International Series 436. Archaeo Press, Oxford, pp. 199–226.
Shipman, P., Foster, G., Schoeninger, M., 1984. Burnt bones and teeth: an experimental study of color, morphology, crystal structure and shrinkage. J. Archaeol. Sci. 11, 307–325.
Sokal, R.R., Oden, N.L., Thomson, B.A., 1998a. Local spatial autocorrelation in biological variables. Biol. J. Linn. Soc. 65, 41–62.
Sokal, R.R., Oden, N.L., Thomson, B.A., 1998b. Local spatial autocorrelation in a Biological Model. Geogr. Anal. 30 (4), 331–354.
Stewart, D., 2014. Strontium. Chemicool Periodic Table. <http://www.chemicool.com/elements/strontium.html> (last visited 05.09.14).
Stinson, K.J., Wright, H.A., 1969. Temperature headfires in the southern mixed prairie of Texas. J. Range Manage. 22, 169–174.
Stone, H.M., 1981. Lead. J. Chem. Educ. 51 (9), 722–724.
Strzyszcz, Z., Magiera, T., 1998. Magnetic susceptibility and heavy metals contamination in soils of Southern Poland. Phys. Chem. Earth 23 (9–10), 1127–1131.
Tylecote, R.F., 1962. Metallurgy in Archaeology. Arnold Press, London, UK.
Von Storch, H., Costa-Cabral, M., Hagner, C., Feser, F., Pacyna, J., Pacyna, E., Kolb, S., 2003. Four decades of gasoline lead emissions and control policies in Europe: a retrospective assessment. Sci. Total Environ. 311 (1–3), 151–176.
Wang, X.S., Qin, Y., 2005. Correlation between magnetic susceptibility and heavy metals in urban topsoil: a case study from the city of Xuzhou, China. Environ. Geol. 49, 10–18.
Wright, H., Bailey, P.W., 1982. Fire Ecology: United States and Southern Canada. John Wiley & Sons, New York.
Yang, T., Liu, Q., Zeng, Q., Chan, L., 2012. Relationship between magnetic properties and heavy metals of urban soils with different soil types and environmental settings: implications for magnetic mapping. Environ. Earth Sci. 66, 409–420.
Zawadzki, J., Fabijańczyk, P., 2008. Reduction of soil contamination uncertainty assessment using magnetic susceptibility measurements and co-est method. Proc. ECOpole 2 (1), 171–174.
Zhang, C., 2006. Using multivariate analyses and GIS to identify pollutants and their spatial patterns in urban soils in Galway, Ireland. Environ. Pollut. 142, 501–511.
Zhang, T., Lin, G., 2007. A decomposition of Moran's I for cluster detection. Comput. Stat. Data Anal. 51, 6123–6137.
Zhang, C., Luo, L., Xu, W., Ledwith, V., 2008. Use of local Moran's I and GIS to identify pollution hotspots of Pb in urban soils of Galway, Ireland. Sci. Total Environ. 398, 212–221.
Zhang, C., Qiao, Q., Appel, E., Huang, B., 2012. Discriminating sources of anthropogenic heavy metals in urban street dusts using magnetic and chemical methods. J. Geochem. Explor. 119–120, 60–75.
Zhu, Z., Han, Z., Bi, X., Yang, W., 2012. The relationship between magnetic parameters and heavy metal contents of indoor dust in e-waste recycling impacted area, Southeast China. Sci. Total Environ. 433, 302–308.
Zhu, Z., Sun, G., Bi, X., Li, Z., Yu, G., 2013. Identification of trace metal pollution in urban dust from kindergartens using magnetic, geochemical and lead isotopic analyses. Atmos. Environ. 77, 9–15.

Environmental Research 155 (2017) 294–306

Contents lists available at ScienceDirect

Environmental Research

journal homepage: www.elsevier.com/locate/envres

Impact of grass cover on the magnetic susceptibility measurements for assessing metal contamination in urban topsoil

Nessa Golden[a], Chaosheng Zhang[a], Aaron P. Potito[a], Paul J. Gibson[b], Norma Bargary[c], Liam Morrison[d,*]

[a] School of Geography and Archaeology, National University of Ireland Galway, Galway, Ireland
[b] Environmental Geophysics Unit, Department of Geography, National University of Ireland, Maynooth, Ireland
[c] Department of Mathematic & Statistics, University of Limerick, Limerick, Ireland
[d] Earth and Ocean Sciences, School of Natural Sciences and Ryan Institute, National University of Ireland Galway, Galway, Ireland

ARTICLE INFO

Keywords:
Magnetic susceptibility
Soil metal contamination
Grass cover
in situ MS
Environmental magnetism

ABSTRACT

In recent decades, magnetic susceptibility monitoring has developed as a useful technique in environmental pollution studies, particularly metal contamination of soil. This study provides the first ever examination of the effects of grass cover on magnetic susceptibility (MS) measurements of underlying urban soils. Magnetic measurements were taken *in situ* to determine the effects on κ (volume magnetic susceptibility) when the grass layer was present (κ^{grass}) and after the grass layer was trimmed down to the root ($\kappa^{no\ grass}$). Height of grass was recorded *in situ* at each grid point. Soil samples (n=185) were collected and measurements of mass specific magnetic susceptibility (χ) were performed in the laboratory and frequency dependence (χ_{fd}%) calculated. Metal concentrations (Pb, Cu, Zn and Fe) in the soil samples were determined and a gradiometry survey carried out *in situ* on a section of the study area. Significant correlations were found between each of the MS measurements and the metal content of the soil at the $p < 0.01$ level. Spatial distribution maps were created using Inverse Distance Weighting (IDW) and Local Indicators of Spatial Association (LISA) to identify common patterns. κ^{grass} (ranged from 1.67 to 301.00×10^{-5} SI) and $\kappa^{no\ grass}$ (ranged from 2.08 to 530.67×10^{-5} SI) measured *in situ* are highly correlated [r=0.966, n=194, $p < 0.01$]. The volume susceptibility datasets in the presence and absence of grass coverage share a similar spatial distribution pattern. This study re-evaluates *in situ* κ monitoring techniques and the results suggest that the removal of grass coverage prior to obtaining *in situ* κ measurements of urban soil is unnecessary. This layer does not impede the MS sensor from accurately measuring elevated κ in soils, and therefore κ measurements recorded with grass coverage present can be reliably used to identify areas of urban soil metal contamination.

1. Introduction

Metal contaminants are a useful indicator of environmental pollution in urban soils. The assessment of magnetic susceptibility of soils has become an established reliable and efficient proxy for metal contamination. The magnetic susceptibility of soils mainly depends on ferromagnetic mineral content which are a result of natural and anthropogenic processes. Natural processes can include weathering of rocks (Kapička et al., 2008) or occur during pedogenic processes which can be mediated by microorganisms (D'Emilio et al., 2007). Magnetic particles occurring in industrial and urban dusts have an anthropogenic source and are referred to as technogenic magnetic particles (TMPs). These iron minerals are formed as a result of technological processes at very high temperatures which are released into the atmosphere (Hanesch and Scholger, 2002; Magiera et al., 2011). Fossil-fuel burning power plants are a significant source of airborne TMPs (Hanesch and Scholger, 2002; Evans and Heller, 2003). Combustion of coal causes the release of sulfur gas and formation of spherical iron particles which can oxidize to form magnetite (Fe_3O_4) (Flanders, 1999; Hanesch and Scholger, 2002), pyrrhotite (Fe_7S_8) and other minerals can also form which are rarely found in the natural environment (technogenic ferrites) (Łukasik et al., 2015). In the event where natural processes are not a significant contributing factor in the magnetization of soil, magnetic susceptibility has emerged as an alternative technique for monitoring environmental metal pollution (Chianese et al., 2006). Particulates resulting from anthropogenic emissions may integrate potentially toxic elements (PTEs) into their structure. Magnetic particles TMPs can act as a host of metals and

* Corresponding author.
E-mail address: liam.morrison@nuigalway.ie (L. Morrison).

http://dx.doi.org/10.1016/j.envres.2017.02.032
Received 9 June 2016; Received in revised form 21 February 2017; Accepted 24 February 2017
Available online 10 March 2017
0013-9351/

contaminants by either incorporating metals into the crystalline structure during combustion, or PTEs may adhere onto their exterior after formation (Chaparro et al., 2006; Kapička et al., 2008).

Magnetic parameters are widely applied in many fields including archaeology and environmental science. The application of magnetic studies to environmental features of archaeology was first established in the 1950's which concerned the magnetic susceptibility of soils. Le Borgne observed enhanced magnetism in topsoils in comparison to the underlying bedrock (Evans and Heller, 2003). Initially, magnetic susceptibility was used to investigate magnetic enhancement of soils relating to fire which could be a result of natural or human activity or pedogenic processes (Dalan, 2008). More modern applications include the locating, mapping and interpretation of earthworks and also as part of the excavation process, carrying out magnetic susceptibility surveys on walls and floors at the microscale to add an additional layer of data to an excavation (Dalan, 2008). Environmental magnetism involves relating magnetic properties of mineral assemblages to the environmental conditions that govern them (Liu et al., 2012). The technique has been developed over the past thirty years and the range of applications of magnetic susceptibility conveyed by many (i.e. Thompson and Oldfield, 1986; Verosub and Roberts, 1995; Maher and Thompson, 1999; Evans and Heller, 2003; Gibson and George, 2013).

The use of magnetic parameters as a proxy for environmental metal contamination in urban environments is established (Canbay et al., 2010; El Baghdadi et al., 2012; Girault et al., 2016; Golden et al., 2015; Liu and Bai, 2006; Morton-Bermea et al., 2009; Yang et al., 2012; Zhang et al., 2012; Zhu et al., 2012). Environmental magnetic methods have been extensively used to examine the extent and causes of anthropogenic contamination, providing a simple, rapid, non-intrusive and feasible tool in the identification of metal pollutants (Chianese et al., 2006; Zhang et al., 2012).

Magnetic susceptibility can be measured in the laboratory as mass specific magnetic susceptibility (χ) and *in situ* as volume magnetic susceptibility (κ) and is a quick and economical technique compared to traditional chemical methods of analysis for soil geochemistry (Jordanova et al., 2003; Soodan et al., 2014).

Volume magnetic susceptibility has been applied as a proxy for metal contamination in many environmental samples such as sediments (Canbay et al., 2010), leaves (Gautam et al., 2005), tree bark (Kletetschka et al., 2003), mosses (Fabian et al., 2011), lichens (Salo et al., 2012), fly ash (Kapička et al., 1999; Zawadzki et al., 2010) and soils (Bityukova et al., 1999; Hoffmann et al., 1999; Boyko et al., 2004; Schmidt et al., 2005; Canbay et al., 2010). The capability of κ to provide instant measurements make it possible to determine relative pollution impacts directly in the field (Jordanova et al., 2003). The main limitation of this technique in relation to environmental studies is the depth of analysis. *In situ* magnetic susceptibility studies are limited to the upper topsoil horizon as significant MS properties may lie below this horizon.

MS mapping has developed as an important technique in soil analyses and monitoring of temporal changes in environmental studies (Dao et al., 2010, 2012, 2013, 2014; Petrovský and Ellwood, 1999; Hanesch et al., 2007). Many studies have incorporated the use of κ to assist in soil metal pollution mapping studies particularly in urban soils (Wang and Qin, 2005; Fialová et al., 2006; Lu et al., 2007). Urban soils occur within populated areas and provide many ecosystem services, natural resources and recreational amenities for communities globally and are considered vulnerable to metal contamination from industrial and domestic sources. Some studies have explored the impact of a vegetative layer on magnetic susceptibility in varying soil environments including a former mining site (Schmidt et al., 2005), a laboratory setting (D'Emilio et al., 2007) and a forest floor (Zawadzki et al., 2010). However, the effects of a vegetative layer on magnetic susceptibility measurements in urban soils remains unknown.

The main aim of this paper was to identify for the first time whether grass coverage significantly affects volume magnetic susceptibility (κ) of underlying urban soils. The study area is a well-established metal contamination hotspot and hence ideal to test this hypothesis. In addition, field-based magnetic susceptibility measurements were evaluated as a proxy for metal contamination in soil by comparing spatial distribution maps of κ and metals. Laboratory-based magnetic susceptibility (χ) and a magnetic gradient survey on a section of the study area was carried out to assess the field-based κ measurements obtained. Percentage frequency dependence (χ_{fd}%) was also calculated to identify the possible locations of anthropogenic magnetic minerals. The findings will potentially impact methodological approaches in environmental soil science.

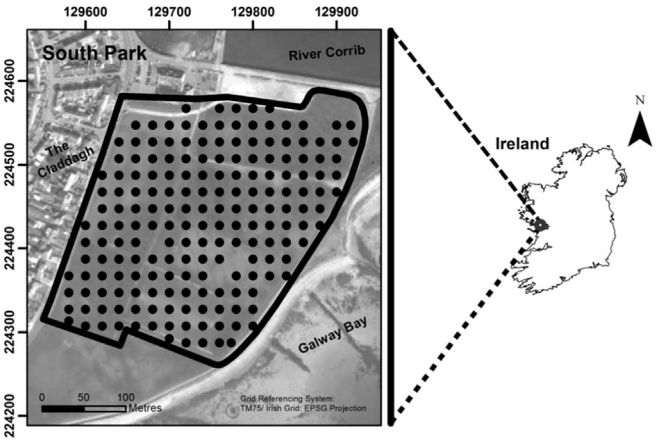

Fig. 1. Map of study area, South Park, Galway, Ireland, featuring 185 soil sampling points and corresponding locations of two datasets of κ measurement taken 1) κ^{grass} - before grass was removed and 2) $\kappa^{no\ grass}$ - after grass layer was removed.

2. Materials and methods

2.1. Study area and vegetation cover

The study site is located in an urban park of approximately 20 acres of former swampy seaside wetland known as South Park in the Claddagh region (O'Dowd, 1993 as cited in Carr et al., 2008) of Galway City (53° 15' 56 N, – 9° 03' 10 E), Ireland (Fig. 1). In the past, the site has been considered a metal contamination hotspot (due to its use as an unregulated waste deposit site) prior to its current use as a green space amenity. A first attempt at reclaiming the flood prone region into a recreational site occurred at the beginning of the twentieth century with the development of a half-mile track around the perimeters of the area (Galway Advertiser, 2008). Much of the track layout is used as a pedestrian walkway/ bicycle path surrounding the green area. This was not a successful undertaking and it was soon after this that the site was used as a municipal landfill. The landfill was potentially in use for twenty to thirty years until in 1931, a grant was provided to develop part of the site into a number of playing pitches. Development occurred gradually until the early 1950's when the area was fully converted into a municipal park (Galway Advertiser, 2008). It is not known whether its use as a municipal dump continued during this development phase. Colloquially, it is claimed that the removal of deposited materials such as glass and tin from the topsoil was required post-development of the playing pitches (Galway Advertiser, 2008). A previous study conducted at the site revealed very high levels of As, Pb and Cu present in the soils. In the past, a fertilizer plant was situated adjacent to the park and the type of pollution identified was similar to the industrial waste originating from a fertilizer plant processing pyrite ores (U.S. EPA 1997 as cited in Carr et al., 2008).

While the main soil type in the region is brown earths, the surface soils in South Park were imported, which were used to cover the rubbish when the sportsground was built. There were no natural

Fig. 2. The site comprises of a number of playing pitches used for various sporting activities including soccer, gaelic football and rugby. Photographs taken at the study site featuring: a) Galway Bay to the east of the park, b) the central eastern pitch and c) north-western pitch and d) the south-eastern pitch.

horizons in the soils and the thickness of the imported soil varied across the study area, e.g. the west and north parts were relatively poorly covered.

The study site (Fig. 2) is comprised of the widespread cultivation of the grass species *Lolium*-mix, predominately *Lolium perenne* L., also known as Ryegrass, Ray Grass or Eavers. This versatile species is commonly found in agricultural settings; in improved or reseeded neutral grassland, livestock grazing pasture and fodder (Beddows, 1967); as a turfgrass species used in domestic gardens, parks, recreational amenities, commercial landscapes and other green belts (Bandaranayake et al., 2003) and on disturbed or waste ground (Averis, 2013). *Lolium perenne* is tolerable to grazing and environmental contamination (Cockerham et al., 1990) and as a result is commercially important globally, with widespread uses in urban and amenity spaces (e.g. football pitches, roadsides and waste places).

2.2. Sampling grid

A systematic 20×20 m ^{2} sampling grid was employed in the collection of 185 soil samples and two datasets of 185 corresponding κ measurements: 1) κ^{grass} – measured with the grass layer present and 2) $\kappa^{no\ grass}$ – measured after the grass layer was trimmed down to the root. The locations of a selection of sampling points were altered due to obstructions present in the field e.g. gravelled areas, tarmacked pavements or water-logged areas. A portable global positioning system (GPS) Trimble GeoExplorer® was used to locate and record sampling point coordinates.

2.3. Soil collection, preparation and analysis

At each point on the sampling grid, three soil samples were collected using a plastic scoop at a depth of ~0–10 cm within 1 m^2 area of the sampling point. The soils samples were combined to form one composite sample and stored in polythene bags. Special attention was paid to ensure the soil samples were removed from the same points as the κ sub-measurements. Soil samples were air-dried at ~20 °C, before being gently disaggregated using a mortar and pestle and sieved using a 2 mm stainless steel sieve.

A portable X-ray fluorescence analyser, Innov-X Alpha Series 6500 (PXRF, ©Innov-X Systems, Inc.) was used to analyse the metal content of the soil samples. PXRF is a non-destructive method of examining possible contaminated sites which can perform accurate quantitative analysis over a whole host of elements including Ba, Hg, Cd, As, Cr, Pb, Mn, Sr, Cu, K, Co, Ti, Fe and Zn (Soodan et al., 2014). XRF measurement uncertainties are within a specified relative standard deviation of the measurement, which are as follows: Cu(± 4), Fe(± 286), Pb(± 13) and Zn(± 9). The XRF was operated for 120 s per sample to generate data for elements lead (Pb), copper (Cu), zinc (Zn) and iron (Fe). The limits of detection are relatively low ranging from ~10 ppm (Innov-X Systems Inc, 2013). Tangible limits are dependent upon the sample type and matrix (Innov-X Systems Inc, 2013).

2.4. Volume magnetic susceptibility (κ)

Volume magnetic susceptibility measurements were obtained using a Bartington MS2 meter (©Bartington Instruments Ltd.) *in situ* with a MS2D search loop. The field penetration depth of the MS2D sensor used is approximately 10 cm. The majority of the susceptibility signal, approximately 95%, comes from the upper 8 cm in the shape of a toroid with an integrated volume of approximately 0.0043 m^3 (Lecoanet et al., 1999). Values of volume magnetic susceptibility (κ) are dimensionless and expressed as 10^{-5} SI units (Zawadzki et al., 2015).

Volume magnetic susceptibility was measured in two phases within a 1 m^2 sampling location: Firstly, three sub-measurements were recorded with the grass layer present. The approximate length of grass coverage was noted to determine whether the presence of this layer had a significant impact on the magnetic measurements obtained. The length of grass was recorded by removing blades of grass from the sampling locations and measuring them. Measurements were rounded to the nearest cm. Lastly, the grass layers were trimmed to the root from each of the three previously measured locations and a secondary κ of the bare soils beneath were recorded. Three sub-measurements were taken at each location because high variability can occur between field measurements even at close distances (Lees et al., 1999). The mean of two air measurements (taken before and after) was subtracted from each surface measurement. The mean of the three surface measurements is then used as the representative measurement for each location.

2.5. Mass specific magnetic susceptibility (χ)

The mass specific magnetic susceptibility of the homogenized soil samples was measured using a Bartington MS2 meter with a dual-frequency MS2B sensor in the laboratory. Samples were measured at the low frequency range (0.46 kHz) expressed as χ_{lf} and at the high frequency range (4.6 kHz) expressed as χ_{hf}. Frequency dependence is the difference between the two frequencies and is expressed in %. Percentage frequency dependence (χ_{fd}%) was calculated to detect the presence of ultrafine (< 0.03 μm) superparamagnetic ferrimagnetic minerals (Dearing, 1999). Samples were measured in compact 10 cm^3 plastic cylinders. In order for true comparisons to be made between magnetic susceptibility measurements, mass specific magnetic susceptibility values were converted to volume magnetic susceptibility in accordance with the methodology applied by Dearing (1999) which states that $\chi(10^{-6}\ m^3\ kg^{-1})$ can be calculated by dividing κ by sample mass and then dividing by 10. Therefore the following formula was used to calculate κ^{lab}:

$$(\chi_{lf} * 10) * sample\ mass = \kappa^{lab}$$

2.6. Fluxgate gradiometry survey

Measurements of magnetic gradient were taken using a Bartington 601 fluxgate gradiometer. These instruments feature two sets of two fluxgate sensors placed vertically above one another, separated by 1 m and measure the vertical component of the Earth's magnetic field (Gaffney and Gater, 2003). Measurements were taken at regular 0.5 m intervals along a series of parallel transects positioned 1 m apart within 8 grid panels measuring 20 m×20 m. Measurements were taken facing north along each transect. The survey grid design was based on the technique employed by Fenwick (2004).

2.7. Quality control

To evaluate the precision of the chemical analysis by PXRF, the determination of the studied elements was performed using the soil certified reference materials (CRMs) San Joaquin (SRM 2709a), Montana I (SRM 2710a) and Montana II (SRM 2711a) from the National Institute of Standards and Technology, USA (NIST). These CRMs have been established for use in technique development, technique validation and routine quality assurance in the analysis of major, minor and trace element concentrations of soils (Mackey et al., 2010). PXRF exhibited particularly good analytical accuracy for Cu and Zn (Table 1).

The field sensor calibration was performed prior to carrying out the survey. Every time the meter was switched on, after an appropriate amount of time (approx. 10 min) a test point was measured ~10 times to check the measurement consistency. Variance was < (±)3%. To maintain the accuracy of field-based κ measurements, air measurements were taken in between surface measurements to allow for any drift in the measurement sequence to be identified. The meter was 'zeroed' if air measurements fell outside the $\pm 0.5\times10^{-5}$ tolerance level applied.

The MS2B sensor is calibrated electronically, to ensure the validity of the κ^{lab} values obtained, a calibration standard was used to check the stability of the measurement (Dearing, 1999). The calibration sample has a value of 3062×10^{-5} SI units. Every 10 samples, the calibration sample measurement was repeated. If a drift in air measurements was detected, samples were removed from the sensor, the meter was zeroed and the measurement repeated. The soil samples were compressed into each container to capacity and weights ranged from 8.48 to 14.55 g.

Table 1
Recovery of metals (Cu, Fe, Pb and Zn) in three soil certified reference materials (Montana I, Montana II and San Joaquin, National Institute of Standards and Technology, USA) (n=3).

CRM		Cu	Fe	Pb	Zn
2709a	Certified	33.9 ± 0.5	33,600 ± 700	17.3 ± 0.1	103 ± 4
San Joaquin	Measured	31 ± 6	32,875 ± 296	13 ± 3	97 ± 5
	Recovery (%)	91.44%	97.84%	75.14%	94.17%
2710a	Certified	3420 ± 50	43,200 ± 800	5520 ± 30	4180 ± 20
Montana I	Measured	3518 ± 46	50,503 ± 497	5564 ± 58	4412 ± 51
	Recovery (%)	102.87%	116.90%	100.80%	105.55%
2711a	Certified	140 ± 2	28,200 ± 400	1400 ± 10	414 ± 11
Montana II	Measured	118 ± 8	25,753 ± 244	1402 ± 18	374 ± 9
	Recovery (%)	84.29%	91.32%	100.14%	90.34%

2.8. Spatial analysis of metals and magnetic susceptibility

Inverse Distance Weighting (IDW) was applied for the interpolation of elemental and magnetic data. Spatial interpolation maps (Fig. 3) were prepared using the extension Geostatistical Analyst within ArcGIS® ArcMap™ v.10.2 (©2013 ESRI). This method is based on the assumption that the value of a particular variable at a location which has not been sampled is the weighted average of known values of that variable within its vicinity. Weights are inversely associated with the distances between the unknown value point location and determined value point locations. The inverse distance weight is dependent on a constant, known as a power parameter. Points closer to the unknown value point can have much more influence over the determined value based on the power parameter (Lu and Wong, 2008). In the current study, a power parameter of 2 was applied to the elemental and magnetic data during geostatistical analysis. Maps produced using a power parameter of 2 attribute more weight to samples closer to the unknown value. This results in a much more abrupt surface which highlights the complexity of the metal concentrations and the magnetic susceptibility signature present.

Local indicators of spatial association (LISA) (Anselin, 1995) maps of metals Pb, Cu, Zn and Fe and magnetic measurements κ and χ_{fd}% (see Fig. 3) were created to identify statistically significant spatial clusters including high value areas ('*high-high*') and low value areas ('*low-low*') within the urban park. Spatial outliers are also featured, these are denoted as '*high-low*' and '*low-high*' on the LISA maps representing statistically significant outliers of high and low values in comparison to surrounding data values. Prior to LISA analysis, each of the datasets were transformed to an approximate normal distribution using a natural logarithm transformation (ln). The weight function used was based on K-nearest neighbours (8 neighbours) (Golden et al., 2015).

2.9. Principal Component Analysis (PCA)

Principal Component Analysis is a technique used for data reduction (Boruvka et al., 2005; Manta et al., 2002). The data must be correlated in order for PCA to be employed. Standardization is applied when variables are measured at different scales or in circumstances where some variables may have much larger variance than others and dominate the first principal component (Miller and Miller, 2005). This

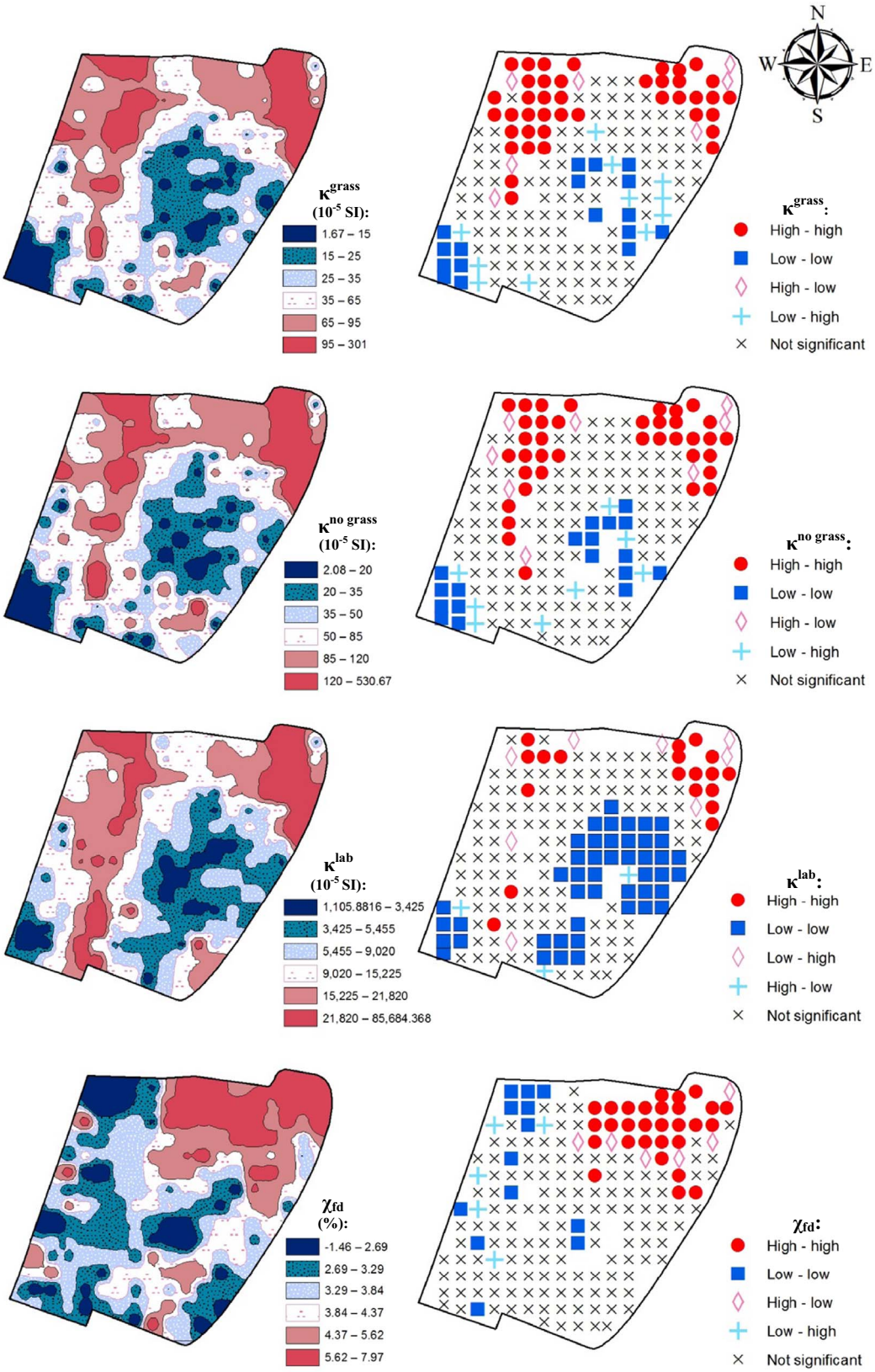

Fig. 3. Total concentration distributions and local Moran's I maps of volume magnetic susceptibility – κ^{grass} and $\kappa^{no\ grass}$ (10^{-5} SI), mass specific magnetic susceptibility – κ^{lab} (10^{-5} SI), percentage frequency dependence – χ_{fd}% and metal concentrations – Cu, Fe, Pb and Zn (mg kg^{-1}).

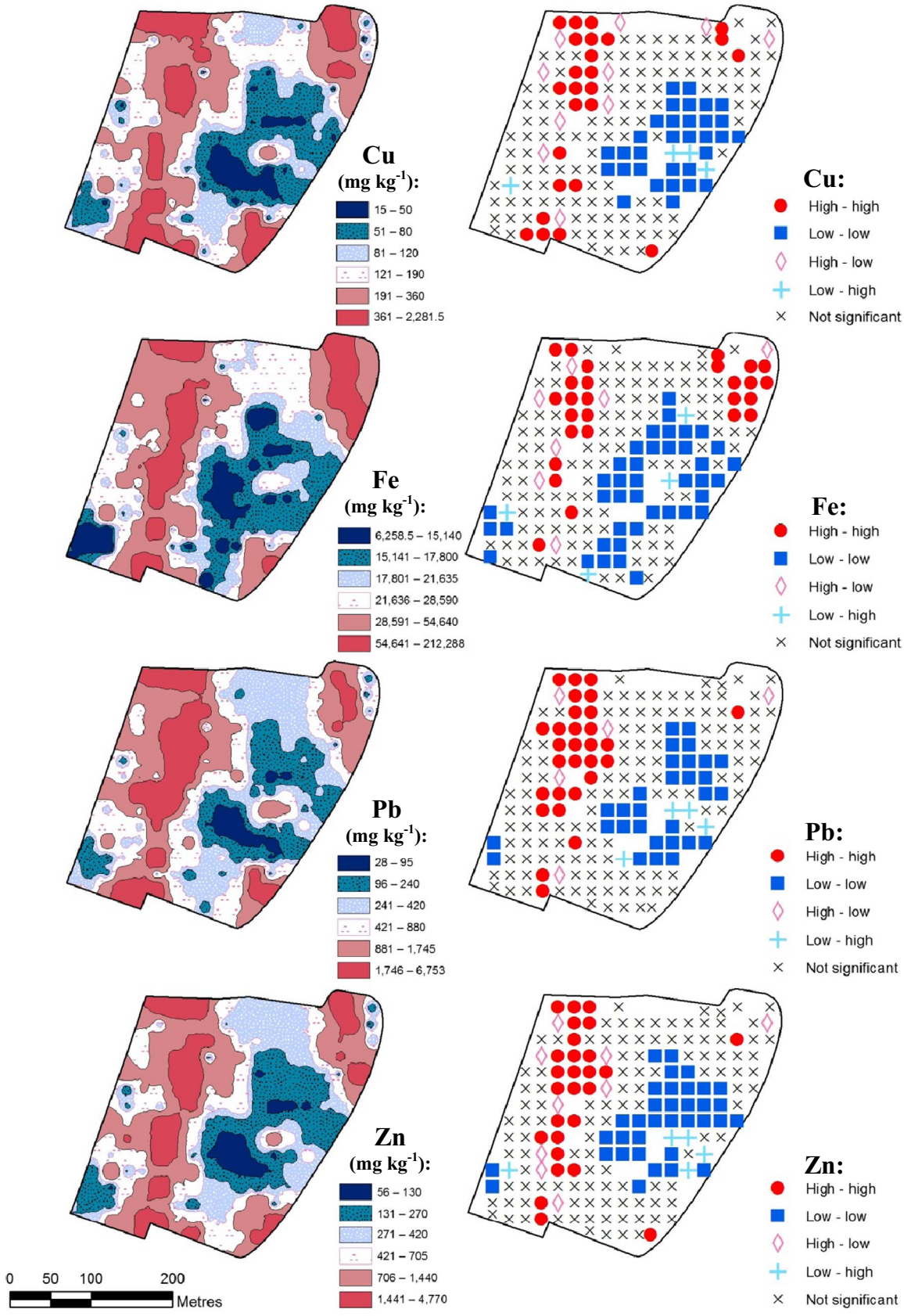

Fig. 3. (*continued*)

is avoided by making all variables carry equal weight. PCA is employed in the current study to aid in the interpretation of interrelations between metals and magnetic susceptibility in the contaminated urban topsoils.

2.10. Data transformation

Due to the heterogenic nature of geochemistry, a Kolmogorov-Smirnov test of normality was applied to the metal and magnetic susceptibility datasets. A Kolmogorov-Smirnov test is based on the maximum deviation of the observed value series from the theoretical model (Webster and Oliver, 2007). Each of the magnetic susceptibility sampled populations (with the exception of χ_{fd}%) were non-normally distributed at the significance level of $p < 0.01$. A natural logarithmic transformation (ln) was performed in an attempt to transform the measured values to a new scale on which the distributions are closer to normality.

2.11. Integrated Pollution Index (IPI)

The degree of metal contamination at the site was also demonstrated by the calculation of an accumulation factor (Integrated Pollution Index (IPI)) (Jung, 2001 as cited in Morton-Bermea et al., 2009) in relation to background regional values (Zhang, 2006) for quantitative purposes. Integrated pollution index (IPI) refers to the mean value of all Pollution Indices (PI) of all the metals being investigated (Morton-Bermea et al., 2009). PI are commonly used to discriminate metal contamination and evaluate the degree of environmental pollution present at a site (Dong et al., 2014). An IPI was calculated for the soil samples defined as:

$$IPI = ((PI_{Cu}) + (PI_{Fe}) + (PI_{Pb}) + (PI_{Zn}))/4$$

where $PI=(Concentration_i^{median}/Background^{median}{}_i)$, $_i$ =metal.

2.12. Data analysis and statistics

Data management was carried out in Microsoft® Excel 2010. Statistical analysis was performed using SPSS 21 (IBM®SPSS® Statistics). Hotspot analysis was applied to the data using GeoDa™1.4.6. (Anselin et al., 2006) and spatial analysis was carried out within a Geographical Information System (ESRI® ArcGIS® ArcMap™ 10.2) using ArcGIS World Imagery basemap service. Mass specific magnetic susceptibility measurements were determined using Multisus v2.44 software.

3. Results and discussion

3.1. Effects of grass coverage on magnetic susceptibility (κ)

A strong linear relationship is shown (Fig. 4) between κ^{grass}, $\kappa^{no\ grass}$ and κ^{lab}. The two κ(ln) datasets exhibited a strong positive pearson's correlation coefficient of r^2=0.966, n=185, $p < 0.01$. In general, κ^{grass} obtained initially, prior to the grass layer being disturbed, are lower than $\kappa^{no\ grass}$. This is because the sensitivity of the sensor for magnetic susceptibility measurements diminishes exponentially with distance from material (Lecoanet et al., 1999). The MS2D search loop is affected by material up to ~14 cm from the sensor. For example, a layer of vegetation 0.5 cm in depth can possibly reduce the MS2D measurement to 75% of the expected value compared to if the sensor was directly placed on the soil surface (Dearing, 1999). The gap between the sensor and the soil surface is a contributing factor in relation to grass height effects. This gap was at least 1.5 cm from the sensor to the soil surface for grasses < 10 cm and 1.5–2 cm for grasses > 10–15 cm.

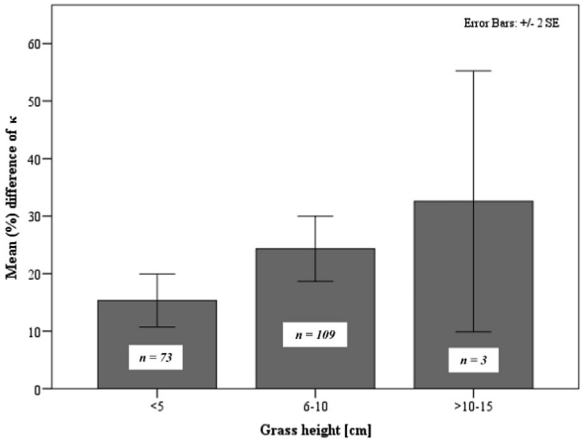

Fig. 5. Effects of grass blade length on approximate mean (%) κ measurement error at grass height ranges: ≤5, 6–10 and > 10–15 cm.

In this study, a substantial amount of magnetic susceptibility data was obtained in the field. The length of grass blades were also recorded at each sampling point. The grass heights ranged from 2 to 15 cm. A possible negative relationship between grass height and the difference in κ values was explored and a Spearman's Rho correlation revealed a weak significant r^2 value between these parameters (r^2=0.253 $p < 0.05$) (see Supplementary materials for graph depicting grass blade lengths at the sub-measurement locations a)1, b)2 and c)3 versus mean % difference in field-based κ measurement). The mean % κ measurement error in relation to grass coverage height was calculated (Please see Fig. 5). Where $\kappa^{no\ grass}$ was considered as the true κ magnetic susceptibility measurement for each sampling point, κ^{grass} measurements were treated as a recovery percentage and the (%) κ measurement error determined using the following calculation: $100 - (\kappa^{no\ grass} - \kappa^{grass}/\kappa^{no\ grass}*100)$. This graph demonstrates a trend in the data and infers an inverse relationship between grass coverage height and κ. Error bars are included to depict the level of variance within each of the three grass height groups. The level of variance is smaller in group 1 (

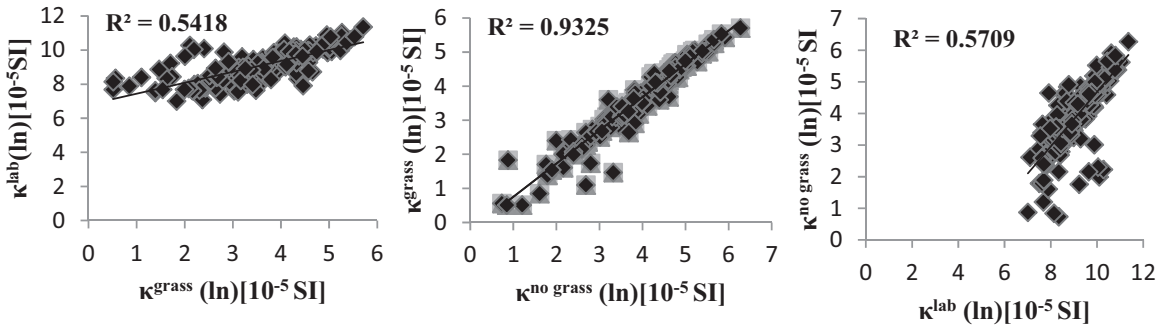

Fig. 4. Relationships between three log-transformed magnetic susceptibility measurements: field-based volume magnetic susceptibility (10^{-5} SI) taken with and without grass coverage (κ^{grass}(ln) and $\kappa^{no\ grass}$(ln), respectively) and volume magnetic susceptibility of soil samples (κ^{lab}(ln)).

Table 2
Summary of volume magnetic susceptibility (10^{-5} SI) taken in the field, mass specific magnetic susceptibility represented as volume magnetic susceptibility of soil samples κ^{lab} (10^{-5} SI) and frequency dependence (%) of soil samples. Volume magnetic susceptibility measurement uncertainties are within a standard deviation of the measurements, which are as follows: κ^{lab} (±0.37), χ_{fd}% (±1.8) and κ (±0.3).

	κlab κ [10^{-5} SI]	χ_{fd}% [%]	κgrass κ [10^{-5} SI]	κno grass κ [10^{-5} SI]
Min	2091	−1.46	1.7	2.1
25%	4328	2.87	21.8	27.5
Median	9022	3.84	37.7	53.3
75%	18,764	4.70	74.8	105.3
Max	85,684	7.97	301.0	530.7
S.D.	12,290	1.51	50.8	73.8

< 5 cm) and group 2 (6–10 cm) in comparison to group 3 (> 10–15 cm). This is related to site specific conditions at the study area. The study site is a well-maintained urban park. Grass is mowed on a regularly basis resulting in a low average blade height of 6 cm at the sampled points. This demonstrates that grass height has the potential to effect measurements but not in the present study where maintained grass dominates the study area.

Based on these results, it is not possible to create a model to identify approximate (%) κ measurement error at varying grass heights. The level of variance across the grass height groups mean the results are not robust enough to back calculate to create a model. The (%) difference calculated in this study can be used as an indicator for other urban soil studies carrying out κ surveys where grass coverage maybe a factor.

It is possible that where very high grasses are present in e.g. wastelands or roadsides that grass height may affect κ measurement obtained. But due to the small number of sample points with grass blade height > 10 cm (n=3), it does not affect the predictive power in the current study.

Four magnetic susceptibility datasets, two volume magnetic susceptibility (κ^{grass} and $\kappa^{no\ grass}$) one mass specific magnetic susceptibility of soil samples converted to volume MS measurement (κ^{lab}) and percentage frequency dependence (χ_{fd}%), were obtained in this study and the descriptive statistics are summarized in Table 2. The measurements revealed elevated and varied levels of magnetic particulates present in these urban soils. Shape parameters of each of the volume datasets were positively skewed to the right (1.724–2.274) with high levels of peakness (3.533–7.625). Fig. 3 depicts the inter-magnetic susceptibility relationships occurring in these urban soils. The majority of the data points are clustered along the linear regression line. This graph and a Pearson's Correlation Coefficient of the log-transformed magnetic susceptibility datasets demonstrate a strong positive correlation between κ^{lab}(ln) and κ^{grass}(ln) r^2=0.752 and $\kappa^{no\ grass}$(ln) r^2=0.756, n=185, $p < 0.01$.

A small number of studies have recognised and addressed the issue of conformity in experimental protocols for field-based magnetic susceptibility monitoring (Schibler et al., 2002; Schmidt et al., 2005; D'Emilio et al., 2007; Zawadzki et al., 2010). As part of the MAGPROX team, Schibler et al. (2002) evaluated the data reproducibility of a magnetic susceptibility sensor. The team established a few standard procedures including: "The preferred surface is covered well in litter and no surface preparation is allowed, except for removing high grass or branches" (Schibler et al., 2002, p.47). Different perspectives exist in the literature on whether the removal of a vegetation layer is necessary (Table 3). Some studies do not explicitly state their methodological approach. In contrast, others have recommended the removal of vegetation prior to measuring magnetic susceptibility, in their unique soil environments. A magnetic susceptibility field survey was carried out at a brownfield site in close proximity to a former industrial iron production and processing site. The strong metal contamination signal and shallow and deep χ measurements of the brownfield site were interpreted to be related to historic localised deposition associated with nearby mining activity whereas the κ of the grass layer was inferred to represent more recent airborne particulate pollution (Schmidt et al., 2005). A forested region was the chosen site for an investigation of the relationship between the κ of different soil horizons of the forest floor. The removal of a thick organic layer was found to increase the magnetic susceptibility measurements of forest topsoils (Zawadzki et al., 2010). In the laboratory, the κ measurement reproducibility of soil, covered by vegetation and after the vegetation was removed was also examined. Based on the distribution shapes of each dataset, the removal of the vegetation layer during field surveys was considered necessary due to its inhomogeneity (D'Emilio et al., 2007).

In regards to urban soils, the results of this study suggest it is not necessary to remove the grass prior to obtaining magnetic susceptibility measurements in the field. Although vegetation can cause reduced contact with the soil surface, the shape and penetration range of the instrument sensor (to a depth of 10 cm) allow for the detections of anthropogenic particles present in deeper horizons. Lower value, diamagnetic minerals in the upper organic layers may dilute the measurement slightly but not detrimentally particularly when greater levels of particles are present. The main argument in favour of removing the vegetation layer is that most anthropogenic contaminants accumulate at a depth of 3–7 cm (Zawadzki et al., 2010) but this may be pathway specific, e.g. atmospheric deposition versus landfill leachate. Furthermore, a vegetative cover, including *Lolium perenne* prevents the spreading of metal-associated particles via wind erosion or water and reduces the mobility of metals through root secretion and precipitation processes (Vangronsveld et al., 1995). Vegetative stabilization also enhances the biological and chemical properties of the contaminated soil by boosting nutrients, biological activities, organic matter content and cation exchange capability (Norland and Veith, 1995; Arienzo et al., 2004).

Thick upper organic layers may significantly influence the measured κ due to limitations of the penetration range, e.g. 50% of the magnetic susceptibility measurement comes from the top 1.5 cm (Lecoanet et al., 1999). Unlike urban soils, undisturbed soils are likely to be allowed to develop over time naturally and accumulate anthropogenic particles via atmospheric deposition. Urban soils are transient as urban environments are constantly modified, leading to a more complicated contamination sources and pathways.

3.2. Metals

The anthropogenic influence at the park is evident in the Pb, Cu and Zn concentrations (see Supplementary materials) as a result of previous municipal and industrial waste disposal activities. However, there is a much smaller PI for Fe between the park soil samples and median regional background values (Zhang, 2006). The maximum pollution indices are 84.5 for Cu, 116.43 for Pb and 56.12 for Zn. Concentrations of Fe did not differ much from background levels and this is reflected in a PI of 1.25. This may be because Fe content in topsoil is largely related to the parent rock (Morton-Bermea et al., 2009). Based on the metal concentration PIs we can speculate that the soils of this urban park remain heavily contaminated with Pb as the largest contributor. The park has a complex history of contamination and remediation activities and this leads to a diverse genetic origin. Pearson correlation values between Pb(ln) and Cu(ln) r^2=0.931, Pb(ln) and Zn(ln) r^2=0.941 and Cu(ln) and Zn(ln) r^2=0.962, n=185, $p < 0.01$ show a strong positive linear correlation suggesting the same contamination source, resulting from industrial waste. There is also a positive correlation between Fe(ln) and Pb(ln) r^2=0.841, Fe(ln) and Cu(ln) r^2=0.883 and Fe(ln) and Zn(ln) r^2=0.863, n=185, $p < 0.01$ but it is slightly lower. These soils subjected to high levels of contamination with elevated concentrations of Pb, Cu and Zn show slightly lower Fe content and this may be due to Fe being associated with low levels of anthropogenic influence (Morton-Bermea et al., 2009).

Table 3
Summary of literature that used a MS2D sensor with the objective of obtaining magnetic susceptibility measurements in soil studies.

Author (s)	Vegetation Cover
Kapička et al. (1997, p. 392)	Not stated. *"Attention was paid to keep constant conditions at the measurement sites (regarding e.g. vegetation cover)"*
Ďurža (1999)	Not stated.
Lecoanet et al. (1999)	Not stated. Measurements taken at graduated distances from ground.
Petrovský et al. (2000)	Not stated.
Strzyszcz and Magiera (2001)	Not stated.
Schibler et al. (2002, p. 47)	Vegetation. *"The preferred measurement surface is covered well in litter. No surface preparation is allowed, except for removing high grass or branches".*
Boyko et al. (2004)	Vegetation. Followed procedure prescribed by Schibler et al. (2002).
Gautam et al. (2004)	Not stated.
Schmidt et al. (2005)	Grass/Grass removed.
D'Emilio et al. (2007)	Grass/Grass removed
Magiera and Zawadzki (2007, p. 21)	Vegetation. "Measurements were taken without any surface preparation, except for cutting of high grass or removal of twigs".
Zawadzki et al. (2007, p. 115)	Vegetation. "Measurements were taken without any surface preparation, except for cutting of high grass or removal of twigs".
Kapička et al. (2008)	Grass
Magiera et al. (2008)	Vegetation. Followed procedure prescribed by Schibler et al. (2002).
D'Emilio et al. (2010)	Grass removed
Zawadzki et al. (2010)	Vegetation/Without vegetation layer (referred to as organic layer (OL)
D'Emilio et al. (2012)	Grass removed
Łukasik et al. (2015)	Surface measured using an MS2D Bartington loop.
Grison et al. (2016)	The soil surface volume magnetic susceptibility was measured.

3.3. Spatial distribution of metals and magnetic susceptibility

Elevated levels of magnetic susceptibility can be found throughout this urban amenity signifying the strong presence of magnetic particles in these soils. The contents of metals Cu, Pb and Zn in the surveyed samples exhibit a considerable enhancement compared to regional background values. Total lead concentrations ranged from 28 to 6753 mg kg^{-1}. Copper concentrations were found to vary from 15 to 2281.50 mg kg^{-1} and zinc ranged from 56 to 4770 mg kg^{-1}. In the north east corner, soils are reddish in colour indicating the presence of industrial waste. Historically, a fertilizer plant was situated adjacent to the park. It processed pyrite ores. There are some high value outliers of Cu, Zn and particularly Pb in this area. In particular, a '*high-high*' value cluster of Fe, κ^{grass}, $\kappa^{no\ grass}$ and κ^{lab} are a feature of this area which coincides with a '*high-high*' value cluster of χ_{fd}%. High χ_{fd}% and Fe are associated with natural processes. Reddish soils can also be found in the central west region of the sports ground, covering the main football pitch where patches of bare soil are visible particularly around goal posts (Carr et al., 2008). The magnetic susceptibility sensor was also capable of detecting these sections of the park as the most highly contaminated. The northern and western sections are the most heavily laden with magnetic particulates; this is demonstrated by the '*high-high*' value clusters featured in Fig. 3. Volume magnetic susceptibility measured with a grass vegetative layer present shared a very similar spatial dispersal pattern of high magnetic susceptibility with measurements taken without the grass layer present and with the laboratory-based mass specific susceptibility of the soil samples.

A small inversely proportional relationship exists between χ_{fd}% and metal concentrations Cu(ln) r^2=−0.176, Fe(ln) r^2=−0.148, Pb(ln) r^2=−0.162 and Zn(ln) r^2=−0.206, n=185, $p < 0.05$. '*Low-low*' value clusters of χ_{fd}% featured in the north western region of the study area contrast with '*high-high*' value clusters in each of the volume magnetic susceptibility and metal concentration spatial distribution maps. A useful magnetic criteria proposed for the identification of soils containing significant concentrations of pollution particles includes elevated $\chi(> 380\times10^{-8}\ m^3\ kg^{-1})$ and frequency dependence of < 3% (Evans and Heller, 2003).

Some remediation work has occurred in the central eastern region of the park and there is a clear distinction in soil depth where soils have been imported and placed there. The less contaminated soils are found in this central eastern area. Volume magnetic susceptibility values are $< 85\times10^{-5}$ SI units in these imported soils. However, there are still some elevated levels of Pb (201–500 mg kg^{-1}) and Zn (201–500 mg kg^{-1}) present which are much greater than the regional background values (Zhang, 2006) (see Supplementary Materials). There is also a statistically significant low level of magnetic particulates featured in each of the magnetic susceptibility maps in the southern western tip of the park. The metal maps feature *relatively* low value concentrations in this area also.

3.4. Comparison between κ and gradiometry surveys

A single magnetic reading cannot determine the exact depth or source of magnetic anomalies in soils. However, with a magnetometer in gradiometer mode acquiring two simultaneous readings from two sensors located at different heights it is possible to estimate the depth of magnetic anomalies based on their associated measurements (Gibson and George, 2013). A spatial distribution map of the surveyed sub-section of the study area can be seen in Fig. 5. It is possible to identify magnetic anomalies in the lower half of the surveyed region visible as white spots. The closer to the surface the more defined the body of the anomaly appears. The appearance of these anomalies suggest the presence of large metallic objects approximately 1–1.5 m below the surface. A comparison to the results obtained in this survey can be made with field- and laboratory-based κ measurements and Fe content of soils samples taken in this section of the park (see Fig. 6). Each of these parameter maps featured elevated measurements in the same locale as the gradiometry survey. This infers that the enhanced magnetic measurements recorded in this area are related to anthropogenic waste as proposed and not naturally occurring.

3.5. Relationship between metals and κ

A Pearson's correlation was performed, after necessary data transformations between magnetic susceptibility datasets κ^{grass}(ln), $\kappa^{no\ grass}$(ln) and κ^{lab}(ln) and metals Cu(ln), Fe(ln), Pb(ln) and Zn(ln). The r coefficients revealed a statistically significant relationship (see Fig. 7) between each of the metals and magnetic susceptibility at the $p < 0.01$ level. As expected, the strongest correlation was present between κ^{lab}(ln) and each of the metals: Cu(ln) 0.855, Fe(ln) 0.859, Pb(ln) 0.826 and Zn(ln) 0.834, $p < 0.01$. However, importantly both κ^{grass} (ln) and $\kappa^{no\ grass}$(ln) are also strongly correlated to each of the metals and share a similarity in r^2 value (κ^{grass}(ln): Cu(ln) 0.589, Fe(ln) 0.599, Pb(ln) 0.601, Zn(ln) 0.591;$\kappa^{no\ grass}$(ln):Cu(ln) 0.591, Fe(ln) 0.600, Pb(ln) 0.605, Zn(ln) 0.587, n=185, $p < 0.01$.

Strong linear relationships are visible between each of the (ln)

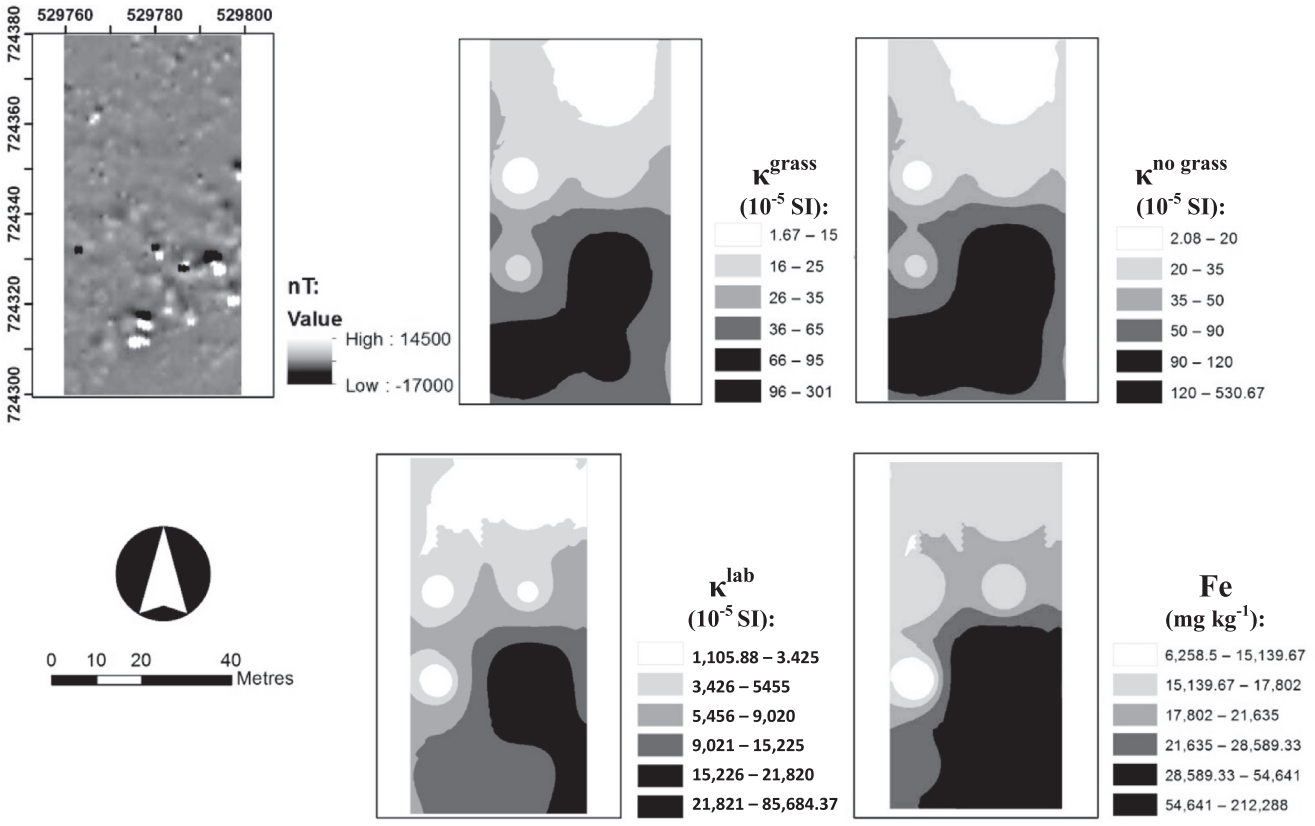

Fig. 6. Fluxgate gradiometry survey of a south eastern section of the park compared to $\kappa^{grass}(10^{-5}$ SI), $\kappa^{no\ grass}(10^{-5}$ SI), $\kappa^{lab}(10^{-5}$ SI) and Fe(mg kg^{-1}).

magnetic susceptibility datasets and the (ln)metals (Fig. 7). It is evident that the magnetic signal is increased for soils affected by anthropogenic waste (Fig. 8).

3.6. Principal Component Analysis (PCA)

A Principal Component Analysis (PCA) was applied to the metal and magnetic susceptibility datasets. Prior to carrying out PCA, the variables were standardised as they were on different measurement scales. Based on the eigenvalues and scree plot results, two principal components (Factor I and Factor II) were selected. The obtained Factors were rotated using varimax which allows an easier interpretation of factor loadings (Boruvka et al., 2005; Manta et al., 2002). The resulting rotated Factor loadings and Communalities can be found in Supp. Mats. The cumulative variance % explained by Factor I and Factor II is > 90%.

A projection of the components is illustrated in Supplementary materials. All three magnetic susceptibility measurements are positively loaded close to the second axis. κ^{grass} and $\kappa^{no\ grass}$ are particularly close reiterating the similarity between the before and after *in situ* magnetic susceptibility measurement of the topsoil. Factor I is dominated by Cu, Fe, Pb and Zn. Based on the history of the site, the spatial distributions and Pearson correlations of these metals, they are interpreted as having an anthropogenic origin. The concentrations of Cu, Pb and Zn are tightly clustered close to the first axis and indicate they are of the same anthropogenic origin in the topsoil sampled. The position of Fe close to this clustering is understandable as Fe is heavily associated with the anthropogenic metals but also naturally occurring in soil. Laboratory-based κ^{lab} features in between both clusters but is more closely associated with Factor II. Based on previous interpretations of the relationships of κ^{lab} and the other soil parameters the reason for this positioning may be related to this technique being a more sensitive measure of the field-based MS measurements and because the measurements were made on the same homogenized soil samples as were used to obtain the metal concentrations. The results of the PCA were also plotted on two maps (see Fig. 8) which correspond well with the spatial distribution maps of magnetic susceptibility and metal concentrations. Factor I which was dominated by the metal variables (Cu, Fe, Pb and Zn mg kg^{-1}) closely resembles the distributions of metals which feature elevated concentrations expanding the length of the western section and dominating the northeast corner. Factor II primary elevated values are spread across the northern section and down the western pitch, a pattern mirrored by the volume magnetic susceptibility distribution maps.

4. Conclusions and recommendations

This study reaffirms the suitability of *in situ* magnetic susceptibility technique as a proxy for metal contamination in soils, particularly where high levels of metal contamination are present. However magnetic susceptibility monitoring may not be as efficient at identifying less contaminated levels of metals in soils. Importantly, it demonstrates that a grass layer has little effect on the ability to identify metal contaminated soils using magnetic susceptibility techniques (in particular, when grass height < 10 cm). Therefore, we suggest that the removal of a grass layer prior to determination of magnetic susceptibility is unnecessary for urban soils. This is reflected in the similarity between the magnetic susceptibility maps and correlation coefficients. Highly spatially associated maps of volume magnetic susceptibility were created from datasets obtained with/without grass layer present during measurement. κ^{grass} also shared a good linear correlation and similarity in spatial distribution with κ^{lab} and concentrations of Cu, Fe, Pb and Zn. Although a robust model to assist in identifying when grass coverage height significantly affects κ measurement could not be calculated. It is worth bearing in mind the % κ measurement errors obtained in this study particularly when surveying in long grasses.

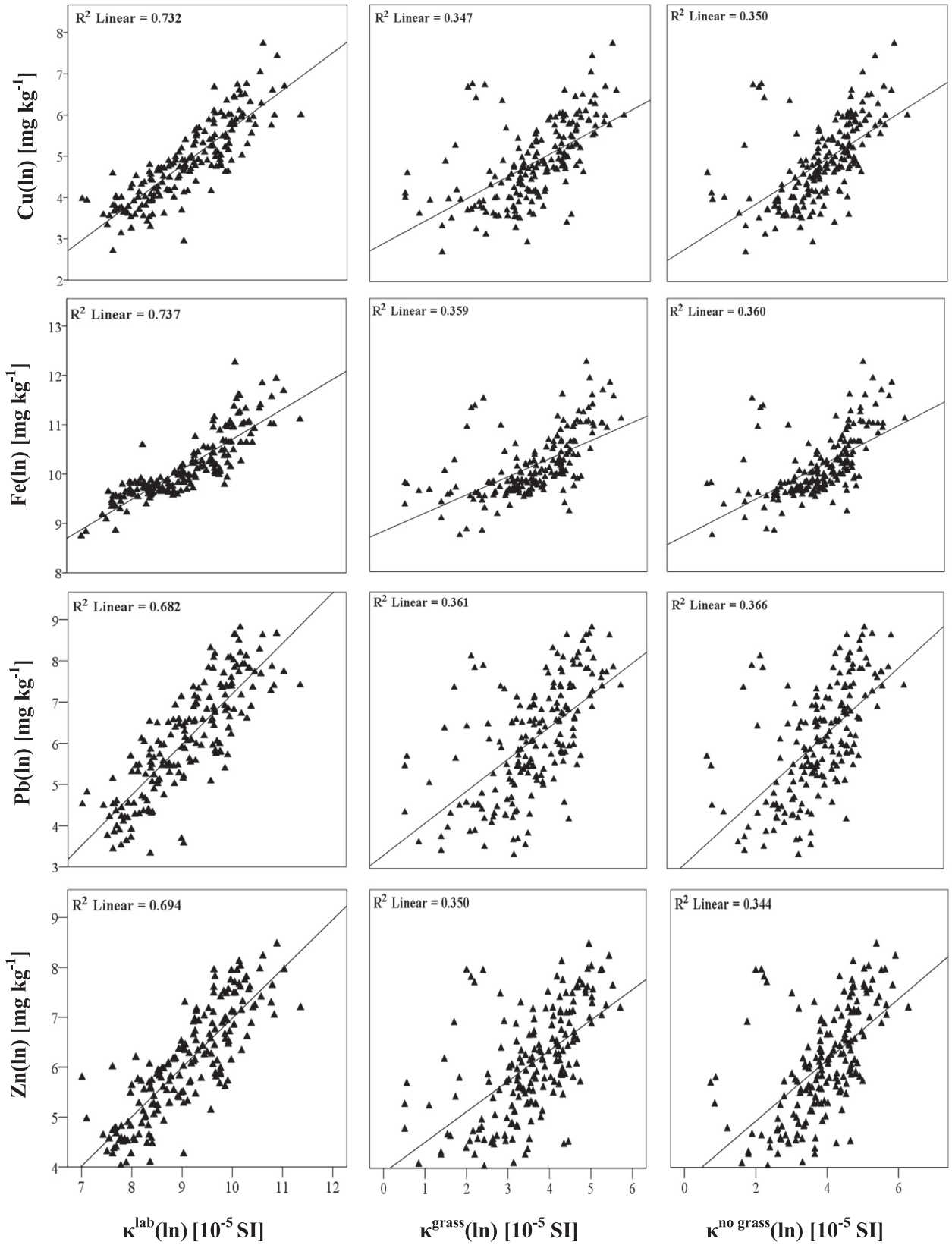

Fig. 7. Scatterplots demonstrating the relationship between log-transformed metal concentrations Cu, Fe, Pb and Zn (mg kg^{-1}) and volume magnetic susceptibility measurements of soil samples (κ^{lab}) and field-based measurements (κ^{grass} and $\kappa^{no\ grass}$) (10^{-5} SI).

Overall, magnetic surveying is a more cost effective alternative to geochemical surveying and can be used for large scale campaigns investigating potentially contaminated soils with anthropogenic particulates.

Funding

This work was supported by the Department of Communications, Energy and Natural Resources under the National Geoscience

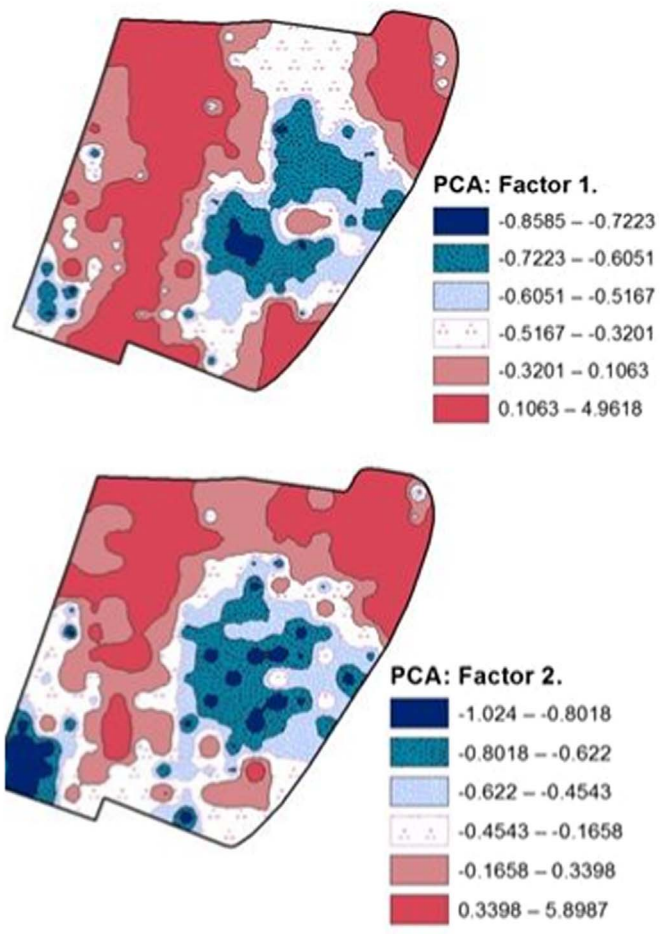

Fig. 8. Map of spatial distribution of Factor I (metal concentrations) and Factor II (magnetic susceptibility).

Programme 2007–2013 (Griffiths Award). The views expressed in the study are the authors' own and do not necessarily reflect the views and opinions of the Minister for Communications, Energy and Natural Resources or any government body. The role of the sponsor did not include any involvement in the study design; the collection, analysis and interpretation of data; the writing of the report or in the decision to submit this manuscript for publication.

Acknowledgements

The authors would like to thank He Yaxin, Ellen McGrory, Sorcha Dolan, Joe Fenwick and Siubhán Comer for their assistance during fieldwork and Dr. Ricardo Bermejo for statistical advice. The authors wish to acknowledge funding from the Department of Communications, Energy and Natural Resources under the National Geoscience Programme 2007–2013 (Griffiths Award). The views expressed in the study are the authors' own and do not necessarily reflect the views and opinions of the Minister for Communications, Energy and Natural Resources or any government body.

Appendix A. Supporting information

Supplementary data associated with this article can be found in the online version at doi:10.1016/j.envres.2017.02.032.

References

Anselin, L., 1995. Local indicators of spatial association – LISA. Geogr. Anal. 27 (2), 93–115.
Anselin, L., Syabri, I., Kho, Y., 2006. GeoDa: an introduction to spatial data analysis. Geogr. Anal. 38 (1), 5–22.
Arienzo, M., Adamo, P., Cozzolino, V., 2004. The potential of *Lolium perenne* for revegetation of contaminated soil from a metallurgical site. Sci. Total Environ. 319, 13–25.
Averis, B., 2013. Plants and habitats: an introduction to common plants and their habitats in Britain and Ireland. Ben Averis, East Linton, UK.
Bandaranayake, W., Qian, Y.L., Parton, W.J., Ojima, D.S., Follett, R.F., 2003. Estimation of soil organic carbon changes in turfgrass systems using the CENTURY model. Agron. J. 95, 558–563.
Beddows, A.R., 1967. Lolium perenne L. J. Ecol. 55 (2), 567–587.
Bityukova, L., Scholger, R., Birke, M., 1999. Magnetic susceptibility as indicator of environmental pollution of soils in Tallinn. Phys. Chem. Earth (A) 24 (9), 829–835.
Boruvka, L., Vacek, O., Jehlička, 2005. Principal component analysis as a tool to indicate the origin of potentially toxic elements in soils. Geoderma 128, 289–300.
Boyko, T., Scholger, R., Stanjek, H., MAGPROX Team, 2004. Topsoil magnetic susceptibility mapping as a tool for pollution monitoring: repeatability of in-situ measurements. J. Appl. Geophys. 55 (3–4), 249–259.
Canbay, M., Aydin, A., Kurtulus, C., 2010. Magnetic susceptibility and heavy metal contamination in topsoils along the Izmit Gulf coastal area and IZAYTAS (Turkey). J. Appl. Geophys. 70 (1), 46–57.
Carr, R., Zhang, C., Moles, N., Harder, M., 2008. Identification and mapping of heavy metal pollution of a sports ground in Galway City, Ireland, using a portable XRF analyser and GIS. Environ. Geochem. Health 30 (1), 45–52.
Chaparro, M.A.E., Gogorza, C.S.G., Chaparro, M.A.E., Irurzun, M.A., Sinito, A.M., 2006. Review of magnetism and pollution studies of various environments in Argentina. Earth Planets Space 58 (10), 1411–1422.
Chianese, D., D'Emilio, M., Bavusi, M., Lapenna, V., Macchiato, M., 2006. Magnetic and ground probing radar measurements for soil pollution mapping in the industrial area of Val Basento (Basilicata Region, Southern Italy): a case study. Environ. Geol. 49 (3), 389–404.
Cockerham, S.T., Gibeault, V.A., Van Dam, J., Leonard, M.K., 1990. Tolerance of several cool- season turfgrasses to simulated sports traffic. In: Schmidt (Ed.), Natural and Artificial Playing Fields: Characteristics and Safety Features. American Society for Testing and Materials, 85–95.
Dalan, R.A., 2008. A review of the role of magnetic susceptibility in archaeogeophysical studies in the USA: recent developments and prospects. Archaeol. Prospect. 15, 1–30.
Dao, L., Morrison, L., Zhang, C., 2012. Bonfires as a potential source of metal pollutants in urban soils, Galway, Ireland. Appl. Geochem. 27 (4), 930–935.
Dao, L., Morrison, L., Zhang, H., Zhang, C., 2014. Influences of traffic on Pb, Cu and Zn concentrations in roadside soils of an urban park in Dublin, Ireland. Environ. Geochem. Health 36 (3), 333–343.
Dao, L., Morrison, L., Kiely, G., Zhang, C., 2013. Spatial distribution of potentially bioavailable metals in surface soils of a contaminated sports ground in Galway, Ireland. Environ. Geochem. Health 35 (2), 227–238.
Dao, L., Morrison, L., Zhang, C., 2010. Spatial variation of urban soil geochemistry in a roadside sports ground in Galway, Ireland. Sci. Total Environ. 408 (5), 1076–1084.
Dearing, J.A., 1999. Environmental Magnetic Susceptibility. Using the Bartington MS2 System second ed. Chi Publishing, Kenilworth, England, UK.
D'Emilio, M., Chianese, D., Coppola, R., Macchiato, M., Ragosta, M., 2007. Magnetic susceptibility measurements as proxy method to monitor soil pollution: development of experimental protocols for field surveys. Environ. Monit. Assess. 125, 137–146.
D'Emilio, M., Caggiano, R., Coppola, R., Macchiato, M., Ragosta, M., 2010. Magnetic susceptibility measurements as proxy method to monitor soil pollution: the case study of S. Nicola di Melfi. Environ. Monit. Assess. 169, 619–630.
D'Emilio, M., Macchiato, M., Ragosta, M., Simoniello, T., 2012. A method for the integration of satellite vegetation activities observations and magnetic susceptibility measurements for monitoring heavy metals in soil. J. Hazard. Mater. 241–242, 118–126.
Dong, C., Zhang, W., Ma, H., Feng, H., Lu, H., Dong, Y., Yu, L., 2014. A magnetic record of heavy metal pollution in the Yangtze River subaqueous delta. Sci. Total Environ. 476–477, 368–377.
Ďurža, O., 1999. Heavy metals contamination and magnetic susceptibility in soils around a metallurgical plant. Phys. Chem. Earth (A) 24, 541–543.
El Baghdadi, M., Barakat, A., Sajieddine, M., Nadem, S., 2012. Heavy metal pollution and soil magnetic susceptibility in urban soil of BeniMellal City (Morocco). Environ. Earth Sci. 66 (1), 141–155.
Evans, M.E., Heller, F., 2003. Environmental Magnetism: Principles and Applications of Enviromagnetics. Academic Press, San Diego, California, USA.
Fabian, K., Reimann, C., McEnroe, S.A., Willemoes-Wissing, B., 2011. Magnetic properties of terrestrial moss (*Hylocomium splendens*) along a north–south profile crossing the city of Oslo, Norway. Sci. Total Environ. 409 (11), 2252–2260.
Fenwick, J., 2004. An Integrated Approach to Archaeological Survey Design, Methodology and Data Management. Computer Applications and Quantitative Methods in Archaeology. Computer Applications in Archaeology, Faculty of Archaeology. Leiden University, 2004.
Fialová, H., Maier, G., Petrovský, E., Kapička, A., Boyko, T., Scholger, R., MAGPROX Team, 2006. Magnetic properties of soils from sites with different geological and environmental settings. J. Appl. Geophys. 59 (4), 273–283.
Flanders, P.J., 1999. Identifying fly ash at a distance from fossil fuel power stations. Environ. Sci. Technol. 33 (4), 528–532.
Gaffney, C.F., Gater, J., 2003. Revealing The Buried Past. Geophysics for Archaeologists. Tempus Publishing Ltd, Stroud, Gloucestershire.
Galway Advertiser, 2008. A May procession in the Claddagh, c1935. Galway Advertiser, (last viewed 22.07.2016)⟨http://www.advertiser.ie/galway/article/2313/a-may-

procession-in-the-claddagh-c1935).
Gautam, P., Blaha, U., Appel, E., Neupane, G., 2004. Environmental magnetic approach towards the quantification of pollution in Kathmandu urban area, Nepal. Phys. Chem. Earth 29, 973–984.
Gautam, P., Blaha, U., Appel, E., 2005. Magnetic susceptibility of dust-loaded leaves as a proxy of traffic-related heavy metal pollution in Kathmandu city, Nepal. Atmos. Environ. 39 (12), 2201–2211.
Gibson, P.J., George, D.M., 2013. Environmental Applications of Geophysical Surveying Techniques 2nd ed. Nova Science Publishers Inc, 360, ISBN: 978-162618-445-9.
Girault, F., Perrier, F., Poitou, C., Isambert, A., Théveniaut, H., Laperche, V., Clozel-Leloup, B., Douay, F., 2016. Effective radium concentration in topsoils contaminated by lead and zinc smelters. Sci. Total Environ. 566–567, 865–876.
Golden, N., Morrison, L., Gibson, P.J., Potito, A.P., Zhang, C., 2015. Spatial patterns of metal contamination and magnetic susceptibility of soils at an urban bonfire site. Appl. Geochem. 52, 86–96.
Grison, H., Petrovský, E., Kapička, A., Stejskalova, S., 2016. Magnetic and chemical parameters of andic soils and their relation to selected pedogenesis factors. Catena 139, 179–190.
Hanesch, M., Scholger, R., 2002. Mapping of heavy metal loadings in soils by means of magnetic susceptibility measurements. Env. Geol. 42 (8), 857–870.
Hanesch, M., Rantitsch, G., Hemetsberger, S., Scholger, R., 2007. Lithological and pedological influences on the magnetic susceptibility of soil: their consideration in magnetic pollution mapping. Sci. Total Environ. 382 (2–3), 351–363.
Hoffmann, V., Knab, M., Appel, E., 1999. Magnetic susceptibility mapping of roadside pollution. Geochem. Int. 66 (1–2), 313–326.
Innov-X Systems, Inc., 2013. Handheld XRF Revolutionizes Environmental Testing. The Best Environmental Analyzer in the World ⟨http://yosemite.epa.gov/r9/sfund/r9sfdocw.nsf/3dc283e6c5d6056f88257426007417a2/e599199dc919b049882576a300616943/$FILE/Attachment%202.pdf⟩.
Jordanova, D., Veneva, L., Hoffmann, V., 2003. Magnetic susceptibility screening of anthropogenic impact on the Danube River sediments in northwestern Bulgaria-preliminary results. Stud. Geophys. Geod. 47, 403–418.
Jung, M.A., 2001. Heavy metal contamination of soils and waters in and around the Imcheon Au-Ag mine, Korea. Appl. Geochem. 16, 1369–1375.
Kapička, A., Petrovský, E., Jordanova, N., 1997. Comparison of in-situ field measurements of soil magnetic susceptibility with laboratory data. Stud. Geophys. Geod. 41 (4), 391–395.
Kapička, A., Petrovský, E., Ustjak, S., Macháčková, K., 1999. Proxy mapping of fly-ash pollution of soils around a coal-burning power plant: a case study in Czech Republic. J. Geochem. Explor. 66 (1), 291–297.
Kapička, A., Petrovský, E., Fialová, H., Podrázský, V., Dvořák, I., 2008. High resolution mapping of anthropogenic pollution in the Giant Mountains Natural Park using soil magnetometry. Stud. Geophys. Geod. 52 (2), 271–284.
Kletetschka, G., Žila, V., Wasilewski, P.J., 2003. Magnetic anomalies on the tree trunks. Stud. Geophys. Geod. 47 (2), 371–379.
Lecoanet, H., Lévêque, F., Segura, S., 1999. Magnetic susceptibility in environmental applications: comparison of field probes. Phys. Earth Planet. Inter. 115, 191–204.
Lees, J.A., 1999. Evaluating magnetic parameters for use in source identification, classification and modelling of natural and environmental materials. In: Walden, J., Oldfield, F., Smith, J. (Eds.), Environmental Magnetism: A Practical Guide, Technical Guide 6. Quaternary Research Association, London.
Liu, S.G., Bai, S.Q., 2006. Study on the correlation of magnetic properties and heavy metals content in urban soils of Hangzhou City, China. J. Appl. Geophys. 60, 1–12.
Liu, Q.S., Roberts, A.P., Larrasoana, J.C., Banerjee, S.K., Guyodo, Y., Tauxe, L., Oldfield, F., 2012. Environmental magnetism: principles and applications. Rev. Geophys. 50 (4), 1–50.
Lu, S.G., Bai, S.Q., Xue, Q.F., 2007. Magnetic properties as indicators of heavy metals pollution in urban topsoils: a case study from the city of Luo Yang, China. Geophys. J. Int. 171, 568–580.
Lu, G.Y., Wong, D.W., 2008. An adaptive inverse-distance weighting spatial interpolation technique. Comput. Geosci. 34, 1044–1055.
Łukasik, A., Szuszkiewicz, M., Magiera, T., 2015. Impact of artifacts on topsoil magnetic susceptibility enhancement in urban parks of the Upper Silesian conurbation datasets. J. Soils Sediment. 15 (8), 1836–1846.
Mackey, E.A., Christopher, S.J., Lindstrom, R.M., Long, S.E., Marlow, A.F., Murphy, K.E., Paul, R.L., Popelka-Filcoff, R.S., Rabb, S.A., Sieber, J.R., Spatz, R.O., Tomlin, B.E., Wood, L.J., Yen, J.H., Yu, L.L., Zeisler, R., Wilson, S.A., Adams, M.G., Brown, Z.A., Lamothe, P.L., Taggart, J.E., Jones, C., Nebelsick, J., 2010. Certification of Three NIST Renewal Soil Standard Reference Materials for Element Content: srm 2709a San Joaquin Soil, SRM 2710a Montana Soil I, and SRM 2711a Montana Soil II. NIST Special Publication 260-172. US Department of Commerce and the National Institute of Standards and Technology.
Magiera, T., Zawadzki, J., 2007. Using of high-resolution topsoil magnetic screening for assessment of dust deposition: comparison of forest and arable soil datasets. Environ. Monit. Assess. 125 (1–3), 19–28.
Magiera, T., Kapička, A., Petrovský, E., Strzyszcz, Z., Fialová, H., Rachwał, M., 2008. Magnetic anomalies of forest soils in the upper Silesia—Northern Moravia region. Environ. Pollut. 156 (3), 618–627.
Magiera, T., Jabłońska, M., Strzyszcz, Z., Rachwal, M., 2011. Morphological and mineralogical forms of technogenic magnetic particles in industrial dusts. Atmos. Environ. 45 (25), 4281–4290.
Maher, B.A., Thompson, R. (Eds.), 1999. Quaternary Climates, Environments and Magnetism. Cambridge University Press, Cambridge, U.K.
Manta, D.S., Angelone, M., Bellanca, A., Neri, R., Sprovieri, M., 2002. Heavy metals in urban soils: a case study from the city of Palermo (Sicily), Italy. Sci. Total Environ. 300, 229–243.
Miller, J.N., Miller, J.C., 2005. Statistics and Chemometrics for Analytical Chemistry. Pearson Education Ltd, England, UK.
Morton-Bermea, O., Hernandez-Alvarez, E., Martinez-Pichardo, E., Soler-Arechalde, A.M., Lozano Santa-Cruz, R., Gonzalez, G., Beramendi-Orosco, L., Urrutia-Fucugauchi, J., 2009. Mexico City topsoils: heavy metals vs. magnetic susceptibility. Geoderma 151 (3–4), 121–125.
Norland, M.R., Veith, D.L., 1995. Revegetation of course taconite iron ore tailing using municipal solid waste compost. J. Hazard. Mater. 41, 123–134.
O'Dowd, P., 1993. Down by the Claddagh. Kenny's Bookshop and Art Galleries Ltd., Galway, Ireland.
Petrovský, E., Ellwood, B., 1999. Magnetic monitoring of air, land and water pollution. In: Maher, B.A., Thompson, R. (Eds.), Quaternary Climates, Environment and Magnetism. Cambridge University Press, Cambridge, 279–322.
Petrovský, E., Kapička, A., Jordanova, N., Knab, M., Hoffmann, V., 2000. Low-field magnetic susceptibility: a proxy method of estimating increased pollution of different environmental systems. Environ. Geol. 39 (3–4), 312–318.
Salo, H., Bućko, M.S., Vaahtovuo, E., Limo, J., Mäkinen, J., Pesonen, L.J., 2012. Biomonitoring of air pollution in SW Finland by magnetic and chemical measurements of moss bags and lichens. J. Geochem. Explor. 115 (1), 69–81.
Schibler, L., Boyko, T., Ferdyn, M., Gajda, M., Höll, S., Jordanova, N., Rösler, N., MAGPROX Team, 2002. Topsoil magnetic susceptibility mapping: data reproducibility and compatibility, measurement strategy. Stud. Geophys. Geod. 46 (1), 43–57.
Schmidt, A., Yarnold, R., Hill, M., Ashmore, M., 2005. Magnetic susceptibility as proxy for heavy metal pollution: a site study. J. Geochem. Explor. 85 (3), 109–117.
Soodan, R.K., Pakade, Y.B., Nagpal, A., Katnoria, J.K., 2014. Analytical techniques for estimation of heavy metals in soil ecosystem: a tabulated review. Talanta 125, 405–410.
Strzyszcz, Z., Magiera, T., 2001. Record of industrial pollution in polish ombrotrophic peat bogs. Phys. Chem. Earth A: Solid Earth Geod. 26 (11–12), 859–866.
Thompson, R., Oldfield, F., 1986. Environmental Magnetism. Allen and Unwin, Winchester, Massachusetts.
Vangronsveld, J., Van Assche, F., Clijsters, H., 1995. Reclamation of a bare industrial area contaminated by non-ferrous metals: In situ metal immobilization and revegetation. Environ. Pollut. 87 (1), 51–59.
Verosub, K.L., Roberts, A.P., 1995. Environmental magnetism: past, present and future. J. Geophys. Res. 100, 2175–2192.
Wang, X.S., Qin, Y., 2005. Correlation between magnetic susceptibility and heavy metals in urban topsoil: a case study from the city of Xuzhou, China. Environ. Geol. 49 (1), 10–18.
Webster, R., Oliver, M.A., 2007. Geostatistics for Environmental Scientists. Statistics in Practice second ed. Wiley & Sons Ltd., Chichester, West Sussex, England.
Yang, T., Liu, Q., Zeng, Q., Chan, L., 2012. Relationship between magnetic properties and heavy metals of urban soils with different soil types and environmental settings: implications for magnetic mapping. Environ. Earth Sci. 66 (2), 409–420.
Zawadzki, J., Fabijańczyk, P., Magiera, T., 2007. The influence of forest stand and organic horizon development on soil surface measurement of magnetic susceptibility. Pol. J. Soil Sci. XL (2), 113–124.
Zawadzki, J., Fabijańczyk, P., Magiera, T., Strzyszcz, Z., 2010. Study of litter influence on magnetic susceptibility measurements of urban forest topsoils using the MS2D sensor. Environ. Earth Sci. 61 (2), 223–230.
Zawadzki, J., Fabijańczyk, P., Magiera, T., Rachwał, 2015. Geostatistical microscale study of magnetic susceptibility in soil profile and magnetic indicators of potential soil pollution. Water, Air Soil Pollut. 226 (5), 142–149.
Zhang, C., 2006. Using multivariate analysis and GIS to identify pollutants and their spatial patterns in urban soils in Galway, Ireland. Environ. Pollut. 142 (3), 501–511.
Zhang, C., Qiao, Q., Appel, E., Haung, B., 2012. Discriminating sources of anthropogenic heavy metals in urban street dusts using magnetic and chemical methods. J. Geochem. Explor. 119–120, 60–75.
Zhu, Z., Han, Z., Bi, X., Yang, W., 2012. The relationship between magnetic parameters and heavy metal contents of indoor dust in e-waste recycling impacted area, Southeast China. Sci. Total Environ. 433, 302–308.